FACULTY OF MEDICINE AND HEALTH SCIENCES

Ghent University, Faculty of Medicine and Health Sciences
Center for Medical Genetics

Identification of novel drug targets downstream of activated ALK in neuroblastoma

Shana Claeys

This thesis is submitted to fulfil the requirements for the degree of Doctor in Biomedical Sciences by Shana Claeys, 2017

Promotor:
Prof. Dr. Franki Speleman

Co-promotor:
Prof. Dr. Ir. Katleen De Preter

Center for Medical Genetics
Ghent University Hospital, Medical Research Building
De Pintelaan 185, 9000 Ghent, Belgium
Shana.Claeys@UGent.be

GHENT UNIVERSITY

Thesis is submitted to fulfil the requirements for the degree of Doctor in Biomedical Sciences, University of Ghent, Faculty of Medicine and Health Sciences, 2017

Promoter: prof. dr. Frank Speleman
Ghent University, Belgium

Co-promoter: prof. dr. ir. Katleen De Preter
Ghent University, Belgium

Members of the examination committee:
prof. dr. Bengt Hallberg
University of Gothenburg, Sweden

prof. dr. Mathieu Bollen
KU Leuven, Belgium

prof. dr. Lennart Martens
Ghent University, Belgium

dr. Tom Vanden Berghe
Ghent University, Belgium

dr. Joni Van der Meulen
Ghent University, Belgium

dr. Tiago França Brazao
Ghent University, Belgium

prof. Jolanda van Hengel
Ghent University, Belgium

The research described in this thesis was conducted at the Center for Medical Genetics, Ghent University, Ghent, Belgium.
This work was supported by a predoctoral fellowship of The Research Foundation – Flanders (FWO) and an Emmanuel van der Schueren grant from “Kom op tegen Kanker (Stand up to Cancer, the Flemish cancer society).

This thesis is addressed to:
all patients and their families & friends, having the courage to beat this disease
Kenny, my parents, my grandparents & my sister
my family
my friends

The two most important days in your life are
the day you are born
and the day you find out why.
~Mark Twain~

Table of Contents

List of abbreviations

ADCC	antibody-dependent cellular cytotoxicity
ADM	adrenomedullin
ADME	absorption, distribution, metabolism and excretion
ALCL	anaplastic large cell lymphoma
ALK	anaplastic lymphoma kinase
AML	acute myeloid leukaemia
AMPK	AMP-dependent kinase
ARTN	artemin
AUG-α/β	augmentor-α/β
AURKA	aurora kinase A
AURKB	aurora kinase B
AHSCT	autologous haematopoietic stem cell transplantation
BBB	blood-brain barrier
BDNF	brain-derived neurotrophic factor
bHLH-Zip	basic-helix-loop-helix-zipper
CAR	chimeric antigen receptor
CAR-T	chimeric antigen receptor T cell
CDC	complement-dependent cytotoxicity
CDK	cyclin-dependent kinase
ChIP-seq	chromatin immunoprecipitation followed by sequencing
CNS	central nervous system
CNTF	ciliary neurotrophic factor
CRA	cis-RA
CTC	circulating tumour cells
ctDNA	circulating or cell-free tumour DNA
DBH	dopamine β-hydroxylase
DEG	delayed early genes
DRTK	developmental receptor tyrosine kinasopathy
EGCG	epigallocatechin-3-gallate
EGFR	epidermal growth factor receptor
EMT	epithelial-to-mesenchymal transformation
FBXW7	F-box and WD repeat domain-containing 7
FDA	food and drug administration
GDNF	glial cell line-derived neurotrophic factor
GEP	gene expression profiling
GFL	GDNF-family ligands
GFR	GDNF-family receptors
GR	glycine-rich
GWAS	genome-wide association study
HAT	histone acetylase
HBP1	HMG-box transcription factor 1

HDAC	histone deacetylase
HDACi	histone deacetylase inhibitor
HMG	high-mobility group
ID-miRs	immediately downregulated microRNAs
IEG	immediately early genes
IMT	inflammatory myofibroblastic tumours
INRG	international neuroblastoma risk group
INSS	international neuroblastoma staging system
LDL	low-density lipoprotein
lncRNA	long non-coding RNA
LTK	leukocyte tyrosine kinase
mAb	monoclonal antibody
miRNA	microRNA
miR	microRNA
MTC	medullary thyroid cancer
MYCN	v-MYC avian myelocytomatosis viral oncogene neuroblastoma
NB	neuroblastoma
NGF	nerve growth factor
NPM	nucleophosmin
NSCLC	non-small cell lung cancer
NTRK	neurotrophin tyrosine receptor kinases
NTRN	neurturin
NT-3/4	neurotrophin-3/4
PDX	patient-derived xenograft
PDOX	patient-derived orthotopic xenograft
PHOX2B	paired-like homeobox 2B
PP2A	protein phosphatase 2A
PSPN	persephin
PTP	protein tyrosine phosphatase
PTPRD	protein tyrosine phosphatase receptor type D
RA	retinoic acid
RET	rearranged during transfection
RNA-seq	RNA sequencing
RTK	receptor tyrosine kinase
shRNA	short hairpin RNA
siRNA	small interfering RNA
SNS	sympathetic nervous system
SRG	secondary response genes
TH	tyrosine hydroxylase
TKD	tyrosine kinase domain
TKI	tyrosine kinase inhibitors

Part I: introduction

Together, we can make a world,
where cancer no longer means
living with fear, without hope or worse.
~Patrick Swayze~

Chapter 1 Introduction

Cancer, a word that immediately awakes a lot of mainly negative emotions by people. During our lifetime, most of us are directly or indirectly confronted with this destructive disease. We all know someone who has suffered or is suffering from cancer. Fortunately, science has helped increasing the survival rate for most cancer entities. For paediatric cancer, the main improvements have been seen in leukaemia. However, the need for more efficient and less toxic treatment is still urgent, as a lot of patients are enduring side effects from the current therapy regimes or are not receiving the most appropriate and effective compounds for their (sub)type of cancer, resulting in a worse clinical outcome. Therefore, to improve the clinical outcome for individual patients, to minimize the side effects and to avoid exposure to costly and potentially toxic compounds to those less likely to response to this treatment, the "precision medicine initiative" has been initiated [1]. Such targeted therapy is directed against components of various deregulated signaling pathways [2]. One of the first and still very important targets for precision drugging are receptor tyrosine kinases of which many are often constitutively activated in cancer, examples being HER/NEU, EGFR, FGFR, and ALK.

The first part of this introduction covers receptor tyrosine kinases, their normal function, their role in cancer and cancer therapy as well as resistance mechanisms to these targeted compounds. In the second part, I provide a short introduction on basic features of neuroblastoma, a paediatric tumour of the peripheral nervous system, which was the topic of my investigations, and an overview of the different receptor tyrosine kinases implicated in normal neuronal development. Finally, I will introduce the receptor tyrosine kinase ALK and the transcription factor MYCN, both recurrently implicated in neuroblastoma, as well as HBP1, an ALK downstream target and newly identified tumour suppressor gene that negatively regulates MYC(N), as described in this thesis.

1.1 Cancer hallmarks as governed by the interplay between oncogenes and tumour suppressors

Cancer is driven by alterations and deregulation of an interplay between the classical oncogenes (e.g. MYC, RAS, ABL1) and tumour suppressors (RB1, TP53, BRCA1) or in other terms drivers, (lineage) dependency genes, care takers, gate keepers and so on [3]. Oncogenes can become activated by chromosomal translocations, gene amplifications, gain-of-function mutations and hypomethylation, while tumour suppressor genes are inactivated by loss-of-function mutations, deletions, insertions or epigenetic silencing. Following the classical Knudson two-hit hypothesis, tumour suppression is lost upon inactivation of both alleles of a tumour suppressor locus, while for other suppressors, haplo-insufficiency may be sufficient to provide cells with a selective growth advantage and initiate or contribute to clonal expansion [3]. Stability genes or caretakers are involved in mechanisms responsible for repairing subtle mistakes made during normal DNA replication or induced by mutagenic exposure, including mismatch repair, nucleotide-excision repair, base-excision repair, and in processes like mitotic recombination and chromosomal segregation. As these genes control accumulation of genetic alterations, inactivation leads to a higher genomic instability, implicating multiple genes over time, including tumour suppressors and oncogenes, driving the tumour formation process [3]. These alterations can arise in the germline, leading to hereditary predispositions for cancer, or in somatic cells. Typically, several genetic insults affecting different genes are required to breach the protection of normal cells against malignant transformation. A germline mutation will affect every cell of the body and in most instances, will cause the first hit of a given tumour suppressor and subsequent alterations in other genes will lead to hyperplasia and finally aggressive and metastazing cancer cells. While germline mutations can lead to highly increased risks for cancer, similar processes can arise in somatic cells either by chance or due to exposure to mutagenic substances and drive cancer formation in individuals with normal populations risk for cancer [3]. While multiple hits are required, also various gene functions can be affected such as receptors, signal transduction molecules, transcription factors, epigenetic regulators, genes implicated in metabolism and so on [3]. As indicated above, industry has invested a lot of efforts to identify druggable targets for cancer therapy. Amongst these, receptor tyrosine

kinases have been a prime target, the BCR/ABL1 fusion gene being the prototypical target for which the first FDA approved target drug imatinib was developed [3-5].

1.2 Receptor Tyrosine Kinases (RTK) as signal transducers

The Epidermal Growth Factor Receptor (EGFR) was the first receptor tyrosine kinase, discovered in 1978 [6]. Since then 57 additional receptor tyrosine kinases (RTKs) have been found, which are part of one of the 20 subfamilies [4,5]. All these receptors are characterized by the same molecular structure, consisting of an extracellular ligand-binding domain, a single-pass transmembrane helix and an intracellular part which contains the tyrosine kinase domain (TKD) and the juxtamembrane regulatory regions [4,5].

Binding of a ligand to the inactive receptor is the first and essential step in receptor activation and essential to initiate further steps towards signal transduction, most often due to subsequent receptor dimerization through different mechanisms (Figure 1) [5]. First, the dimerization can be completely “ligand mediated”. The bivalent ligand interacts with both receptors and crosslinks them, thereby circumventing that the extracellular regions of the two receptors contact each other (Figure 1A) [5]. Secondly, the formation of the dimer can be entirely “receptor mediated”. In this situation, the bivalent activating ligands bind two sites in only a single receptor, thereby boosting a conformation change, so that the two receptors bind to each other (Figure 1C) [5]. Thirdly, the dimerization can be a consequence of the combination of ligand-receptor crosslinking and receptor-receptor binding (Figure 1B) [5]. Sometimes, even an accessory molecule can be involved to further link the receptors and ligands to each other. Furthermore, in the case of the RET (Rearranged during Transfection, see section “RET”) receptor, the ligands first have to form a complex with a co-receptor, namely the GDNF-family receptors (GFRs), before they can activate the dimerization of the receptor itself [5].

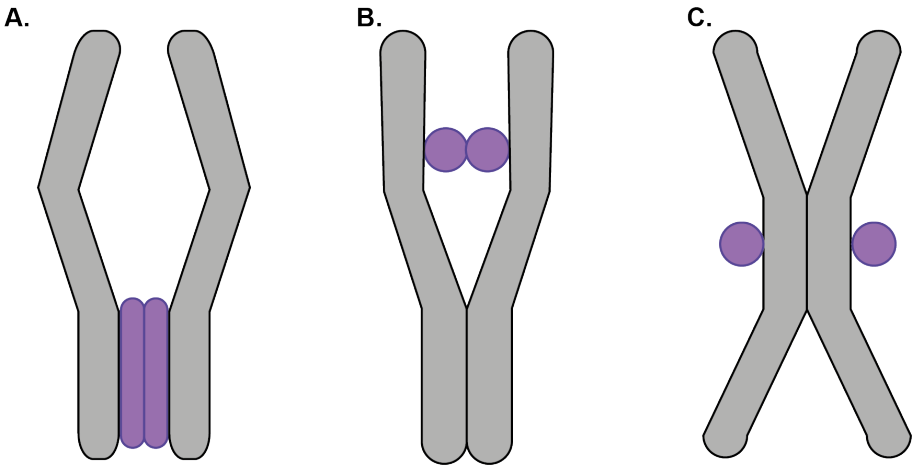

Figure 1: dimerization of the extracellular domain of receptor tyrosine kinases.
In general, dimerization is induced upon binding of the ligand to the receptor tyrosine kinases. This can happen through different mechanisms.
A. A dimer of ligands crosslinks two receptors, while these do not make any contact with each other (ligand mediated only). **B.** Crosslinking of two receptors is caused by a dimer of ligands and an interaction of the two receptors themselves (ligand and receptor mediated). **C.** Each ligand binds to only one receptor, causing them to dimerize, while the ligands are not forming a dimer (receptor mediated only). Adapted from [5].

Dimerization is always followed by activation of the intracellular kinase domains [4,5]. Most receptors are in an inactive configuration, which means that the kinase is folded in such a way that the substrate-binding and/or the ATP-binding sites are inaccessible [7]. As each tyrosine kinase domain is uniquely *cis*-auto-inhibited by a set of specific intramolecular interactions, the release of this inhibition as consequence of the dimerization can happen via diverse processes and is the most important event in the activation procedure of the signaling pathway. Several parts of the kinase domain (Figure 2) can be involved in this activation procedure. One method involves the activation loop (Figure 2, green), which can either interact with other residues in the active site, blocking both the substrate-binding as the ATP-binding sites (Figure 2, orange), or participate in intramolecular interactions thereby hindering the protein-substrate-binding place. In both scenario's, dimerization induces *trans*-phosphorylation of the tyrosines in the activation loop, which will together with the αC-helix (Figure 2, blue) adopt to an active configuration state, making the ATP-binding and protein-substrate-binding sites available for ATP and substrates. For other receptor tyrosine kinases, the tyrosine kinase domain is inhibited by interactions of his juxtamembrane region with amongst others the activation loop.

Upon dimerization, *trans*-phosphorylation will disrupt these interactions, inducing receptor activation [4,5]. Moreover, some receptors, including Tie2K, have their activation loop already in an active-like state, so the substrate- and/or ATP-binding sites are not blocked by this activation loop [8]. However, a region in the C-terminal part is hindering the substrates to bind to this active-like site. Upon auto-phosphorylation of sites in the C-terminal, the blockade will be removed and the receptor will become fully activated. There are two kind of receptors that do not require such *trans*-phosphorylation, namely the EGFR family and RET [4,5]. For the RET receptor, it was shown that the kinase domain is in an active configuration, even without phosphorylation [9]. Moreover, the substrate- or ATP-binding sites are not structurally hindered [9]. However, the kinase domains of RET associate as dimers with mutually occluded binding sites [9]. Disruption of these *trans*-inhibitory interactions is required for RET activation, while for EGFR yet another mechanism is implicated [4,5].

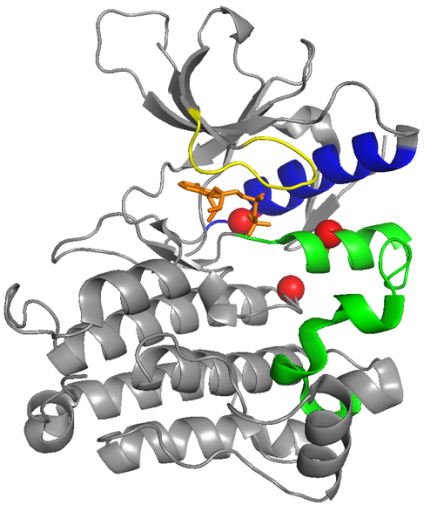

Figure 2: detailed figure of the ALK kinase domain.

The ALK kinase domain is shown in more detail, with the A-loop or activation loop in green, the αC-helix in blue, the glycine loop in yellow and the ATP-binding site in orange. The ALK hotspot mutations are shown in red. Figure provided by prof. dr. Bengt Hallberg.

Upon activation of the receptor, different phosphorylation steps are initiated by the RTK [4,5].The receptors are the first substrates that are phosphorylated. Importantly, these phosphorylations are occurring in a precise order. The first-phase auto-

phosphorylation involves the activation loop and the juxtamembrane region, which enhances the catalytic activity of the kinase. This is followed by auto-phosphorylation of other cytoplasmic regions in the RTK, resulting in the generation of the phospho-tyrosine-based binding sites that recruit other signaling molecules. Moreover, to further boost the ability of the kinase to phosphorylate downstream targets, some RTKs undergo *trans*-phosphorylation [4,5].

The phospho-tyrosines in the cytoplasmic part of the receptor recruit and activate downstream signal-transducing proteins, which have SH2 or PTB domains to bind these phosphorylated tyrosines in the RTK [4,5,10]. The recruitment can be directly or indirectly by the involvement of docking proteins, which are phosphorylated by the RTK itself. These docking proteins can be mobilized by multiple receptors or restricted to a subset.

These recruited molecules will bind to other downstream targets, mainly by protein-protein interactions or phospho-lipid-binding, to pass the signal through the cell [4,5].

As RTKs have multiple auto-phosphorylation sites that can recruit several docking proteins or molecules harbouring SH2/PTB domains, which are able as well to interact with multiple other downstream targets, complex signaling networks are built. The SH2 domains have a high degree of selectivity for their interactions with the downstream targets [11]. These SH2 domains cluster in different families based on peptide binding, defined by their consensus binding motif [11]. Moreover, binding of the SH2 domain to the peptide can be blocked through steric conflict or charge repulsion, further increasing the selectivity of the binding [11].

Furthermore, the outcome is determined by the dynamics and extent of the network activation. These networks are further complicated by the existence of cross-talk between the different signaling pathways a well as positive and negative feedback mechanisms [4,5].

The auto-phosphorylation events of the RTK are normally reversed by dephosphorylation by protein tyrosine phosphatases (PTPs) [4,5]. In some situations, these PTPs can be temporary or constantly repressed. Other mechanisms of such positive feedback include autocrine activation of the receptor and translocation of the adaptor proteins to the membrane. In this way, the signaling response is further enhanced and prolonged and the cell is more sensitive to input. In contrast, negative feedback is needed to prevent activation of the signaling pathways by small changes in the environment. Activation of the PTPs, phosphorylation of certain sites of the

receptor or docking proteins by downstream protein kinases and signal-dependent transcription of negative regulators are types of negative feedback. Furthermore, receptor endocytosis and ubiquitination will result in downregulation of the signaling. Activation of the cell-surface receptor is generally followed by ligand-stimulated endocytosis, where after the receptor is dephosphorylated and ubiquitinated. Next, the receptors will be recycled from these endosomes to the plasma membrane or they will be degraded, in order to terminate RTK activation. However, some receptors will continue the recruitment of intracellular pathway molecules from within these endosomes, in this way further activating downstream signaling pathways [4,5].

1.2.1 Receptor tyrosine kinases and diseases, kinasopathies and cancer

Giving the important role of these receptors in controlling the cellular response upon a stimulus during normal homeostasis and given the strict regulation of these RTKs, not surprisingly, aberrations in a receptor or his downstream pathways are involved in diseases.

The "developmental receptor tyrosine kinasopathies" (DRTK) are congenital malformations, caused by germline mutations disrupting such RTK signaling pathways [4]. These malignancies are characterized by a phenotypic heterogeneity, as the location and type of the mutation together with the impact of the aberration on the receptor and his kinase activity influences the phenotype. While different mutations affecting the same RTK can result in different phenotypes, one malignancy can be caused by mutations in different receptors or by mutations in diverse signaling components of the involved pathway [4]. Moreover, somatic mutations can also cause developmental disorders, presented in a milder or atypical form of the disease [4].
More importantly, these RTKs are frequently mutated in cancer. This dysregulation can be caused by four different mechanisms: overexpression, genomic rearrangements, autocrine activation and gain- or loss-of-function mutations, which result in constitutively stimulated or activated RTKs [4,5,10].
Furthermore, abnormalities in these receptors or their downstream signaling pathways can also cause other diseases, including diabetes, immune-deficiencies and inflammation [5,10].

1.2.2 Receptor tyrosine kinase inhibitors as cancer drug targets

Given their pivotal role in tumorigenesis and strong addiction of cancer cells to particular constitutively activating mutations, RTKs are the ideal target for precision medicine. A plethora of drugs have been developed targeting these molecules and they can be divided into two distinct groups: the small molecule inhibitors or tyrosine kinase inhibitors (TKI) and the monoclonal antibodies (mAb) [5]. In contrast to conventional chemotherapy, that kills all rapidly dividing cells, including normal cells, these TKIs and mAbs target specific molecules, mainly located in the tumour cell or in endothelial cells in the neighbourhood. Therefore, they cause less toxic side effects as compared to conventional chemotherapy. Moreover, they are often combined with chemotherapy or radiation to more effectively kill the cancer cells, while keeping the toxicity and adverse effects as low as possible [2].

The monoclonal antibodies can repress RTK signaling directly as well as indirectly (Figure 3) [10,12]. As first mechanism, they can block the signaling by impeding the interaction between the ligand and his receptor, by inhibiting the receptor dimerization or by increasing the downregulation and internalisation of the receptors (Figure 3A-B-C) [10,12]. Secondly, by cross-linking to the RTK, they can modulate the signaling in order to trigger apoptosis or growth inhibition instead of increasing survival in cells (Figure 3D) [10,12]. Thirdly, when conjugated with toxins, DNA molecules or small molecules, they can selectively eliminate the tumour cells upon interaction with the receptor (Figure 3E) [10,12]. For the indirect effect, the mAbs are using the immune system, including complement-dependent cytotoxicity (CDC) and antibody-dependent cellular cytotoxicity (ADCC) [12].

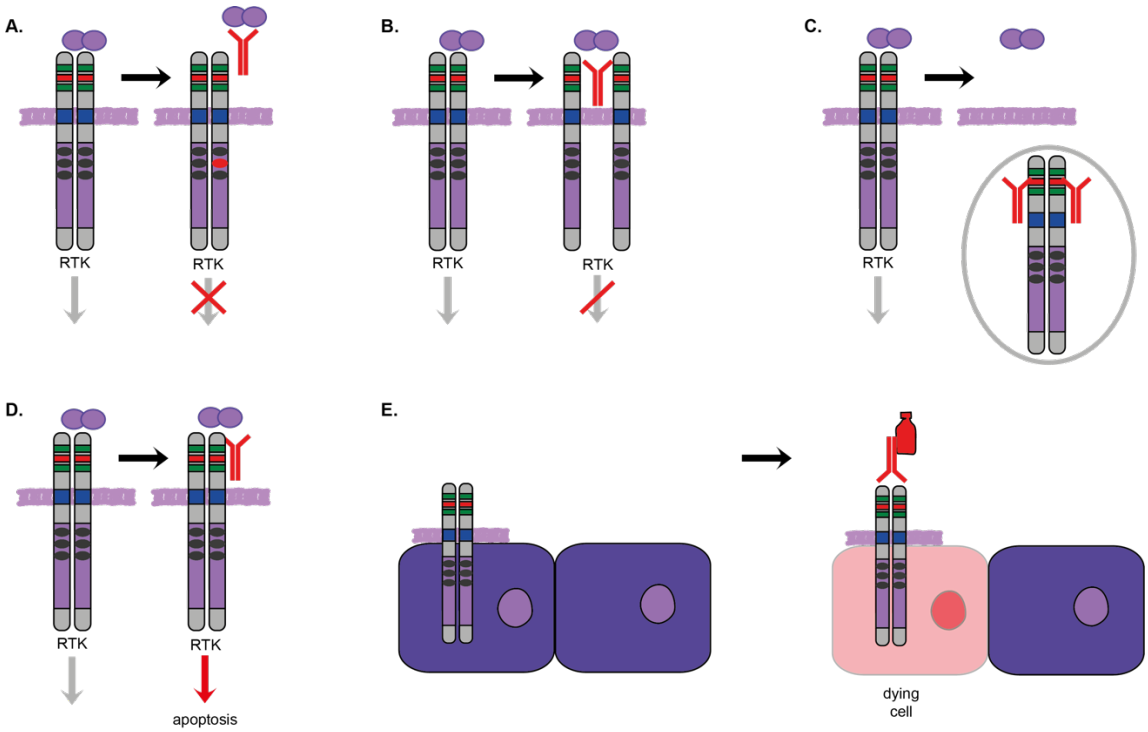

Figure 3: different mechanisms used by monoclonal antibodies to repress RTK.
The monoclonal antibodies can repress RTK signaling through direct and indirect mechanisms.
A. The mAb can repress the signaling by impeding the interaction between the ligand and his receptor. **B.** The dimerization of the receptors can be hindered by the mAb. **C.** The mAbs can increase the downregulation and internalisation of the receptors. **D.** The mAb can modulate the RTK signaling in order to trigger apoptosis or growth inhibition instead of increasing survival in cells by cross-linking the receptor. **E.** The mAbs can, when conjugated with toxins, DNA molecules or small molecules, selectively eliminate the tumour cells upon interaction with the receptor. Figure based on [10,12].

Nevertheless, the small molecule RTK inhibitors have the advantage that they can penetrate the plasma membrane to interact with the intracellular kinase domain. More specific, most of them will bind in close proximity to the ATP-binding domain within the tyrosine kinase domain, thereby competitively inhibiting the substrate-binding site and competing with endogenous ATP for binding [10,12]. Additionally, through binding at alternative sites in the receptor, a subset of the inhibitors will induce conformational changes, resulting in a decrease in kinase activity of the involved RTK [13]. Furthermore, irreversible inhibitors have been generated that covalently bind to the kinase domain of the RTK in order to completely abolish his catalytic activity [10]. Moreover, these inhibitors have a smaller molecular weight compared to the mAbs,

making it possible for them to bypass the blood-brain barrier (BBB) to treat brain cancers [12]. Despite that inhibitors have the same molecular weight, difference in anti-tumour activity against brain metastases have also been observed for different ALK small molecule inhibitors [14]. The ALK inhibitor lorlatinib has a superior anti-tumour activity against brain metastases compared to other ALK inhibitors, including crizotinib or alectinib [14]. This superior intracranial efficacy is probably caused by the enhanced potency of the compound and its increased ability to cross the BBB by avoiding transporter-mediated efflux [14].

In addition to these receptor tyrosine kinases, protein tyrosine phosphatases (PTPs) are also involved in cancer. These proteins are enzymes that remove phosphate groups from proteins [15]. Most of the time, these dephosphorylation events result in termination of the signaling pathways, activated by the RTKs. Next to these tumour suppressive PTPs, they can also function as oncogenes by promoting tumour initiation, progression and metastasis [15]. For this last group of PTPs, small molecule inhibitors have been generated. However, the main problem is the specificity, as the active site is conserved both in the tumour suppressive as the oncogenic PTPs, resulting in adverse effects and unsafety [15]. Therefore, the inhibitors must be designed so that they bind to regions located outside this active site, in order to increase their specificity towards the oncogenic PTPs [15].

However, the use of such small molecules and monoclonal antibodies targeting either the RTKs or the PTPs as single compounds are not always as successful. The first step towards an efficient compound is to identify the crucial event driving tumour progression. Further, to evaluate the compound properly, a suitable selection of patients for the clinical trial is required, as there will be lack of tumour response in the general population, emphasizing the need for appropriate biomarkers for the drugs [2]. Moreover, tumours harbour multiple mutations, so the compound should be able to target them all or combination therapy should be advised. More importantly, resistance rapidly occur when using single compound therapy. Nevertheless, in patients with relapsed anaplastic large cell lymphoma (ALCL), treatment with the ALK inhibitor crizotinib as a single agent achieved a response rate of 90%, while in ALK-positive unresectable inflammatory myofibroblastic tumour (IMT), the response rate was 86% [16]. These response rates exceeded those seen in early-phase clinical trials

in children with relapsed/refractory disease, suggesting that durability of response is tissue-context dependent [16].

1.2.3 Resistance to targeted drugs and strategies to circumvent resistance

Despite the generation of receptor tyrosine kinase inhibitors and monoclonal antibodies, the long-term efficacy of these drugs is still disappointingly low due to primary and acquired resistance [10,17-19]. Primary resistance means there is no initial response, while acquired is an "escape" mechanism during the treatment, resulting in disease progression after an initial response. Different mechanisms of resistance are found, which can be pharmacological- or biological-driven (Figure 4) [18,20].

Patient-specific pharmacokinetic differences in drug absorption, distribution, metabolism and excretion (ADME), cause changes in drug plasma levels, while drug delivery can be hindered by the blood-brain barrier [10,17-19]. All these pharmacological-based processes, together with drug – drug interactions, compliance or missed doses, result in an inadequate drug exposure of the cancer cell, leading to reduced efficacy of the compounds. In addition, tumour-intrinsic factors, including the coexistence of multiple genetic aberrations in the drug target or his downstream signaling molecules, will result in a lack of tumour response [10,17-19]. Moreover, during drug exposure, certain tumour cells from the heterogeneous tumour mass will often escape therapeutic effects leading to the emergence of resistant clones or genomic instable tumour cells will actively acquire resistance mutations (Figure 4) [18,20]. For example, the occurrence of a secondary mutation in the targeted RTK can result in a conformation change, hindering the binding for the inhibitor or increasing the affinity for ATP, while amplification of the target gene will increase the number of receptors expressed at the cell surface and thus the need for higher concentrations of the inhibitor [10,17-19] (Figure 4A-B) [18,20]. Moreover, aberrations in the downstream signaling or the activation of bypass pathways will cause resistance, resulting in a continued signaling through downstream networks. Similarly, the inhibitor-mediated inactivation of a negative feedback loop can reactivate the downstream networks, as seen for RAF inhibitors [21]. RAF inhibitors are able to block the proliferation of BRAF mutant cell lines, but are surprisingly ineffective against RAS mutant cells [21]. In these cells, RAF inhibitors cause activation of the RAF-MEK-ERK pathway, since mutant RAS

recruits and activates CRAF, which is only partially inactivated by the RAF inhibitors [21]. This is the so-called RAF paradox [21]. Furthermore, while a given mutant RTK is blocked, one or more RTKs may become activated, taking over the downstream signaling (Figure 4C-D) [18,20]. Another mechanism involves phenotypic and histologic transformation [10,17-19]. In non-small cell lung cancer (NSCLC), it has been shown that the tumour cell underwent epithelial-to-mesenchymal transformation (EMT) at the time of acquired resistance (Figure 4E) [18,20]. However, the exact underlying process is not yet fully resolved. Finally, increased production of the appropriate ligand has also been observed to cause resistance against TKIs [10,17-19] (Figure 4F) [18,20].

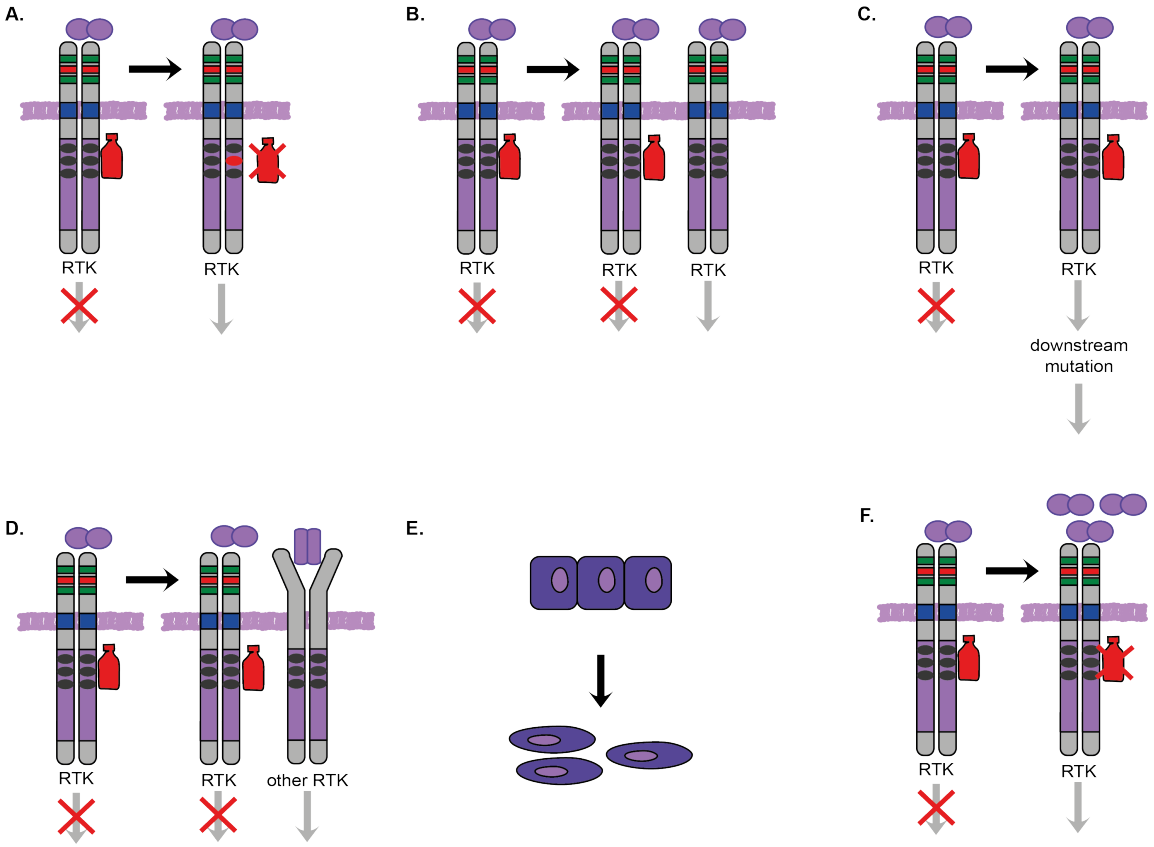

Figure 4: biological-driven resistance mechanisms to receptor tyrosine kinases

A. Resistance can be caused by a second-site mutation, blocking the drug binding. **B.** Amplification of the targeted kinase can cause resistance. **C.** A mutation downstream the targeted kinase can reactivate the downstream pathways **D.** Another (redundant) RTK can be activated upon treatment, resulting in a bypass mechanism and reactivation of the downstream pathways. **E.** Histologic changes, including epithelial-to-mesenchymal transformation (EMT) can cause resistance. **F.** Increased expression of the ligand can result as well in resistance. Adapted from [18,20].

There are several options to avoid these resistance mechanisms. If the resistance is the consequence of gene amplifications or secondary mutations, adapting the dose and schedule or using a more potent, second-generation inhibitor can solve the problem [10,17-19]. To solve the above-mentioned RAF paradox [21], several second-generation inhibitors have been developed, which are known as paradox-breaking RAF inhibitors [22,23]. These inhibitors efficiently block RAF-MAPK pathway in RAF and RAS mutant cell lines, by hindering the MAPK reactivation through inhibiting SRC-family kinase signaling [22] or by evading the paradoxical MAPK activation [23]. Moreover, using the monoclonal antibodies alone or in combination with a TKI, so called dual target blockade, can enhance efficiency, as the mAbs will use the immune system as indirect tool to further boost the elimination of the targeted tumour cell. However, most of the tumours are the consequence of defects in more than one signaling pathway or use a compensatory pathway to evade the inhibitor [10,12,17-19]. Therefore, combination therapy might be more promising to efficiently eliminate the cancer cells and to circumvent resistance. Indeed, combining a TKI with an inhibitor targeting the bypass pathway has proved to be efficient for several cancers, including melanoma [10,17-20]. Moreover, the combination of a TKI with an inhibitor targeting the molecular chaperone HSP90, which is necessary for protein folding and stabilisation, has been proposed to delay or overcome acquired resistance [10,17-20]. Indeed, HSP90 inhibitors have been shown to overcome ligand-triggered resistance to ALK inhibitors in EML4-ALK NSCLC, resulting in a more successful treatment [24,25]. Similarly, HSP90 inhibitors can effectively block the paradoxical MAPK reactivation seen upon treatment with RAF inhibitors [26]. Additionally, a phase I clinical study in paediatric patients with recurrent and refractory solid tumours, including neuroblastoma, showed that such HSP90 inhibitors can be safely administered twice weekly for 2 of 3 weeks [27]. Furthermore, these HSP90 inhibitors are effective against a variety of oncogene addicted cancers, including those that have developed resistance to specific receptors [28]. Moreover, the combination of small molecule inhibitors with chemo- or immune therapy, has shown promising results in several cancers.

However, to combine the TKI with a small molecule inhibitor targeting the bypass pathway, a good understanding of the downstream signaling networks is needed. Therefore, a deep investigation of the transcriptome and proteome downstream of the targeted receptor is pivotal.

1.3 Neuroblastoma

Almost ten years ago, in 2008, activating point mutations in the receptor tyrosine kinase "Anaplastic Lymphoma Kinase" (ALK) were described to be involved in neuroblastoma, a devastating childhood cancer [29-34]. In Belgium alone, between 2004 and 2009, 130 children and young adolescents were diagnosed with a sympathetic nervous system (SNS) tumour and 98% of them were classified as neuroblastoma [22].

1.3.1 Neuroblastoma, a leading cause of cancer-related death by children

Neuroblastoma (NB) is an embryonic tumour of the developing sympathetic nervous system and is the most common extracranial solid cancer of early childhood. It is the primary cause of cancer-related death by young children between one and five years old and accounts for approximately 13% of all paediatric cancer mortality [35,36]. The median age at diagnosis is 18 months [37], but neuroblastoma rarely occurs in adolescents and young adults and regresses in some infants before being medically noticed [35,36]. In the majority of the patients, neuroblastoma arises sporadically. However, in at least 1% to 2% of the patients, a familial history of neuroblastoma, characterized by bilateral or multifocal primary tumours and an earlier median age at diagnosis, is observed, which points toward a hereditary predisposition [36,38]. The pattern of inheritance is autosomal dominant with incomplete penetrance [36]. Furthermore, neuroblastoma is characterized by a clinical heterogeneity with respect to age at diagnosis, location of the primary tumour, stage of the disease, as well as a heterogeneous genetic landscape of the tumour, impacting on tumour behaviour that can vary from spontaneously regression to a highly aggressive, metastatic disease unresponsive to therapy [39].

The tumour arises from cells of the sympatho-adrenal lineage of developing neural crests, that fail to differentiate into sympathetic ganglion and adrenal chromaffin cells [36,37]. Primary tumours can therefore arise anywhere along the sympathetic nervous system, with most arising in the adrenal medulla or the abdominal paraspinal ganglia, while others develop from sympathetic ganglia in the chest, pelvis or neck (Figure 5)

[35]. The site of this primary tumour is associated with age and outcome [36]. Furthermore, metastatic lesions are detected in approximately 50% of patients at diagnosis and occur frequently in the regional lymph nodes, bone marrow and bone, while liver and skin metastases are most frequently seen in young children < 18 months at diagnosis [37]. At relapse, metastases in the central nervous system (CNS) are increasingly common [36]. The metastases occur through both the lymphatic and haematogenous routes [36].

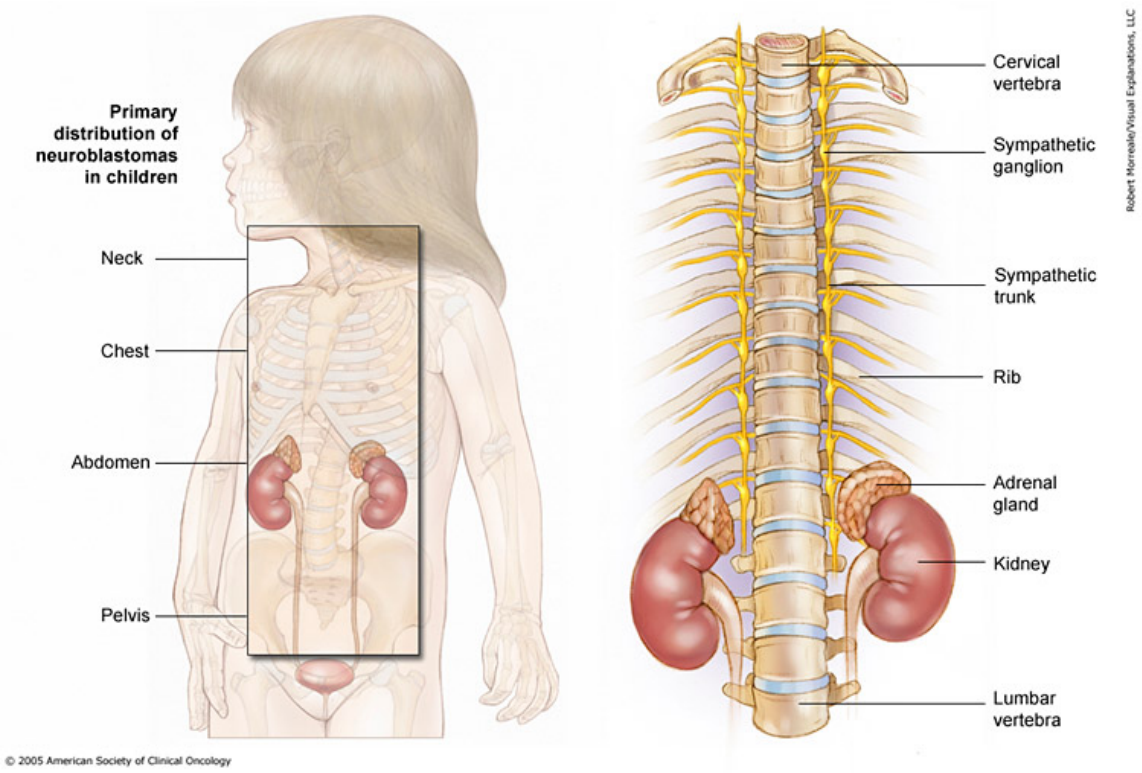

Figure 5: locations of neuroblastoma tumours.

Neuroblastoma tumours arise along the sympathetic nervous system. The primary locations are the abdomen, more specific the adrenal glands, the neck, chest and pelvis. Figure from www.cancer.net.

The clinical signs and symptoms of this cancer entity are dependent on the locations of the primary tumour and his metastases [36,37]. As mentioned before, primary tumours occur mainly in the medulla of the adrenal glands, which are associated with a poorer survival than those arising in other sites [35]. Localized primary tumours often give no clinical symptoms, while large abdominal masses can lead to hypertension and pain. If the tumour arises in the neck, it might cause damage to the cervical ganglion, leading to the Horner syndrome, while neuroblastoma tumours in the

paraspinal sympathetic ganglia can cause spinal cord compression. Metastatic disease can give rise to constitutional signs, as pain, weight loss or fever [36,37].

1.3.2 Risk staging

The oldest classification system is the widely accepted International Neuroblastoma Staging System (INSS), in which tumours are classified into a stage based on the aggressiveness of the surgical approach needed [35,36]. Stage 1 tumours are localized tumours without metastasis, which can be completely surgically excised, while stage 2 tumours are localized tumours that cannot be completely surgically removed and are further subdivided into two groups [36,37]. The stage 2A neuroblastoma tumours have no metastasis to the lymph nodes, while the stage 2B have metastatic lesions in the ipsilateral lymph nodes [36,37]. Stage 3 tumours are unresectable tumours with or without lymph node metastasis, while stage 4 tumours have metastatic lesions in distant lymph nodes and/or other organs [36,37]. A special subgroup of stage 4 is stage 4S, which consists of localized primary tumours, which mostly spontaneously regress, in young patients (age < 1year) and with metastases limited to the skin, liver or bone marrow [36,37].

To have a more standardised and international used classification system, the International Neuroblastoma Risk Group (INRG) Staging System has been initiated, which subdivide the tumours in four different stages, irrespective of the surgery needed [33,35-37,40]. Stage L1 and L2 are localized tumours, but they differ as L2 tumours involve vital structures [35]. Stage M consist of tumours with metastases at distant places, while patients younger than 18 months, who have metastatic disease in the skin, liver and/or bone marrow, are grouped as stage MS [35].

However, to define which tumour benefit from which treatment regimen, disease stage is combined with other prognostic factors, including age at diagnosis, stage, histopathology and genomic characterization like *MYCN* amplification and DNA index (table 1) [36,37,41]. In this way, tumours can be classified as (very)-low-risk, intermediate- or high-risk neuroblastoma. Very-low- and low-risk neuroblastoma cover stage L1, L2 and MS tumours with favourable genomic features, while the intermediate tumours are the *MYCN* non-amplified stage L2, the MS with

unfavourable genomic features and those patients younger than 18 months at diagnosis with *MYCN* non-amplified stage M disease [35,37,40]. The high-risk group are patients older than 18 months with stage M tumours as well as the children younger than 18 months with stage M tumours with unfavourable biological features, such as *MYCN* amplification [35,37,40]. Despite intensive treatment and incorporation of current immunotherapies, long-term survival for these high-risk patients remains 40 to 50% [36]. In contrast, the overall survival for patients with (very)-low- to intermediate-risk disease is greater than 90% with only surgical or minimal medical interventions [36].

Risk group	INRG	Distant metastases	Age (months)	Histological category	Grade of diff	MYCN	Genomic profile	Ploidy
Very-low	L1	Absent	Any	GNBnod, NB	Any	-	Any	Any
Very-low	L1/L2	Absent	Any	GN, GNBinter	Any	-	Any	Any
Low	L2	Absent	<18	GNBnod, NB	Any	-	No SCA	Any
Low	L2	Absent	≥18	GNBnod, NB	2	-	No SCA	Any
Low	MS	Present	<12	Any	Any	-	No SCA	Any
Intermediate	L2	Absent	<18	GNBnod, NB	Any	-	SCA	Any
Intermediate	L2	Absent	≥18	GNBnod, NB	2	-	SCA	Any
Intermediate*	L2	Absent	≥18	GNBnod, NB	1	-	Any	Any
Intermediate	M	Present	<18	Any	Any	-	Any	Hyper
Intermediate	M	Present	<12	Any	Any	-	SCA and/or	diploid
Intermediate	MS	Present	12-18	Any	Any	-	No SCA	Any
Intermediate	MS	Present	<12	Any	Any	-	SCA	Any
High	L1	Absent	Any	GNBnod, NB	Any	+	Any	Any
High	L2	Absent	≥18	GNBnod, NB	1	+	Any	Any
High	M	Present	12-18	Any	Any	-	SCA and/or	diploid
High	M	Present	<18	Any	Any	+	Any	Any
High	M	Present	≥18	Any	Any	Any	Any	Any
High	MS	Present	12-18	Any	Any	-	SCA	Any
High	MS	Present	<18	Any	Any	+	Any	Any

Table 1: International Neuroblastoma Risk Group (INRG) consensus pretreatment classification scheme.

Abbreviations and definitions: GN, ganglioneuroma; GNB, ganglioneuroblastoma; GNBnod, GNB nodular; GNBinter, GNB intermixed; NB, neuroblastoma; +, amplified; -, non-amplified; diff, differentiation; 1, poorly or undifferentiated; 2, differentiating; hyper, hyperdiploid. No SCA corresponds to absence and SCA to the presence of segmental chromosome alterations. *Some clinical trials consider patients with stage L2 neuroblastoma with unfavourable pathology who are >18 months as high-risks, since excellent prognosis was achieved with intensive chemotherapy, often followed by radiation and autologous haematopoietic stem cell transplantation [37]. Table adapted from [36,37,41].

Moreover, epigenetic differences, like hypermethylation to downregulate tumour suppressor genes and hypomethylation to upregulate the expression of oncogenes, are discovered [40]. These DNA methylation changes are not only able to distinguish neuroblastoma tumours from healthy individuals, but are also linked to distinguish these clinically and biologically relevant neuroblastoma subgroups [40]. High-risk neuroblastoma tumours show hypermethylation of several genes compared to the low-risk group, which is characterized by some specific hypomethylated regions [40]. Moreover, genes are differentially methylated between the 4 and 4S stage neuroblastoma tumours. Additionally, such differences are discovered as well between *MYCN* amplified and non-amplified cancers [40].

1.3.3 Current therapy regimes

Induction chemotherapy to reduce the tumour size is often the first treatment that is given to neuroblastoma patients, followed by a surgical removal of the primary tumour [37]. This removal is often difficult for patients with high-risk neuroblastoma, even after chemotherapy. Therefore, high-risk neuroblastoma patients frequently undergo myeloablative therapy and autologous haematopoietic stem cell transplantation (AHSCT). After these treatments, maintenance therapy, which consists of an oral differentiation compound like 13-cis-retinoic acid and immunotherapy, including the use of anti-GD2 monoclonal antibodies, is given to prevent relapse. If the patient relapses, chemotherapy alone or together with small molecules like ALK inhibitors, is considered [37,42]. Recurrently, such targeted approaches rapidly lead to resistance due to activation of other downstream pathways or bypass mutations. Therefore, current treatment regimens are reoriented to combine different small molecules, trying to circumvent this signal rewiring and completely blocking the downstream pathways. Such approach in combination with chemotherapy or immune therapy will hopefully lead to a better and longer survival of the patients [10,17-20]. Indeed, recently, it has been shown that the combination of melphalan, a chemotherapeutic used to treat high-risk neuroblastoma, with BSO, a GSH synthesis inhibitor, was tolerable with haematopoietic stem cell support and achieved good responses in patients with recurrent/refractory high-risk neuroblastoma [43].

Next to further research to improve targeted therapy and since anti-GD2 is quite toxic due to the presence of this cell surface protein on noci-receptor-containing peripheral nerves, alternative immunotherapeutic strategies are urgently needed [44] (described in more detail in discussion). Bosse *and colleagues* have identified GPC2 as a promising immunotherapeutic target by searching for genes encoding proteins with extracellular domains, which are differentially expressed on neuroblastoma compared to normal tissue [44]. Indeed, a GPC2 targeting antibody-drug conjugate resulted in cellular cytotoxicity *in vitro* in neuroblastoma cells and was efficacious and safe *in vivo* in neuroblastoma mouse models [44].

1.3.4 The genetic landscape of neuroblastoma

Recent sequencing efforts have further characterized the genomic landscape of neuroblastoma in great detail. At the mutational level, the diagnostic tumour exhibit few recurrent driver mutations in a background of highly recurrent DNA copy number alterations [45]. These recurrent copy number alterations include gains of 17q, 1q, 2p or losses of 1p, 11q, 3p, 4p, 14q [36,37]. Moreover, in familial NB, candidate chromosomal predisposition regions have been identified at 16p, 12p and 2p [36]. More importantly, outcome is associated with type of chromosomal alterations [36,46]. Tumours with numerical chromosomal abnormalities due to whole chromosome gains and losses have an excellent outcome, while patients with segmental chromosomal alterations due to gains and losses of parts of chromosomes, have an inferior outcome [36,46]. Additionally, the acquisition of new segmental chromosomal aberrations occurs at the time of relapse [46]. Furthermore, hyperdiploid tumours have a more favourable prognosis compared to diploid tumours [36,46].

The most common focal genetic lesion is the amplification of *MYCN* (>10 copies), located on 2p24, which occurs in approximately 20% of neuroblastoma tumours and half of the high-stage tumours. *MYCN* amplifications are linked with a particularly poor prognosis (as described in more detail in the “MYCN” paragraph further in this thesis) [35,39]. In addition, amplification or overexpression of *LIN28B* is frequently found in high-risk neuroblastoma, leading to increased *MYCN* levels and depletion of the *let-7* family of microRNAs (miRNAs) [35,47]. Moreover, such *let-7* family disruption seems to be an important mechanism for neuroblastoma developments, since multiple mechanisms have been found to neutralize *let-7* [48]. In addition to the

repression by LIN28B, loss of chromosomes 3p and 11q, containing *let-7* family members, is frequently observed in neuroblastoma tumours [48]. Moreover, in *MYCN*^{amplified} neuroblastoma tumours, *MYCN* mRNA sponges *let-7* members, in this way hindering the activity of these miRNAs [48].

Activating mutations in the Anaplastic Lymphoma Kinase (*ALK*) receptor have been found to be oncogenic drivers in both familial as sporadic cases of neuroblastoma (as described in more detail in the "ALK" section) [35,36]. In addition, germline mutations can be found in the Paired-like Homeobox 2B (*PHOX2B*) gene in familial tumours and in approximately 4% of sporadic neuroblastoma [35,36]. This transcription factor, located on chromosome 4p12, is necessary for normal development of the autonomic nervous system [46,49]. Moreover, patients harbouring such a mutation have a higher risk for developing neurocristopathies, which are diseases arising from tissues consisting of cells derived from the neural crest [36,38,49]. Additionally, whole exome sequencing of families with no *PHOX2B* or *ALK* mutations revealed functionally damaging mutations in *GALNT14* [38,49]. Rare germline mutations in association with occurrence of neuroblastoma have been found in genes involved in the RAS pathway, including *HRAS*, *PTPN11*, *ODZ3*, *SOS1*, *KRAS*, *NRAS*, *RAF1*, *BRAF*, *MEK1*, *RIT1* and *NF1* [38,46,49]. In small percentages of neuroblastoma patients, rare germline mutations have been found in *TP53*, *CDKN1C*, *SDHB*, *APC*, *BRCA1*, *BRCA2*, *CHEK2* and *PINK1* [38,49]. Of particular interest, genome-wide association studies (GWAS) identified *CASC15*, *BARD1*, *LMO1*, *LIN28B*, *HACE1*, *DUSP12*, *DDX4*, *IL31RA*, *HSD17B12*, *NEFL*, *TP53* and *NBPF23* as associated with high-risk and low-risk neuroblastoma predisposition [36,46,49]. Moreover, individuals with risk alleles in *BARD1* and *LMO1* are more likely to develop neuroblastoma and more likely to have metastatic disease and worse clinical outcome [46]. However, BARD1 has mostly tumour suppressive functions in cancer. Nevertheless, in neuroblastoma, the disease-associated variations are correlated with the expression of an oncogenetically activated isoform, namely BARD1β, that has growth-promoting effects through cooperation with the Aurora kinases [46]. Additionally, a single G>T transversion in a super-enhancer element in the *LMO1* gene allows GATA3 transcription factor binding, enhancing the expression of *LMO1* [46]. Moreover, LMO1 synergizes with MYCN to promote neuroblastoma development and metastasis [50,51]. Furthermore, in *MYCN* non-amplified cases, structural variants affecting TERT

expression are highly recurrent and *ATRX* inactivating mutations are mostly found in tumours from adolescent and young adult patients [36,46,52,53]. Next to *ATRX*, other genes in the Rho/Rac signaling cascade, a pathway important for migration and differentiation of neural crest cells, are frequently mutated in neuroblastoma tumours [54]. Moreover, high expression of ROCK2, a kinase of the Rho/Rac pathway, is associated with poor survival [54]. Further recurrent mutations include those inactivating *ARID1A* and *ARID1B* [36,39,46], while an emergence of *ALK* mutations at relapse have been demonstrated, suggesting that *ALK* mutations might occur as subclones at diagnosis, contributing to tumour progression [55]. Moreover, RAS/MAPK pathway mutations were shown to be enriched in relapsed cases [46,56].

1.3.5 Models of neuroblastoma disease

The first transgenic neuroblastoma mice model system has been established in 1997 by Weiss *and colleagues* [57], to test the effect of *MYCN* on the transformation of neuroblasts *in vivo*. Therefore, they cloned the human *MYCN* gene after the tyrosine hydroxylase (*Th*) promoter, since this promoter is active in migrating cells of the neural crest. In this way, the mice will develop targeted expression of *MYCN* in the sympathetic ganglia and the adrenal, the places where neuroblastoma tumours appear [57]. They were able to show that overexpression of MYCN in these cells leads to neuroblastoma tumours which resemble the human ones. In 2012 [58], a *Th-ALK*^{F1174L} mouse model was created by injecting a *Th-ALK*^{F1174L} construct, which consist of the human *ALK*^{F1174L} cDNA cloned after the *Th* promoter, in mice blastocysts. These mice were crossed with the *Th-MYCN* mice of Weiss *and colleagues* [57], to create *ALK*^{F1174L}*/MYCN* compound hemizygote mice. In this way, the interaction between the ALK and MYCN downstream pathways can be investigated (see further). Recently, Althoff *and colleagues* [59] created the LSL-*MYCN*;*Dbh*-iCre mice, which is a Cre-conditional MYCN-driven neuroblastoma mouse model with the neuroblastoma-specific marker dopamine β-hydroxylase (*Dbh*) as promoter and has several advantages compared to the *Th-MYCN* mice. One important advantage is that the LSL-*MYCN*;*Dbh*-iCre tumours arise not only from the adrenals, but as well from the celiac and the superior cervical ganglia, from which a minority of human neuroblastoma tumours develops [59]. From a LSL-*MYCN*;*Dbh*-iCre

tumour, a cell line has been generated, named mNB-A1. The growth of these cells was MYCN-dependent, showing oncogene addiction. Therefore, this cell line is an ideal model system to test new drugs targeting MYCN. Additionally, these cells can be used to be re-engrafted into nude mice, to test the compounds *in vivo* [59]. As last, the LSL-*Lin28b*;*Dbh*-iCre mouse model was created to test the effect of LIN28B on neuroblastoma [47].

Next to mice, zebrafish are often used as model system, because they are easier to house, have a larger number of offspring and they reproduce rapidly compared to mice. In 2012, Zhu *and colleagues* [60] created a stable transgenic zebrafish line, *Tg(dβh:EGFP-MYCN)*, which overexpresses the human *MYCN* gene under the control of the *dβh* promoter and fused to EGFP to monitor the tumour formation easily with microscopy. Simultaneously, they created the *Tg(dβh:EGFP; dβh:ALK^{F1174L})* zebrafish line. After breeding these zebrafish with the *MYCN* heterogeneous zebrafish line, zebrafish overexpressing both *MYCN* and *ALK^{F1174L}* were generated [60]. This strategy can also be used for crossing *MYCN* zebrafish with a zebrafish with an overexpression or knock-out from your gene of interest to evaluate tumour acceleration, onset and penetrance compared to *MYCN* only zebrafish. Recently, the high-risk neuroblastoma susceptibility gene *LMO1* has been injected into zebrafish embryos, creating the *Tg(dbh:LMO1),Tg(dbh:mCherry)* zebrafish lines [50,51]. Interbreeding of the *LMO1* and *MYCN* transgenic fish showed that high levels of *LMO1* enhance neuroblastoma initiation *in vivo* [50,51]. Transgenic *LMO1* expression increases the proliferation of sympatho-adrenal cells, thereby overcoming the MYCN-induced apoptotic response [50,51]. Moreover, *LMO1* expression promote expression of LOX family members, which contribute to metastasis by promoting tumour cell invasion and migration [50,51]. Thereafter, it is shown [61] that zebrafish can be used to evaluate the metastatic capacity of human cancer cells. The adaptive immune system of zebrafish arises after 14 days' post-fertilization, so human cancer cells can survive and form metastatic lesions when transplanted into zebrafish larvae. In this way, it is possible to evaluate in a rapid, robust and inexpensive way the effect of a genetic manipulation on metastasis [61].

To evaluate the effect of the mutations and DNA copy number alterations on initiation and/or tumour progression in neural crest progenitor cells, murine JoMa1 cells, which are kept in an undifferentiated state by special culture medium and by supplementation with 4-OHT to have low c-MYC activity, were transfected with DNA for MYCN or ALK^{F1174L} [62]. The low levels of c-MYC hold the cells in undifferentiated state, but make it impossible to initiate transformation. The JoMa-ALK^{F1174L} and JoMa-MYCN were able to proliferate even after inactivation of c-MYC by withdrawal of 4-OHT, which shows that both MYCN and ALK are capable of inducing an immortalized phenotype [62]. Furthermore, injection of these cell lines in mice resulted in tumours, which resemble human neuroblastoma tumours. In this way, it was shown that both mutated ALK and MYCN are capable of driving neuroblastoma development [62].

More recently, the group of Kevin Freeman [63] was able to generate tumours that molecularly and phenotypically mimic human neuroblastoma tumours by enforced expression of *MYCN* in wild type neuronal crest cells, which are highly migratory, multipotent cells and the proposed embryonic precursor cell of neuroblastoma [63]. Moreover, this approach should be ideal to study the early phases of neuroblastoma development as well as to evaluate the functional role of established and newly identified oncogenic drivers in these first steps towards a full-blown tumour [63].

Since half of the patients present with metastatic disease, a model system to investigate the metastatic processes is crucial. The mechanisms driving metastasis in neuroblastoma are challenging and poorly recapitulated in the existing mouse model systems [64], but can be modelled in zebrafish [50,51]. Additionally, Delloye-Bourgeois *and colleagues* have shown the power of the chick embryo to model neuroblastoma metastasis [64,65]. They have injected neuroblastoma cell lines and patient-derived xenografts into chick embryos, which are naturally immune-deficient [64,65]. These neuroblastoma cells followed migration patterns of the endogenous avian neural crest cells to reach sympathetic ganglia, where they formed dense, proliferating masses. Metastatic spread was often seen 7 days' post-engraftment and proceeded through the dorsal aorta and peripheral nerves [64,65]. Moreover, neuroblastoma dissemination is induced by downregulation of SEMA3C, a pro-cohesion autocrine

signal, known to regulate axon and cell migration, including that of the neural crest [64,65].

Another option to evaluate the characteristics of the manipulation of a certain gene or chromosome *in vivo* as follow up to cell culture experiments is by using xenografted mice. Well-established neuroblastoma cell lines are subcutaneously injected in immune-deficient mice, to prevent destruction by the immune system of the mice [66,67]. These subcutaneously xenografted mice have several benefits as they are easy to use and relatively inexpensive, while being reproducible [68]. However, they also have several drawbacks, with the most important being the inappropriate microenvironment of the sympathetic ganglion, the location of the injection and the lack of metastasis [69,70]. One way to circumvent these caveats, is by generating an orthotopically xenografted mouse model. In this model system, the tumour cells are injected directly into the organ of origin, so they recapitulate more faithfully the human disease [66,67]. The tumour evolved from the subcutaneously or orthotopically injected human neuroblastoma cells, can be excised and brought into culture to create a mouse tumour cell line. These cells can then be re-engrafted in immune-deficient mice to create new tumours or to test drugs in *vivo* on these tumour cells.

As these model systems are still based on the use of cell lines that have been cultured for several years and that can undergo irreversible genetic changes [71], generation of a patient-derived xenografted (PDX) mouse is a better alternative. In this model system, a part of the viable tumour from a cancer patient is directly implanted into the mice, which circumvent the generation of *in vitro* induced modifications. As establishment of neuroblastoma PDXs are challenging due to the sporadic access to fresh tumour material form this rare disease, Braekeveldt *and colleagues* [71-73] recently generated patient-derived orthotopic xenografts (PDOXs) by orthotopically implanting viably cryopreserved neuroblastoma samples. The tumours of these PDXs and PDOXs retain the characteristics of their corresponding patient tumour. From these PD(O)X-tumours, cell lines can be derived. These cells preserve the genotypic as well as the phenotypic features of the tumour they arise from and have tumour initiating and metastatic characteristics if re-injected in mice [71-73]. These mice and the derived cell lines are especially valuable to test therapeutic compounds in a patient-dependent manner [71-73]. Other well-established mouse models are the

transgenic mice (discussed above), which have the advantage that the gene is induced in immunocompetent mice, so the effect of the immune system can be monitored as well [68]. Additionally, their tumours have histologically and genetically the same characteristic as the human neuroblastoma cancers, in contrast to xenografts [68].

An overview of the different models of neuroblastoma disease can be found in table 2.

In vitro model systems	Transgenic mice	Zebrafish	Others
neuroblastoma cell lines	*Th-MYCN*	*Tg(dβh:EGFP-MYCN)*	Subcutaneously xenografted mice
JoMa-*ALK*^{F1174L}	*Th-ALK*^{F1174L}	*Tg(dβh:EGFP; dβh:ALK*^{F1174L}*)*	Orthotopically xenografted mice
JoMa-*MYCN*	*Th-ALK*^{F1174L}*/MYCN*	*Tg(dbh:LMO1),Tg(dbh:mCherry)*	PDX mice
Neural crest cells	LSL-*MYCN;Dbh-i*Cre		PDOX mice
PDX cell lines	LSL-*Lin28b;Dbh-i*Cre		Chick embryo

Table 2: overview of the model systems for neuroblastoma.
Different models for neuroblastoma disease exist. First, to evaluate effects *in vitro*, neuroblastoma cell lines, JoMa-*ALK*^{F1174L} or JoMa-*MYCN*, neural crest cells and PDX cell lines have been used. Secondly, different transgenic mouse models have been generated. Thirdly, in parallel, zebrafish lines have been created. Additionally, xenografted mice, PDX mice, PDOX mice and chick embryos have been generated to evaluate diverse aspects of neuroblastoma disease or the effect of gene manipulation on tumorigenesis.

1.4 RTKs in sympathetic nervous system development and neuroblastoma

1.4.1 The TRK neurotrophin receptors are associated with neuroblastoma prognosis

The Neurotrophin Tyrosine Receptor Kinases family, NTRK or TRK, consists of three homologous members, namely TRKA or NTRK1, TRKB or NTRK2 and TRKC or

NTRK3 [74,75]. These three receptors have a crucial role in the normal development of the peripheral nervous system as shown by knockout mice models. These model systems showed both unique and overlapping nervous system abnormalities, suggesting that the three receptors have redundant as well as unique functionalities [74,75]. Additionally, these mice models revealed that TRKA is the most important receptor involved in later stages of sympathetic neuron development, while TRKC is needed during the early stages of sympathetic and sensory neuron development and TRKB is more important for normal development of motor neurons [74-76]. Therefore, the TRK gene expression profile reflects the stage of neuronal differentiation of the sympathetic neurons [77].

Similar to other receptor tyrosine kinases, signal transduction starts with binding of the appropriate ligand to the receptor. The nerve growth factor (NGF) binds to TRKA, while brain-derived neurotrophic factor (BDNF) interacts with TRKB and neurotrophin-3 (NT3) with TRKC. Moreover, neurotrophin-4 (NT4) can bind as well to TRKB and NT3 can activate all three receptors [74,75]. Upon binding of the ligand, receptor homodimerization activates the receptor, leading to auto-phosphorylation as well as phosphorylation of other downstream effectors. In this way, the RAS-MAPK, PI_3K-AKT as well as the PLCγ1-PKC signaling pathways are activated, leading to proliferation, aggressiveness, metastases and neuronal differentiation, depending on which genes are activated and/or repressed by these activated signaling pathways [74,75].

These receptors have been shown to be constitutively activated through gene fusions or to be highly (over)-expressed in several cancers, including glioma, lung cancer, breast cancer and neuroblastoma. The gene fusions and (over)-expressions lead to more active receptors on the surface, highly activated pathways and induced gene expression. These gene expression changes result in malignant transformation, chemotaxis, metastasis and survival [77,78]. In neuroblastoma, the expression of these receptors has been associated with clinical outcome. TRKB is highly expressed together with his ligand BDNF in 36% of all neuroblastoma cases and 50-60% of the unfavourable high-risk group, more specific in those with *MYCN* amplification. The higher expression of the receptor leads to increased BNDF expression, resulting in further autocrine activation of the involved pathways [74-76]. Moreover, activation of this TRKB-BDNF pathway is associated with drug resistance, metastasis, angiogenesis and invasion. In contrast, high expression of TRKA and TRKC has been observed in

favourable neuroblastoma. Furthermore, TRKA expression is inversely associated with *MYCN* amplification status. Interestingly, TRK receptors have also been suggested to be involved in spontaneous regression frequently observed in stage 4S tumours. The TRKA and TRKC receptors are dependence receptors, meaning that in absence of their ligands, neuroblastoma cells undergo apoptosis, leading to spontaneous regression, while upon ligand activation, these cells will undergo neuronal differentiation, which is a feature of favourable neuroblastoma tumours [74,75,79]. However, no genomic rearrangements or mutations involving one of these receptors have been observed in neuroblastoma so far.

Given their important role in tumorigenesis, both small drug molecules as monoclonal antibodies and specific siRNAs targeting these TRKs have been developed and evaluated in several paediatric and adult cancer entities, including neuroblastoma [77,78]. Growth of neuroblastoma cells *in vitro* and *in vivo* was compromised by treatment with the pan-TRK inhibitor leslaurtinib in combination with or without chemotherapy [80]. In a later phase, this inhibitor was evaluated in a phase 1 clinical trial for refractory neuroblastoma, showing promising results, but clinical trials were stopped due to corporate takeover [80,81]. Additionally, other pan-TRK inhibitors, such as GNF-4256 [82] and AZ623 [78], were evaluated in neuroblastoma, both *in vitro* and *in vivo*, confirming the effective growth inhibition and the enhanced anti-tumour efficacy in combination with chemotherapeutics such as irinotecan, temozolomide or topotecan [78,80,82]. Moreover, combining AZ623 with topotecan resulted in nearly complete inhibition of tumour regrowth after discontinuation of the therapy [78]. Additionally, entrectinib, which is a second-generation pan-TRK inhibitor that also targets ALK and ROS, resulted in dose-dependent inhibition of TRK phosphorylation and growth in neuroblastoma cell lines and xenografts [80]. A more enhanced tumour inhibiting effect was observed in combination with the chemotherapeutics irinotecan and temozolomide [80].

1.4.2 The oncogene RET is involved in TRK-induced differentiation in neuroblastoma

Another receptor tyrosine kinase which is required for normal development, maturation and maintenance of different cell types, including neurons of both the central and the peripheral nervous system, is the REarranged during Transfection

(*RET*) proto-oncogene, located on chromosome 10q. The receptor is expressed during early embryogenesis in neural crest cells and is necessary for the migration of these cells to the developing enteric nervous system [83]. Once the cells reach their final destination, RET is needed for their proliferation, differentiation and survival. Moreover, the receptor is a guide for axon growth and is required for the survival of neurons of the adult brain and peripheral neurons of the sympathetic and parasympathetic nervous systems [83].

Similar to other receptor tyrosine kinases, RET signaling is activated by binding of his ligands, a group of soluble proteins of the glial cell line-derived neurotrophic factor (GDNF) family ligands (GFLs), namely GDNF, neurturin (NTRN), artemin (ARTN) and persephin (PSPN). However, in contrast to other RTKs, RET needs an additional co-receptor for this binding, one of the four GDNF family receptor-α (GFRα) family members, which are anchored in the cell membrane on the cell surface by a glycosylphosphatidylinositol binding [83]. GDNF, NRTN, ARTN and PSPN bind respectively to GFRα1, GFRα2, GFRα3 and GFRα4, providing selectivity and specificity for RET-activation complexes in different cells. Upon binding of one of these ligand–co-receptor complexes, RET will dimerize and auto-phosphorylate intracellular tyrosine residues, which will recruit adaptors and other signaling proteins leading to stimulation of the different downstream pathways, including STAT3, RAS-MAPK and PI_3K-AKT [83].

Due to its pivotal role in regulating several cellular processes, dysregulated expression of RET results in human diseases and cancers. Germline loss-of-function mutations lead to the congenital abnormality Hirschsprung disease or to congenital abnormalities of the kidney and urinary tract. Promoter methylation and heterozygous missense mutations, resulting in reduced RET expression, are frequently found in colon and colorectal cancer. However, in many other sporadic and heritable cancers, gain-of-function mutations and the formation of fusion proteins are most frequently found, further pointing at an important oncogenic role of RET [83]. Activation of RET results in cancer cell proliferation and survival, local and distant metastasis, increased tumour-associated inflammation and invasion [83]. Whereas no RET mutations have been observed in neuroblastoma tumours, RET has been found to play an important role in neuroblastoma tumorigenesis. Indeed, RET is highly expressed in neuroblastoma cells and constitutively active RET leads to enhanced tumour metastasis in neuroblastoma [84]. In addition, neuroblastoma tumours arise in

mice with transgenic *RET* overexpression [84]. Moreover, expression of activated RET suppresses cell growth, while inducing differentiation in the SK-N-BE neuroblastoma cell line [85]. Treatment of this cell line with retinoic acid (RA) further boosted the observed differentiation [85]. More importantly, it has been shown that RET cooperates with both TRKA [86] and TRKB [87] to regulate neuroblastoma differentiation. GDNF-mediated RET activation causes a G_0/G_1 cell cycle arrest in neuroblastoma cells and further boosts ciliary neurotrophic factor (CTNF)-induced TRKA expression. The cooperation between RET and TRKA results in a decrease in MYCN expression and enhances neuronal differentiation in several neuroblastoma cell lines, showing that the cross-talk is necessary to promote neuronal differentiation [86]. Interestingly, treatment with RA overexpresses and activates TRKB, which in his way phosphorylates and activates RET in a GDNF-independent manner, leading to differentiation of neuroblastoma cells. Moreover, both TRKB and RET activation are necessary for the differentiation caused by RA treatment [87].

Analogously to other RTKs, the RET receptor has an ATP-binding domain and can be targeted by several small molecule inhibitors that have been generated to block other RTKs, such as vandetanib, cabozantinib and sorafenib. Both vandetanib and cabozantinib have been approved for treatment of medullary thyroid carcinoma (MTC) and are in phase II clinical trial for NSCLC, while sorafenib is in clinical trials for thyroid cancer. Moreover, acquired resistance is also observed for these inhibitors, further emphasizing the need for combination therapy options [83]. In neuroblastoma, treatment with vandetanib causes dephosphorylation of RET and reduced cell viability *in vitro* and *in vivo*, while inducing apoptosis [84,88]. Moreover, Zage *and colleagues* [88] combined vandetanib with cis-retinoic acid (CRA). They observed that while CRA increases RET phosphorylation, this could be blocked by treatment with vandetanib. Furthermore, the combination resulted in a synergistic decrease in number of viable cells *in vitro* and in a synergistic inhibition of tumour growth *in vivo*, led to a potent anti-angiogenic effect and induced apoptosis in xenografts [88].

1.4.3 The ALK tyrosine kinase receptor in normal neuronal development and neuroblastoma

The Anaplastic Lymphoma Kinase (ALK) gene is located on human chromosome 2p23 and on mouse chromosome 17 [89]. It encodes for the receptor tyrosine kinase ALK, a member of the insulin receptor protein-tyrosine kinase superfamily and is most related to the leukocyte tyrosine kinase (LTK) [90]. The full-length receptor has the typical structure of an RTK, whereby it consists of a signal peptide, a long extracellular domain, a transmembrane segment and the intracellular part (Figure 6) [39]. The extracellular domain consists of two MAM segments, one low-density lipoprotein (LDL) domain and a glycine-rich part (GR), which is unique for both LTK and ALK [90]. Only the function of the MAM segments is known, as they are involved in cell-cell interactions. The intracellular part contains a juxtamembrane segment, a carboxy-terminal tail and the protein kinase domain, with the latter being important to modify other proteins by adding a phosphate group (= phosphorylation) to them. This domain consists of an amino-terminal lobe that is linked by a 'hinge' region to the carboxy-terminal lobe, creating a binding pocket for ATP, which is needed to phosphorylate its substrates [91] (Figure 2 for detailed structure). The molecular weight of ALK is 176 kDa, while as the result of N-linked glycosylation of the extracellular domain, the weight changes to 220 kDa [90]. Additionally, a 140 kDa form of ALK is formed due to cleavage within the extracellular domain of the full-length receptor. This isoform becomes phosphorylated as well upon ALK stimulation [92].

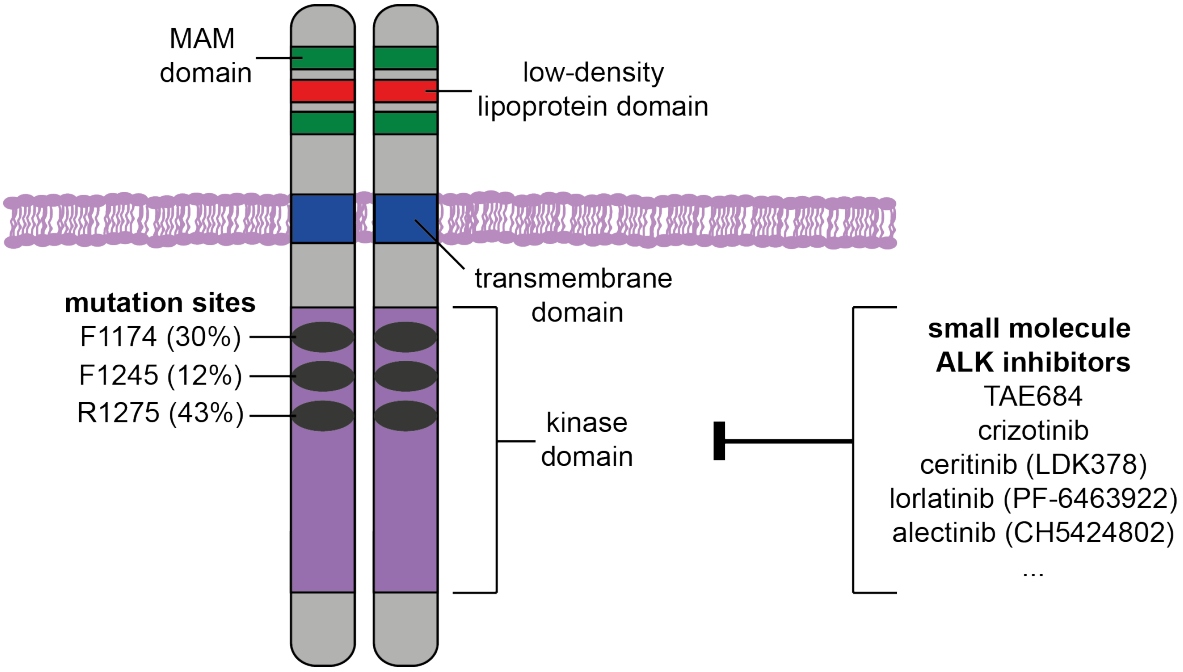

Figure 6: structure of the ALK receptor

A schematic representation of the ALK structure. The extracellular part consists of two MAM domains and a low-density lipoprotein (LDL) domain. The transmembrane domain passes through the cell membrane. The intracellular domain harbours the kinase domain. The hotspot mutations found in neuroblastoma are depicted. Several ALK inhibitors have been generated, targeting this kinase domain. Adapted from [39].

ALK is mainly expressed in the central and peripheral nervous system of developing mice [93,94], but mRNA and protein levels decrease soon after birth. In human, ALK has a role in the development of the nervous system, but is also expressed at low levels in the adult central nervous system, while it is undetectable in other human tissues [93,94]. Its expression pattern, together with its structure, supports the hypothesis that ALK may function as a receptor for ligands with a specific role in regulating the proliferation or differentiation of neural cells [94]. However, ALK has long been considered an orphan receptor, as identified ligands such as midkine and pleiotrophin could not be confirmed to activate ALK signaling [90]. Nevertheless, in 2015, heparin [95] was identified as an ALK modulatory ligand, while FAM150A or augmentor-β (AUG-β) and FAM150B or augmentor-α (AUG-α) [96,97] were discovered and confirmed as major ALK activating ligands, resolving the problem of unknown ligands for this receptor. As described for all RTKs, the ALK receptor can be phosphorylated at different tyrosines and can have numerous docking proteins. Consequently, these docking proteins can activate a large number of downstream

signaling pathways, which are often interconnected and overlapping [5,90]. As such, ALK activates the RAS-MAPK, PI_3K-AKT, JAK-STAT and the PLC-γ pathways [89,90]. Moreover, giving the important role of ALK in the development of the nervous systems, deregulated expression of ALK can result in the formation of neuroblastoma tumours, further described in the next chapter.

1.5 ALKoma: cancers with activated ALK

ALK was described for the first time as an oncogene in 1994. It was identified as fusion partner of nucleophosmin (NPM) in anaplastic large cell lymphoma (ALCL) [91,94]. Since then, diverse ALK fusion proteins as well as ALK activating mutations or alterations have been described in various cancer entities, called ALKoma, which include ALCL, NSCLC, rhabdomyosarcoma, renal cell carcinoma, inflammatory myofibroblastic tumour (IMT), inflammatory breast cancers and of particular interest, neuroblastoma [94,98].

1.5.1 ALK rearrangements and gene fusions

Chromosomal rearrangements leading to fusion genes are the most recurrent *ALK* alterations observed in cancer. These fusions comprise the 3' part of *ALK* and the 5' half of a different gene. In this way, the promoter of another gene is placed before the kinase domain of *ALK*. Around 30 different fusion partners have been identified, which can result in fusions with differential stability and a broad range of sensitivity to ALK inhibitors [91], including *NPM-ALK* in ALCL, *EML4-ALK* in NSCLC, *TPM3/4-ALK* in IMT and *VCL-ALK* in renal cell carcinoma [94]. Other *ALK* fusions have been found in diffuse, large B-cell lymphoma and thyroid tumours [98,99]. More intriguingly, both in neuroblastoma cell lines and tumours, ALK rearrangements have been found. While the intergenic rearrangements do not result in the formation of fusion proteins, as the genes involved are in opposite transcriptional directions, they can lead to truncated proteins (e.g. ALK^{del2-3}, $ALK^{del4-11}$ and $ALK^{del1-5)}$, which are phosphorylated and strongly active, resulting in increased downstream signaling and tumorigenicity [100-102].

1.5.2 ALK copy number alterations

In some cancer types, additional copies of the *ALK* locus or *ALK* amplifications have been observed [98]. Such alterations have been found in NSCLC, oesophageal cancer, colorectal cancer and breast cancer. However, in these entities, increased *ALK* copy numbers do not result in increased ALK mRNA or protein expression, while it is often correlated with poor prognosis and sensitivity to ALK inhibitors [98]. In contrast, *ALK* amplification in rhabdomyosarcoma and neuroblastoma does correlate with higher ALK mRNA and protein expression and poor prognosis [98]. Next to copy number alterations, wild type ALK can be overexpressed, as frequently observed in metastatic neuroblastoma and this overexpression is correlated with poor clinical outcome [99,103,104].

1.5.3 Activating ALK mutations

The most frequent genomic ALK aberrations found in neuroblastoma are point mutations. Also in lung cancer and anaplastic thyroid cancer, gain-of-function mutations have been reported [91,94,98]. In neuroblastoma, the mutations are located mainly in the kinase domain, with the hotspot mutations being F1174, R1275 and F1245 [91,98] (Figure 2 & 6) [39] and they can be grouped in 3 classes: ligand-independent activating mutations, ligand-dependent mutations and a kinase-dead mutation [105,106]. These mutations are observed in 8-10% of sporadic neuroblastoma tumours, while the ALK^{R1275Q} mutation is also frequently found in familial cases [29-32]. ALK^{F1174L} mutations have been shown to have a higher degree of ALK phosphorylation and a higher potential to drive tumorigenesis in neuroblastoma compared to the other hotspot mutation ALK^{R1275Q} [107].

Deep sequencing of neuroblastoma tumours at diagnosis revealed the presence of small ALK mutant subclones that could not be detected at normal sequencing depth and might lead to therapy resistance and relapse [108]. Indeed, other studies confirmed that relapsed neuroblastoma tumours and post-chemotherapy tumours more frequently present with *ALK* mutations, but also mutations in the RAS-MAPK and YAP pathway or EMT [55,56,109-111].

1.5.4 ALK as therapeutic target

The discovery of these ALK aberrations has opened new venues for therapeutic targeting of patients harbouring an ALKoma tumour. One of the first generated ALK inhibitors was TAE684, which is a small molecule inhibitor that binds in the ATP-binding pocket of ALK, thereby competing with ATP and inhibiting phosphorylation of ALK and its substrates [112]. This compound was first tested in NPM-ALK fusion positive ALCL [112], but also showed effect in neuroblastoma cell lines with ALK^{F1174L} or ALK^{R1275Q} mutations [32]. However, TAE684 was shown not to be clinically useful due to some toxic effects arising over time [113]. Another compound with more clinical potential is crizotinib, which like TAE684 binds the ATP-binding pocket of ALK. This compound has been tested in several clinical trials, where it has shown promising effects for diverse ALKoma tumours, including neuroblastoma [114]. Importantly, it has been shown that the ALK inhibitors have different effects on the different ALK mutations [113,115-117]. For example, tumour cells with ALK^{F1174L} mutation are resistant to crizotinib. This can be explained by an increased ATP-binding affinity of this mutation, which reduces the potency of ATP-competitive inhibitors [115-119]. Moreover, not only the mutations status, but also the expression levels of ALK mRNA and protein determine how the response on the inhibitor will be, as shown by Duijkers *and colleagues* [120].

As seen for multiple small molecule inhibitors, cells rapidly acquire resistance to compounds upon an initial promising response of the tumour. This can be due to diverse mechanisms, ranging from activation of bypass signaling or the development of resistance mutations in the tyrosine kinase domain of the ALK receptor [20,119,121-124]. These mutations hinder the binding of the compound to the ATP-binding pocket of the receptor or they increase the affinity of this binding place for ATP [20,119,121]. Therefore, second- and third-generation ALK inhibitors have been developed, including alectinib, ceritinib (LDK-378) and lorlatinib (PF-06463922), which are currently evaluated in paediatric clinical trials [109,122]. Alectinib has been shown to effectively inhibit cell growth and colony formation, while inducing apoptosis by blocking the PI_3K/AKT/mTOR pathway in neuroblastoma cells with different ALK mutation status, in neuroblastoma xenografts and the *Th-MYCN* transgenic neuroblastoma mice model [125]. Moreover, in NSCLC, it has been shown that ceritinib

can overcome crizotinib resistance [126,127], while in neuroblastoma the same has been shown for lorlatinib [128].

In addition, other options to target ALK and circumvent the resistance have been developed, including antagonistic ALK monoclonal antibodies [129]. Moreover, HSP90 inhibitors [24,25] might be useful to target ALK^{F1274L} mutant neuroblastoma tumours that have become resistant to ALK inhibitors. These tumours present AXL activation and induction of EMT, which make these cells more sensitive to HSP90 inhibitors [130]. Last but not least, ALK-positive tumours can also be targeted by blocking the signaling pathways downstream of ALK, like PI_3K inhibitors [131].

However, in most single compound treatment regiments, resistance and subsequent relapse frequently occur. There is thus an urgent need for new therapy regimens, where different compounds are combined to attack the signaling pathways from different angles, avoiding escape mechanisms.

A first way of targeting the ALK pathway from different angles, is by combining an ALK inhibitor, which inhibits the ALK protein and his activity, with siRNA-mediated knockdown of *ALK* mRNA in neuroblastoma. These siRNAs were packed in liposomes and they specifically targeted neuroblastoma cells, in this way diminishing side-effects. Indeed, this combination enhanced the anti-tumorigenic potential of the single compounds [132]. Additionally, combining an ALK inhibitor, such as crizotinib, with an ALK inhibitory antibody, results in almost complete growth inhibition in neuroblastoma cells [133]. Crizotinib induces accumulation of ALK at the cell surface, in this way sensitizing the neuroblastoma cells for ALK antibody treatment [133]. Moreover, ALK antibody treatment can restore crizotinib resistance as well [133]. Interestingly, another study has shown that blocking PI_3K pathway components restored the sensitivity of the neuroblastoma cells for TAE684 treatment, resulting in synergistic inhibition of proliferation by combining an PI_3K inhibitor with an ALK inhibitor [131]. Moreover, in $MYCN^{amplified}$ and ALK^{mutant} neuroblastoma cells, the use of the ALK inhibitor crizotinib alone does not inactivate mTORC1 [134]. In order to shutdown mTORC1 signaling, crizotinib has been combined with a mTOR inhibitor, showing reduced tumour growth and prolonged survival in ALK^{F1174L}/*MYCN*-positive models compared to single treatment [134]. Recently, it has been observed that ALK inhibition in combination with the chemotherapeutics topotecan and cyclophosphamide enhanced survival by reducing tumour growth in *TP53* wild type neuroblastoma cells, xenografts and PDX models with both sensitive *ALK* mutations

as *de novo*-resistant *ALK* aberrations [135]. Furthermore, using an ALK inhibitor in combination with a dual inhibitor of cyclin-dependent kinase (CDK) 4 and 6 synergistically decreased pALK and pRB levels in neuroblastoma cells, while promoting cell-cycle arrest *in vitro* [136]. Moreover, this synergistic combination showed complete and sustained tumour regression in two PDX neuroblastoma models, harbouring ALK^{F1174L} and ALK^{F1245C} as *de novo* crizotinib resistance mutations [136]. Similarly, the combination of an ALK inhibitor with a MDM2 inhibitor synergistically increased anti-tumour activity in *ALK* mutant, *TP53* wild type neuroblastoma cells and xenografts by inducing antiproliferative and pro-apoptotic proteins [124]. Interestingly, the MDM2 inhibitor restored the sensitivity to the ALK inhibitor by downregulating MYCN, which was identified as driving resistance in a subset of neuroblastoma cells and xenografts [124].

1.6 ALK and MYCN cooperate to control tumorigenesis

Intriguingly, a subset of neuroblastoma patients has both an ALK^{F1174L} mutation and *MYCN* amplification, leading to worse prognosis compared to tumours with only one of these alterations [89,107], suggesting that a cooperative mechanism is involved. This cooperative effect was confirmed in both mice and zebrafish neuroblastoma models [58,60]. The zebrafish harbouring both activated ALK and MYCN show accelerated onset of tumour formation and increased tumour penetrance [60]. Furthermore, ALK expression enhanced the MYCN oncogenic activity by blocking the MYCN-induced apoptotic death [60]. Also in the mice model [58], it was confirmed that combined expression results in higher tumour penetrance as well as earlier time of onset. Additionally, these mice had a decreased survival probability compared to mice with expression of only one of the oncogenes [58]. In these double transgenic mice, genes involved in the PI_3K-AKT and MAPK pathways were upregulated compared to MYCN-only mice [58]. Moreover, it was recently shown that the cooperation between MYCN and ALK leads to proliferation and survival of neuroblasts, which may represent initial steps toward neuroblastoma development [137].

Until now, 3 mechanisms have been described in literature, explaining the observed cooperativity between MYCN and ALK (Figure 7) [58,138-143]. Firstly, ALK activates the PI_3K-AKT pathway, which will phosphorylate and inactivate GSK3β [141].

Consequently, GSK3β can no longer phosphorylate MYCN, which is needed for poly-ubiquitination and subsequent proteasomal degradation [141,144]. In this way, the MYCN protein stability is enhanced by mutant ALK^{F1174L} [58]. Additionally, mutant ALK^{F1174L} increases *MYCN* mRNA levels through increased initiation of transcription of the promoter upstream of the *MYCN* gene, driven by ALK-mediated ERK activity [138]. Likewise, stimulated ALK phosphorylates and activates ERK5 through the PI_3K-AKT-MEKK3-MEK5 pathway and ERK5 will on his turn increase transcriptional initiation of *MYCN* [139]. Furthermore, the ERK5 inhibitor XMD8-92 leads to a decrease in MYCN levels and a simultaneous reduction in cell viability, while combination with an ALK inhibitor further boosts these effects leading to a synergistic decline in MYCN abundance and cell survival *in vitro* and *in vivo* [139]. Additionally, MYCN can activate apoptosis through downregulation of anti-apoptotic proteins [58,60,145]. Moreover, a positive feedback loop has been found, as MYCN itself also directly regulates *ALK* mRNA expression by binding to the *ALK* promoter as shown by ChIP assays with anti-MYCN antibodies [142].

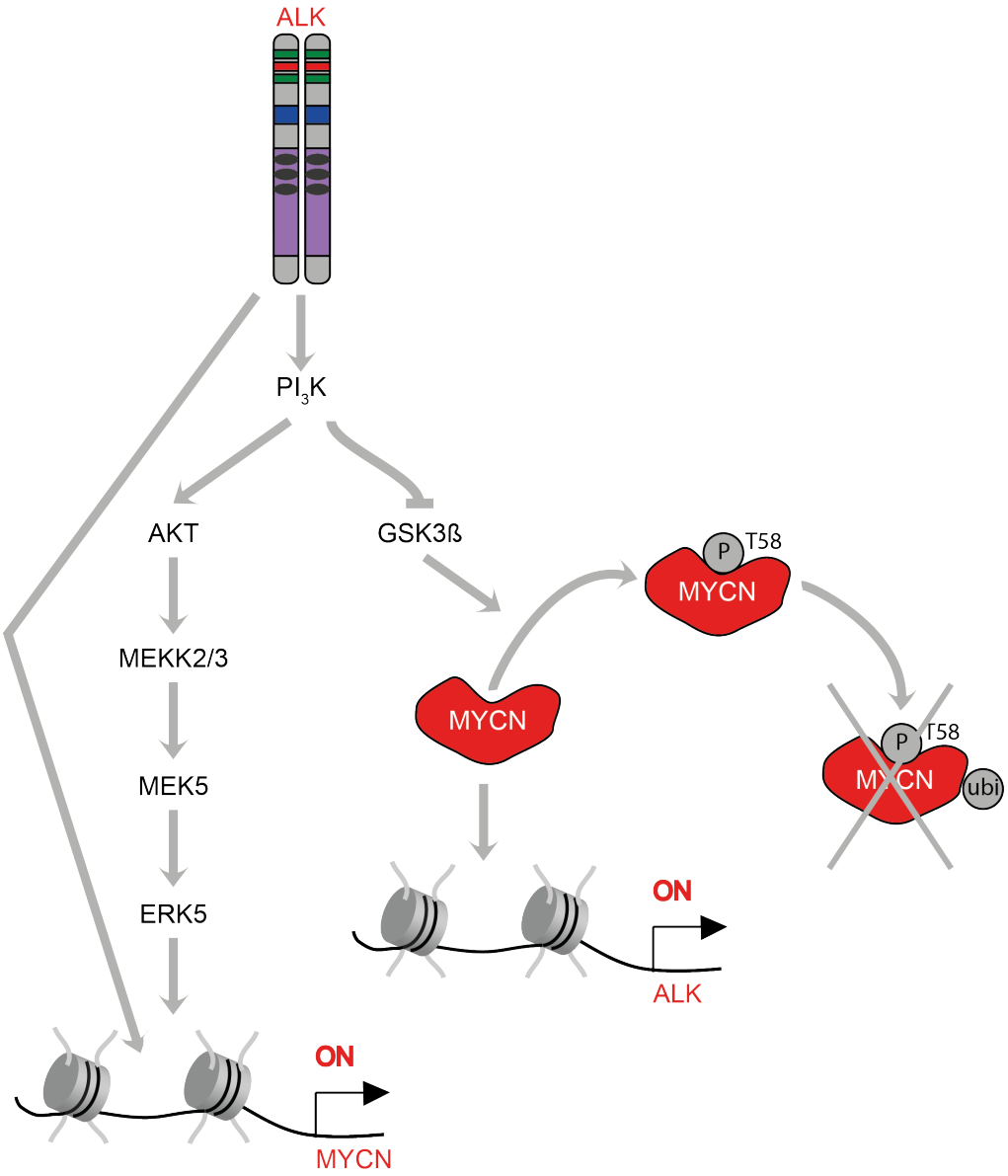

Figure 7: cooperation between ALK and MYCN in neuroblastoma

Different mechanisms are found for the ALK and MYCN cooperativity in neuroblastoma. Firstly, ALK induces *MYCN* mRNA levels by increased transcriptional initiation of the *MYCN* gene. Secondly, ALK enhances MYCN protein levels through the PI_3K-AKT-GSK3β pathway. Thirdly, *MYCN* transcription is further boosted by the PI_3K-AKT-MEKK3-MEK5-ERK5 pathway. Moreover, MYCN itself enhances *ALK* transcription, creating a positive feedback loop. Based on [58,138-143].

1.7 MYCN as oncogenic driver of neuroblastoma

1.7.1 The role of MYC family members in normal development and cancer

The *MYCN* gene is located on the short arm of chromosome 2 at band p24 [145,146] and is part of the MYC family of proto-oncogenes, which further also includes c-MYC and L-MYC. These MYC proteins belong to the basic-helix-loop-helix-zipper (bHLH-Zip) class of transcription factors and regulate the expression of genes involved in several cellular processes, including proliferation, differentiation, growth and apoptosis [145,146]. Structurally, the *MYCN* gene encodes for a nuclear protein with a size of 64 kDa. MYCN consists of an N-terminal transcriptional domain for interaction with co-activators or co-repressors, containing the MYC boxes and a nuclear localization sequence, and a C-terminal DNA-binding domain with the bHLH-Zip motif, required for dimerization with MAX and for interaction with DNA [146-148]. There is a high sequence as well a structural homology between MYCN and c-MYC, but their expression pattern is different [145,146]. While expression of c-MYC is generally high in most rapidly proliferating cells, MYCN is expressed following a restricted temporal, tissue-specific pattern. During embryogenesis, the highest expression of MYCN is observed in developing brains, while it is not expressed in adults [145,146]. Of interest, MYCN is expressed in the developing sympathetic nervous system [145,146] and required for proliferation of immature neuronal precursor cells in the neural crest [146].

1.7.2 Regulatory mechanisms for MYCN expression, protein stability and activity

MYCN is involved in several key cellular processes with its expression being tightly controlled through different mechanisms [146]. A first level of regulation is by controlling MYCN protein stabilization and degradation (Figure 8) [141,145,146,149-151]. MYCN proteins are stabilized by phosphorylation of a serine (S62) by CK1 or MAPK, followed by a phosphorylation of a threonine (T58) by GSK3β [141,146]. In order to target MYCN for protein degradation, the protein phosphatase 2A (PP2A) dephosphorylates the S62, which allows that F-box and WD repeat domain-containing 7 (FBXW7) or other ligases can bind this MYCN harbouring only the T58 phosphorylation [145,146]. Next, FBXW7 ubiquitinylates MYCN, thereby targeting it for proteasomal degradation

via the ubiquitin-proteasome system. Normally, GSK3β is repressed by AKT, so activation of the PI_3K-AKT pathway results in MYCN protein stabilization. Moreover, the ERK pathway is involved as well in regulation of protein levels, as it can either stabilize or destabilize MYCN proteins by phosphorylation of serine 62 or threonine 58 through the ERK pathway respectively [149]. Additionally, *ZAR1*, a possible transcriptional regulator, is involved in regulating MYCN protein levels, as *ZAR1* knockdown result in differentiation through loss of MYCN protein, but the exact mechanism of this regulation is still unknown [152]. Moreover, the *MYCNOS* gene has a dual role in regulating MYCN. First of all, it encodes for a protein, also named NCYM, which is always co-amplified with MYCN and interacts with GSK3β, thereby stabilizing MYCN protein without effect on *MYCN* mRNA levels [150,151]. Furthermore, NCYM and MYCN enhances each other's protein expression [150,151]. Secondly, *MYCNOS* also functions as a lncRNA by recruiting protein complexes to the upstream *MYCN* promoter instead of to its internal promoter, leading to a switch in *MYCN* isoform transcription [151]. Another lncRNA, *LncUSMycN* is frequently co-amplified with MYCN and located upstream of the *MYCN* transcription start site. Reduction of this lncRNA results in downregulation of MYCN mRNA and protein levels by interacting with NonO, a RNA binding protein that binds *MYCN* [153,154]. Aurora kinase A (AURKA) provides an additional level of MYCN regulation, by preventing the FBXW7-mediated MYCN protein degradation [145,146]. However, dephosphorylation of AURKA by protein tyrosine phosphatase receptor type D (PTPRD) destabilizes AURKA, leading to subsequently degradation of MYCN [145,146]. Furthermore, interaction of MYC(N) with MIZ-1 enhances MYC(N) stabilization by inhibiting its ubiquitination and degradation [148].

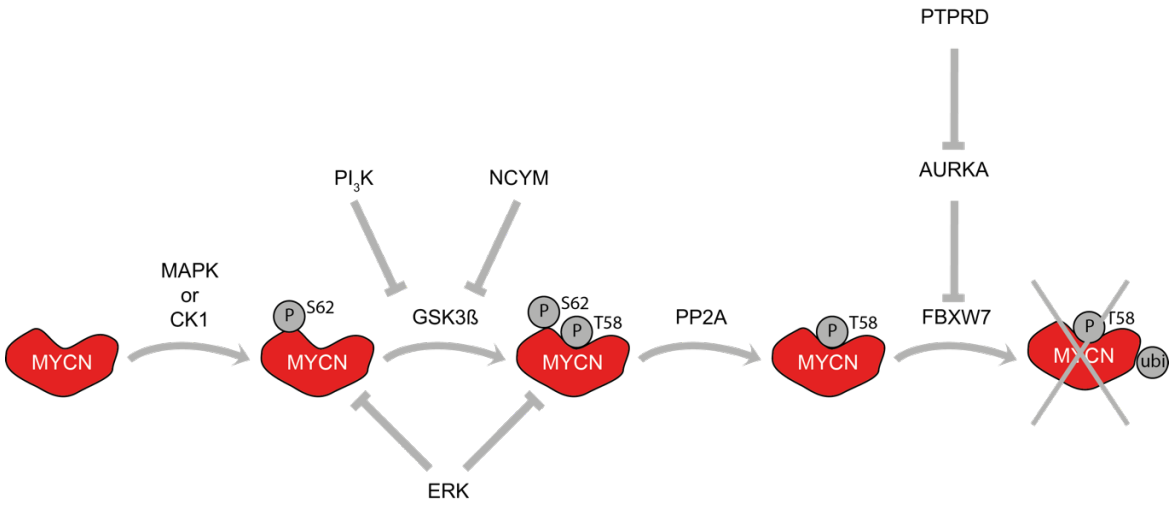

Figure 8: regulation of MYCN protein levels

Different mechanisms regulate MYCN protein levels. CK1 or MAPK phosphorylates a serine in the MYCN protein (S62), followed by phosphorylation of a threonine (T58) by GSK3β. Protein phosphatase 2A (PP2A) dephosphorylates the S62, which allows that F-box and WD repeat domain-containing 7 (FBXW7) or other ligases can ubiquitinylate MYCN harbouring only the T58 phosphorylation, thereby targeting it for proteasomal degradation via the ubiquitin-proteasome system. GSK3β is repressed by AKT, while the ERK pathway can phosphorylate serine 62 or threonine 58. The MYCNOS protein, also named NCYM interacts with GSK3β. Based on [117,121,122,125-12].

Another mechanism of controlling MYCN expression is through transcriptional regulation. ALK itself as well as through ERK5, a member of the MAPK pathway, increases *MYCN* transcription initiation [138,139]. Moreover, the Wnt/β-catenin pathway enhances the transcription factor Tcf-4 to bind to tissue-specific enchancers upstream of the *MYC(N)* gene in order to promote *MYC(N)* transcription [149]. Additionally, it has been shown that microRNAs (miRNAs), like miR-34a or let-7 family members, can bind to the 3'UTR of *MYCN*, leading to mRNA degradation [146,155]. Recently, our group has identified 29 miRNAs targeting the 3'UTR of *MYCN*, of which 12 miRNAs are inversely correlated with MYCN expression or activity in neuroblastoma [156]. Furthermore, 10 of these miRNAs are downregulated during mouse MYCN-driven neuroblastoma tumour formation, suggesting that MYCN negatively controls the expression of these miRNAs to safeguard his own expression [156]. Moreover, another neuroblastoma oncogene, LIN28B, regulates MYCN expression through downregulation of let-7 [35,47].

1.7.3 MYC(N) acts as transcriptional activator and repressor

Despite the high structural and sequence homology and the functional redundancy of c-MYC and MYCN, they exert independent and tissue-specific functions through their regulation of different target genes [146,157]. High expression of MYCN results in manipulation of the expression of genes regulating apoptosis, cell differentiation cell-cycle and proliferation [146,148]. To modulate the expression of these genes, MYCN uses a number of strategies. One of these approaches is by heterodimerization with MAX through the bHLH-Zip domains of both proteins, forming a functional transcriptional activator [146]. This stable complex binds to specific DNA sequences, known as E-boxes, and is essential for stimulation of transcription at these E-boxes proximal of promoters of genes involved in diverse cellular processes [146-148]. MYCN normally binds to the canonical CACGTG as well as the E-box CATGTG, while when amplified, it recognizes additional E-box motifs, like CATTTG, CATCTG and CAACTG [146]. Moreover, MYCN can bind to the nuclear co-factor TRRAP, which is part of a complex involving histone acetyl transferases (HATs), which are responsible for acetylating the histones around promoters, resulting in an open chromatin structure so that transcription can be enhanced [148,158]. Furthermore, MYCN recruits pTEF-β, which induces phosphorylation of the RNA polymerase C-terminal domain, in this way enhancing transcriptional elongation [148]. Next to transcriptional activation, MYCN also transcriptionally represses the expression of genes, independent from recognition of E-box places. Therefore, MYCN recruits through his bHLH-Zip domain the transcriptional activator Myc-interacting zinc finger protein 1 or Miz-1 to the promoters of these genes to form together a repressive complex, which leads to transcriptional silencing partly through recruitment of DNA methyltransferases, like DNMT3a or EZH2, as well as histone deacetylases (HDACs) [146,148,157,159-161]. Similarly, MYCN can interact via its MB2 domain with the basal transcription factor 1 (SP1) and can in this way recruit HDACs, including HDAC1, HDAC2, HDAC3 and SIRT1 [148]. More intriguingly, MYCN directly interacts with both Miz-1 and SP1 to recruit HDAC1 to silence expression of amongst others TRKA [162]. Additionally, MYCN indirectly modulates expression by protein-protein interactions. In this way, it upregulates AURKA, thereby creating a positive feedback loop [146]. Moreover, MYCN not only directly activates or represses the transcription of genes, but also indirectly influences the expression of multiple genes by modulating the expression of several

miRNAs, including miR-17~92 [146,155,163,164] and lncRNAs [146]. Furthermore, as mentioned earlier, MYCN downregulates the expression of 10 miRNAs, that are themselves negative regulators of MYCN, to safeguard his own expression [156]. Additionally, MYCN enhances the expression of LIN28B by two mechanisms [165]. Firstly, it directly interacts with the promoter of *LIN28B* to promote its transcription. Secondly, MYCN indirectly represses miR-26a-5p, which is a negative regulator of LIN28B, in this way creating a double regulatory feed-forward loop as LIN28B enhances MYCN by repressing let-7 family members [35,47,165]. Recently, it has been discovered that *MYCN* mRNA itself sponges the *let-7* family in *MYCN*^{amplified} neuroblastoma tumours to hinder the activity of these miRNAs [48]. In summary, MYCN is a transcriptional activator and repressor of several genes implicated in normal development.

1.7.4 MYCN acts as oncogene in neuroblastoma and other cancers

As MYCN regulates the expression of a large number of genes involved in key cellular processes including positive regulation of the cell cycle, it is not surprising that MYCN overexpression results in cancer formation [148]. MYCN overexpression has been reported predominantly in tumours originating from neuronal or neuroendocrine origin including neuroblastoma, medulloblastoma, glioblastoma multiforme, small-cell lung cancer, neuroendocrine/small-cell prostate cancer and retinoblastoma as well as rhabdomyosarcoma and breast cancer [146].

In neuroblastoma, MYCN is an independent prognostic factor and is involved in almost every cancer hallmark as described by Huang and Weiss (Figure 9) [145]. First of all, *MYCN* expression levels correlate with invasive and metastatic behaviour [145]. MYCN is involved in every step of metastasis: adhesion, motility and invasion, by direct or indirect repression of specific genes. To achieve this, MYCN downregulates amongst others integrins, caveolin-1 and a specific subset of ABC transporters controlling cell motility and invasion, while increasing other factors like miRNAs and matrix metalloproteinase activity, which finally leads to detachment from the extracellular matrix in order to allow the cells to migrate and invade other tissues [145,148]. Secondly, MYCN also modulates antigens expressed on the tumour cells in order to mislead our immune system [145]. Thirdly, anti-angiogenic factors are transcriptionally repressed, while pro-angiogenic factors become upregulated

following MYCN amplification or overexpression [145,148]. Additionally, MYCN promotes self-renewal and pluripotency, while blocking differentiation, which are stem cell characteristics [145]. MYCN is able to form several complexes which regulate both directly and indirectly the expression of genes involved in neuronal differentiation, including downregulation of the TRKA receptor [148,162]. Furthermore, MYCN can repress apoptosis by inhibiting several pro-apoptotic genes, including nerve growth factor receptor (NGFR), while it can activate as well apoptosis due downregulation of anti-apoptotic proteins, such as Galectin-3 [145,148]. This MYCN-induced apoptotic response can turn into a complete proliferative response, especially if the anti-apoptotic factors are also upregulated by other mechanisms like the acquisition of an ALK mutation [58,60,145]. Additionally, MYCN promotes cell cycle progression and proliferation, as it enhances the re-entry of quiescent cells into the cell cycle and shortens the time needed to progress through the cell cycle by up- or downregulation of the expression of several cell cycle-related genes [145,148]. Recently, it has been shown that c-MYC is involved as well in neuroblastoma by driving the expression of an ESC-like cancer-activated signature in the high-risk tumours, which are characterized by poor prognosis [166].

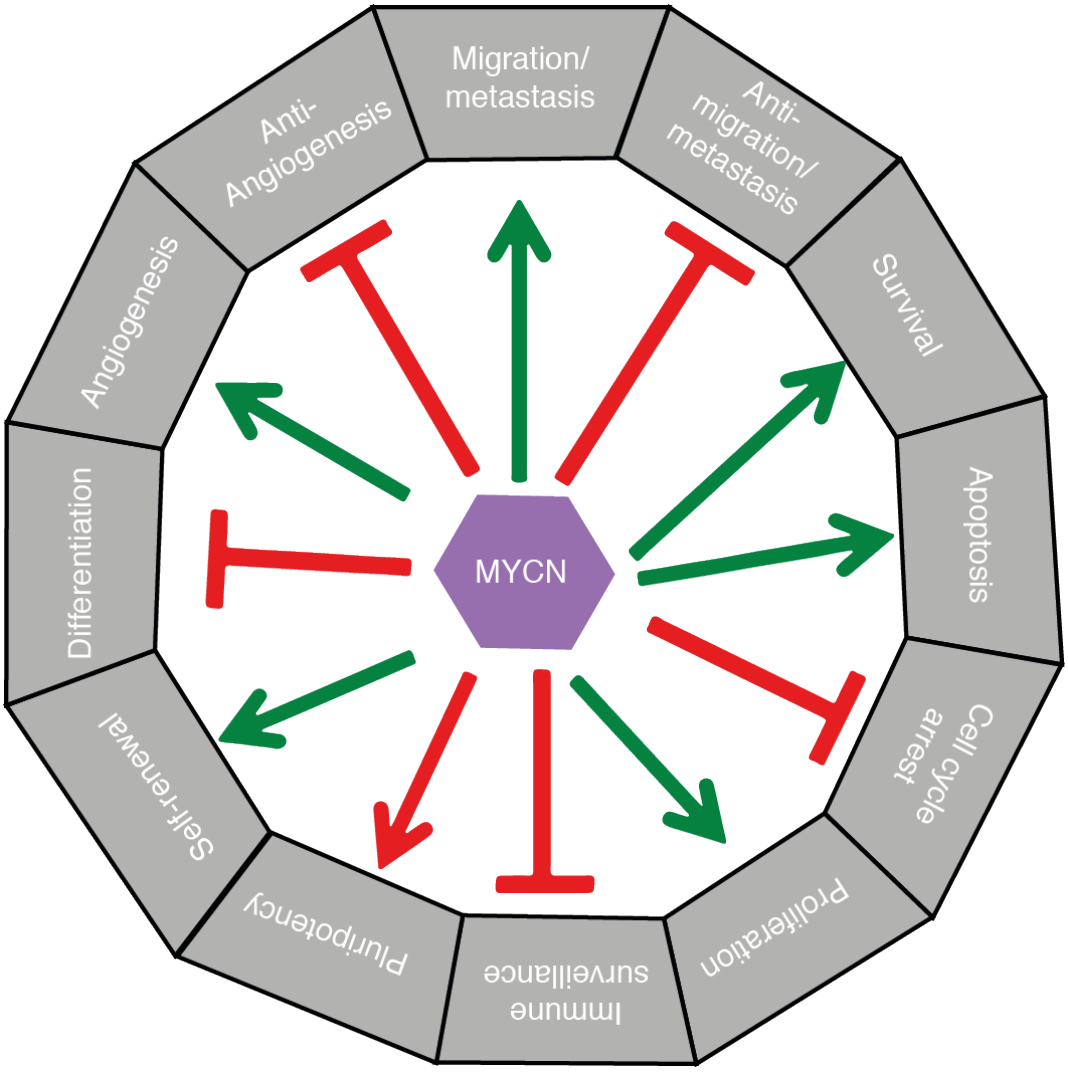

Figure 9: MYCN is involved in every cancer hallmark

MYCN has an important role in cancer, since it is involved in every cancer hallmark. Firstly, MYCN activates transcription of genes involved in metastasis, survival, proliferation, pluripotency, self-renewal and angiogenesis. Secondly, MYCN represses genes promoting differentiation, cell cycle arrest and immune surveillance, and blocks the transcription of genes that inhibit metastasis and angiogenesis. Figure adapted from [145].

1.7.5 Therapeutic targeting of MYC(N)

Considering the important role of MYCN in several tumour-driven cellular pathways, targeting MYCN has long been proposed as a valid therapeutic option for several tumour entities harbouring *MYCN* overexpression or amplification, amongst others *MYCN*-driven neuroblastoma [145,146]. However, as MYCN is a transcription factor and structurally consists of α-helices without a binding place for ligands and thus for small

molecule inhibitors, it has long been considered to be undruggable [145,146]. Moreover, MYCN is mainly localized in the nucleus, making it inaccessible for antibody-based compounds [149,158]. Therefore, several approaches have been developed to indirectly target MYCN. As MYC and MYCN are closely related, a lot of studies focusing on targeting MYC can be extrapolated to MYCN therapy.

A first strategy could be by hindering the interaction between MYCN and MAX by using small molecules like 10058-F4 and KJ-Pyr9 [149,158] or by Omomyc, which is a dominant-negative MYC mutant and as a result of binding to MYC(N) impairs the dimerization with MAX [146,158,167]. However, these small molecules are non-specific as several proteins contain the bHLH-Zip domain that they target and Omomyc is ineffective as it is unable to penetrate human tumours [158]. Another strategy that has been developed, acts through targeting MYCN through its coactivator proteins, required for transcriptional initiation and elongation driven by MYCN [149]. One such approach is based on displacement of BET bromodomains from chromatin by competitively binding of the compound with the acetyl lysines in histone tails [145,146,167-169]. BRD4 contains BET bromodomains and has been shown to bind to the promoter of *MYCN* as well as to several MYCN target genes to promote active transcription of these genes. JQ1 is the first reported BET bromodomain inhibitor, which represses transcription of *MYCN* and MYCN targets, followed by cell cycle arrest and apoptosis in mainly *MYCN*^{amplified} neuroblastoma cell lines [168]. Moreover, treatment of *MYCN*^{amplified} neuroblastoma mouse models with JQ1 resulted in a prolonged overall survival [168]. Furthermore, dBET1, a novel compound that targets BRD4 for protein degradation, also strongly affects the MYC proteins and their targets [158]. Similarly, MYC proteins interact with TRRAP, which is part of a complex with HATs, to open chromatin and enhance transcription [149]. Therefore, HAT inhibitors may also be considered for therapeutic targeting of MYCN activity [149]. Furthermore, giving the predisposition of the MYC locus for the formation of G-quadruplexes, small molecules stabilizing these complexes have been shown to have MYC-specific effects [149]. However, MYCN not only activates genes, but also silences tumour suppressor genes by recruiting DNA methyltransferases and by elevating HDAC expression. This opens the way to use HDAC inhibitors to indirectly target MYCN activity [145]. As shown by Cortés *and colleagues* [170], the HDAC inhibitor SAHA decreased MYCN mRNA and protein levels, while simultaneously decreasing cell viability in neuroblastoma cell lines with or without MYCN amplification. However, such

epigenetic-based compounds are often non-specific, targeting multiple genes and proteins at the same moment [171]. Therefore, another method to destabilize MYCN is by targeting genes involved in MYCN degradation [145,146,167]. As mentioned above, AURKA is needed to protect MYCN from degradation [145,146]. AURKA inhibitors hinder the interaction between MYCN and AURKA by inducing a conformational change in the kinase domain of the latter, thereby making MYCN available for degradation while simultaneously decreasing cell viability in neuroblastoma cells [145,146,167]. Another kind of inhibitors influencing MYCN degradation, are those inhibiting proteins from the PI_3K-AKT pathway, which through GSK3β play an important role in MYCN stabilization, while via ERK5 this pathway has an impact on *MYCN* transcription initiation [139]. Therefore, several PI_3K-AKT, mTOR, ERK5 or GSK3β inhibitors have been evaluated and showed potential as therapeutic interventions for MYCN-driven tumours, including neuroblastoma [139-141,143,145,146,167,172,173]. Moreover, ROCK inhibitors have shown to inhibit GSK3β-dependent MYCN phosphorylation, resulting in differentiation of the neuroblastoma cells and a reduction in cell growth, migration and invasion [54]. However, NCYM expression makes cell lines and tumours less sensitive to the PI_3K-AKT inhibitors [150]. Nevertheless, combination of an ERK5 inhibitor with an ALK inhibitor synergistically reduced MYCN levels, cell viability *in vitro* and tumour growth *in vivo* [139]. Furthermore, GSK3β inhibitors not only effect MYCN protein stabilization, but have as well an effect on *MYCN* mRNA stability, probably by transcriptional regulation of miRNAs of other MYCN repressing genes [173]. Moreover, the MAPK pathway is involved as well in regulating MYCN protein stability, so inhibitors targeting this signaling network are another opportunity for MYCN targeting [149]. More intriguingly, MDM2 repression showed significant effect on $MYCN^{amplified}$ neuroblastoma [145]. The working mechanism of this inhibition consists of two parts. First of all, MDM2 loss destabilizes *MYCN* mRNA, while in parallel blocking MYCN protein expression. Secondly, MDM2 blockade stabilizes p53, which results in p53-dependent apoptosis. Another approach is by using compounds targeting the expression or function of MYCN [145,167]. THZ1 and THZ2 are CDK7 inhibitors that downregulate MYCN in *MYCN*-driven neuroblastoma, an effect which is attributed by the presence of super-enhancers upstream of *MYCN* [174]. Furthermore, inhibitors of the Wnt/β-catenin pathway will block the binding of Tcf-4 to enhancers upstream of *MYC*, which will result in less *MYC* transcription [149]. Moreover, retinoic acids induce

differentiation, so counteracting the differentiation block by MYCN, and reduce as well *MYCN* levels. A final approach is based on the observation that MYC-dependent cancer cells are addicted to the MYC oncogene [149,158]. In this way, it has been observed that small molecules against the Aurora kinase B (AURKB) and Cdk-1 kinases have antiproliferative effects in MYC-addicted cancers [149]. Moreover, it has been shown that compounds against the AMP-dependent kinase (AMPK) protein, spliceosome core factors or metabolic pathways are effective in MYC-overexpressing cells [158]. Furthermore, cells depending on high MYC expression for their survival were sensitive to the multikinase inhibitor, dasatinib [158]. However, until now, there are no small molecule inhibitors available that directly target the MYCN protein, but diverse strategies are generated to target its transcription, stabilization or activity.

1.8 The discovery of HBP1 and its proposed role as tumour suppressor

1.8.1 Interaction partners of the HBP1 transcription factor

The High-Mobility Group (HMG)-box protein 1 or *HBP1* gene was discovered in 1994 through a screen for new mammalian potassium channels in yeast [175]. Subsequent analysis of the gene revealed a HMG-box DNA-binding domain and thus assigned HBP1 to the transcription factor family of HMG proteins [175]. These transcription factors have a role in the assembly of multifactor transcriptional complexes, ensuring correct enhancer specificity [176].

Transcriptional regulation by HBP1 acts through two mechanisms, namely by direct binding to the promoter of its target or by physical inhibitory interaction with transcriptional activators [177] through its HMG-box DNA-binding domain as well as its AXH transcriptional repression domain [178]. Furthermore, this AXH domain is needed to form a repression complex with SIN3 and HDACs through PAH2 domains [163,179]. In addition, HBP1 has also two RB1 and one p38 binding site [176,180,181]. By associating with RB1, HBP1 can recruit as well HDAC1 to repress various target genes. Intriguingly, HBP1 has also a role in DNA methylation, as it inhibits DNMT1, leading

to a gene-specific as well as global DNA hypomethylation pattern in lung fibroblast cells [182]. Moreover, through activation of the Histone $H1^0$ gene, HBP1 may play a role in remodelling of chromatin [181].

1.8.2 The role of HBP1 in controlling proliferation and differentiation during normal development

HBP1 has been defined as transcriptional repressor as well as cell cycle regulator involved in control of proliferation and differentiation [175,176,180,181,183-185].

As indicated above, the HBP1 protein harbours two binding sites allowing interaction with the so-called pocket proteins RB1 and p130 [176,180]. These proteins suppress cell growth by negatively regulating the G_1/S transition by controlling the activity of several cell cycle involved transcription factors including the E2F family, thus inducing a G_1 phase cell cycle arrest as a critical step during differentiation [175,176]. In addition, the p38 MAPK signaling cascade induces G1 arrest by extending the protein stability of HBP1 through binding and phosphorylation [181], further suggesting a role of HBP1 in cell cycle regulation and differentiation. Indeed, HBP1 is responsible for cell cycle progression regulation during normal development of different cell types and tissues [175,176,183,185]. In the liver, expression of *HBP1* in differentiating cells results in a significant delay in S phase, caused by a prolonged G1 progression, which has been supported by the extended immediate-early response and delayed cyclin E expression [185]. Moreover, *HBP1* mRNA expression was highly increased during differentiation of both adipocytes and myogenic cells [175]. Additionally, in C2 muscle cells, overexpression of HBP1 results in a reduction in number of cells in the S-phase, suggesting cell cycle arrest [176]. Furthermore, in skin keratinocytes, HBP1 is repressed by p63, a homologue of the DNA-damage response regulator p53, to promote growth of the lower layers of the epidermis, while it is activated in differentiating skin keratinocytes in order to further boost their differentiation, showing that HBP1 has a key role in the stratification of the human skin [183].

In summary, HBP1 is important in driving differentiation of most cell types through controlling cell cycle progression and cell proliferation. This effect is partly mediated

by the repression of c-MYC and MYCN, two genes involved in proliferation and whose expression levels decrease during differentiation [176]. The regulation of the c-MYC gene by HBP1 is dual (Figure 10) [176,184] : first, through interaction with the β-catenin/TCF complex, the transcription of *c-MYC* itself is blocked, secondly, HBP1 interacts with the c-MYC/MAX complex, preventing its interaction with DNA sequences like the E-box in the promoter region of genes, resulting in the inability of activation of c-MYC downstream target genes [184]. In addition, HBP1 has been shown to have docking sites in the promoter of *MYCN* (Figure 10) [176,184], showing transcriptional repression of *MYCN* [101].

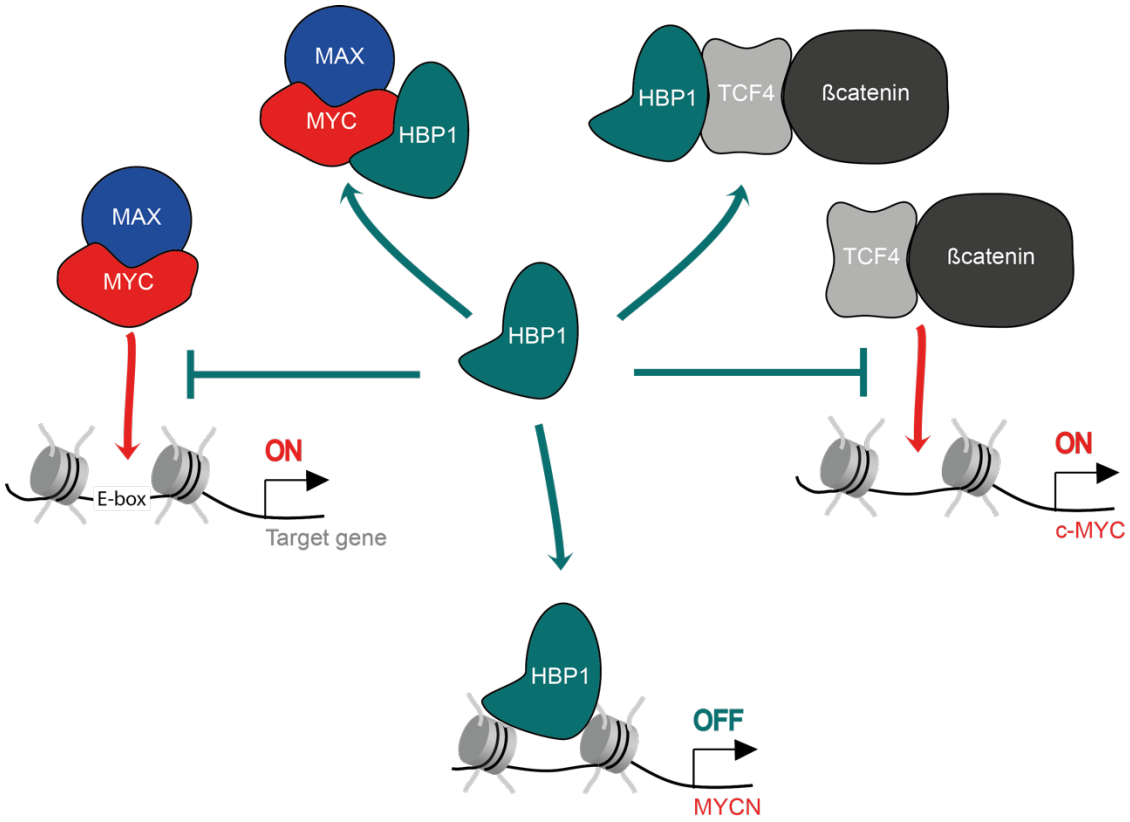

Figure 10: HBP1 negatively regulates c-MYC, c-MYC targets and MYCN

The effect of HBP1 on c-MYC is dual. First, HBP1 interacts with the TCF4- βcatenin complex, thereby preventing its binding with the promoters of target genes, including *c-MYC*. Secondly, by binding with c-MYC, HBP1 prevents the interaction of c-MYC with DNA, thereby impeding the activation of c-MYC target genes. Furthermore, HBP1 represses *MYCN* transcription by binding with its promoter. Figure adapted from [184] and based on [176].

Next to its role in controlling cell cycle, proliferation and differentiation, the observation that HBP1 levels rise during RAS-induced premature senescence,

suggested a possible role of HBP1 in this cellular process (Figure 11) [163,175,176,179-181,183-189], that is frequently overcome by additional mutations to promote tumorigenesis [187,188]. Further experiments confirmed that binding of HBP1 to RB1 is required downstream of the RAS-p38 MAPK signaling in order to trigger senescence [188]. Therefore, HBP1 interacts through its DNA-binding domain with the affinity sites in the *p16*^{INK4A} promoter, resulting in activation of this gene [187]. Simultaneously, to further boost premature senescence, HBP1 interacts via its repression domain with MDM2, thus repressing the negative control of MDM2 on *TP53*. As a consequence, the ubiquitination and degradation of p53 is blocked, leading to enhanced protein stability and more transcriptional activity, resulting in more p21 expression. Additionally, through inhibition of the WNT pathway, HBP1 represses EZH2, followed by loss of H3K27me3 on p21, further increasing p21 levels [186]. Additionally, the p38 MAPK – HBP1 pathway is also involved in induction of senescence following DNA damage, through the formation of senescence-associated heterochromatin foci after binding of HBP1 to RB1 [189].

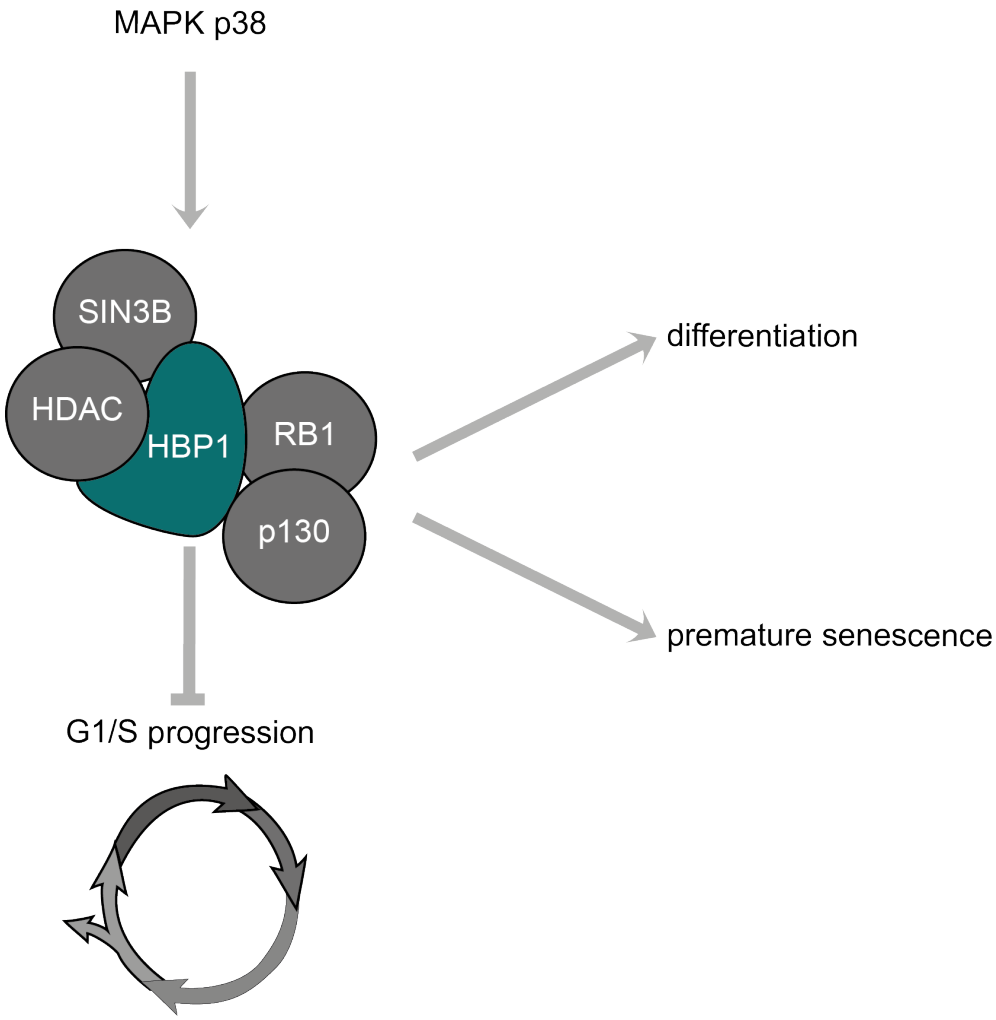

Figure 11: HBP1 controls differentiation, cell cycle progression and premature senescence

The MAPK p38 enhances HBP1 levels to drive differentiation or premature senescence, while it represses the G1/S progression, resulting in cell cycle arrest. HBP1 can therefore bind with RB1 and p130 to mainly activate genes, while interaction with HDACs and SIN3B results in repression of targets. Based on [163,175,176,179-181,183-189].

1.8.3 HBP1 as tumour suppressor gene in several cancer types by inducing cell cycle arrest and differentiation

Given the central role of HBP1 in transcriptional control of differentiation and cell cycle arrest, deregulated expression of HBP1 has been found in diverse cancer entities. Moreover, the chromosomal location of *HBP1* pinpoints towards a possible role as tumour suppressor, as 7q31 is a region that is frequently deleted, mutated or translocated in cancers.

One of the cancer types that is characterized by frequent 7q31 deletions, is myeloid leukaemia and indeed, *HBP1* alterations are found in acute myeloid leukaemia (AML) [181]. Therefore, the role of HBP1 in these tumours was further studied by overexpressing in myeloid cells [190]. HBP1 was shown to have tumour suppressive characteristics, as overexpression resulted in decreased cell proliferation and cell cycle progression by downregulation of cyclin D1 and D3, while upregulating p21. HBP1 simultaneously induces apoptosis, by increasing FasL and in this way activating the Fas/FasL apoptosis pathway [190]. Furthermore, HBP1 simultaneously influences the expression of lineage-specific transcription factors involved in differentiation. Upon HBP1 overexpression, GATA-1, which promotes erythroid, megakaryocytic or combined differentiation in myeloid cells, is upregulated [190]. Similarly, the expression of RUNX1, JunB, C/EBPα, involved in respectively megakaryocytic and myeloid cell differentiation, is increased, while the important factor for granulocyte differentiation, PU.1, is repressed. Moreover, the expression of c-MYB and c-MYC is decreased, which is seen during myeloid differentiation [190]. Furthermore, in leukemic and lymphoid cells, HBP1 interaction with SIN3B promotes HDAC recruitment to repress the transcription of AURKB, MYBL2, CDC6 and BUB1B, which are genes implicated in cell proliferation [163]. Moreover, in MYC-driven leukaemia and lymphoma, MYC maintains a neoplastic state by upregulating the miR-17~92 cluster, which amongst others negatively regulates HBP1, thereby creating a feedback loop to further boost the MYC levels [163].

Another tumour type that frequently harbours 7q deletions is breast cancer [181]. Indeed, reduced *HBP1* levels or mutant HBP1 proteins were found in a subset of invasive breast cancers [181,191]. These *HBP1* variants and mutants were unable to fulfil their transcriptional repressive role, which resulted in a deregulation of the WNT pathway, more invasion and tumorigenic growth [191]. Furthermore, reduced HBP1 expression significantly predicted poor breast cancer outcome and relapse [191]. Additionally, another mechanism through which HBP1 levels are decreased in breast cancer cells is by inducing the PI_3K-AKT axis, which in its turn represses FOXO transcription factors by phosphorylation on certain conserved sites, which results in export from the nucleus to the cytoplasm, where sequestration or ubiquitination is followed by proteasomal degradation [192,193]. In this way, FOXO1 and FOXO3

transcription factors no longer bind directly to the promoter of their targets, including *HBP1* [192]. Additionally, diverse breast cancers harbour dysregulated miR-17~92 expression, which also results in increased proliferation, invasion and migration [194]. These oncogenic effects can partly be explained by the capacity of this miR-17~92 cluster to repress HBP1 and in this way, deregulate the WNT pathway [194]. The inhibition of the WNT pathway is mediated by repressive binding of HBP1 to the β-catenin/TCF complex [195]. As these data show the importance of deregulated *HBP1* expression and overactivity of the WNT pathway in breast cancer, a search for drugs was initiated in order to promote HBP1 function and thus boost its tumour suppressor function to repress invasiveness and proliferation of tumour cells through the WNT pathway. The green tea component, epigallocatechin-3-gallate or EGCG, was found to inhibit the WNT pathway by inducing *HBP1* mRNA and protein levels through an increase in *HBP1* mRNA stability and not through transcriptional initiation [196]. Moreover, sensitivity of tumour cells to EGCG are dependent upon *HBP1* levels, suggesting that HBP1 is an important target for the activity of EGCG [196].

Such deregulated expression of the WNT pathway and activation of its downstream targets, including c-MYC and cyclin D2, by repressed HBP1 has been observed in several other cancer types, including osteosarcoma, glioma, melanoma and NSCLC [197-201]. In osteosarcoma, WNT signaling is reactivated by suppression of *HBP1* through miR-155 binding to its 3'UTR, resulting in proliferation, cell cycle progression and drug resistance by inducing autophagy [198]. Also in glioma, miR-155 was higher expressed to reactivate the WNT signaling by suppression of *HBP1* to boost proliferation of the tumour cells [200]. Moreover, this HBP1–WNT pathway seems to be intriguingly important in glioma, as, next to miR-155, also miR-96 inhibits *HBP1* in order to activate WNT signaling to upregulate in this way the proliferation and tumorigenicity of the glioma cells [201]. Similarly, in melanoma, HBP1 is repressed by NRAS mutations to boost tumorigenesis by reactivation of this WNT pathway [197]. Additionally, also in NSCLC, promoter hypermethylation is responsible for low levels of the *HBP1* tumour suppressor gene, resulting in activation of the WNT signaling [199]. Moreover, low HBP1 expression correlates with poor prognosis of these NSCLC patients [199].

Furthermore, in prostate cancer, loss of HBP1 binding to the promoter of *MIF1* results in an upregulation of this oncogenic, pro-inflammatory cytokine, which results in more cancer cell growth and invasion [177]. Furthermore, *HBP1* and *MIF* expression levels were negatively correlated in a cohort of patients harbouring prostate tumours [177]. More importantly, prostate malignancies that have low *HBP1* and high *MIF* expression, have a statistically significant increased chance to relapse, leading to a worse relapse-free survival [177].

In EGFR-overexpressing oral cancer, EGFR activates the AKT signaling pathway, resulting in HBP1 downregulation. More intriguingly, the anti-cancer adjuvant NAC represses AKT activity to re-induce HBP1, which results in growth inhibition in this cancer type [178].

Intriguingly, HBP1 was identified as being upregulated in stage 4S neuroblastoma tumours, mainly in the ones that were spontaneously regressing [202]. However, no further investigation had been performed to understand the role of HBP1 in neuroblastoma.

In this thesis, we show that HBP1 is downregulated by mutant ALK with effects on proliferation and clonogenicity and impact on MYCN activity, thus representing a fourth mechanism for ALK-driven MYCN activation. Furthermore, we show that HBP1 is also regulated through the miR-17~92 cluster which itself is a major direct upregulated MYCN target (see Chapter 5).

1.9 References

1 Jameson, J. L. & Longo, D. L. Precision medicine--personalized, problematic, and promising. *The New England journal of medicine* **372**, 2229-2234, doi:10.1056/NEJMsb1503104 (2015).

2 Arora, A. & Scholar, E. M. Role of tyrosine kinase inhibitors in cancer therapy. *The Journal of pharmacology and experimental therapeutics* **315**, 971-979, doi:10.1124/jpet.105.084145 (2005).

3 Vogelstein, B. & Kinzler, K. W. Cancer genes and the pathways they control. *Nature medicine* **10**, 789-799, doi:10.1038/nm1087 (2004).

4 McDonell, L. M., Kernohan, K. D., Boycott, K. M. & Sawyer, S. L. Receptor tyrosine kinase mutations in developmental syndromes and cancer: two sides

of the same coin. *Human molecular genetics* **24**, 6, doi:10.1093/hmg/ddv254 (2015).
5 Lemmon, M. A. & Schlessinger, J. Cell signaling by receptor tyrosine kinases. *Cell* **141**, 1117-1134, doi:10.1016/j.cell.2010.06.011 (2010).
6 Gschwind, A., Fischer, O. M. & Ullrich, A. The discovery of receptor tyrosine kinases: targets for cancer therapy. *Nature reviews. Cancer* **4**, 361-370, doi:10.1038/nrc1360 (2004).
7 Nolen, B., Taylor, S. & Ghosh, G. Regulation of protein kinases; controlling activity through activation segment conformation. *Mol Cell* **15**, 661-675, doi:10.1016/j.molcel.2004.08.024 (2004).
8 Shewchuk, L. M. *et al.* Structure of the Tie2 RTK domain: self-inhibition by the nucleotide binding loop, activation loop, and C-terminal tail. *Structure* **8**, 1105-1113 (2000).
9 Knowles, P. P. *et al.* Structure and chemical inhibition of the RET tyrosine kinase domain. *J Biol Chem* **281**, 33577-33587, doi:10.1074/jbc.M605604200 (2006).
10 Madhusudan, S. & Ganesan, T. S. Tyrosine kinase inhibitors in cancer therapy. *Clinical biochemistry* **37**, 618-635, doi:10.1016/j.clinbiochem.2004.05.006 (2004).
11 Liu, B. A. *et al.* SH2 domains recognize contextual peptide sequence information to determine selectivity. *Mol Cell Proteomics* **9**, 2391-2404, doi:10.1074/mcp.M110.001586 (2010).
12 Imai, K. & Takaoka, A. Comparing antibody and small-molecule therapies for cancer. *Nature reviews. Cancer* **6**, 714-727, doi:10.1038/nrc1913 (2006).
13 Gharwan, H. & Groninger, H. Kinase inhibitors and monoclonal antibodies in oncology: clinical implications. *Nature reviews. Clinical oncology* **13**, 209-227, doi:10.1038/nrclinonc.2015.213 (2016).
14 Zou, H. Y. *et al.* PF-06463922, an ALK/ROS1 Inhibitor, Overcomes Resistance to First and Second Generation ALK Inhibitors in Preclinical Models. *Cancer Cell* **28**, 70-81, doi:10.1016/j.ccell.2015.05.010 (2015).
15 Bollu, L. R., Mazumdar, A., Savage, M. I. & Brown, P. H. Molecular Pathways: Targeting Protein Tyrosine Phosphatases in Cancer. *Clinical cancer research : an official journal of the American Association for Cancer Research* **23**, 2136-2142, doi:10.1158/1078-0432.CCR-16-0934 (2017).
16 Mosse, Y. P. *et al.* Targeting ALK With Crizotinib in Pediatric Anaplastic Large Cell Lymphoma and Inflammatory Myofibroblastic Tumor: A Children's Oncology Group Study. *J Clin Oncol* **35**, 3215-3221, doi:10.1200/JCO.2017.73.4830 (2017).
17 Camidge, D. R., Pao, W. & Sequist, L. V. Acquired resistance to TKIs in solid tumours: learning from lung cancer. *Nature reviews. Clinical oncology* **11**, 473-481, doi:10.1038/nrclinonc.2014.104 (2014).
18 Lovly, C. M. & Shaw, A. T. Molecular pathways: resistance to kinase inhibitors and implications for therapeutic strategies. *Clinical cancer research : an official journal of the American Association for Cancer Research* **20**, 2249-2256, doi:10.1158/1078-0432.CCR-13-1610 (2014).
19 Mancini, M. & Yarden, Y. Mutational and network level mechanisms underlying resistance to anti-cancer kinase inhibitors. *Seminars in cell & developmental biology* **50**, 164-176, doi:10.1016/j.semcdb.2015.09.018 (2016).

20 Knight, Z. A., Lin, H. & Shokat, K. M. Targeting the cancer kinome through polypharmacology. *Nature reviews. Cancer* **10**, 130-137, doi:10.1038/nrc2787 (2010).
21 Cox, A. D. & Der, C. J. The raf inhibitor paradox: unexpected consequences of targeted drugs. *Cancer Cell* **17**, 221-223, doi:10.1016/j.ccr.2010.02.029 (2010).
22 Girotti, M. R. *et al.* Paradox-breaking RAF inhibitors that also target SRC are effective in drug-resistant BRAF mutant melanoma. *Cancer Cell* **27**, 85-96, doi:10.1016/j.ccell.2014.11.006 (2015).
23 Zhang, C. *et al.* RAF inhibitors that evade paradoxical MAPK pathway activation. *Nature* **526**, 583-586, doi:10.1038/nature14982 (2015).
24 Sang, J. *et al.* Targeted Inhibition of the Molecular Chaperone Hsp90 Overcomes ALK Inhibitor Resistance in Non–Small Cell Lung Cancer. *Cancer Discovery* **3**, 430-443, doi:10.1158/2159-8290.CD-12-0440 (2013).
25 Tanimoto, A. *et al.* Receptor ligand-triggered resistance to alectinib and its circumvention by Hsp90 inhibition in EML4-ALK lung cancer cells. *Oncotarget* **5**, 4920-4928, doi:10.18632/oncotarget.2055 (2014).
26 Vido, M. J. & Aplin, A. E. The Broad Stroke of Hsp90 Inhibitors: Painting over the RAF Inhibitor Paradox. *J Invest Dermatol* **135**, 2355-2357, doi:10.1038/jid.2015.239 (2015).
27 Bagatell, R. *et al.* Phase I pharmacokinetic and pharmacodynamic study of 17-N-allylamino-17-demethoxygeldanamycin in pediatric patients with recurrent or refractory solid tumors: a pediatric oncology experimental therapeutics investigators consortium study. *Clin Cancer Res* **13**, 1783-1788, doi:10.1158/1078-0432.CCR-06-1892 (2007).
28 Wang, H., Lu, M., Yao, M. & Zhu, W. Effects of treatment with an Hsp90 inhibitor in tumors based on 15 phase II clinical trials. *Mol Clin Oncol* **5**, 326-334, doi:10.3892/mco.2016.963 (2016).
29 Mossé, Y. P. *et al.* Identification of ALK as a major familial neuroblastoma predisposition gene. *Nature* **455**, 930-935, doi:10.1038/nature07261 (2008).
30 Janoueix-Lerosey, I. *et al.* Somatic and germline activating mutations of the ALK kinase receptor in neuroblastoma. *Nature* **455**, 967-970, doi:10.1038/nature07398 (2008).
31 Chen, Y. *et al.* Oncogenic mutations of ALK kinase in neuroblastoma. *Nature* **455**, 971-974, doi:10.1038/nature07399 (2008).
32 George, R. E. *et al.* Activating mutations in ALK provide a therapeutic target in neuroblastoma. *Nature* **455**, 975-978, doi:10.1038/nature07397 (2008).
33 Shohet, J. & Foster, J. Neuroblastoma. *BMJ*, doi:10.1136/bmj.j1863 (2017).
34 Carén, H., Abel, F., Kogner, P. & Martinsson, T. High incidence of DNA mutations and gene amplifications of theALKgene in advanced sporadic neuroblastoma tumours. *Biochemical Journal* **416**, 153-159, doi:10.1042/bj20081834 (2008).
35 Louis, C. U. & Shohet, J. M. Neuroblastoma: molecular pathogenesis and therapy. *Annual review of medicine* **66**, 49-63, doi:10.1146/annurev-med-011514-023121 (2015).
36 Irwin, M. S. & Park, J. R. Neuroblastoma: paradigm for precision medicine. *Pediatr Clin North Am* **62**, 225-256, doi:10.1016/j.pcl.2014.09.015 (2015).
37 Matthay, K. K. *et al.* Neuroblastoma. *Nature Reviews Disease Primers* **2**, 16078, doi:10.1038/nrdp.2016.78 (2016).

38 Kamihara, J. *et al.* Retinoblastoma and Neuroblastoma Predisposition and Surveillance. *Clinical Cancer Research* **23**, doi:10.1158/1078-0432.CCR-17-0652 (2017).

39 Cheung, N.-K. V. & Dyer, M. A. Neuroblastoma: developmental biology, cancer genomics and immunotherapy. *Nature Reviews Cancer* **13**, 397-411, doi:10.1038/nrc3526 (2013).

40 Mayol, G. *et al.* DNA Hypomethylation Affects Cancer-Related Biological Functions and Genes Relevant in Neuroblastoma Pathogenesis. *PLoS ONE* **7**, doi:10.1371/journal.pone.0048401 (2012).

41 Louis, C. U. & Shohet, J. M. Neuroblastoma: molecular pathogenesis and therapy. *Annu Rev Med* **66**, 49-63, doi:10.1146/annurev-med-011514-023121 (2015).

42 Berlanga, P., Cañete, A. & Castel, V. Advances in emerging drugs for the treatment of neuroblastoma. *Expert Opinion on Emerging Drugs*, doi:10.1080/14728214.2017.1294159 (2017).

43 Villablanca, J. G. *et al.* A Phase I New Approaches to Neuroblastoma Therapy Study of Buthionine Sulfoximine and Melphalan With Autologous Stem Cells for Recurrent/Refractory High-Risk Neuroblastoma. *Pediatr Blood Cancer* **63**, 1349-1356, doi:10.1002/pbc.25994 (2016).

44 Bosse, K. R. *et al.* Identification of GPC2 as an Oncoprotein and Candidate Immunotherapeutic Target in High-Risk Neuroblastoma. *Cancer Cell* **32**, 295-309 e212, doi:10.1016/j.ccell.2017.08.003 (2017).

45 Molenaar, J. J. *et al.* Sequencing of neuroblastoma identifies chromothripsis and defects in neuritogenesis genes. *Nature* **483**, 589-593, doi:10.1038/nature10910 (2012).

46 Bosse, K. R. & Maris, J. M. Advances in the translational genomics of neuroblastoma: From improving risk stratification and revealing novel biology to identifying actionable genomic alterations. *Cancer* **122**, 20-33, doi:10.1002/cncr.29706 (2016).

47 Molenaar, J. J. *et al.* LIN28B induces neuroblastoma and enhances MYCN levels via let-7 suppression. *Nature genetics* **44**, 1199-1206, doi:10.1038/ng.2436 (2012).

48 Powers, J. T. *et al.* Multiple mechanisms disrupt the let-7 microRNA family in neuroblastoma. *Nature* **535**, 246-251, doi:10.1038/nature18632 (2016).

49 Tolbert, V. P., Coggins, G. E. & Maris, J. M. Genetic susceptibility to neuroblastoma. *Current Opinion in Genetics & Development* **42**, 81-90, doi:10.1016/j.gde.2017.03.008 (2017).

50 Liu, Z. & Thiele, C. J. When LMO1 Meets MYCN, Neuroblastoma Is Metastatic. *Cancer Cell* **32**, 273-275, doi:10.1016/j.ccell.2017.08.014 (2017).

51 Zhu, S. *et al.* LMO1 Synergizes with MYCN to Promote Neuroblastoma Initiation and Metastasis. *Cancer Cell* **32**, 310-323 e315, doi:10.1016/j.ccell.2017.08.002 (2017).

52 Valentijn, L. J. *et al.* TERT rearrangements are frequent in neuroblastoma and identify aggressive tumors. *Nature genetics* **47**, 1411-1414, doi:10.1038/ng.3438 (2015).

53 Peifer, M. *et al.* Telomerase activation by genomic rearrangements in high-risk neuroblastoma. *Nature* **526**, 700-704, doi:10.1038/nature14980 (2015).

54 Dyberg, C. *et al.* Rho-associated kinase is a therapeutic target in neuroblastoma. *Proc Natl Acad Sci U S A* **114**, E6603-E6612, doi:10.1073/pnas.1706011114 (2017).

55 Schleiermacher, G. *et al.* Emergence of new ALK mutations at relapse of neuroblastoma. *Journal of clinical oncology : official journal of the American Society of Clinical Oncology* **32**, 2727-2734, doi:10.1200/JCO.2013.54.0674 (2014).
56 Eleveld, T. F. *et al.* Relapsed neuroblastomas show frequent RAS-MAPK pathway mutations. *Nature genetics* **47**, 864-871, doi:10.1038/ng.3333 (2015).
57 Weiss, W. A., Aldape, K., Mohapatra, G., Feuerstein, B. G. & Bishop, J. M. Targeted expression of MYCN causes neuroblastoma in transgenic mice. *The EMBO Journal* **16**, 2985-2995, doi:10.1093/emboj/16.11.2985 (1997).
58 Berry, T. *et al.* The ALKF1174L Mutation Potentiates the Oncogenic Activity of MYCN in Neuroblastoma. *Cancer Cell* **22**, 117-130, doi:10.1016/j.ccr.2012.06.001 (2012).
59 Althoff, K. *et al.* A Cre-conditional MYCN-driven neuroblastoma mouse model as an improved tool for preclinical studies. *Oncogene* **34**, 3357-3368, doi:10.1038/onc.2014.269 (2015).
60 Zhu, S. *et al.* Activated ALK Collaborates with MYCN in Neuroblastoma Pathogenesis. *Cancer Cell* **21**, 362-373, doi:10.1016/j.ccr.2012.02.010 (2012).
61 Teng, Y. *et al.* Evaluating human cancer cell metastasis in zebrafish. *BMC Cancer* **13**, 1-12, doi:10.1186/1471-2407-13-453 (2013).
62 Schulte, J. H. *et al.* MYCN and ALKF1174L are sufficient to drive neuroblastoma development from neural crest progenitor cells. *Oncogene* **32**, 1059-1065, doi:10.1038/onc.2012.106 (2013).
63 Olsen, R. R. *et al.* MYCN induces neuroblastoma in primary neural crest cells. *Oncogene* **36**, 5075-5082, doi:10.1038/onc.2017.128 (2017).
64 Zheng, T., Menard, M. & Weiss, W. A. Neuroblastoma Metastases: Leveraging the Avian Neural Crest. *Cancer Cell* **32**, 395-397, doi:10.1016/j.ccell.2017.09.012 (2017).
65 Delloye-Bourgeois, C. *et al.* Microenvironment-Driven Shift of Cohesion/Detachment Balance within Tumors Induces a Switch toward Metastasis in Neuroblastoma. *Cancer Cell* **32**, 427-443 e428, doi:10.1016/j.ccell.2017.09.006 (2017).
66 Teitz, T. *et al.* Preclinical Models for Neuroblastoma: Establishing a Baseline for Treatment. *PLoS ONE* **6**, doi:10.1371/journal.pone.0019133 (2011).
67 Dyer, M. A. Mouse models of childhood cancer of the nervous system. *Journal of Clinical Pathology* **57**, 561-576, doi:10.1136/jcp.2003.009910 (2004).
68 Becher, O. J., Holland, E. C., Sausville, E. A. & Burger, A. M. Genetically Engineered Models Have Advantages over Xenografts for Preclinical Studies. *Cancer Research* **66**, 3355-3359, doi:10.1158/0008-5472.CAN-05-3827 (2006).
69 Daudigeos-Dubus, E. *et al.* Establishment and characterization of new orthotopic and metastatic neuroblastoma models. *In vivo (Athens, Greece)* **28**, 425-434 (2014).
70 Francia, G. & Kerbel, R. S. Raising the bar for cancer therapy models. *Nature biotechnology* **28**, 561-562, doi:10.1038/nbt0610-561 (2010).
71 Braekeveldt, N. *et al.* Neuroblastoma patient-derived orthotopic xenografts retain metastatic patterns and geno- and phenotypes of patient tumours. *International Journal of Cancer* **136**, doi:10.1002/ijc.29217 (2015).
72 Braekeveldt, N. & Bexell, D. Patient-derived xenografts as preclinical neuroblastoma models. *Cell and Tissue Research*, 1-11, doi:10.1007/s00441-017-2687-8 (2017).

73 Persson, C. U. *et al.* Neuroblastoma patient-derived xenograft cells cultured in stem-cell promoting medium retain tumorigenic and metastatic capacities but differentiate in serum. *Scientific reports* **7**, 10274, doi:10.1038/s41598-017-09662-8 (2017).
74 Brodeur, G. M. & Bagatell, R. Mechanisms of neuroblastoma regression. *Nature Reviews Clinical Oncology* **11**, doi:10.1038/nrclinonc.2014.168 (2014).
75 Brodeur, G. M. *et al.* Trk Receptor Expression and Inhibition in Neuroblastomas. *Clinical Cancer Research* **15**, 3244-3250, doi:10.1158/1078-0432.CCR-08-1815 (2009).
76 Brodeur, G. M. *et al.* Therapeutic targets for neuroblastomas. *Expert Opinion on Therapeutic Targets* **18**, 277-292, doi:10.1517/14728222.2014.867946 (2014).
77 Meldolesi, J. Reviews of Physiology, Biochemistry and Pharmacology. *Reviews of Physiology, Biochemistry and Pharmacology*, 1-13, doi:10.1007/112_2017_6 (2017).
78 Zage, P. E. *et al.* The selective Trk inhibitor AZ623 inhibits brain-derived neurotrophic factor–mediated neuroblastoma cell proliferation and signaling and is synergistic with topotecan. *Cancer* **117**, 1321-1391, doi:10.1002/cncr.25674 (2011).
79 Rosenzweig, S. A. Acquired resistance to drugs targeting receptor tyrosine kinases. *Biochemical pharmacology* **83**, 1041-1048, doi:10.1016/j.bcp.2011.12.025 (2012).
80 Iyer, R. *et al.* Entrectinib is a potent inhibitor of Trk-driven neuroblastomas in a xenograft mouse model. *Cancer Letters* **372**, 179-186, doi:10.1016/j.canlet.2016.01.018 (2016).
81 Minturn, J. E. *et al.* Phase I trial of lestaurtinib for children with refractory neuroblastoma: a new approaches to neuroblastoma therapy consortium study. *Cancer Chemotherapy and Pharmacology* **68**, 1057-1065, doi:10.1007/s00280-011-1581-4 (2011).
82 Croucher, J. L. *et al.* TrkB inhibition by GNF-4256 slows growth and enhances chemotherapeutic efficacy in neuroblastoma xenografts. *Cancer Chemotherapy and Pharmacology* **75**, 131-141, doi:10.1007/s00280-014-2627-1 (2015).
83 Mulligan, L. M. RET revisited: expanding the oncogenic portfolio. *Nature Reviews Cancer* **14**, doi:10.1038/nrc3680 (2014).
84 Beaudry, P. *et al.* Potent antitumor effects of ZD6474 on neuroblastoma via dual targeting of tumor cells and tumor endothelium. *Molecular Cancer Therapeutics* **7**, 418-424, doi:10.1158/1535-7163.mct-07-0568 (2008).
85 D'Alessio, A. *et al.* Expression of the RET oncogene induces differentiation of SK-N-BE neuroblastoma cells. *Cell Growth Differ* **6**, 1387-1394 (1995).
86 Peterson, S. & Bogenmann, E. The RET and TRKA pathways collaborate to regulate neuroblastoma differentiation. *Oncogene* **23**, 213-225, doi:10.1038/sj.onc.1206980 (2004).
87 Esposito, C., D'Alessio, A., de Franciscis, V. & Cerchia, L. A Cross-Talk between TrkB and Ret Tyrosine Kinases Receptors Mediates Neuroblastoma Cells Differentiation. *PLoS ONE* **3**, doi:10.1371/journal.pone.0001643 (2008).
88 Zage, P. E. *et al.* A novel therapeutic combination for neuroblastoma. *Cancer* **116**, 2465-2475, doi:10.1002/cncr.25017 (2010).

89 Azarova, A. M., Gautam, G. & George, R. E. Emerging importance of ALK in neuroblastoma. *Seminars in Cancer Biology* **21**, 267-275, doi:10.1016/j.semcancer.2011.09.005 (2011).
90 Roskoski, R. Anaplastic lymphoma kinase (ALK): Structure, oncogenic activation, and pharmacological inhibition. *Pharmacological Research* **68**, 68-94, doi:10.1016/j.phrs.2012.11.007 (2013).
91 Hallberg, B. & Palmer, R. H. The role of the ALK receptor in cancer biology. *Annals of oncology : official journal of the European Society for Medical Oncology / ESMO* **27 Suppl 3**, doi:10.1093/annonc/mdw301 (2016).
92 Mourali, J. *et al.* Anaplastic Lymphoma Kinase Is a Dependence Receptor Whose Proapoptotic Functions Are Activated by Caspase Cleavage. *Molecular and Cellular Biology* **26**, 6209-6222, doi:10.1128/MCB.01515-05 (2006).
93 Hallberg, B. & Palmer, R. H. Mechanistic insight into ALK receptor tyrosine kinase in human cancer biology. *Nature Reviews Cancer* **13**, 685-700, doi:10.1038/nrc3580 (2013).
94 Mano, H. ALKoma: a cancer subtype with a shared target. *Cancer discovery* **2**, 495-502, doi:10.1158/2159-8290.CD-12-0009 (2012).
95 Murray, P. B. *et al.* Heparin is an activating ligand of the orphan receptor tyrosine kinase ALK. *Science signaling* **8**, doi:10.1126/scisignal.2005916 (2015).
96 Guan, J. *et al.* FAM150A and FAM150B are activating ligands for anaplastic lymphoma kinase. *eLife* **4**, doi:10.7554/eLife.09811 (2015).
97 Reshetnyak, A. V. *et al.* Augmentor α and β (FAM150) are ligands of the receptor tyrosine kinases ALK and LTK: Hierarchy and specificity of ligand–receptor interactions. *Proceedings of the National Academy of Sciences* **112**, 15862-15867, doi:10.1073/pnas.1520099112 (2015).
98 Holla, V. R. *et al.* ALK: a tyrosine kinase target for cancer therapy. *Molecular Case Studies* **3**, doi:10.1101/mcs.a001115 (2017).
99 De Mariano, M. *et al.* A genome-wide microRNA profiling indicates miR-424-5p and miR-503-5p as regulators of ALK expression in neuroblastoma. *Oncotarget* **8**, 56518-56532, doi:10.18632/oncotarget.17033 (2017).
100 Okubo, J. *et al.* Aberrant activation of ALK kinase by a novel truncated form ALK protein in neuroblastoma. *Oncogene* **31**, 4667-4676, doi:10.1038/onc.2011.616 (2012).
101 Cazes, A. *et al.* Characterization of Rearrangements Involving the ALK Gene Reveals a Novel Truncated Form Associated with Tumor Aggressiveness in Neuroblastoma. *Cancer Research* **73**, 195-204, doi:10.1158/0008-5472.CAN-12-1242 (2013).
102 Fransson, S. *et al.* Intragenic anaplastic lymphoma kinase (ALK) rearrangements: Translocations as a novel mechanism of ALK activation in neuroblastoma tumors. *Genes, Chromosomes and Cancer* **54**, 99-109, doi:10.1002/gcc.22223 (2015).
103 Schulte, J. H. *et al.* High ALK Receptor Tyrosine Kinase Expression Supersedes ALK Mutation as a Determining Factor of an Unfavorable Phenotype in Primary Neuroblastoma. *Clinical Cancer Research* **17**, 5082-5092, doi:10.1158/1078-0432.CCR-10-2809 (2011).
104 Passoni, L. *et al.* Mutation-Independent Anaplastic Lymphoma Kinase Overexpression in Poor Prognosis Neuroblastoma Patients. *Cancer Research* **69**, 7338-7346, doi:10.1158/0008-5472.CAN-08-4419 (2009).

105 Chand, D. *et al.* Cell culture and Drosophila model systems define three classes of anaplastic lymphoma kinase mutations in neuroblastoma. *Disease Models & Mechanisms* **6**, 373-382, doi:10.1242/dmm.010348 (2013).
106 Schönherr, C. *et al.* The Neuroblastoma ALK(I1250T) Mutation Is a Kinase-Dead RTK In Vitro and In Vivo. *Translational Oncology* **4**, 258, doi:10.1593/tlo.11139 (2011).
107 De Brouwer, S. *et al.* Meta-analysis of Neuroblastomas Reveals a Skewed ALK Mutation Spectrum in Tumors with MYCN Amplification. *Clinical Cancer Research* **16**, doi:10.1158/1078-0432.CCR-09-2660 (2010).
108 Bellini, A. *et al.* Deep Sequencing Reveals Occurrence of Subclonal ALK Mutations in Neuroblastoma at Diagnosis. *Clinical Cancer Research* **21**, 4913-4921, doi:10.1158/1078-0432.CCR-15-0423 (2015).
109 Chen, L. *et al.* Identification of different ALK mutations in a pair of neuroblastoma cell lines established at diagnosis and relapse. *Oncotarget* **7**, 87301-87311, doi:10.18632/oncotarget.13541 (2016).
110 Schramm, A. *et al.* Mutational dynamics between primary and relapse neuroblastomas. *Nature genetics* **47**, 872-877, doi:10.1038/ng.3349 (2015).
111 Padovan-Merhar, O. M. *et al.* Enrichment of Targetable Mutations in the Relapsed Neuroblastoma Genome. *PLoS Genet* **12**, e1006501, doi:10.1371/journal.pgen.1006501 (2016).
112 Galkin, A. V. *et al.* Identification of NVP-TAE684, a potent, selective, and efficacious inhibitor of NPM-ALK. *Proceedings of the National Academy of Sciences* **104**, 270-275, doi:10.1073/pnas.0609412103 (2007).
113 Schönherr, C. *et al.* Activating ALK mutations found in neuroblastoma are inhibited by Crizotinib and NVP-TAE684. *Biochemical Journal* **440**, 405-414, doi:10.1042/BJ20101796 (2011).
114 Mossé, Y. P. *et al.* Safety and activity of crizotinib for paediatric patients with refractory solid tumours or anaplastic large-cell lymphoma: a Children's Oncology Group phase 1 consortium study. *The Lancet Oncology* **14**, 472-480, doi:10.1016/S1470-2045(13)70095-0 (2013).
115 Bresler, S. C. *et al.* Differential inhibitor sensitivity of anaplastic lymphoma kinase variants found in neuroblastoma. *Science translational medicine* **3**, doi:10.1126/scitranslmed.3002950 (2011).
116 Heuckmann, J. M. *et al.* ALK Mutations Conferring Differential Resistance to Structurally Diverse ALK Inhibitors. *Clinical Cancer Research* **17**, 7394-7401, doi:10.1158/1078-0432.CCR-11-1648 (2011).
117 Sasaki, T. *et al.* The Neuroblastoma-Associated F1174L ALK Mutation Causes Resistance to an ALK Kinase Inhibitor in ALK-Translocated Cancers. *Cancer Research* **70**, 10038-10043, doi:10.1158/0008-5472.CAN-10-2956 (2010).
118 Amin, A. D. *et al.* TKI sensitivity patterns of novel kinase-domain mutations suggest therapeutic opportunities for patients with resistant ALK+ tumors. *Oncotarget* **7**, 23715-23729, doi:10.18632/oncotarget.8173 (2016).
119 Carpenter, E. L. & Mossé, Y. P. Targeting ALK in neuroblastoma--preclinical and clinical advancements. *Nature reviews. Clinical oncology* **9**, 391-399, doi:10.1038/nrclinonc.2012.72 (2012).
120 Duijkers, F. A. M. *et al.* Anaplastic lymphoma kinase (ALK) inhibitor response in neuroblastoma is highly correlated with ALK mutation status, ALK mRNA and protein levels. *Cellular Oncology* **34**, 409-417, doi:10.1007/s13402-011-0048-2 (2011).

121 Huang, D. *et al.* Multiplexed deep sequencing analysis of ALK kinase domain identifies resistance mutations in relapsed patients following crizotinib treatment. *Genomics* **102**, 157-162, doi:10.1016/j.ygeno.2013.02.006 (2013).
122 Pall, G. The next-generation ALK inhibitors. *Current Opinion in Oncology* **27**, 118, doi:10.1097/CCO.0000000000000165 (2015).
123 Toyokawa, G. & Seto, T. Updated Evidence on the Mechanisms of Resistance to ALK Inhibitors and Strategies to Overcome Such Resistance: Clinical and Preclinical Data. *Oncology research and treatment* **38**, 291-298, doi:10.1159/000430852 (2015).
124 Wang, H. *et al.* Combined ALK and MDM2 inhibition increases antitumor activity and overcomes resistance in human ALK mutant neuroblastoma cell lines and xenograft models. *eLife* **6**, doi:10.7554/eLife.17137 (2017).
125 Lu, J. *et al.* The second-generation ALK inhibitor alectinib effectively induces apoptosis in human neuroblastoma cells and inhibits tumor growth in a TH-MYCN transgenic neuroblastoma mouse model. *Cancer Letters* **400**, 61-68, doi:10.1016/j.canlet.2017.04.022 (2017).
126 Friboulet, L. *et al.* The ALK Inhibitor Ceritinib Overcomes Crizotinib Resistance in Non–Small Cell Lung Cancer. *Cancer Discovery* **4**, 662-673, doi:10.1158/2159-8290.CD-13-0846 (2014).
127 Shaw, A. T. *et al.* Ceritinib in ALK-Rearranged Non–Small-Cell Lung Cancer. *The New England Journal of Medicine* **370**, 1189-1197, doi:10.1056/NEJMoa1311107 (2014).
128 Infarinato, N. R. *et al.* The ALK/ROS1 Inhibitor PF-06463922 Overcomes Primary Resistance to Crizotinib in ALK-Driven Neuroblastoma. *Cancer discovery* **6**, 96-107, doi:10.1158/2159-8290.CD-15-1056 (2016).
129 Mazot, P. *et al.* The constitutive activity of the ALK mutated at positions F1174 or R1275 impairs receptor trafficking. *Oncogene* **30**, 2017-2025, doi:10.1038/onc.2010.595 (2011).
130 Debruyne, D. N. *et al.* ALK inhibitor resistance in ALK(F1174L)-driven neuroblastoma is associated with AXL activation and induction of EMT. *Oncogene* **35**, 3681-3691, doi:10.1038/onc.2015.434 (2016).
131 Yang, L. *et al.* Blocking the PI3K pathway enhances the efficacy of ALK-targeted therapy in EML4-ALK-positive nonsmall-cell lung cancer. *Tumor Biology* **35**, 9759-9767, doi:10.1007/s13277-014-2252-y (2014).
132 Paolo, D. *et al.* New therapeutic strategies in neuroblastoma: combined targeting of a novel tyrosine kinase inhibitor and liposomal siRNAs against ALK. *Oncotarget* **6**, 28774-28789, doi:10.18632/oncotarget.4342 (2015).
133 Carpenter, E. L. *et al.* Antibody targeting of anaplastic lymphoma kinase induces cytotoxicity of human neuroblastoma. *Oncogene* **31**, 4859-4867, doi:10.1038/onc.2011.647 (2012).
134 Moore, N. F. *et al.* Molecular rationale for the use of PI3K/AKT/mTOR pathway inhibitors in combination with crizotinib in ALK-mutated neuroblastoma. *Oncotarget* **5**, 8737-8749, doi:10.18632/oncotarget.2372 (2014).
135 Krytska, K. *et al.* Crizotinib Synergizes with Chemotherapy in Preclinical Models of Neuroblastoma. *Clinical Cancer Research* **22**, 948-960, doi:10.1158/1078-0432.CCR-15-0379 (2016).
136 Wood, A. C. *et al.* Dual ALK and CDK4/6 Inhibition Demonstrates Synergy against Neuroblastoma. *Clinical Cancer Research* **23**, 2856-2868, doi:10.1158/1078-0432.CCR-16-1114 (2017).

137 Kramer, M., Ribeiro, D., Arsenian-Henriksson, M., Deller, T. & Rohrer, H. Proliferation and Survival of Embryonic Sympathetic Neuroblasts by MYCN and Activated ALK Signaling. *The Journal of Neuroscience* **36**, 10425-10439, doi:10.1523/JNEUROSCI.0183-16.2016 (2016).
138 Schönherr, C. *et al.* Anaplastic Lymphoma Kinase (ALK) regulates initiation of transcription of MYCN in neuroblastoma cells. *Oncogene* **31**, doi:10.1038/onc.2012.12 (2012).
139 Umapathy, G. *et al.* The kinase ALK stimulates the kinase ERK5 to promote the expression of the oncogene MYCN in neuroblastoma. *Sci. Signal.* **7**, doi:10.1126/scisignal.2005470 (2014).
140 Cage, T. A. *et al.* Downregulation of MYCN through PI3K Inhibition in Mouse Models of Pediatric Neural Cancer. *Frontiers in oncology* **5**, 111, doi:10.3389/fonc.2015.00111 (2015).
141 Chesler, L. *et al.* Inhibition of phosphatidylinositol 3-kinase destabilizes Mycn protein and blocks malignant progression in neuroblastoma. *Cancer research* **66**, 8139-8146, doi:10.1158/0008-5472.CAN-11-0412 (2006).
142 Hasan, K. *et al.* ALK is a MYCN target gene and regulates cell migration and invasion in neuroblastoma. *Scientific Reports* **3**, 3450, doi:10.1038/srep03450 (2013).
143 Vaughan, L. *et al.* Inhibition of mTOR-kinase destabilizes MYCN and is a potential therapy for MYCN-dependent tumors. *Oncotarget* **7**, 57525-57544, doi:10.18632/oncotarget.10544 (2016).
144 Gustafson, W. C. & Weiss, W. A. Myc proteins as therapeutic targets. *Oncogene* **29**, 1249-1259, doi:10.1038/onc.2009.512 (2010).
145 Huang, M. & Weiss, W. A. Neuroblastoma and MYCN. *Cold Spring Harbor Perspectives in Medicine* **3**, doi:10.1101/cshperspect.a014415 (2013).
146 Beltran, H. The N-myc Oncogene: Maximizing its Targets, Regulation, and Therapeutic Potential. *Molecular Cancer Research* **12**, 815-822, doi:10.1158/1541-7786.MCR-13-0536 (2014).
147 Conacci-Sorrell, M., McFerrin, L. & Eisenman, R. N. An Overview of MYC and Its Interactome. *Cold Spring Harbor Perspectives in Medicine* **4**, doi:10.1101/cshperspect.a014357 (2014).
148 Gherardi, S., Valli, E., Erriquez, D. & Perini, G. MYCN-mediated transcriptional repression in neuroblastoma: the other side of the coin. *Frontiers in Oncology* **3**, 42, doi:10.3389/fonc.2013.00042 (2013).
149 McKeown, M. R. & Bradner, J. E. Therapeutic Strategies to Inhibit MYC. *Cold Spring Harbor Perspectives in Medicine* **4**, doi:10.1101/cshperspect.a014266 (2014).
150 Suenaga, Y. *et al.* NCYM, a Cis-Antisense Gene of MYCN, Encodes a De Novo Evolved Protein That Inhibits GSK3β Resulting in the Stabilization of MYCN in Human Neuroblastomas. *PLoS Genetics* **10**, doi:10.1371/journal.pgen.1003996 (2014).
151 Vadie, N. *et al.* MYCNOS functions as an antisense RNA regulating MYCN. *RNA Biology* **12**, doi:10.1080/15476286.2015.1063773 (2015).
152 Watanabe, Y. *et al.* ZAR1 knockdown promotes the differentiation of human neuroblastoma cells by suppression of MYCN expression. *Medical Oncology* **34**, 158, doi:10.1007/s12032-017-0999-x (2017).
153 Liu, P. Y. *et al.* Effects of a Novel Long Noncoding RNA, lncUSMycN, on N-Myc Expression and Neuroblastoma Progression. *JNCI: Journal of the National Cancer Institute* **106**, doi:10.1093/jnci/dju113 (2014).

154 Pandey, G. & Kanduri, C. Long noncoding RNAs and neuroblastoma. *Oncotarget* **6**, 18265-18275, doi:10.18632/oncotarget.4251 (2015).
155 Buechner, J. & Einvik, C. N-myc and Noncoding RNAs in Neuroblastoma. *Molecular Cancer Research* **10**, 1243-1253, doi:10.1158/1541-7786.MCR-12-0244 (2012).
156 Beckers, A. *et al.* MYCN-targeting miRNAs are predominantly downregulated during MYCN-driven neuroblastoma tumor formation. *Oncotarget* **6**, 5204-5216, doi:10.18632/oncotarget.2477 (2015).
157 Vo, B. T. *et al.* The Interaction of Myc with Miz1 Defines Medulloblastoma Subgroup Identity. *Cancer Cell* **29**, 5-16, doi:10.1016/j.ccell.2015.12.003 (2016).
158 Posternak, V. & Cole, M. D. Strategically targeting MYC in cancer. *F1000Research* **5**, 408, doi:10.12688/f1000research.7879.1 (2016).
159 Corvetta, D. *et al.* Physical Interaction between MYCN Oncogene and Polycomb Repressive Complex 2 (PRC2) in Neuroblastoma FUNCTIONAL AND THERAPEUTIC IMPLICATIONS. *Journal of Biological Chemistry* **288**, 8332-8341, doi:10.1074/jbc.M113.454280 (2013).
160 He, S., Liu, Z., Oh, D.-Y. Y. & Thiele, C. J. MYCN and the epigenome. *Frontiers in oncology* **3**, 1, doi:10.3389/fonc.2013.00001 (2013).
161 Peukert, K. *et al.* An alternative pathway for gene regulation by Myc. *The EMBO journal* **16**, 5672-5686, doi:10.1093/emboj/16.18.5672 (1997).
162 Iraci, N. *et al.* A SP1/MIZ1/MYCN Repression Complex Recruits HDAC1 at the TRKA and p75NTR Promoters and Affects Neuroblastoma Malignancy by Inhibiting the Cell Response to NGF. *Cancer Research* **71**, 404-412, doi:10.1158/0008-5472.CAN-10-2627 (2011).
163 Li, Y., Choi, P. S., Casey, S. C., Dill, D. L. & Felsher, D. W. MYC through miR-17-92 Suppresses Specific Target Genes to Maintain Survival, Autonomous Proliferation, and a Neoplastic State. *Cancer Cell* **26**, 262-272, doi:10.1016/j.ccr.2014.06.014 (2014).
164 Mestdagh, P. *et al.* MYCN/c-MYC-induced microRNAs repress coding gene networks associated with poor outcome in MYCN/c-MYC-activated tumors. *Oncogene* **29**, 1394-1404, doi:10.1038/onc.2009.429 (2009).
165 Beckers, A. *et al.* MYCN-driven regulatory mechanisms controlling LIN28B in neuroblastoma. *Cancer Letters* **366**, 123-132, doi:10.1016/j.canlet.2015.06.015 (2015).
166 Yang, X. H., Tang, F., Shin, J. & Cunningham, J. M. A c-Myc-regulated stem cell-like signature in high-risk neuroblastoma: A systematic discovery (Target neuroblastoma ESC-like signature). *Sci Rep* **7**, 41, doi:10.1038/s41598-017-00122-x (2017).
167 Barone, G., Anderson, J., Pearson, A., Petrie, K. & Chesler, L. New Strategies in Neuroblastoma: Therapeutic Targeting of MYCN and ALK. *Clinical Cancer Research* **19**, 5814-5821, doi:10.1158/1078-0432.CCR-13-0680 (2013).
168 Puissant, A. *et al.* Targeting MYCN in Neuroblastoma by BET Bromodomain Inhibition. *Cancer Discovery* **3**, 308-323, doi:10.1158/2159-8290.CD-12-0418 (2013).
169 Filippakopoulos, P. *et al.* Selective inhibition of BET bromodomains. *Nature* **468**, 1067-1073, doi:10.1038/nature09504 (2010).
170 Cortés, C., Kozma, S. C., Tauler, A. & Ambrosio, S. MYCN concurrence with SAHA-induced cell death in human neuroblastoma cells. *Cellular Oncology* **38**, 341-352, doi:10.1007/s13402-015-0233-9 (2015).

171 Schnepp, R. W. & Maris, J. M. Targeting MYCN: A Good BET for Improving Neuroblastoma Therapy? *Cancer Discovery* **3**, 255-257, doi:10.1158/2159-8290.CD-13-0018 (2013).
172 Chanthery, Y. H. *et al.* Paracrine Signaling Through MYCN Enhances Tumor-Vascular Interactions in Neuroblastoma. *Science Translational Medicine* **4**, doi:10.1126/scitranslmed.3002977 (2012).
173 Duffy, D. J., Krstic, A., Schwarzl, T., Higgins, D. G. & Kolch, W. GSK3 Inhibitors Regulate MYCN mRNA Levels and Reduce Neuroblastoma Cell Viability through Multiple Mechanisms, Including p53 and Wnt Signaling. *Molecular Cancer Therapeutics* **13**, 454-467, doi:10.1158/1535-7163.MCT-13-0560-T (2014).
174 Chipumuro, E. *et al.* CDK7 inhibition suppresses super-enhancer-linked oncogenic transcription in MYCN-driven cancer. *Cell* **159**, 1126-1139, doi:10.1016/j.cell.2014.10.024 (2014).
175 Lesage, F. *et al.* Expression cloning in K+ transport defective yeast and distribution of HBP1, a new putative HMG transcriptional regulator. *Nucleic acids research* **22**, 3685-3688 (1994).
176 Tevosian, S. G. *et al.* HBP1: a HMG box transcriptional repressor that is targeted by the retinoblastoma family. *Genes & Development* **11**, 383-396, doi:10.1101/gad.11.3.383 (1997).
177 Chen, Y. C. *et al.* Macrophage migration inhibitory factor is a direct target of HBP1-mediated transcriptional repression that is overexpressed in prostate cancer. *Oncogene* **29**, 3067-3078, doi:10.1038/onc.2010.97 (2010).
178 Lee, M.-F. *et al.* N-acetylcysteine (NAC) inhibits cell growth by mediating the EGFR/Akt/HMG box-containing protein 1 (HBP1) signaling pathway in invasive oral cancer. *Oral Oncology* **49**, 129-135, doi:10.1016/j.oraloncology.2012.08.003 (2013).
179 Swanson, K. A. *et al.* HBP1 and Mad1 repressors bind the Sin3 corepressor PAH2 domain with opposite helical orientations. *Nature Structural & Molecular Biology* **11**, 738-746, doi:10.1038/nsmb798 (2004).
180 Lavender, P., Vandel, L., Bannister, A. J. & Kouzarides, T. The HMG-box transcription factor HBP1 is targeted by the pocket proteins and E1A. *Oncogene* **14**, 2721-2728, doi:10.1038/sj.onc.1201243 (1997).
181 Yee, A. S. *et al.* The HBP1 transcriptional repressor and the p38 MAP kinase: unlikely partners in G1 regulation and tumor suppression. *Gene* **336**, 1-13, doi:10.1016/j.gene.2004.04.004 (2004).
182 Pan, K. *et al.* HBP1-Mediated Transcriptional Regulation of DNA Methyltransferase 1 and Its Impact on Cell Senescence. *Molecular and Cellular Biology* **33**, 887-903, doi:10.1128/MCB.00637-12 (2013).
183 Borrelli, S. *et al.* The p63 target HBP1 is required for skin differentiation and stratification. *Cell Death & Differentiation* **17**, 1896-1907, doi:10.1038/cdd.2010.59 (2010).
184 Escamilla-Powers, J. R. *et al.* The Tumor Suppressor Protein HBP1 Is a Novel c-Myc-binding Protein That Negatively Regulates c-Myc Transcriptional Activity. *Journal of Biological Chemistry* **285**, 4847-4858, doi:10.1074/jbc.M109.074856 (2010).
185 Shih, H. H. *et al.* HMG box transcriptional repressor HBP1 maintains a proliferation barrier in differentiated liver tissue. *Molecular and cellular biology* **21**, 5723-5732 (2001).

186 Chen, Y. *et al.* HBP1-mediated Regulation of p21 Protein through the Mdm2/p53 and TCF4/EZH2 Pathways and Its Impact on Cell Senescence and Tumorigenesis. *Journal of Biological Chemistry* **291**, 12688-12705, doi:10.1074/jbc.M116.714147 (2016).
187 Li, H. *et al.* Transcriptional factor HBP1 targets P16INK4A, upregulating its expression and consequently is involved in Ras-induced premature senescence. *Oncogene* **29**, 5083-5094, doi:10.1038/onc.2010.252 (2010).
188 Zhang, X. *et al.* The HBP1 Transcriptional Repressor Participates in RAS-Induced Premature Senescence. *Molecular and Cellular Biology* **26**, 8252-8266, doi:10.1128/MCB.00604-06 (2006).
189 Zhang, Y. *et al.* Mitogen-activated protein kinase p38 and retinoblastoma protein signalling is required for DNA damage-mediated formation of senescence-associated heterochromatic foci in tumour cells. *FEBS Journal* **280**, 4625-4639, doi:10.1111/febs.12435 (2013).
190 Yao, C. J., Works, K., Romagnoli, P. A. & Austin, G. E. Effects of overexpression of HBP1 upon growth and differentiation of leukemic myeloid cells. *Leukemia* **19**, 1958-1968, doi:10.1038/sj.leu.2403918 (2005).
191 Paulson, E. K. *et al.* Alterations of the HBP1 Transcriptional Repressor Are Associated with Invasive Breast Cancer. *Cancer Research* **67**, 6136-6145, doi:10.1158/0008-5472.CAN-07-0567 (2007).
192 Coomans de Brachène, A. *et al.* The expression of the tumour suppressor HBP1 is down-regulated by growth factors via the PI3K/PKB/FOXO pathway. *The Biochemical journal* **460**, doi:10.1042/BJ20131467 (2014).
193 Santo, E. E. *et al.* FOXO3a Is a Major Target of Inactivation by PI3K/AKT Signaling in Aggressive Neuroblastoma. *Cancer Research* **73**, 2189-2198, doi:10.1158/0008-5472.CAN-12-3767 (2013).
194 Li, H., Bian, C., Liao, L., Li, J. & Zhao, R. miR-17-5p promotes human breast cancer cell migration and invasion through suppression of HBP1. *Breast Cancer Research and Treatment* **126**, 565-575, doi:10.1007/s10549-010-0954-4 (2011).
195 Sampson, E. M. *et al.* Negative regulation of the Wnt–β-catenin pathway by the transcriptional repressor HBP1. *The EMBO Journal* **20**, 4500-4511, doi:10.1093/emboj/20.16.4500 (2001).
196 Kim, J. *et al.* Suppression of Wnt signaling by the green tea compound (-)-epigallocatechin 3-gallate (EGCG) in invasive breast cancer cells. Requirement of the transcriptional repressor HBP1. *The Journal of biological chemistry* **281**, 10865-10875, doi:10.1074/jbc.M513378200 (2006).
197 Eskandarpour, M., Huang, F., Reeves, K. A., Clark, E. & Hansson, J. Oncogenic NRAS has multiple effects on the malignant phenotype of human melanoma cells cultured in vitro. *International Journal of Cancer* **124**, 16-26, doi:10.1002/ijc.23876 (2009).
198 Sun, X., Geng, X., Zhang, J., Zhao, H. & Liu, Y. miR-155 promotes the growth of osteosarcoma in a HBP1-dependent mechanism. *Molecular and Cellular Biochemistry* **403**, 139-147, doi:10.1007/s11010-015-2344-z (2015).
199 Tseng, R. C. *et al.* HBP1 promoter methylation augments the oncogenic β-catenin to correlate with prognosis in NSCLC. *Journal of Cellular and Molecular Medicine* **18**, 1752-1761, doi:10.1111/jcmm.12318 (2014).
200 Yan, Z. *et al.* miR-155 contributes to the progression of glioma by enhancing Wnt/β-catenin pathway. *Tumor Biology* **36**, 5323-5331, doi:10.1007/s13277-015-3193-9 (2015).

201 Yan, Z. *et al.* miR-96/HBP1/Wnt/β-catenin regulatory circuitry promotes glioma growth. *FEBS Letters* **588**, 3038-3046, doi:10.1016/j.febslet.2014.06.017 (2014).
202 Benard, J. *et al.* MYCN-non-amplified metastatic neuroblastoma with good prognosis and spontaneous regression: a molecular portrait of stage 4S. *Mol Oncol* **2**, 261-271, doi:10.1016/j.molonc.2008.07.002 (2008).

Part II: research objectives

Everything is theoretically impossible,
until it is done.
~Robert A. Heinlein~

Chapter 2 Research objectives

The discovery of constitutive activating mutations in the ALK receptor tyrosine kinase in familial and sporadic neuroblastoma offers the possibility to design novel therapeutic strategies. However, as indicated above, despite the development of potent inhibitors, tumours often acquire resistance due to second-line aberrations in ALK or due to interference with downstream components of targeted signaling pathways or bypass networks. Therefore, in-depth research into the ALK downstream events is aimed at detecting new vulnerable nodes for therapy of neuroblastoma patients.

2.1.1 Unravelling the mutant ALK downstream signaling pathways in neuroblastoma

The first aim of my PhD thesis was to contribute to the in-depth characterization of the transcriptomic landscape of ALK in neuroblastoma (**paper 1**). For this purpose, gene expression profiling was performed on 10 neuroblastoma cell lines with different ALK status, before and after ALK aberration, both by shRNA-mediated knockdown as pharmacological inhibition. Further, this human, mutant ALK-driven transcriptome was compared with the transcriptionally perturbed genes common in *MYCN/ALK*^{F1174L}-double transgenic versus *MYCN* transgenic mouse. By this strategy, a 77-gene signature was established, which are genes being either consistently up- or downregulated in ALK mutant neuroblastoma. Further, the PI_3K-AKT-mTOR, MAPK and MYC(N) signaling pathways were identified as major ALK downstream axes in neuroblastoma. Moreover, a strong upregulation of MAPK negative feedback loop regulators, RET and RET-driven cholinergic neuronal markers was uncovered in mutant ALK neuroblastoma cells.

2.1.2 Dissecting dynamic gene regulation following ALK inhibition in neuroblastoma

Resistance against a small molecule targeting a receptor tyrosine kinase like ALK, occurs within two years following an initial response. Different resistance mechanisms upon ALK inhibition have been revealed in ALK-driven tumours. For neuroblastoma, it has been shown that the type of mutation can influence the efficiency of a given small molecule. To discover additional genes or pathways

implicated in acquired resistance, the dynamic response upon pharmacological ALK inhibition was investigated in the neuroblastoma CLB-GA (ALK^{R1275Q}) cell line (**paper 2**). This analysis confirmed the downregulation of the PI_3K-AKT-mTOR, MAPK and MYC(N) signaling pathways upon ALK repression in neuroblastoma, starting within 2 hours after treatment. More intriguingly, there was an initial upregulation of positively regulated MYCN target genes, which was followed by the expected downregulation of the overall MYCN activity. Additionally, adrenomedullin (ADM), previously reported to be involved in sunitinib resistance in renal cancer, was identified as the earliest differentially expressed gene upon ALK inhibition.

2.1.3 Investigating the role of HBP1, a possible tumour suppressor gene in neuroblastoma and providing a fourth mechanism for the ALK – MYCN cooperativity.

An ultra-high-risk patient subgroup with both *MYCN* amplification as ALK^{F1174L} mutation has been observed in a previously reported meta-analysis. Subsequently, accelerated tumour formation was observed in a mouse and a zebrafish neuroblastoma model system, when both *MYCN* and ALK^{F1174L} were expressed in sympathetic neuronal progenitor cells. Moreover, ALK controls *MYCN* transcription levels directly and through ERK5, while ALK regulates MYCN protein stabilization via the PI_3K-AKT-GSK3β pathway. Moreover, MYCN transcriptionally activates *ALK*. To identify additional mechanisms for this ALK – MYCN cooperativity, we explored our previously established 77-ALK gene signature. In this way, we identified HBP1, a negative regulator of MYC(N) activity and unravelled a fourth mechanism through which ALK further boosts MYCN (**paper 3**). This study shows that HBP1 is negatively regulated by ALK through the PI_3K-AKT-FOXO3 signaling axis and by MYCN through induction of the miR-17~92 cluster. Moreover, HBP1 inhibits both the transcriptional activation as repressing activity of MYCN, partly through repression of the PRC2 complex. HBP1 overexpression was performed in a neuroblastoma cell line, showing tumour repressive characteristics. More importantly, combined targeting of HBP1 by PI_3K antagonists and MYCN signaling by BET or HDAC inhibitors synergistically represses MYCN activity and significantly reduces tumour growth, suggesting a novel targeted therapy option for the ultra-high-risk patient subgroup with both *MYCN* amplification and ALK^{F1174L} mutation.

Part III: results

Success is the sum of small efforts,
repeated day in and day out.
~Robert Collier~

Part III: results

Chapter 3: Upregulation of MAPK negative feedback regulators and RET in mutant ALK neuroblastoma: implications for targeted treatment

The discovery of constitutive activating mutations in the ALK receptor tyrosine kinase in familial and sporadic neuroblastoma offers the possibility to design novel therapeutic strategies. However, despite potent ALK inhibitors, neuroblastoma tumours often acquire resistance by other aberrations or bypass networks. Therefore, an in-depth characterization of the transcriptomic landscape of ALK in neuroblastoma is needed. In our first paper, we revealed the downstream pathways of mutant ALK in neuroblastoma, by performing gene expression profiling on 10 neuroblastoma cell lines with different ALK status, before and 6 hours after ALK inhibition.

Translational relevance: ALK mutations were the first druggable genetic targets in neuroblastoma patients. While clinical studies were rapidly initiated based on previous experience in adult cancer (mainly lymphoma and lung cancer), the understanding of the downstream consequences of constitutive ALK signaling in neuroblastoma was very limited. This study was amongst the first to provide a detailed insight into the transcriptional effects of activated ALK in neuroblastoma cells and yields the required insights in order to anticipate to putative resistance to ALK targeted therapy or as a guide to further study the causes of emerging drug resistance in the current ongoing trials.

Chapter 4: Early and late effects of pharmacological ALK inhibition on the neuroblastoma transcriptome

To discover additional genes or pathways implicated in acquired resistance upon ALK small molecules, the dynamic response upon pharmacological ALK inhibition was investigated in the neuroblastoma CLB-GA (ALK^{R1275Q}) cell line by gene expression profiling on different time points, between 0 and 6 hours upon treatment with TAE684.

Translational relevance: This study was a follow-up on our first paper describing the ALK-driven transcriptome in neuroblastoma cells and explored the dynamic regulation of ALK target genes. It yielded an unexpected finding of adrenomedullin as regulated gene with putative impact on drugging efficacy and warrants further

investigation. Also, this work should trigger further, more in-depth similar analysis using the newly identified ALK ligands which allow ALK activation studies.

Chapter 5: ALK positively regulates MYCN activity through repression of HBP1 expression

Different groups have confirmed the cooperativity between ALK and MYCN in neuroblastoma tumorigenesis. To identify additional mechanisms for this ALK – MYCN cooperativity and to find possible druggable nodes, we explored our previously established 77-ALK gene signature and identified HBP1, a negative regulator of MYC(N) activity, as a fourth mechanism through which ALK further boosts MYCN.

Translational relevance: Given the previously established observation of the host lab that combined MYCN amplification and ALK mutation marks a patient subgroup with very poor outcome, a deeper understanding of the mechanistic basis of this genetic interaction is of utmost importance. My work allowed to unravel a novel mechanism of ALK-driven regulation of MYCN activity and, in a more broader context, identified for the first time HBP1 as an important regulator of MYCN signaling in neuroblastoma, with a potential to exploit novel drugging options towards targeting MYCN, the major driver oncogene in this tumour.

Chapter 3 Upregulation of MAPK Negative Feedback Regulators and RET in Mutant ALK Neuroblastoma: Implications for Targeted Treatment

Authors: Irina Lambertz, Candy Kumps, Shana Claeys, Sven Lindner, Anneleen Beckers, Els Janssens, Daniel R. Carter, Alex Cazes, Belamy B. Cheung, Marilena De Mariano, An De Bondt, Sara De Brouwer, Olivier Delattre, Jay Gibbons, Isabelle Janoueix-Lerosey, Geneviève Laureys, Chris Liang, Glenn M. Marchall, Michael Porcu, Junko Takita, David Camacho Trujillo, Ilse Van Den Wyngaert, Nadine Van Roy, Alan Van Goethem, Tom Van Maerken, Piotr Zabrocki, Jan Cools, Johannes H. Schulte, Jorge Vialard, Frank Speleman, Katleen De Preter

Paper published in Clinical Cancer Research in 2015

Author contribution:

Irina Lambertz and Candy Kumps performed laboratory experiments and were responsible for the coordination of the experiments, generation of the figures and writing of the paper. Shana Claeys performed laboratory experiments and was involved in the design of the experiments with the second-generation ALK inhibitors, the downstream pathway inhibitors (BEZ-235, Trametinib, Vandetanib) and the treatment of the SK-N-AS cell lines with inducible ALK constructs with TAE684. Furthermore, she was involved in generation of the figures (Fig. 1B, 2A, 5H, 5G, 6 and supplemental data 1, 2A, 7, 11, 15, 16) and provided help in writing the manuscript. Katleen De Preter was responsible for the bio-informatics analysis. Sven Lindner, Anneleen Beckers, Els Janssens, Daniel R. Carter, Alex Cazes, Belamy B. Cheung, Marilena De Mariano, An De Bondt, Sara De Brouwer, Olivier Delattre, Jay Gibbons, Isabelle Janoueix-Lerosey, Geneviève Laureys, Chris Liang, Glenn M. Marchall, Michael Porcu, Junko Takita, David Camacho Trujillo, Ilse Van Den Wyngaert, Nadine Van Roy, Alan Van Goethem, Tom Van Maerken, Piotr Zabrocki, Jan Cools, Johannes H. Schulte, Jorge Vialard, provided valuable discussions and feedback. Katleen De Preter and Frank Speleman coordinated the research, designed experiments and helped writing the paper.

Upregulation of MAPK negative feedback regulators and RET in mutant ALK neuroblastoma: implications for targeted treatment

Authors: Irina Lambertz[1*], Candy Kumps[1*], **Shana Claeys**[1], Sven Lindner[2], Anneleen Beckers[1], Els Janssens[1], Daniel R. Carter[3], Alex Cazes[4], Belamy B. Cheung[3], Marilena De Mariano[5], An De Bondt[6], Sara De Brouwer[1], Olivier Delattre[4], Jay Gibbons[7], Isabelle Janoueix-Lerosey[4], Geneviève Laureys[8], Chris Liang[7], Glenn M. Marchall[3], Michael Porcu[9], Junko Takita[10], David Camacho Trujillo[1], Ilse Van Den Wyngaert[6], Nadine Van Roy[1], Alan Van Goethem[1], Tom Van Maerken[1], Piotr Zabrocki[9], Jan Cools[9], Johannes H. Schulte[2,11,12,13,14], Jorge Vialard[15], Frank Speleman[1**$], Katleen De Preter[1**]

** shared first authors, ** shared last authors*

3.1.1 Affiliations:

1. Center for Medical Genetics, Ghent University Hospital, Ghent, Belgium
2. Department of Pediatric Oncology and Haematology, University Children's Hospital Essen, Germany
3. Kids Cancer Center, Sydneys Childrens Hospital; Children's Cancer Institute, Lowy Cancer Centre, University of New South Wales, Sydney, Australia
4. Unité Inserm U830, Centre de Recherche, Institut Curie, Paris, France
5. Biotherapy Unit, IRCCS AOU San Martino-IST, Istituto Nazionale per la Ricerca sul Cancro, Genoa, Italy
6. Oncology Discovery Research and Early Development, Johnson & Johnson, Beerse, Belgium
7. VP Oncology, Xcovery LLC, West Palm Beach, Florida
8. Department of Pediatric Oncology and Haematology, Ghent University Hospital, Ghent, Belgium
9. Center for Human Genetics, K.U.Leuven - VIB, Leuven, Belgium
10. Department of Pediatrics, Graduate School of Medicine, the University of Tokyo, Tokyo, Japan
11. German Cancer Consortium (DKTK), Germany
12. Translational Neuro-Oncology, West German Cancer Center, University Hospital Essen, University Duisburg-Essen, Essen, Germany
13. German Cancer Research Center (DKFZ), Heidelberg, Germany
14. Centre for Medical Biotechnology, University Duisburg-Essen, Essen, Germany
15. Oncology Discovery Biology, Janssen Research & Development, a division of Janssen Pharmaceutica NV, Beerse, Belgium

3.1.2 Abstract

Purpose: Activating *ALK* mutations are present in almost 10% of primary neuroblastomas and mark patients for treatment with small molecule ALK inhibitors in clinical trials. However, recent studies have shown that multiple mechanisms drive resistance to these molecular therapies. We anticipated that detailed mapping of the oncogenic ALK-driven signaling in neuroblastoma can aid to identify potential fragile nodes as additional targets for combination therapies.

Experimental design: To achieve this goal, transcriptome profiling was performed in neuroblastoma cell lines with the A*LK*^{F1174L} or *ALK*^{R1275Q} hotspot mutations, *ALK* amplification or wild type *ALK* following pharmacological inhibition of ALK using four different compounds. Next, we performed cross-species genomic analyses to identify commonly transcriptionally perturbed genes in *MYCN/ALK*^{F1174L} double transgenic versus *MYCN* transgenic mouse tumours as compared to the mutant ALK-driven transcriptome in human neuroblastomas.

Results: A 77-gene ALK signature was established and successfully validated in primary neuroblastoma samples, in a neuroblastoma cell line with *ALK*^{F1174L} and *ALK*^{R1275Q} regulatable overexpression constructs and in other ALKomas. In addition to the previously established PI_3K/AKT/mTOR, MAPK/ERK and MYC/MYCN signaling branches, we identified that mutant ALK drives a strong upregulation of MAPK negative feedback regulators and upregulates RET and RET-driven sympathetic neuronal markers of the cholinergic lineage.

Conclusions: We provide important novel insights into the transcriptional consequences and the complexity of mutant ALK signaling in this aggressive paediatric tumour. The negative feedback loop of MAPK pathway inhibitors may impact on novel ALK inhibition therapies while mutant ALK induced RET signaling can offer novel opportunities for testing ALK-RET oriented molecular combination therapies.

3.1.3 Statement of translational relevance

Single molecule therapies almost invariably lead to resistance due to oncogene switching and modulation of various regulatory loops. Therefore, a deeper understanding of the nature and plasticity of targeted pathways is required in order to identify fragile nodes that may act as additional targets for combination therapies and to design robust and sustainable treatment strategies. In this study, we established and validated a 77-gene ALK signature in ALK mutant neuroblastomas. We identified a strong upregulation of MAPK negative feedback regulators. While this did not render the cells more sensitive to MEK inhibitors, ablation of negative feedback regulation upon ALK inhibition can impact on other signaling axes within the mutant cells and should be taken into account when monitoring the molecular effects of such treatment or treatment failure. Next, we also discovered mutant ALK upregulation of RET and RET-driven cholinergic markers offering novel opportunities for testing ALK-RET oriented molecular combination therapies.

3.1.4 Introduction

Neuroblastoma is a paediatric malignancy arising from sympatho-adrenergic neural crest progenitor cells of the peripheral nervous system (1). Neuroblastoma originates from a subset of neural progenitor cells that normally differentiate into adrenal chromaffin cells and sympathetic ganglia (2).

Treating neuroblastoma remains a major therapeutic challenge for paediatric oncologists as overall survival for patients with aggressive disease remains disappointingly low despite intensified and optimized treatment protocols (1). Previous research work from our laboratory and others have identified activating mutations in the tyrosine kinase domain of the ALK transmembrane receptor tyrosine kinase, which are found in the majority of hereditary neuroblastoma and occur as somatic defects in 7–10% of sporadic cases (3-6). During embryonic development, ALK is expressed in the central and peripheral nervous system (7), where it may regulate the interplay between cell proliferation and differentiation of the developing sympatho-adrenal cells of the neural crest (1, 8, 9).

The identification of activated ALK in neuroblastoma as a tractable therapeutic target has raised hope for more successful treatment: several small molecule ALK inhibitors have recently gone into clinical trials such as a recent phase 1 clinical trial for crizotinib in patients with refractory neuroblastoma (10, 11). Moreover, these small molecules are also emerging as important novel treatment options for other tumour entities with aberrant ALK activity, including a subset of lung cancers (12). Notwithstanding these encouraging findings, intrinsic and acquired resistance almost inevitably occurs when using single compound treatment for receptor tyrosine kinases or other kinases (13-15), warranting the development of higher affinity inhibitors and the exploration of opportunities for rationally designed combinatorial treatment approaches. To achieve this goal, a more comprehensive understanding of the mutant ALK controlled regulatory network is required including feedforward and feedback loops as well as pathway cross-talk, as these are critical in the adaptive responses of cancer cells leading to therapy resistance.

In this study, we established a robust 77-gene signature marking ALK activity in neuroblastoma cells, using transcriptome profiling. Next, we showed that this signature is preserved in other ALK-driven tumour entities and across *ALK*^{F1174L} -

driven human and murine neuroblastoma tumours and cell lines. First, we confirm the activation of the PI_3K/AKT/mTOR, MAPK/ERK and MYC/MYCN signaling pathways. Secondly, we describe important novel specific insights related to mutant ALK signaling: we demonstrate a strong upregulation of MAPK negative feedback regulators and cross-species genomic analysis revealed that mutant ALK drives the expression of the tyrosine kinase RET as well as a set of RET controlled cholinergic markers. We consider these novel findings as important leads for further studies exploring novel therapeutic combination strategies in ALK mutant neuroblastomas and also offering first insights towards a deeper understanding of the role of ALK signaling in normal sympathetic nervous system development.

3.1.5 Materials and Methods

Cell lines and cell culture

Human neuroblastoma cell lines, anaplastic large cell lymphoma (ALCL) cell lines and non-small cell lung cancer (NSCLC) cell lines (Supplemental Data 1) were cultured in RPMI 1640 medium (Invitrogen) supplemented with foetal bovine serum (10%), kanamycin (1%), penicillin/streptomycin (1%), L-glutamin (1%) and HEPES (25mM) (Life Technologies). Cells were kept at 37°C in a 5%$C0_2$/95%0_2 humidified environment. Details on determining GI_{50} values are described in the Supplemental M&M file.

Pharmacological ALK and RET inhibition and shRNA mediated ALK knockdown in neuroblastoma cell lines

Detailed information can be found in Supplemental M&M. In summary: Human wild type *ALK* (SK-N-AS, NGP, IMR-32), ALK^{R1275Q} (CLB-GA, LAN-5, UKF-NB-3), ALK^{F1174L} (SK-N-SH, Kelly, SMS-KCNR) and *ALK* amplified (NB-1) neuroblastoma cell lines were treated in triplicate with 0.3μM NPV-TAE-684 (Novartis/SelleckChem, further referred to as TAE-684) or DMSO (VWR) for 6 hours, followed by RNA isolation and gene expression profiling (see further). CLB-GA was further treated with ALK, MEK, PI_3K/mTOR or RET inhibitors. A gene expression time series for ALK inhibition was performed in CLB-GA cells at 0 – 10’ – 30’ – 60’ – 120’ – 240’ – 360’

time points. For shRNA mediated knockdown, pGIPZ-ALK shRNAmir and pGIPZ-non-silencing control shRNAmir vectors were used (Open Biosystems).

Establishment of inducible SK-N-AS *ALK*^{wt}, *ALK*^{F1174L} and *ALK*^{R1275Q} cell lines

Human neuroblastoma SK-N-AS cells were electroporated with pcDNA6/TR (Invitrogen) using the Neon® Transfection System (Life Techologies). Single cell clones were generated using blasticidin (7.5µg/ml) and limited dilution. Using a TetR antibody (Clonetech), the clone with the highest TetR expression was selected (named SK-N-AS-TR) and used for the transfection with pT-REx-DEST30-*ALK*, *ALK*^{F1174L} or *ALK*^{R1275Q}. After transfection of SK-N-AS-TR with the *ALK* variants, single cell clones were raised using geneticin (500 µg/ml) and limited dilution, while blasticidin treatment was continued as described above. Clones with moderate expression of the *ALK* variants were selected for further experiments using RT-qPCR (ALK_fwd: ccatcattttggagaggattgaat; ALK_rev: gaacccccctcagggtcctt) and Western Blot.

***Th-MYCN* neuroblastoma progression model**

Homozygous *Th-MYCN* transgenic mice (16) were sacrificed at day seven (n=4) and day fourteen (n=4) of life to harvest sympathetic ganglia containing foci of neuroblast hyperplasia and at week 6 to harvest advanced neuroblastoma tumours (n=4). Additionally, we have dissected the same sympathetic ganglia from wild type mice at day seven (n=4), day fourteen (n=4) and week 6 (n=4) to control for mRNA expression changes during normal development (17).

RNA extraction, RT-qPCR and gene expression profiling

Details on RNA extraction and RT-qPCR are described in Supplemental M&M. Gene expression profiling was performed using Affymetrix HG-U133plus2 arrays or Sureprint G3 human GE or G3 Mouse GE 8x60K microarrays (Agilent Technologies). Data were summarized and normalized with the gcRMA and vsn method (for Affy and Agilent data, respectively) (18), in the R statistical programming language using the affy, gcrma and limma packages. Data can be accessed via ArrayExpress (E-MTAB-3205, E-MTAB-3206, E-MTAB-3207).

Protein isolation, antibodies and Western blotting

Total protein lysates were harvested after washing with ice-cold PBS and total protein isolation was carried out using RIPA lysis buffer, containing Complete Protease Inhibitor Cocktail (Roche Diagnostics) and PhosSTOP Phosphatase Inhibitor (Roche Diagnostics). Antibodies directed against phosphorylated ALK (Y1604), total ALK (C26G7), phosphorylated RET (Y905), total RET (C31B4), secondary anti-rabbit and anti-mouse antibodies were obtained from Cell Signaling. Antibodies directed against the loading control proteins β-actin and α-tubulin were obtained from Sigma Aldrich.

Published datasets

Validation of the ALK signature was performed using signature score analysis in published datasets of neuroblastoma tumours (E-MTAB-161 (19), Oberthuer dataset), neuroblastoma mice tumours (GSE32386 (20)) and other ALK-driven tumour entities, including NSCLC (GSE25118 (21)) and ALCL (GSE14879 (22), GSE6184 (23)). In addition, signature score analysis was performed in a partly published dataset of mRNA expression data of 283 neuroblastoma tumour samples (NRC dataset (24, 25)). In addition, GSE42762 (26) was used to check RET levels upon FOXO3a activation and PI_3K/AKT inhibition.

Data-mining

ALK-, RET-, MAPK/ERK-, PI_3K/AKT/mTOR- signature identification

An ALK signaling signature was established using differential expression analysis with the Rank Product (RP) algorithm. Genes that were significantly ($p<0.05$) up- or downregulated after TAE-684 treatment in at least 3 cell lines and that showed a (log)fold-change of at least 1.2 after shRNA treatment were included in the ALK signature (Figure 1A). MAPK/ERK, PI_3K/AKT/mTOR and RET signature genes were established by differential expression analysis (Limma) of CLB-GA cells treated with the respective inhibitor versus DMSO treatment.

Signature score analyses

Signature score analysis was performed using a rank-scoring algorithm as described in Fredlund *and colleagues* (27). In short, for each sample expression values were transformed to ranks (a rank of 1 matching with the lowest expressing gene). Next,

rank scores for the signature genes were summed for each sample generating a signature score. Correlation of the score with survival was tested using Kaplan-Meier plots and log-rank analysis by grouping the samples in four quartiles (R-survival package). Comparison of signature scores or expression between groups of samples was done using the Mann-Whitney test (R-base package). Signature score correlation analysis was performed using Pearson correlation analysis (R-base package).

Pathway analysis: GO, GSEA, CMAP and cross-species genomics analysis

The probe-id lists of the ALK signature were submitted to DAVID for gene ontology (GO) analysis (28) and to the Connectivity Map database (29) for identification of drugs with similar transcriptional responses as ALK inhibition. Geneset enrichment analysis (30, 31) was performed using the C2 geneset catalogue (genetic and chemical perturbations). This analysis was performed on each cell line separately using the fold changes of TAE-684 versus DMSO treatment and the shALK versus scrambled control transduction. Genesets that were overrepresented in at least 3 cell lines after both ALK inhibitor treatment and shRNA knockdown were withheld. Cross-species genomic analysis was performed by looking for the overlap of the ALK signature genes and the list of differentially expressed genes (RP analysis) for *MYCN* versus ALK^{F1174L}-driven or double transgenic tumours.

3.1.6 Results

A 77-gene signature marks constitutive ALK signaling in neuroblastoma cells

The transcriptional consequences of constitutive oncogenic ALK signaling were determined through ALK perturbation experiments in 10 neuroblastoma cell lines with either of the two hotspot mutations ALK^{F1174} and ALK^{R1275}, high-level *ALK* amplification (ALK^{amp}) or wild type *ALK* (ALK^{wt}) [protein levels of phospho-ALK (pALK) and ALK are provided in Supplemental Data 3]. We performed pharmacological inhibition with ALK inhibitor TAE-684 and controlled for off-target effects by shRNA treatment directed against ALK. Gene expression profiling was performed following 6 hours of TAE-684 treatment or 2 days post shRNA transduction (mRNA and protein expression levels of ALK are provided in

Supplemental Data 4). Importantly, TAE-684 treatment resulted in a marked transcriptome perturbation in all ALK activated cell lines whereas no significant effects on the transcriptome were observed in the SK-N-AS cell line with undetectable *ALK* protein expression. Overall, transcriptional responses in shALK treated cell lines showed similar direction of responses in the majority of up- or downregulated genes albeit with lower fold changes, probably due to incomplete knockdown of ALK (Supplemental Data 5).

Next, we established a gene expression signature recapitulating constitutive ALK signaling in neuroblastoma. Using differential expression analysis of the above described transcriptome data (of both TAE-684 treated cell lines and shALK treated cells to control for off-target effects), we generated an ALK signature, consisting of 32 downregulated (49 probe-ids) and 45 upregulated (61 probe-ids) genes (see M&M and Figure 1A for details). The expression of these signature genes is visualized in Figure 1B for CLB-GA upon ALK inhibition and for the 10 cell lines in Supplemental Data 6 for TAE-684 ALK inhibition. The differential expression pattern for these 77-genes was highly reminiscent in the CLB-GA cell line treated with three additional ALK small molecule inhibitors currently under evaluation in clinical trials: crizotinib, X-396 and LDK-378 (10, 32) further supporting the validity of the established 77-gene ALK signature (Figure 1B). In addition, significant correlation was found between the signature scores for TAE-684 versus the three other compounds in 2 independent datasets as shown in Figure 1C and D. about 44%, 49% and 66% of the 77 signature genes were shown to be significantly differentially expressed in CLB-GA upon crizotinib, X-396 and LDK-378 treatment, respectively (with significant overlap according to Fisher's exact test, data not shown).

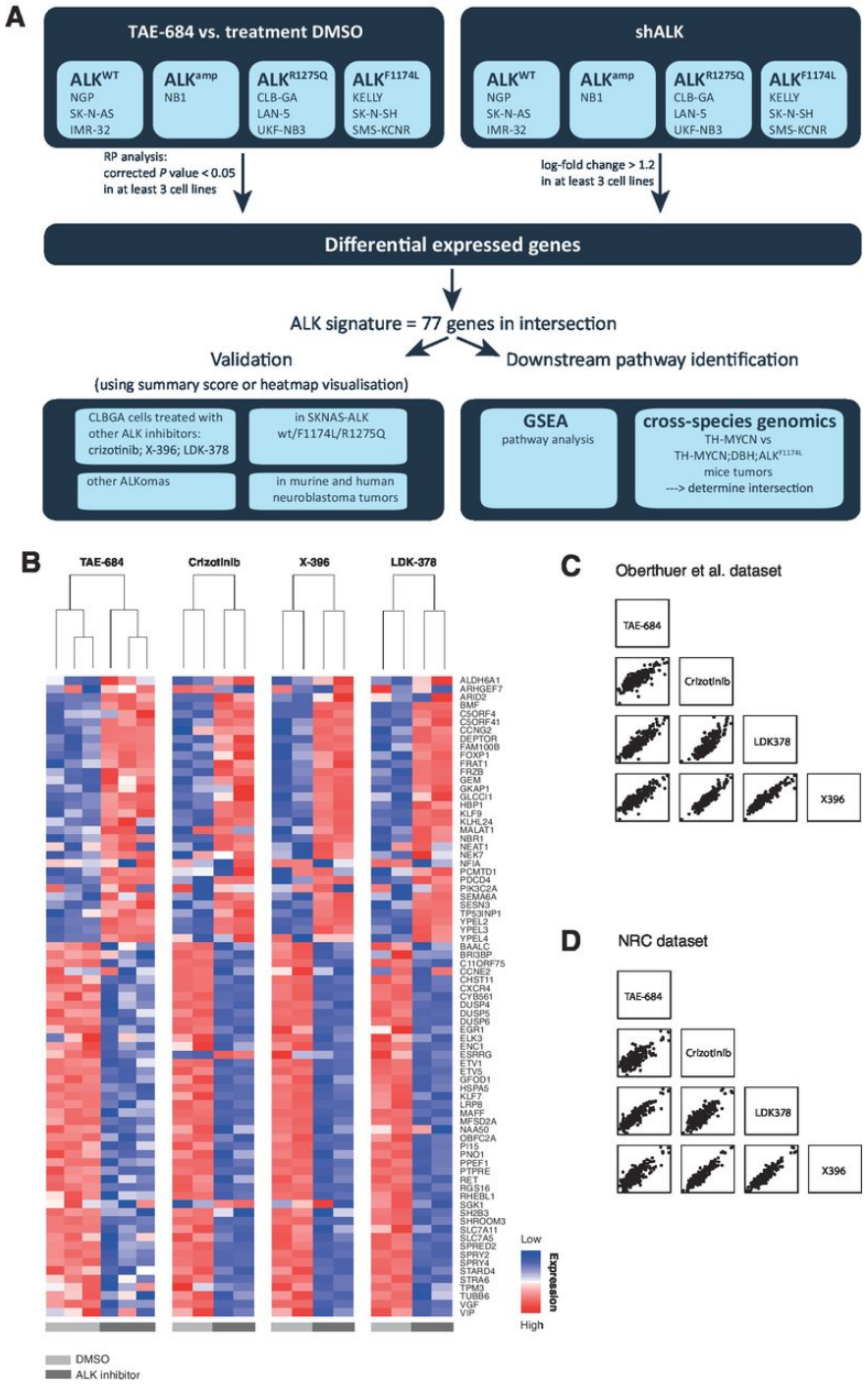

Figure 1: The 77-gene signature marks constitutive ALK signaling in neuroblastoma.

A. Data-mining workflow. **B.** Hierarchical clustering and heatmap representation of the expression levels of the 32 down- and 45 upregulated genes from the ALK signature in the neuroblastoma cell line CLB-GA after pharmacological ALK inhibition using four different small molecule inhibitors (TAE-684, crizotinib, X-396 and LDK-378). **C. & D**. Signature scores for each of the three different ALK compounds are all significantly correlated with the 77-gene ALK signature scores in 2 independent neuroblastoma patient sample sets (i.e. the Oberthuer dataset and the NRC dataset).

The ALK signature score is elevated in SK-N-AS cells overexpressing the *ALK*^{F1174L} and *ALK*^{R1275Q} hotspot mutations, but not in *ALK*^{wt}-overexpressing SK-N-AS cells

Next, we investigated whether the ALK signature also marks *de novo* constitutive activation of the mutant ALK receptor. To this end, we generated and performed transcriptome profiling of the SK-N-AS cell lines with tetracycline-inducible overexpression of *ALK*^{F1174L}, *ALK*^{R1275Q} and *ALK*^{wt}. Whereas overexpression of all ALK isoforms resulted in robust accumulation of the protein upon tetracycline-induction, only *ALK*^{F1174L} and *ALK*^{R1275Q} showed constitutive Y1604 phosphorylation (Supplemental data 7A). Indeed, it has been shown previously that even upon overexpression, wild type ALK displays significantly reduced (to absent) kinase activity compared to the mutant ALK isoforms and is inefficient in transforming NIH3T3 cells (4). Consistent with these data, *de novo* mutant ALK activation in the SK-N-AS cell line showed to be very well represented by an increased ALK signature score (i.e. a summary score of the expression of the 77-gene ALK signature) when compared to cells overexpressing wild type *ALK*, thus confirming the robustness of the developed gene signature list (Figure 2A; Supplemental Data 7B & C).

ALK signature scores are elevated in primary human and murine mutant *ALK* neuroblastomas and downregulated in crizotinib treated *MYCN/ALK*-driven mice tumours

To validate how well the cell line-based ALK downstream transcriptional profile recapitulates ALK oncogenic activity, we evaluated ALK signature scores in two independent gene expression datasets consisting of respectively 252 and 283 neuroblastoma tumours (19, 24, 25), as well as data of two *in vivo* neuroblastoma model systems (20). In human primary tumours with *ALK* amplification or *ALK* mutations, ALK signature scores were significantly higher as compared to *ALK* wild type tumours (Figure 2B & D). Moreover, increased ALK signature scores correlate to poor overall (OS) (Figure 2C & E) and event-free survival (EFS) (Supplemental Data 8A & B) also in tumours with wild type *ALK*, pointing at a possible role of ALK signaling in wild type *ALK* tumours. Additionally, we could show that *Dbh-ALK*^{F1174L}-driven murine neuroblastoma tumours have significantly higher ALK signature scores

than *Th-MYCN*-driven murine neuroblastoma tumours and normal adrenal tissue (published in (20)).

Most interestingly, we could confirm the validity of the ALK signature in compound treated tumour samples. Indeed, crizotinib treated *Th-MYCN;KI-Alk*^{R1297Q} tumours have reduced ALK signature scores compared to untreated tumours (Figure 2F).

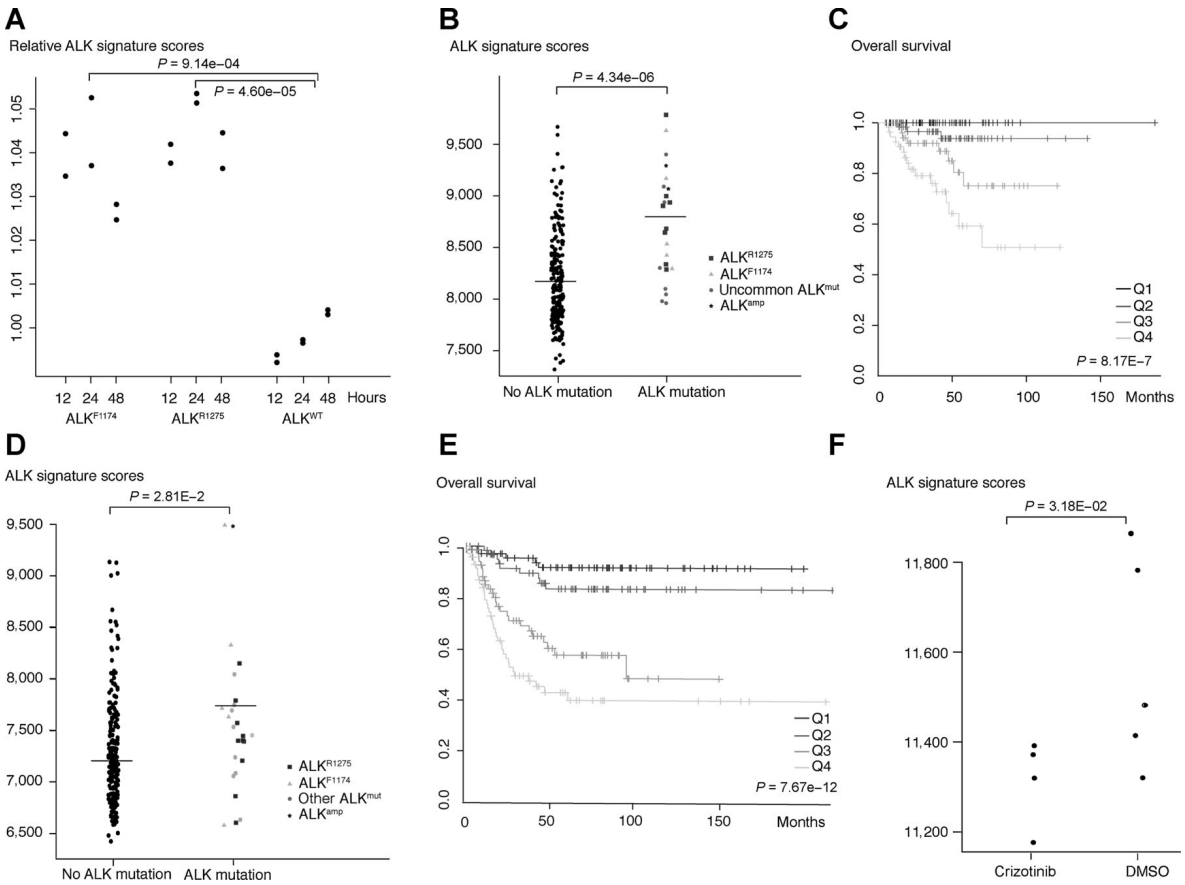

Figure 2: *In vitro* and *in vivo* validation of the ALK signature in SK-N-AS cells overexpressing mutant ALK, in primary human tumours and crizotinib treated mice tumours.

A. Relative ALK signature scores (relative to non-induced SK-N-AS) are significantly higher in SK-N-AS cells after tetracycline induction of *ALK*^{F1174L} and *ALK*^{R1275Q} as compared to SK-N-AS cells with tetracycline-induced *ALK*^{wt}. **B & D.** ALK signature scores are significantly higher in tumours with ALK mutations compared to tumours without ALK mutations (uncommon ALK mutation types include: F1245V, G1128A, I1170S, I1170T, L1240V and T1151M). **C & E.** ALK signature score significantly correlates with overall survival of the neuroblastoma patients (Q1 – Q4= lowest– highest quartile of scores) in 2 independent datasets. **F.** ALK signature scores in tumours of *Th-MYCN;KI-Alk*^{R1297Q} transgenic mice treated with crizotinib are lower than in control (DMSO) treated tumours.

ALK signature score assessment in other primary ALKomas and compound treated tumours shows a common ALK-deregulated transcriptome

Next, we analysed publically available gene expression datasets from other ALK-driven tumour entities (ALKomas). Indeed, we identified high activity scores in primary ALK rearranged anaplastic large cell lymphoma tumours (ALCLs) (Figure 3A) (22). Furthermore, activity scores also decreased in non-small cell lung carcinoma (NSCLC) xenografts and in ALCL cell lines following ALK abrogation (either through tyrosine kinase inhibitors or ALK shRNA) (21, 23) (Figure 3B & C). This observation suggests a significant overlap in activated downstream signaling pathways in different ALKoma entities.

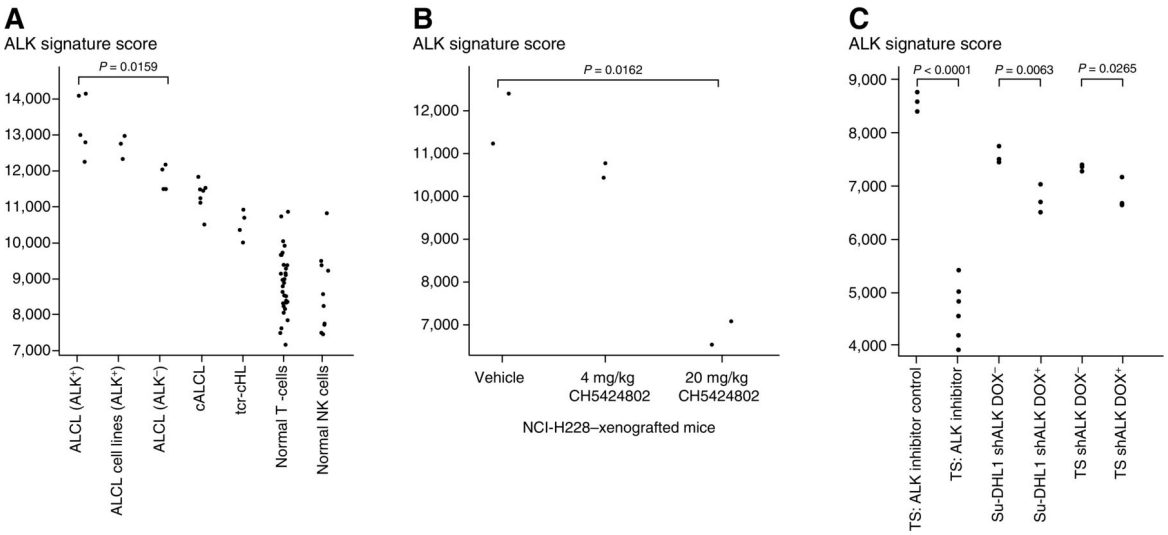

Figure 3: *In vitro* and *in vivo* validation of the ALK signature in other primary ALKomas and ALK-inhibited tumours and cell lines.

A. ALK signature scores are significantly higher in ALK-positive ALCL tumours and cell lines compared to ALK negative ALCL tumours (cALCL = cutaneous ALCL tumours, tcr-cHL = tumour cell rich-classical Hodgkin Lymfoma tumours). **B.** ALK signature scores are significantly lower for NCI-H2228 (NSCLC) xenografts treated with 20 mg/kg of the ALK inhibitor CH5424802 (alectinib). **C.** ALK signature scores are significantly lower in ALCL cell lines TS and Su-DHL1 treated with ALK inhibitor or DOX activated shALK compared to control treated cell lines.

Mutant ALK activates PI_3K/AKT/mTOR, MAPK and MYC/MYCN signaling

Gene set enrichment analysis (GSEA) on ALK inhibitor treated cell lines yielded enriched gene sets linked to EGFR, PI_3K/AKT/mTOR, and MYC/MYCN signaling

pathways (Supplemental Data 9) in keeping with previous reports (3-6, 20, 33, 34). Subsequent gene ontology (GO) analysis applied to the list of 77 ALK regulated genes showed that MAPK signaling genes were enriched among the ALK upregulated genes, whereas genes driving cell cycle arrest and apoptosis were represented in the downregulated gene set (Supplemental Data 10).

To further examine which genes are under control of the MAPK and PI_3K/AKT/mTOR signaling branches activated by mutant ALK, we measured the transcriptional effects of trametinib (MEK inhibitor) and BEZ-235 (a dual PI_3K/mTOR inhibitor) in the *ALK*^{R1275Q}-mutant CLB-GA cell line. Using this approach, we identified 19 and 42 ALK signature genes, which were differentially expressed following trametinib or BEZ-235 treatment respectively (Supplemental data 11). A prominent role for mutant ALK-driven PI_3K/AKT/mTOR signaling also emerged from Connectivity Map analysis, yielding LY-294002, sirolimus and wortmannin as top ranked inhibitors targeting the PI_3K/AKT/mTOR pathway (Supplemental data 12).

Mutant ALK upregulates MAPK feedback inhibition regulators

Time series analysis (10'-30'-60'-120'-240'-360') of gene expression profiles after exposure of the *ALK*^{R1275Q} positive CLB-GA cells to TAE-684 showed a gradual decrease in ALK signature score starting from 2h towards near extinction 6h after treatment (Figure 4A). This is also represented in the time-dependent modulation of transcription levels of ALK regulated genes (Figure 4B). Furthermore, GSEA analysis reveals that the overall transcriptional response following ALK inhibition is obvious from 2h at which point MAPK pathway driven gene expression shows the most prominent decrease (Supplemental Data 13). Indeed, six of these genes, DUSP4, DUSP5, DUSP6, SPRY2, SPRY4 and MAFF, mark the earliest transcriptional responses with a strong decrease two hours after ALK inhibition (Supplemental Data 14; Figure 4B red arrows). Interestingly, these genes are upregulated in SK-N-AS cell lines upon regulable mutant *ALK* overexpression, indicating that this negative feedback loop is readily installed subsequent to ALK-driven pathway activation (Figure 4C).

These genes are known negative regulators of growth factor signaling, controlling transcription-dependent feedback attenuation. This observation is reminiscent to the effects of MAPK feedback inhibition as described in BRAF^{V600E}-mutant melanoma

(35), but has so far not been observed in mutant receptor tyrosine kinase signaling. This observation prompted us to test MEK inhibitor (trametanib) in a panel of neuroblastoma cell lines. However, responses to the compound were very modest (Supplemental Data 16).

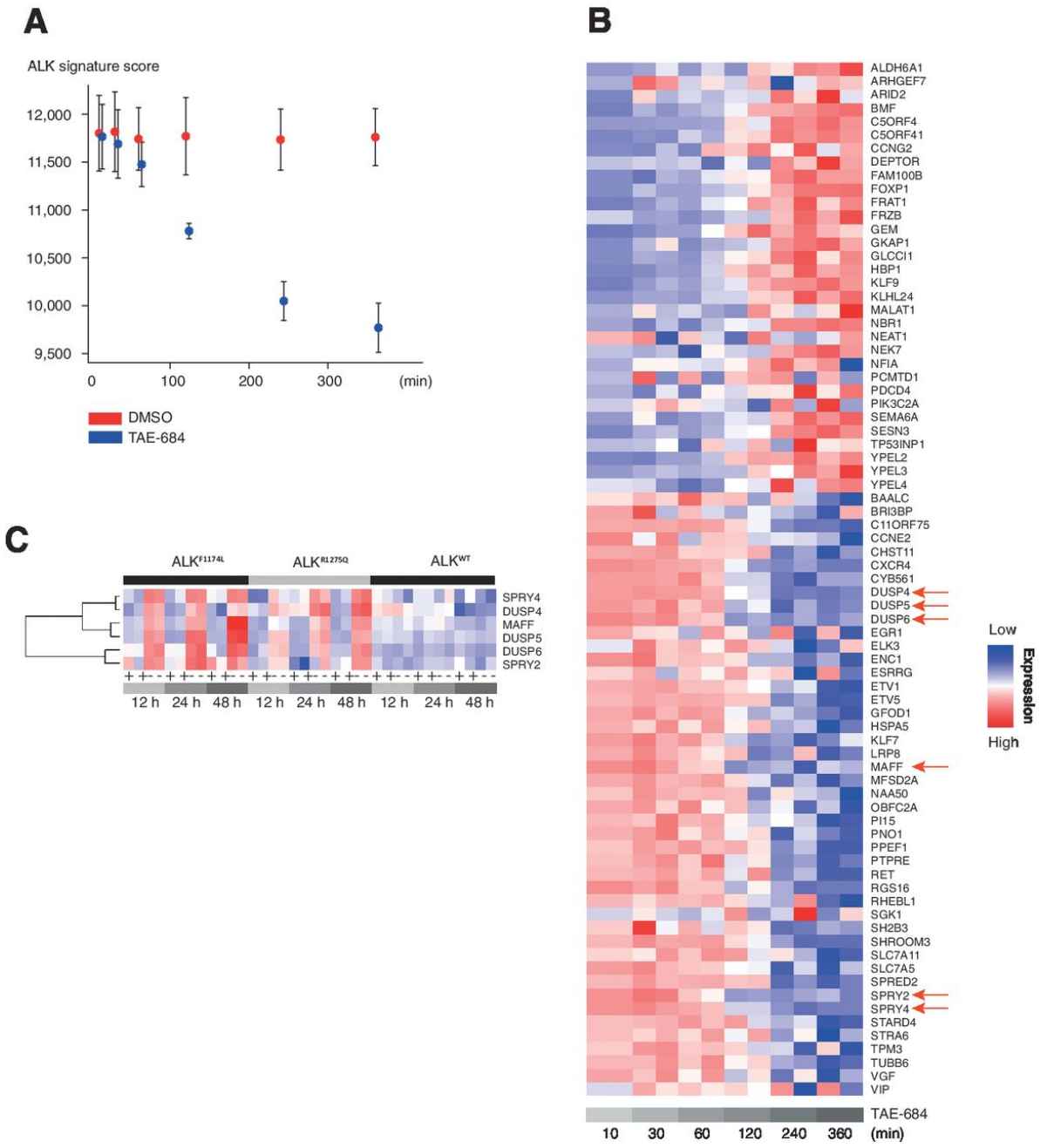

Figure 4: Time series analysis of ALK inhibitor treated CLB-GA reveals increased expression of MAPK inhibitors.

A. ALK signature score significantly decreases from 120 minutes after pharmacological ALK inhibition of the CLB-GA cell line using TAE-684 (red = DMSO, blue = TAE-684). **B.** Heatmap representation of the expression levels of the ALK signature genes at different time points

after pharmacological ALK inhibition using TAE-684 in the neuroblastoma cell line CLB-GA. The red arrows in the heatmap indicate 6 MAPK pathway genes that are inhibited 2 hours after ALK inhibition. **C.** The expression of the 6 genes that mark the earliest transcriptional response upon ALK inhibition is increased upon mutant ALK activation and not upon wild type ALK activation in the SK-N-AS model system.

Mutant ALK upregulates markers of adrenergic and cholinergic neuronal differentiation

Next, a stringent cross-species genomics analyses for differentially expressed genes in *MYCN*- versus *ALK*^{F1174L}-driven murine neuroblastoma tumours (16, 20), yielded 7 genes expressed significantly higher in *ALK*^{F1174L}*;Dbh-i*Cre positive neuroblastoma tumours. In addition to 3 known MAPK regulated genes (*SPRY4, DUSP6, ETV5*) also 4 neuronal markers were identified*: RET*, *ENC1*, *VGF* and *VIP*. Interestingly, additional comparison between the 77-gene ALK signature and the differentially expressed genes between *Th-MYCN;ALK*^{F1174L}*;Dbh-i*Cre-driven versus *Th-MYCN*-driven murine tumours, further reduced this list to *RET*, *ETV5*, *VGF* and *VIP*. Importantly, RET and VIP are part of a gene regulatory network determining noradrenergic and cholinergic sympathetic subtypes during neuronal development (36). Moreover, VGF is expressed in the developing adrenal gland and it is transcriptionally regulated by RET in PC12 cells (37, 38).

Further investigation of additional adrenergic and cholinergic markers in the mice tumours showed higher expression levels for both cholinergic and adrenergic marker genes in double transgenic *Th-MYCN;ALK*^{F1174L}*;Dbh-i*Cre tumours compared to those from *Th-MYCN* mice (Figure 5A). This was confirmed in an independent set of tumours obtained from *Th-MYCN;Th-ALK*^{F1174L} mice (Figure 5B) (20, 33). Moreover, in a dataset of primary human neuroblastoma tumours, we observed that the expression of the cholinergic genes is significantly higher in human primary neuroblastoma with aberrant ALK activation (Figure 5C) (19).

Further, we also observed low expression of both cholinergic and adrenergic markers in *Th-MYCN* tumours. Interestingly, in pre-neoplastic lesions isolated from *Th-MYCN* mice (17), dramatic downregulation of both the adrenergic and cholinergic markers was observed in full-blown tumours as compared to early hyperplastic lesions in sympathetic ganglia of transgenic mice, whereas expression levels remained unchanged during development of wild type mice ganglia (Figure 5D).

Collectively, these data point to a very distinct cholinergic/adrenergic phenotype in *MYCN* versus *MYCN;ALK*-driven neuroblastomas.

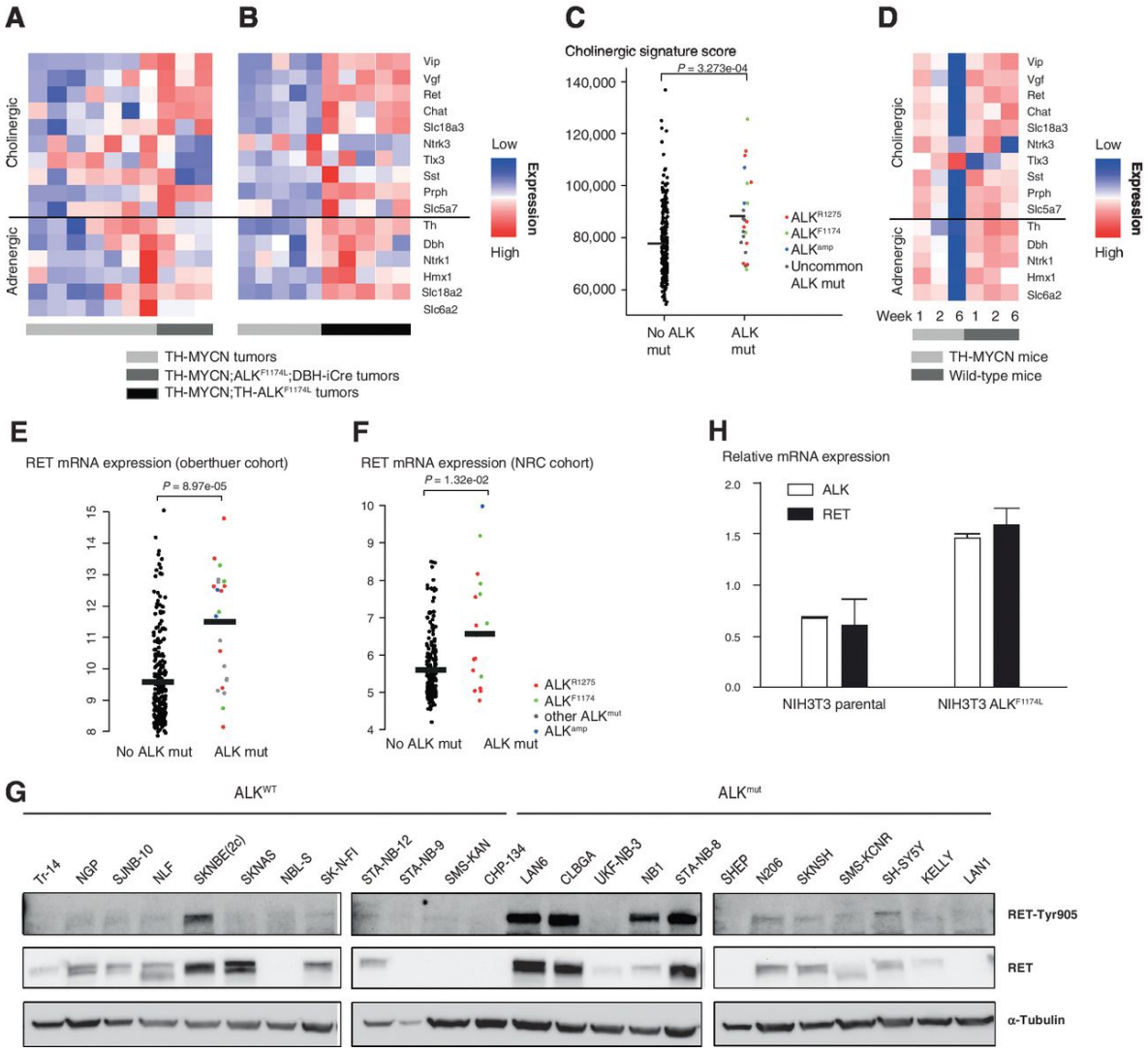

Figure 5: Mutant ALK upregulates markers of adrenergic and cholinergic neuronal differentiation including RET.

A-B. Hierarchical clustering and heatmap representation of the expression levels of cholinergic and adrenergic marker genes in two independent sets of *MYCN/ALK^{F1174L}* double transgenic versus *Th-MYCN*-driven mice tumours. There is an upregulation of these markers in the double transgenic mice tumours compared to the *Th-MYCN* mice tumours. **C.** Cholinergic signature scores are significantly higher in human primary neuroblastomas tumours with mutant ALK (uncommon ALK mutation types include: F1245V, G1128A, I1170S, I1170T, L1240V and T1151M). **D.** The expression of the adrenergic and cholinergic marker genes decrease steeply during tumour initiation from pre-neoplastic lesions (at week 1 and 2) to full-blown tumours in the *Th-MYCN* mouse model (at week 6). **E & F.** RET expression levels are significantly higher in primary tumours with mutant ALK versus tumours

with wild type ALK in 2 independent primary tumour datasets. **G.** RET protein expression and phosphorylation status in 12 ALK^{wt} and 12 ALK^{mutant} cell lines. **H.** Upregulation of RET expression levels in NIH3T3 cell line transformed by ALK^{F1174L} (RT-qPCR).

Increased RET expression in primary neuroblastomas and cell lines

An important driver of the sympathetic neuronal markers of the cholinergic lineage is the RET gene. Comparison of RET expression levels in ALK mutated and wildtype neuroblastoma tumour samples showed a significant higher expression in ALK mutant versus ALK wild type samples in 2 independent datasets of primary neuroblastoma tumour samples (Figure 5E & F).

In addition, RET expression levels showed strong correlation with the 77-gene ALK signature scores in two independent patient sample datasets, providing strong support for ALK regulation of RET transcription (Figure 6D & E).

Importantly, we also confirmed RET total protein expression in 8 out of 12 *ALK* wild type neuroblastoma cell lines (66.7%) and in 10 out of 12 neuroblastoma cell lines with *ALK* mutation (83%), with moderate to strong RET phosphorylation (Tyr905) observed in 7 out of 12 ALK mutant cell lines (58%) and in one ALK wild type cell line (8%) (Figure 5G). Taken together, these data show more pRET-positive mutant ALK cell lines and also more pronounced pRET levels in ALK mutant cell lines versus ALK wild type cell lines (Fischer exact test: p-value = 2.72e-2).

Mutant ALK regulates the expression of RET through FOXO3 and renders cells sensitive to RET pharmacological inhibition

Given the above findings, we sought for further mechanistic evidence for regulation of RET mRNA levels by mutant ALK. To this end, we determined RET expression levels in NIH3T3 cells transformed by mutant ALK^{F1174L}. These cells were previously reported by Chen *and colleagues* (4) as a cellular model that demonstrates the transforming capacity of the ALK^{F1174L} mutation. Using this model system, we observed a robust 2-fold upregulation of RET mRNA levels in NIH3T3-ALK^{F1174L} cells compared to the parental NIH3T3 cell line (Figure 5H).

Given the previously described regulation of FOXO3a by PI_3K/AKT signaling (26) and the observation that the related FOXO1 controls RET expression in mouse spermatogonial stem cells (39), we tested the possibility that FOXO3a could regulate RET under the control of mutant ALK. Pharmacological inhibition of mutant ALK

using LDK-378 clearly leads to the expected loss of FOXO3a phosphorylation (leading to activation of FOXO3a) (Supplemental Data 15 B). Next, we investigated published data on overexpression of FOXO3a in neuroblastoma cells (26) and observed strong repression of RET mRNA expression following activation of FOXO3a in combination with PI_3K/AKT inhibition (Supplemental Data 15 A). Taken together, these data convincingly show that RET expression is under direct control of mutant ALK.

Next, we explored the effect of RET inhibition for the clinically approved drug vandetanib (RET knock-down in Figure 6A) in 5 neuroblastoma cell lines (4 ALK mutant cell lines with varying RET phosphorylation levels, and 1 ALK wild type cell line with RET phosphorylation). All mutant ALK cell lines responded to vandetanib, with strongest effects observed for CLB-GA cells, while the ALK wild type cell line SK-N-BE2C showed no significant response to the compound (Figure 6B).

Finally, to determine on a more global scale whether RET-driven-signaling partially recapitulates mutant *ALK* signaling, we performed gene expression analysis of CLB-GA cells following vandetanib treatment. Strikingly, the 77-ALK signature genes identified following TAE-684 treatment also showed to be regulated in the same direction following vandetanib treatment, strongly suggesting that RET contributes to ALK-driven neuroblastoma tumours (Figure 6C). This was further illustrated by the strong correlation observed between vandetanib and ALK signature scores in two independent tumour datasets (Figure 6D & E).

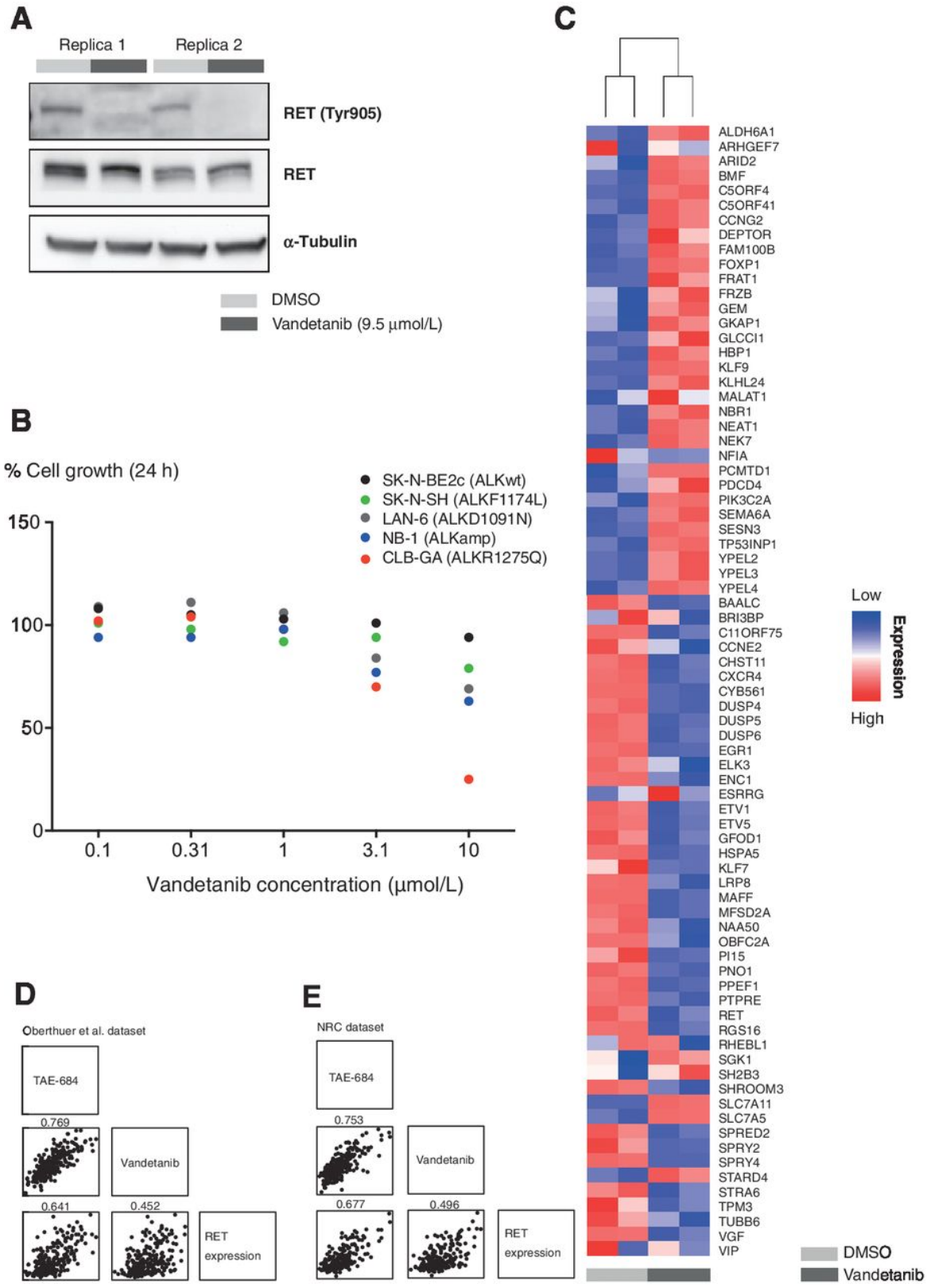

Figure 6: Expression of ALK signature genes after RET-inhibition.

A. Western blot analysis of phospho-RET and total RET in CLB-GA cell line after pharmacological inhibition of RET using the small molecule inhibitor vandetanib shows clear decrease of (p)RET expression. **B.** Sensitivity of wild type and mutant ALK cell lines to

vandetanib in cell lines SK-N-SH (with low pRET levels) and SK-N-BE2c, NB-1, LAN-6, CLB-GA (with high pRET levels). **C.** Hierarchical clustering and heatmap representation of the expression levels of the 77 genes of the ALK signature in neuroblastoma cell line CLB-GA after pharmacological RET inhibition using the small molecule inhibitor vandetanib. **D & E.** scatter plots of the TAE-684 and vandetanib signature scores and ALK and RET expression levels in 2 independent datasets. Correlation coefficients are indicated on top of the scatter plots.

3.1.7 Discussion

Detailed insights into ALK signaling and its possible interference with other signaling pathways is of utmost importance when introducing small molecule inhibitors in the clinic, as this may yield improved tools for measuring and predicting therapy response. Also, a deeper understanding of signaling cascades driven by genetic changes and their complex intertwined compensatory regulatory programs activated during tumorigenesis will be a prerequisite for identification of druggable downstream targets for novel combination therapies.

Here, we describe the repertoire of ALK-driven transcriptional alterations in neuroblastoma cells. Using a combined approach of pharmacological inhibition and shRNA knockdown of ALK, we identified a signature of 32 up- and 45 downregulated genes (ALK signature) and validated this signature in an *in vitro* cellular model for regulable ALK^{F1174L} as well as human and murine neuroblastomas. Of further interest, also other ALK-driven tumour entities displayed higher ALK signature scores, thus underscoring the robustness of the developed gene list and revealing a significant overlap in activated downstream signaling pathways in different ALKoma entities. Finally, pathway dissection of the mutant ALK-driven transcriptome was in accordance with activation of the MAPK/ERK, PI_3K/AKT/mTOR and MYC/MYCN signaling as described (3-6, 20, 33, 34, 40). Connectivity Map analysis as well as comparison of the ALK gene signature and the transcriptionally regulated genes upon PI_3K/mTOR inhibition pointed at a major role of the PI_3K/AKT/mTOR pathway downstream of ALK in neuroblastoma. These findings are in concordance with the observations of Berry *and colleagues* (33), who showed a synergistic effect of crizotinib and Torin2 treatment of double transgenic mouse tumours. Both

observations further emphasize the possible role of PI_3K/mTOR inhibitors in new combinatorial treatment schemes for ALK-positive neuroblastoma tumours.

Importantly, our study uncovered two major novel insights, that is, (i) the observation of upregulation of MAPK feedback inhibitors including DUSPs, SPRYs and MAFF and (ii) regulation of RET and cholinergic/adrenergic neuronal differentiation genes through mutant ALK. Of notice, despite the fact that DUSP genes function as negative regulators of MAPKs, their gain of expression has often been correlated with cancer progression, drug resistance and poor prognosis (41). A similar constitutively activated MAPK feedback loop has been observed in $BRAF^{V600E}$-mutant melanoma cells (35). The exact role of this aberrant feedback loop is poorly understood but could reflect the cellular response to cell cycle arrest and oncogene-induced senescence, keeping in mind that these can be triggered by sustained over-activation of ERK and presence of $BRAF^{V600E}$-mutations (41). In this scenario, elevated expression of DUSPs and other negative feedback regulators might dampen the primary cellular response to sustained MAPK activation, allowing mutant cells to proliferate. For $BRAF^{V600E}$-mutant melanoma it has been shown that MEK inhibition can counteract the effects from relief of negative feedback loop components as shown in recent clinical trials (42). Therefore, we tested the effects of MEK inhibition *in vitro* on selected neuroblastoma cell lines but, overall, effects of MEK inhibition were modest.

Feedback loop mechanisms present in normal cells to control for unwanted or temporarily interruption (or activation) of signaling may negatively impact upon molecular treatment and ultimately lead to therapy resistance. In this context, recent work from the Rosen team showed that BRAF inhibitors in $BRAF^{V600E}$-mutant melanoma cells leads to derepression of RAS signaling due to downregulation of the negative feedback components as evidenced by a pERK rebounce (43, 44). Moreover and even more worrysome, this same mechanism can also unleash the activity of other receptor tyrosine kinase receptors, further aggravating the unwanted effects of the initial pathway inhibition. Recent work, has pointed to increased occurrence of RAS mutations in relapsed neuroblastomas (45). Such mutations may invoke stronger effects on MAPK pathway activation and render cells more sensitive to MEK inhibition. Taken together, the present new insights into downstream

signaling of mutant ALK in neuroblastoma cells, points at potential risks of abrogating intrinsic mutant ALK induced negative feedback regulation of MAPK signaling which may render these cells more sensitive to subsequent accumulation of upstream RAS pathway mutations leading to therapy resistance. Also, our findings are in keeping with our initial finding of predominant AKT signaling in neuroblastoma (24) and more recent papers (33, 46, 47).

A second important novel finding from our study was that mutant ALK controls expression of the RET tyrosine kinase receptor. We first reported a possible role for RET in *ALK* mutant neuroblastomas first based on cross-species comparative genomic analysis on MYCN versus *ALK*^{F1174L} and *MYCN/ALK*^{F1174L}-driven mouse tumours and neuroblastoma cell lines (48). Further evidence was provided for this regulation, including the finding that mutant ALK likely controls RET expression levels through FOXO3a signaling. The FOXO3a forkhead transcription factor was previously shown as a key target of the PI_3K/AKT pathway in neuroblastoma and essential for their survival (26). Here, we showed that mutant ALK signaling blocks FOXO3a phosphorylation through PI_3K/AKT and that FOXO3a regulates RET expression thus strongly indicating the existence of a mutant ALK-PI_3K/AKT-FOXO3a-RET signaling axis in neuroblastoma cells.

This finding has several important consequences. First, this provides novel insights into the regulatory networks controlling early differentiation of sympathetic neuronal progenitors, particularly in relation to ALK and RET. RET regulates cholinergic properties in mouse sympathetic neurons and participates in cross-regulatory interactions which segregate cells towards adrenergic or cholinergic fate in the developing sympathetic ganglia (36, 49). In addition to RET, several genes implicated in cholinergic fate acquisition were identified as being part of the ALK signature including VGF and VIP. Early neural crest RET/TRKC positive progenitors committed to sympathetic fate express a hybrid noradrenergic/cholinergic phenotype marked by adrenergic markers TH, DBH, VMAT2 and cholinergic markers ChAT, VAChT, RET, NT3, TRKC and PRPH expression and are marked by high proliferation levels (36). Shortly hereafter at E15.5, VAChT positive neurons segregate with RET, PRPH, VIP and SST and develop towards cholinergic neurons whereas TRKA expression is initiated in VMAT2 positive neurons that will differentiate towards DBH/TH-positive noradrenergic neurons (50).

Secondly, the discovery of an ALK-RET regulatory pathway paves the way for novel experiments to deepen our understanding of *MYCN* and mutant *ALK*-driven tumour formation. Indeed, analysis of both cholinergic and adrenergic neuronal differentiation genes showed dramatic downregulation during *MYCN*-driven tumour formation, whereas these marker genes show relatively higher expression levels in *MYCN/ALK*^{F1174L} double transgenic mice tumours. This could indicate a possible mutant ALK-driven attenuation of the steep decline of the expression levels of these genes but requires further investigation in hyperplastic preneoplastic lesions from these double transgenic mice tumours. During tumour formation in *Th-MYCN* mice, we speculate that overexpression of MYCN imposes a very immature phenotype with steeply decreased levels of both adrenergic and cholinergic differentiation markers. We hypothesize, based on our current findings, that mutant ALK may drive the cells slightly further along the differentiation path with installment of the biphenotypic RET/TRKC positive proliferative progenitor cell type (see Supplemental Data 17). Possibly, this sustained ALK signaling and upregulation of RET may positively impact on the survival of the cells during tumour initiation, thereby counteracting the initially observed apoptotic loss of most of the tumour precursor cells in early stages of tumour formation (51). Further investigations probing deeper into the mechanisms of the interrelationship between MYCN, ALK and RET in normal neuron diversification are needed to understand how perturbation of this early gene regulatory network governing the adrenergic/cholinergic switch may impact on neuroblastoma tumour formation.

Thirdly, this study should trigger further work investigating novel therapeutic angles based on our observations. In particular, our data suggest possible co-regulation between mutant ALK and RET (52) and show vandetanib sensitivity in ALK mutant neuroblastoma cell lines. Moreover, a recent study showed impaired tumour growth *in vivo* in both *MYCN/KI-Alk*^{R1279Q} and *MYCN/KI-Alk*^{F1178L} mice upon inhibition of RET by vandetanib (48). Further dissection of the role of RET signaling in neuroblastoma and its impact on therapeutic targeting of the mutant ALK receptor with small molecules is therefore warranted.

In conclusion, we provide the first in depth analysis of the mutant ALK-driven transcriptome in neuroblastoma cells offering an important resource for future studies

towards designing and assessing novel therapies for *ALK*-driven tumours. In the present study, we were able to (i) establish a mutant ALK activity score which is also recapitulated in other ALKomas, (ii) uncover a MAPK negative feedback loop which may potentially play an important role in molecular rewiring of mutant ALK neuroblastoma cells following prolonged exposure to inhibitors, (iii) show that ALK regulates RET and propose RET as a bona fide target for molecular treatment of neuroblastoma. Taken together, these novel findings should fuel further studies towards understanding the complex interrelationship between ALK and RET signaling in the early steps of sympathetic nervous system and tumour development and provide a basis for further exploration of novel therapeutic strategies, especially in relation to the interplay between ALK and RET signaling.

3.1.8 Disclosure of Potential Conflicts of Interest

J. Gibbons and C. Liang hold ownership interest (including patents) in Xcovery. No potential conflicts of interest were disclosed by the other authors.

3.1.9 Acknowledgements

We would like to acknowledge Jeroen Schacht, Fanny De Vloed, Els De Smet, Justine Nuytens, Lies Vantomme and Shalina Baute for their outstanding technical support.

3.1.10 Grant Support

This work was supported by NIH grants R01CA102074 and R01CA134878 (D. Danielpour) and the Case Comprehensive Cancer Center P30 CA43703 (for Cytometry and athymic mouse cores). R.S. Wahdan-Alaswad was supported, in part, by a predoctoral fellowship from Research Oncology Training Grant 5T32CA059366-15 (2009) and a National Research Service Award Individual Fellowship Application 1F31CA142311-01 (2010–2011).
C. Kumps was indebted to the Institute for the Promotion of Innovation by Science and Technology (IWT-Vlaanderen; http://www.iwt.be/) for a predoctoral fellowship (grant number 081373); K. De Preter, I. Lambertz, S. Claeys, and T. Van Maerken are supported by the Fund for Scientific Research Flanders (FWO;

http://www.fwo.be/). This work was supported by the FWO (grant number: G.0198.08), the Belgian program of Interuniversity Poles of Attraction (IUAP; http://www.belspo.be/belspo/iap/index_en.stm), initiated by the Belgian State, Prime Minister's Office, Science Policy Programming, by the GOA (http://www.ugent.be/nl/onderzoek/financiering/bof/GOA; grant number 01G01910), the FOD (http://www.health.belgium.be/eportal; grant number: NKP_29_014). The research leading to these results has received funding from the European Union's Seventh Framework Program (FP7/2010-2015) under grant agreement n 259348.

3.1.11 References

1. Cheung NK, Dyer MA. Neuroblastoma: developmental biology, cancer genomics and immunotherapy. Nat Rev Cancer. 2013;13(6):397-411.
2. De Preter K, Vandesompele J, Heimann P, Yigit N, Beckman S, Schramm A, et al. Human fetal neuroblast and neuroblastoma transcriptome analysis confirms neuroblast origin and highlights neuroblastoma candidate genes. Genome Biol. 2006;7(9):R84.
3. Mosse YP, Laudenslager M, Longo L, Cole KA, Wood A, Attiyeh EF, et al. Identification of ALK as a major familial neuroblastoma predisposition gene. Nature. 2008.
4. Chen Y, Takita J, Choi YL, Kato M, Ohira M, Sanada M, et al. Oncogenic mutations of ALK kinase in neuroblastoma. Nature. 2008;455(7215):971-4.
5. George RE, Sanda T, Hanna M, Frohling S, Luther W, 2nd, Zhang J, et al. Activating mutations in ALK provide a therapeutic target in neuroblastoma. Nature. 2008;455(7215):975-8.
6. Janoueix-Lerosey I, Lequin D, Brugieres L, Ribeiro A, de Pontual L, Combaret V, et al. Somatic and germline activating mutations of the ALK kinase receptor in neuroblastoma. Nature. 2008;455(7215):967-70.
7. Azarova AM, Gautam G, George RE. Emerging importance of ALK in neuroblastoma. Semin Cancer Biol. 2011;21(4):267-75.
8. Reiff T, Huber L, Kramer M, Delattre O, Janoueix-Lerosey I, Rohrer H. Midkine and Alk signaling in sympathetic neuron proliferation and neuroblastoma predisposition. Development. 2011;138(21):4699-708.
9. Hallberg B, Palmer RH. Mechanistic insight into ALK receptor tyrosine kinase in human cancer biology. Nat Rev Cancer. 2013;13(10):685-700.
10. Mossé YP, Lim MS, Voss SD, Wilner K, Ruffner K, Laliberte J, et al. Safety and activity of crizotinib for paediatric patients with refractory solid tumours or anaplastic large-cell lymphoma: a Children's Oncology Group phase 1 consortium study. The Lancet Oncology. 2013;14(6):472-80.

11. Carpenter EL, Mosse YP. Targeting ALK in neuroblastoma--preclinical and clinical advancements. Nature reviews Clinical oncology. 2012;9(7):391-9.
12. Mano H. ALKoma: A Cancer Subtype with a Shared Target. Cancer discovery. 2012;2(6):495-502.
13. Katayama R, Shaw AT, Khan TM, Mino-Kenudson M, Solomon BJ, Halmos B, et al. Mechanisms of acquired crizotinib resistance in ALK-rearranged lung Cancers. Science translational medicine. 2012;4(120):120ra17.
14. Workman P, Clarke PA. Resisting targeted therapy: fifty ways to leave your EGFR. Cancer Cell. 2011;19(4):437-40.
15. Lovly CM, Shaw AT. Molecular pathways: resistance to kinase inhibitors and implications for therapeutic strategies. Clin Cancer Res. 2014;20(9):2249-56.
16. Weiss WA, Aldape K, Mohapatra G, Feuerstein BG, Bishop JM. Targeted expression of MYCN causes neuroblastoma in transgenic mice. EMBO J. 1997;16(11):2986 - 95.
17. Beckers A, Van Peer G, Carter D, Mets E, Althoff K, Cheung BB, et al. MYCN-targeting miRNAs are predominantly downregulated during MYCN-driven neuroblastoma tumour formation. Oncotarget. 2014.
18. Wu ZI, Rafael A.; Gentleman, Robert; Murillo, Francisco Martinez; and Spencer, Forrest. Adjustment for Oligonucleotide Expression Arrays" (May 2004). Johns Hopkins University, Dept. of Biostatistics Working Papers. 2004.
19. Oberthuer A, Hero B, Berthold F, Juraeva D, Faldum A, Kahlert Y, et al. Prognostic impact of gene expression-based classification for neuroblastoma. J Clin Oncol. 2010;28(21):3506-15.
20. Heukamp LC, Thor T, Schramm A, De Preter K, Kumps C, De Wilde B, et al. Targeted Expression of Mutated ALK Induces Neuroblastoma in Transgenic Mice. Science translational medicine. 2012;4(141):141ra91.
21. Sakamoto H, Tsukaguchi T, Hiroshima S, Kodama T, Kobayashi T, Fukami TA, et al. CH5424802, a selective ALK inhibitor capable of blocking the resistant gatekeeper mutant. Cancer Cell. 2011;19(5):679-90.
22. Eckerle S, Brune V, Doring C, Tiacci E, Bohle V, Sundstrom C, et al. Gene expression profiling of isolated tumour cells from anaplastic large cell lymphomas: insights into its cellular origin, pathogenesis and relation to Hodgkin lymphoma. Leukemia. 2009;23(11):2129-38.
23. Piva R, Pellegrino E, Mattioli M, Agnelli L, Lombardi L, Boccalatte F, et al. Functional validation of the anaplastic lymphoma kinase signature identifies CEBPB and BCL2A1 as critical target genes. J Clin Invest. 2006;116(12):3171-82.
24. De Preter K, De Brouwer S, Van Maerken T, Pattyn F, Schramm A, Eggert A, et al. Meta-mining of neuroblastoma and neuroblast gene expression profiles reveals candidate therapeutic compounds. Clin Cancer Res. 2009;15(11):3690-6.
25. Schramm A, Schowe B, Fielitz K, Heilmann M, Martin M, Marschall T, et al. Exon-level expression analyses identify MYCN and NTRK1 as major determinants of alternative exon usage and robustly predict primary neuroblastoma outcome. Br J Cancer. 2012;107(8):1409-17.

26. Santo EE, Stroeken P, Sluis PV, Koster J, Versteeg R, Westerhout EM. FOXO3a is a major target of inactivation by PI3K/AKT signaling in aggressive neuroblastoma. Cancer Res. 2013;73(7):2189-98.
27. Fredlund E, Ringner M, Maris JM, Pahlman S. High Myc pathway activity and low stage of neuronal differentiation associate with poor outcome in neuroblastoma. Proc Natl Acad Sci U S A. 2008;105(37):14094-9.
28. Huang da W, Sherman BT, Lempicki RA. Bioinformatics enrichment tools: paths toward the comprehensive functional analysis of large gene lists. Nucleic Acids Res. 2009;37(1):1-13.
29. Lamb J, Crawford ED, Peck D, Modell JW, Blat IC, Wrobel MJ, et al. The Connectivity Map: using gene-expression signatures to connect small molecules, genes, and disease. Science. 2006;313(5795):1929-35.
30. Subramanian A, Tamayo P, Mootha VK, Mukherjee S, Ebert BL, Gillette MA, et al. Gene set enrichment analysis: a knowledge-based approach for interpreting genome-wide expression profiles. Proc Natl Acad Sci U S A. 2005;102(43):15545-50.
31. Mootha VK, Lindgren CM, Eriksson KF, Subramanian A, Sihag S, Lehar J, et al. PGC-1alpha-responsive genes involved in oxidative phosphorylation are coordinately downregulated in human diabetes. Nat Genet. 2003;34(3):267-73.
32. Chen J, Jiang C, Wang S. LDK378: a promising anaplastic lymphoma kinase (ALK) inhibitor. J Med Chem. 2013;56(14):5673-4.
33. Berry T, Luther W, Bhatnagar N, Jamin Y, Poon E, Sanda T, et al. The ALK(F1174L) Mutation Potentiates the Oncogenic Activity of MYCN in Neuroblastoma. Cancer Cell. 2012;22(1):117-30.
34. Schonherr C, Ruuth K, Kamaraj S, Wang CL, Yang HL, Combaret V, et al. Anaplastic Lymphoma Kinase (ALK) regulates initiation of transcription of MYCN in neuroblastoma cells. Oncogene. 2012.
35. Pratilas CA, Taylor BS, Ye Q, Viale A, Sander C, Solit DB, et al. (V600E)BRAF is associated with disabled feedback inhibition of RAF-MEK signaling and elevated transcriptional output of the pathway. Proc Natl Acad Sci U S A. 2009;106(11):4519-24.
36. A, Lubke M, Adameyko I, Lallemend F, Ernfors P. The transcription factor Hmx1 and growth factor receptor activities control sympathetic neurons diversification. EMBO J. 2013;32(11):1613-25.
37. Salton SR, Ferri GL, Hahm S, Snyder SE, Wilson AJ, Possenti R, et al. VGF: a novel role for this neuronal and neuroendocrine polypeptide in the regulation of energy balance. Frontiers in neuroendocrinology. 2000;21(3):199-219.
38. Xing S. Signal Transduction Pathways Activated by RET Oncoproteins in PC12 Pheochromocytoma Cells. Journal of Biological Chemistry. 1998;273(9):4909-14.
39. Goertz MJ, Wu Z, Gallardo TD, Hamra FK, Castrillon DH. Foxo1 is required in mouse spermatogonial stem cells for their maintenance and the initiation of spermatogenesis. J Clin Invest. 2011;121(9):3456-66.

40. Passoni L, Longo L, Collini P, Coluccia AM, Bozzi F, Podda M, et al. Mutation-independent anaplastic lymphoma kinase overexpression in poor prognosis neuroblastoma patients. Cancer Res. 2009;69(18):7338-46.
41. Caunt CJ, Keyse SM. Dual-specificity MAP kinase phosphatases (MKPs): shaping the outcome of MAP kinase signalling. The FEBS journal. 2013;280(2):489-504.
42. Long GV, Stroyakovskiy D, Gogas H, Levchenko E, de Braud F, Larkin J, et al. Combined BRAF and MEK inhibition versus BRAF inhibition alone in melanoma. N Engl J Med. 2014;371(20):1877-88.
43. Lito P, Pratilas CA, Joseph EW, Tadi M, Halilovic E, Zubrowski M, et al. Relief of profound feedback inhibition of mitogenic signaling by RAF inhibitors attenuates their activity in BRAFV600E melanomas. Cancer Cell. 2012;22(5):668-82.
44. Lito P, Saborowski A, Yue J, Solomon M, Joseph E, Gadal S, et al. Disruption of CRAF-mediated MEK activation is required for effective MEK inhibition in KRAS mutant tumours. Cancer Cell. 2014;25(5):697-710.
45. Eleveld T, Schild L, Ebus ME, van Sluis PG, Zwijnenburg DA, Westerhout EM, et al. Whole Genome Sequencing of Relapse Neuroblastoma Identifies the RAS-MAPK Pathway as a Potential Therapeutic Target in Neuroblastoma. ANR. 2014;PL007.
46. Moore N, Azarova A, Bhatnagar N, Ross KN, Drake L, Frumm S, et al. Molecular rationale for the use of PI3K/AKT/mTOR pathway inhibitors in combination with crizotinib in ALK-mutated neuroblastoma. Oncotarget. 2014;5(18):8737-49.
47. Chesler L, Schlieve C, Goldenberg DD, Kenney A, Kim G, McMillan A, et al. Inhibition of phosphatidylinositol 3-kinase destabilizes Mycn protein and blocks malignant progression in neuroblastoma. Cancer Res. 2006;66(16):8139-46.
48. Cazes A, Lopez-Delisle L, Tsarovina K, Pierre-Eugene C, De Preter K, Peuchmaur M, et al. Activated Alk triggers prolonged neurogenesis and Ret upregulation providing a therapeutic target in ALK-mutated neuroblastoma. Oncotarget. 2014;5(9):2688-702.
49. Burau K, Stenull I, Huber K, Misawa H, Berse B, Unsicker K, et al. c-ret regulates cholinergic properties in mouse sympathetic neurons: evidence from mutant mice. The European journal of neuroscience. 2004;20(2):353-62.
50. Bourdeaut F, Janoueix-Lerosey I, Lucchesi C, Paris R, Ribeiro A, de Pontual L, et al. Cholinergic switch associated with morphological differentiation in neuroblastoma. J Pathol. 2009;219(4):463-72.
51. Zhu S, Lee JS, Guo F, Shin J, Perez-Atayde AR, Kutok JL, et al. Activated ALK collaborates with MYCN in neuroblastoma pathogenesis. Cancer Cell. 2012;21(3):362-73.
52. Xu AM, Huang PH. Receptor tyrosine kinase coactivation networks in cancer. Cancer Res. 2010;70(10):3857-60.

3.1.12 Supplemental Material and Methods

Determining GI_{50} values for compounds in neuroblastoma cell lines

In order to determine GI_{50} values in neuroblastoma cell lines for the compounds used, cell lines were seeded in 96-well tissue culture plates at 30% confluency, allowed to recover overnight and subsequently treated with a range of inhibitor concentrations. Cell viability was assessed in triplicate using Cell-Titer Glo at 24h and 48h and 72h following treatment (Promega), according to the manufacturer's protocol. The GI_{50} values were calculated for each cell line using the CalcuSyn software (BioSoft).

Pharmacological ALK, MEK, PI_3K/mTOR and RET inhibition and shRNA mediated ALK knockdown in neuroblastoma cell lines

Human wild type ALK (SK-N-AS, NGP, IMR-32), ALKR1275Q (CLB-GA, LAN-5, UKF-NB-3), ALKF1174L (SK-N-SH, Kelly, SMS-KCNR) and ALK amplified (NB-1) neuroblastoma cell lines were treated in triplicate with 0.3μM NPV-TAE-684 (Novartis/SelleckChem, further referred to as TAE-684) or DMSO (VWR) for 6 hours, followed by RNA isolation and gene expression profiling (see further). Sensitivity to TAE-684 was monitored by determination of the GI_{50} values (see above), which showed to be stronger in ALK mutant versus wild type cell lines, as expected (Supplemental Data 2). Treatment of cells with 0.3μM TAE-684 for 6h was selected based on the survival response of cells to a range of concentrations as well as expression data in the neuroblastoma cell lines of published ALK regulated genes from a study on NPM-ALK-driven ALCL.

Treatment of the CLB-GA cell line with complementary ALK, MEK, PI_3K/mTOR or RET inhibitors (and DMSO (VWR) as control) was performed in duplicate for each drug using the GI_{50} concentrations (see further): 0.5μM Crizotinib (Pfizer/Sigma-Aldrich); 0.06μM X-396 (VWR); 0.2μM LDK378 (Hoelzel Biotech); 0.05uM Trametinib (SelleckChem); 0.5μM BEZ-235 (SelleckChem); 9.5μM Vandetanib (SelleckChem). Cells were collected at 6h following treatment and further profiled. The selected inhibitor concentrations were used based on determined GI_{50} values.

For generation of gene expression time series following ALK inhibition, CLB-GA cells were treated with 0.3uM TAE-684 (and DMSO as control treatment) and RNA was harvested at 0 – 10' – 30' – 60' – 120' – 240' – 360' time points.

For shRNA mediated knockdown, pGIPZ-ALK shRNAmir and pGIPZ-non-silencing control shRNAmir vectors were used (Open Biosystems). The ALK shRNA was directed against a part of exon 26 in the tyrosine kinase domain of ALK (target sequence: TGGAAGGAATATTCACTTCTAA). Lentiviral particles were produced according to manufacturer's protocol (Open Biosystems). On day 2 post-transduction of neuroblastoma cells, the transduction efficiency was determined by flow cytometry and microscopic analysis of GFP-positive cells (>90% so no further selection was performed). Cells were subsequently harvested for expression profiling.

RNA extraction and RT-qPCR

Total RNA of (treated) cell lines, transgenic mice tumours and ganglia was isolated using the miRNeasy kit (Qiagen) according to the manufacturer's instructions, including on-column DNase treatment. The RNA integrity was verified using Experion (Bio-Rad). cDNA was synthesized from total RNA using an iScript cDNA synthesis kit (Bio-Rad). qPCR reactions were performed with Sybr green detection chemistry, using the LC480 real-time PCR detection system (Bio-Rad). qPCR reactions were performed in duplicate in a total volume of 5 µl consisting of 2.5 µl of Sso advanced qPCR master mix (Bio-Rad), 0.25 µl forward and reverse primer (5 µM) and 2 µl of 2.5 ng/µl cDNA (total RNA equivalents), with cycling conditions: 2 minutes at 95°C, 44 cycles of 5 seconds at 95°C, 30 seconds at 60°C and 1 second at 72°C. Primers for the genes were obtained from IDT (Belgium). mRNA expression levels of target genes *ETV5* (ID 8595), *ALK* (ID 8596), *RET* (ID 8761) were normalized to at least two internal reference genes (TBP (ID 653), *YWHAZ* (ID 9), *B2M* (ID 2) and *UBC* (ID 8)). All primer sequences are available in RTPrimerDB (http://www.rtprimerdb.org) (1). The primers used for detection of mouse Ret have previously been described (2). Expression analysis as well as error propagation was done using qbasePLUS software 1.5 (http://www.biogazelle.com) (3).

1. Lefever S, Vandesompele J, Speleman F, Pattyn F. RTPrimerDB: the portal for real-time PCR primers and probes. Nucleic Acids Res. 2009;37(Database issue):D942-5.

2. Uesaka T, Nagashimada M, Yonemura S, Enomoto H. Diminished Ret expression compromises neuronal survival in the colon and causes intestinal aganglionosis in mice. J Clin Invest. 2008;118(5):1890-8.

3. Hellemans J, Mortier G, De Paepe A, Speleman F, Vandesompele J. qBase relative quantification framework and software for management and automated analysis of real-time quantitative PCR data. Genome Biol. 2007;8(2):R19.

3.1.13 Supplemental figures, tables and data

Supplemental data 1

SampleID	Origin	tumor	ALK status	MYCN status
CLB-GA	Combaret	NB	R1275Q	NA
IMR-32	Versteeg	NB	wt	A
LAN-5	Versteeg	NB	R1275Q	A
NB-1	JHSF	NB	wt	A
NGP	Versteeg	NB	wt	A
SK-N-AS	ATCC	NB	wt	NA
SK-N-BE	Versteeg	NB	wt	A
SK-N-SH	Versteeg/ Cohn/ Pålman	NB	F1174L	NA
SMS-KCNR	Versteeg	NB	F1174L	A
UKF-NB-3	Michaelis	NB	R1275Q	A
Kelly	Eggert/Schramm	NB	F1174L	A
Karpas-299	/	ALCL	NPM-ALK fusion gene	/
H3122	/	NSCLC	EML4-ALK fusion gene	/

Supplemental data 1: Cell line information.

Summary of the characteristics of cell lines used in this study including origin, tumour type, ALK and MYCN status (wt = wild type, NA = non amplified, A = amplified).

Supplemental data 2

A

Cell line	ALK status	GI_{50} (µM) 24h	GI_{50} (µM) 48h	GI_{50} (µM) 72h
UKF-NB3	R1275Q	3.76	0.69	0.64
CLB-GA	R1275Q	21.82	0.44	0.33
LAN-5	R1275Q	1.39	0.33	0.19
SK-N-SH	F1174L	1.80	0.58	0.68
KELLY	F1174L	28.91	0.56	0.20
SMS-KCNR	F1174L	1.66	0.28	0.19
NB-1	A	4.19	0.18	0.00
SK-N-AS	wt	1.94	0.77	0.63
NGP	wt	1.65	0.81	0.63
IMR-32	wt	3.61	0.60	0.44

B

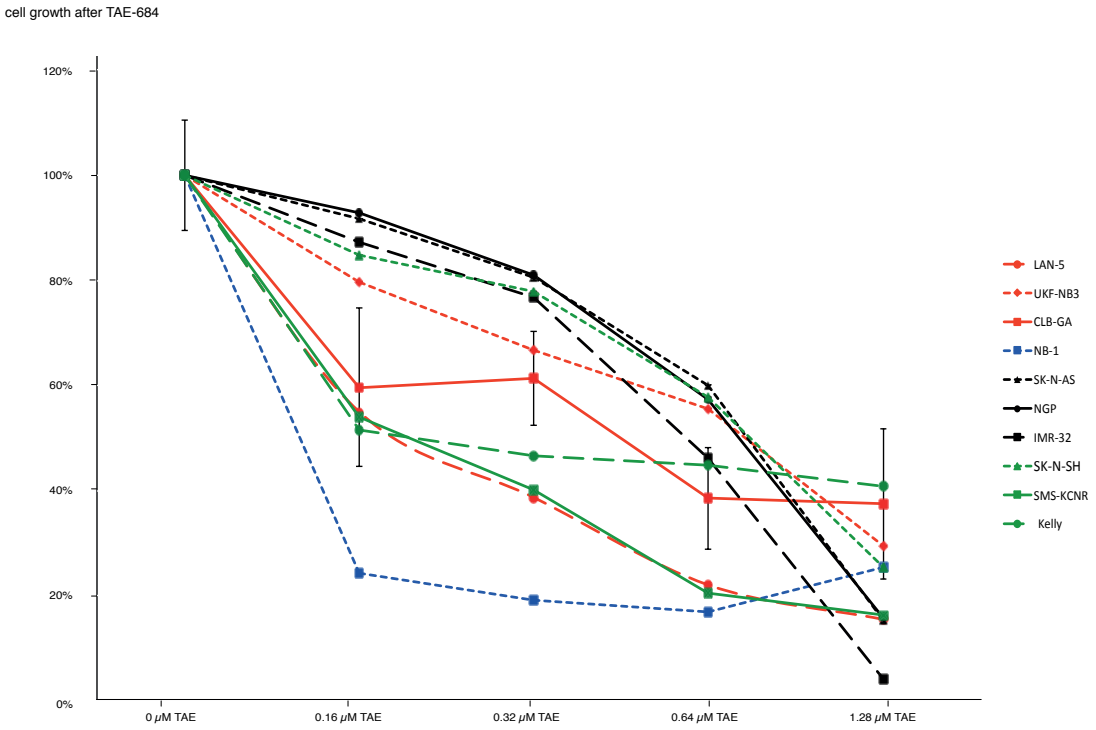

Supplemental data 2: GI_{50} concentration of TAE-684 in neuroblastoma cell lines.

A. GI_{50} – values at different time points following pharmacological ALK inhibition using TAE-684 in 10 neuroblastoma cell lines. (A = amplified, wt= wild type) **B.** Cell growth graphs at 72 hours following pharmacological ALK inhibition using TAE-684 in different cell lines.

Supplemental data 3

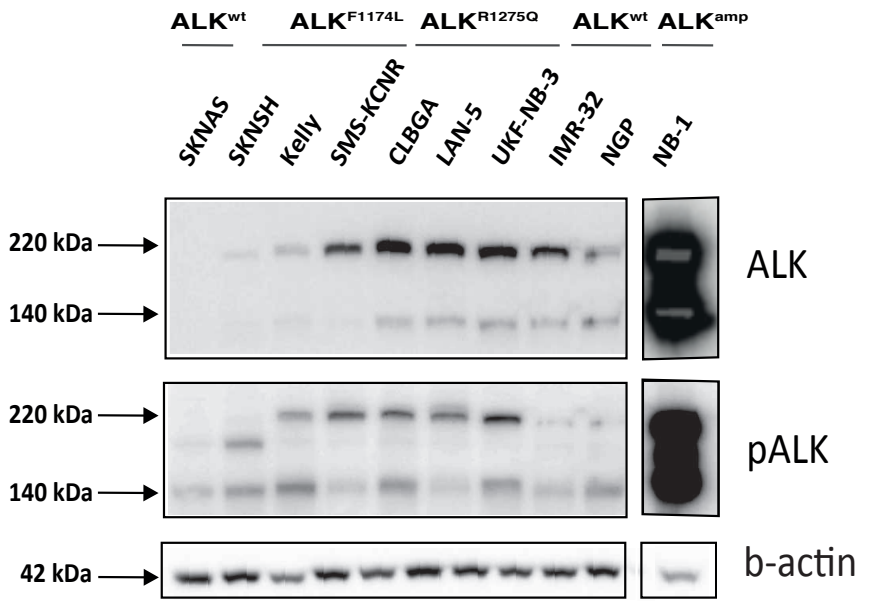

Supplemental data 3: phospho-ALK and total ALK expression in a panel of 10 neuroblastoma cell lines.

Western blot analysis of phospho-ALK and total ALK protein levels (**β**-actin as loading control) for different neuroblastoma cell lines.

Three bands are visualized upon ALK Western blotting: doublet at 220 kDa (upper: plasma-membrane ALK, lower: intracellular pool of ALK) and a singlet at 140 kDa (extracellular cleavage of 220 kDa).

Supplemental data 4

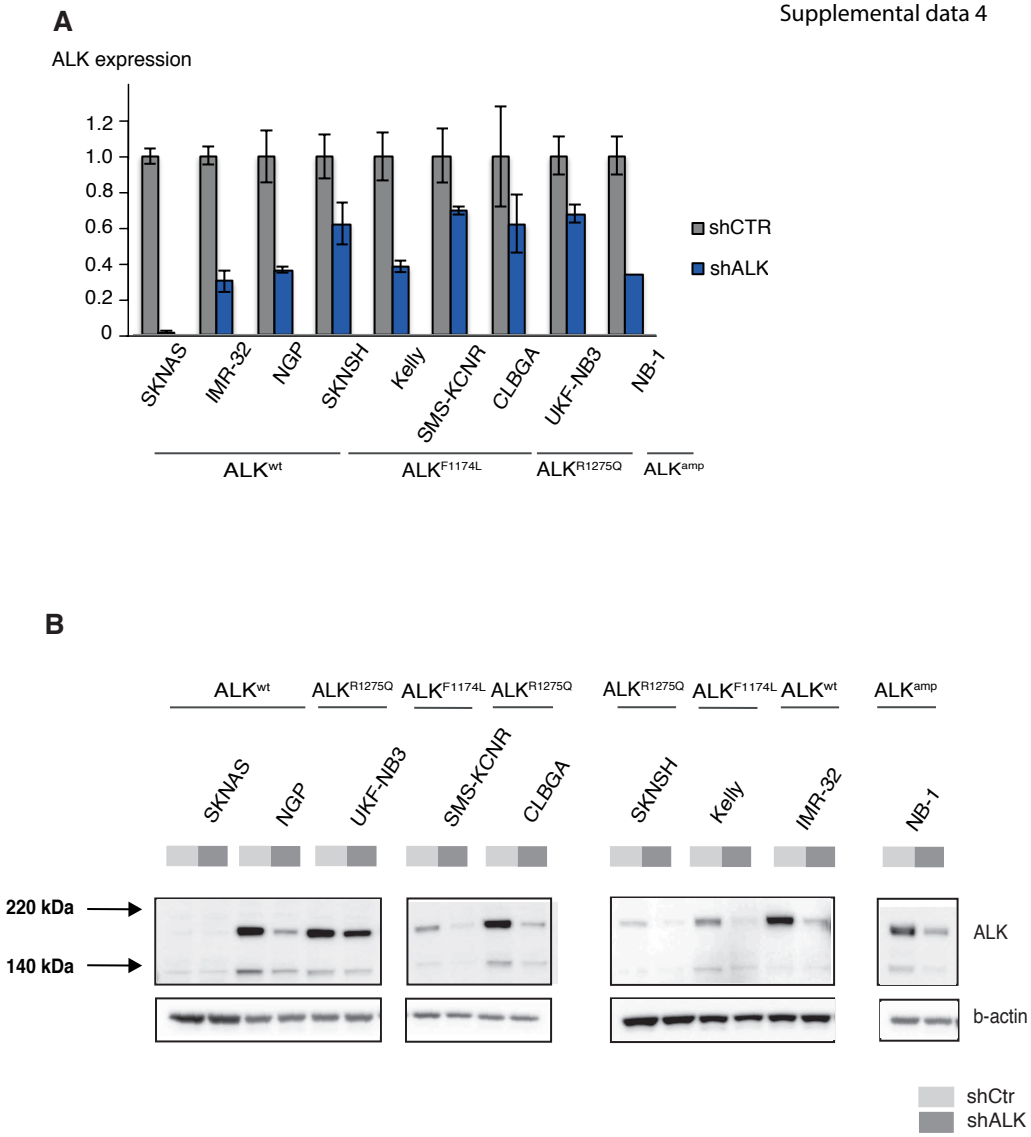

Supplemental data 4: ALK expression upon ALK inhibition using shALK.

A. ALK expression in different neuroblastoma cell lines after ALK inhibition using shALK. The expression decreases after shALK compared to shControl (shCtr). **B.** Western blot analysis of total ALK protein levels in different neuroblastoma cell lines after ALK inhibition using shALK (**β**-actin as loading control). ALK protein levels decrease after shALK compared to shControl (shCtr).

Supplemental data 5: Differential expression analysis upon ALK inhibition.

Differentially expressed genes were identified using Rank Product analysis and fold-change analysis on the data generated after pharmacological inhibition of 10 neuroblastoma cell lines using TAE-684 and shALK. The full list can be sent upon request.

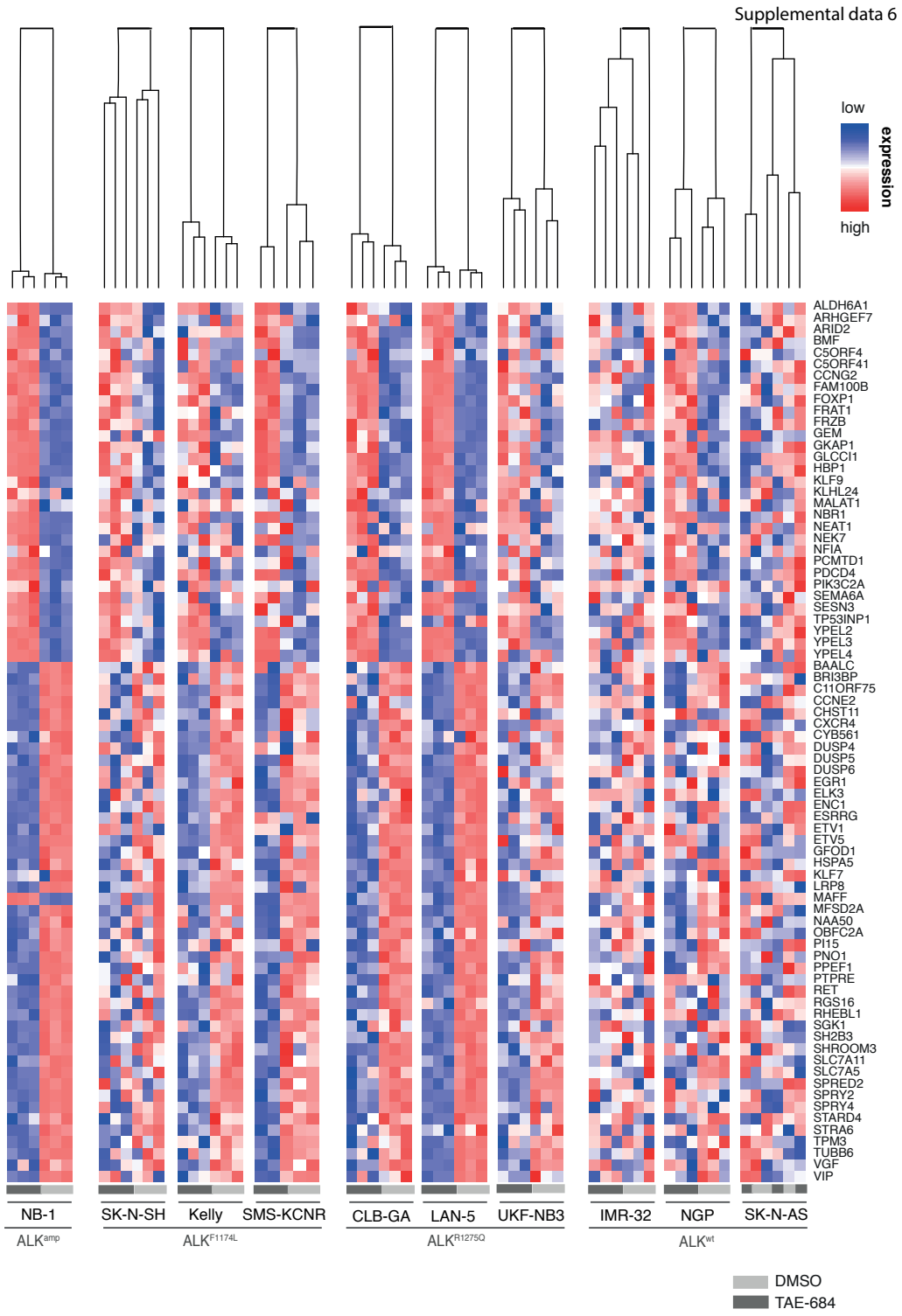

Supplemental data 6: Expression of 77 ALK regulated genes in a panel of 10 neuroblastoma cell lines treated with ALK inhibitor TAE-684.

Hierarchical clustering and heatmap representation of the expression levels of the 77 genes of the ALK signature in 10 neuroblastoma cell lines with different ALK status after pharmacological ALK inhibition using the small molecule inhibitor TAE-684.

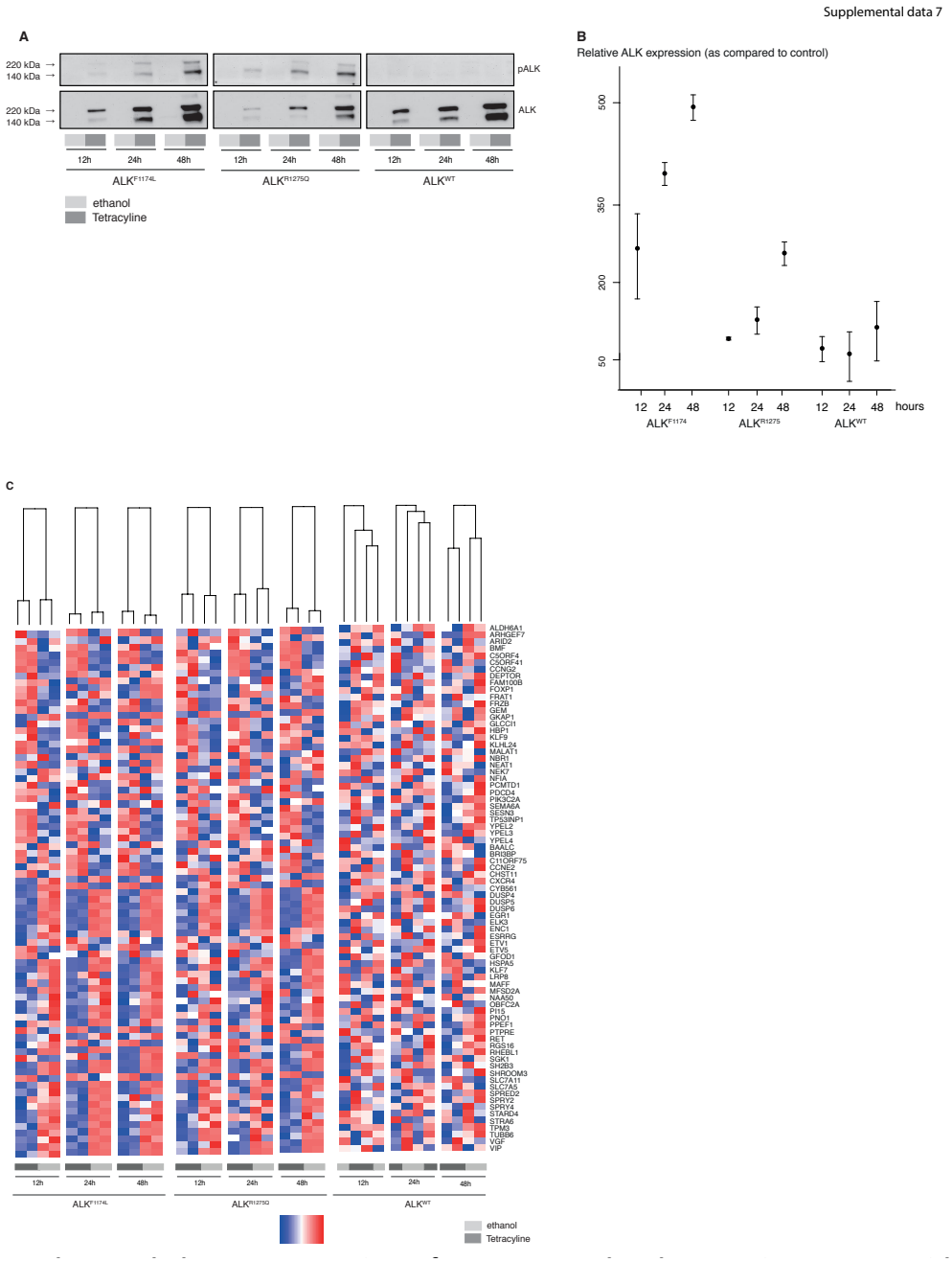

Supplemental data 7: Expression of 77 ALK regulated genes in SK-N-AS with induced ALK.

A. Western blot analysis for phospho-ALK and total ALK protein levels before and after TET-induction of *ALK*^{F1174L}, *ALK*^{R1275Q} or *ALK*^{wt} in SK-N-AS. **B.** Relative ALK expression levels (as compared to non-induced SK-N-AS) were higher for SK-N-AS cells with tetracycline-induced *ALK*^{F1174L} and *ALK*^{R1275Q} as compared to SK-N-AS cells with tetracycline-induced *ALK*^{wt}. **C.** Hierarchical clustering and heatmap representation of the expression levels of the 77 genes of the ALK signature as measured in the SK-N-AS cell line before and after induction of *ALK*^{F1174L}, *ALK*^{R1275Q} or *ALK*^{wt}.

Supplemental data 8

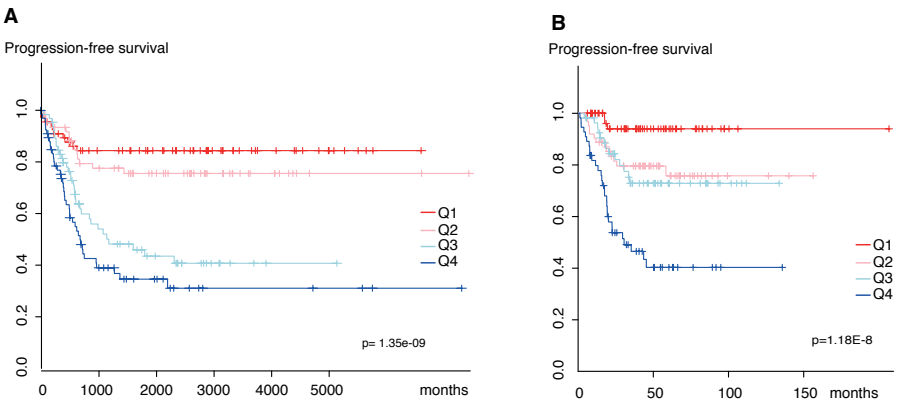

Supplemental Data 8: Progression-free survival versus ALK signature scores.

A-B. ALK signature score significantly correlates with progression-free survival in the NRC dataset as well as in the Oberthuer dataset (30) (Q1 – Q4= lowest quartile of scores – highest quartile of scores).

Supplemental data 9: Summary of Gene Set Enrichment analysis results performed on expression data upon ALK inhibition in 10 cell lines.

The full list can be sent upon request.

Supplemental data 10: Results of gene ontology analysis performed on the 77 ALK signature genes.

The full list can be sent upon request.

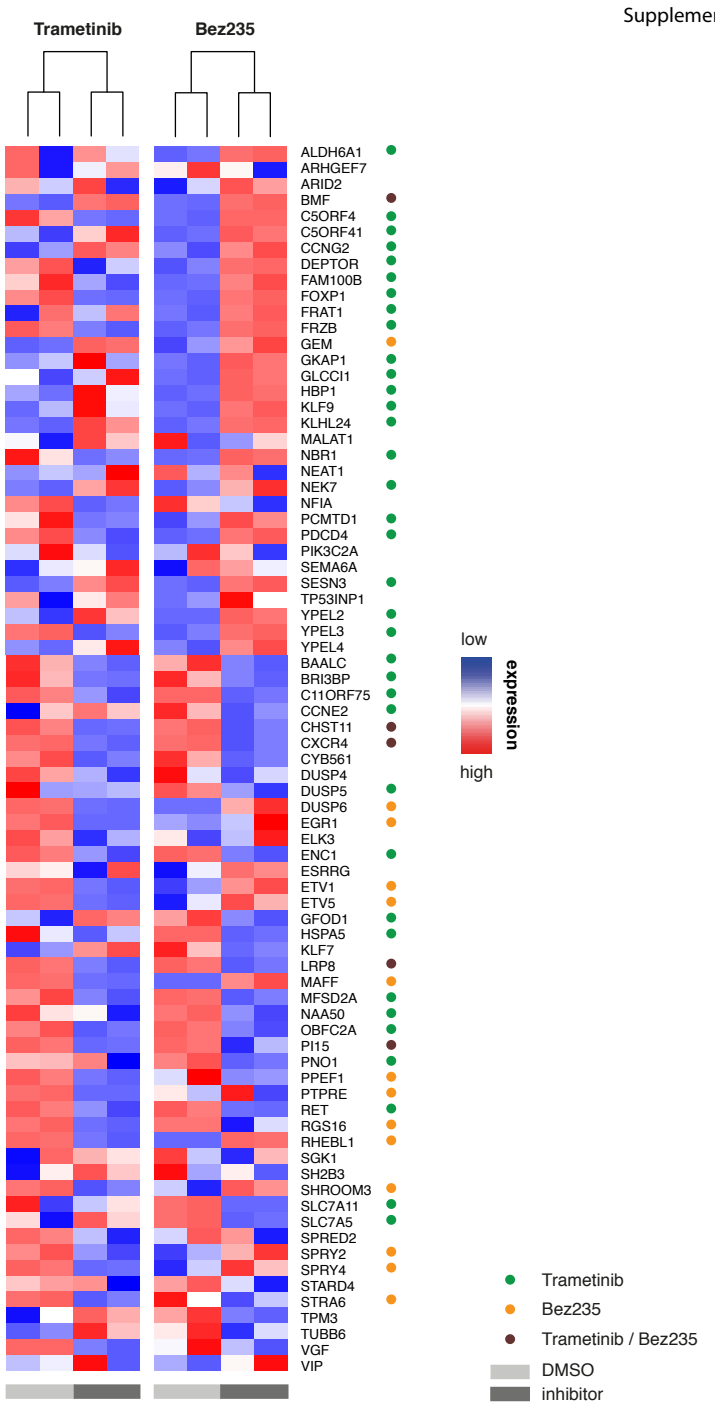

Supplemental data 11: ALK signature gene analysis upon inhibition of two ALK downstream pathways.

Hierarchical clustering and heatmap representation of the expression levels of the 77 genes of the ALK signature in neuroblastoma cell line CLB-GA after pharmacological pathway inhibition using small molecule inhibitors targeting ALK downstream pathways MAPK/ERK and PI3K/AKT/mTOR (using Trametinib and BEZ-235 respectively). Significantly differentially expressed genes are indicated with green/yellow/brown dots.

Supplemental data 12: Results of Connectivity map analysis performed on ALK signature genes.

The full list can be sent upon request.

Supplemental data 13: Summary of Gene Set Enrichment analysis results obtained on expression profiling data of CLB-GA on different time points (10' – 30' – 60' – 2h – 4h – 6h) after pharmacological inhibition using TAE-684.

The full list can be sent upon request.

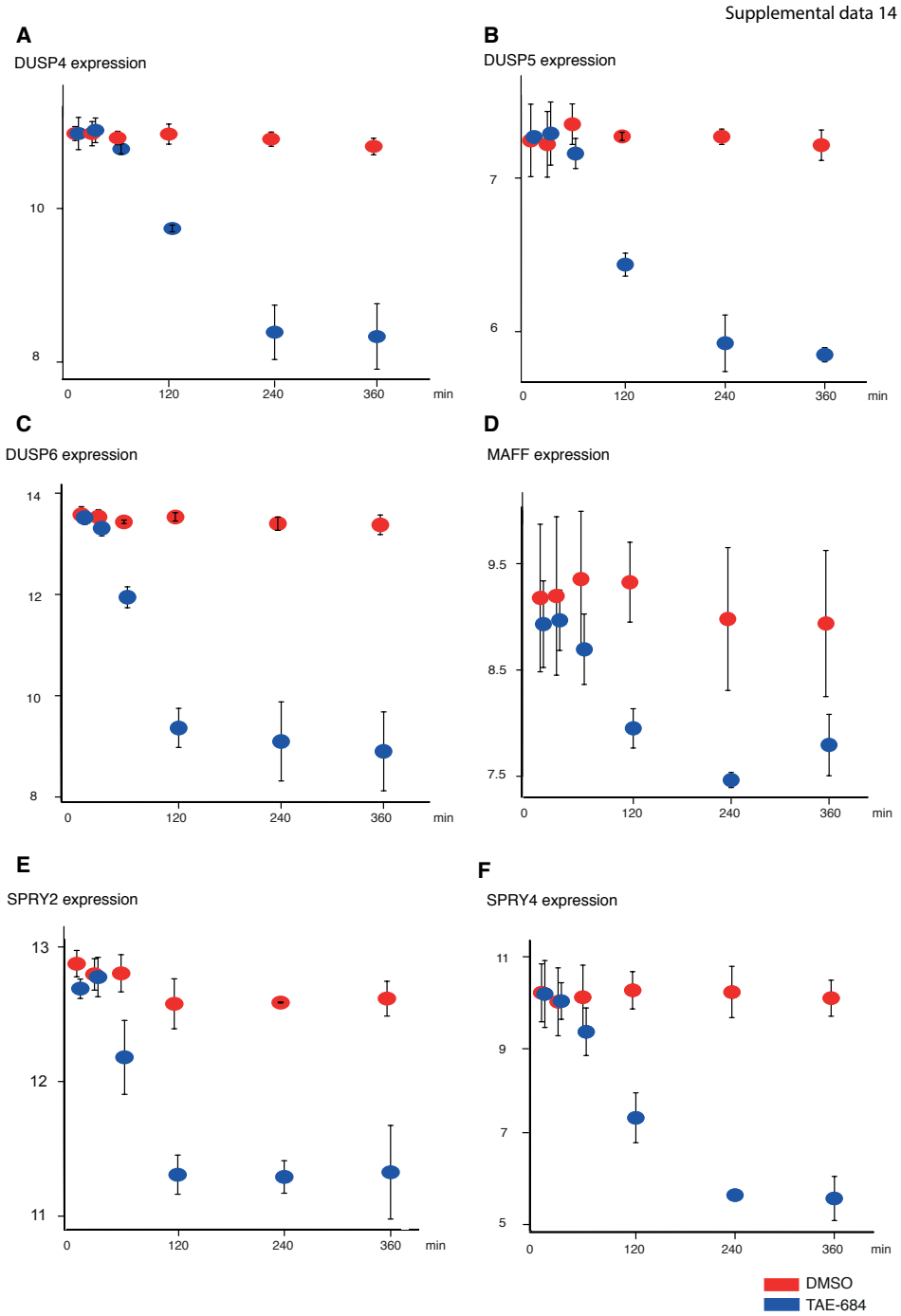

Supplemental data 14: Expression of MAPK genes in CLB-GA after ALK inhibition.

A-F. Expression levels of 6 MAPK genes (DUSP4, DUSP5, DUSP6, MAFF, SPRY2 and SPRY4) over the different time points (10' – 30' – 60' – 120' – 240' – 360') in the neuroblastoma cell line CLB-GA after pharmacological ALK inhibition with TAE384. These 6 genes show a significant decrease in expression from 60 min or 120 min after ALK inhibition.

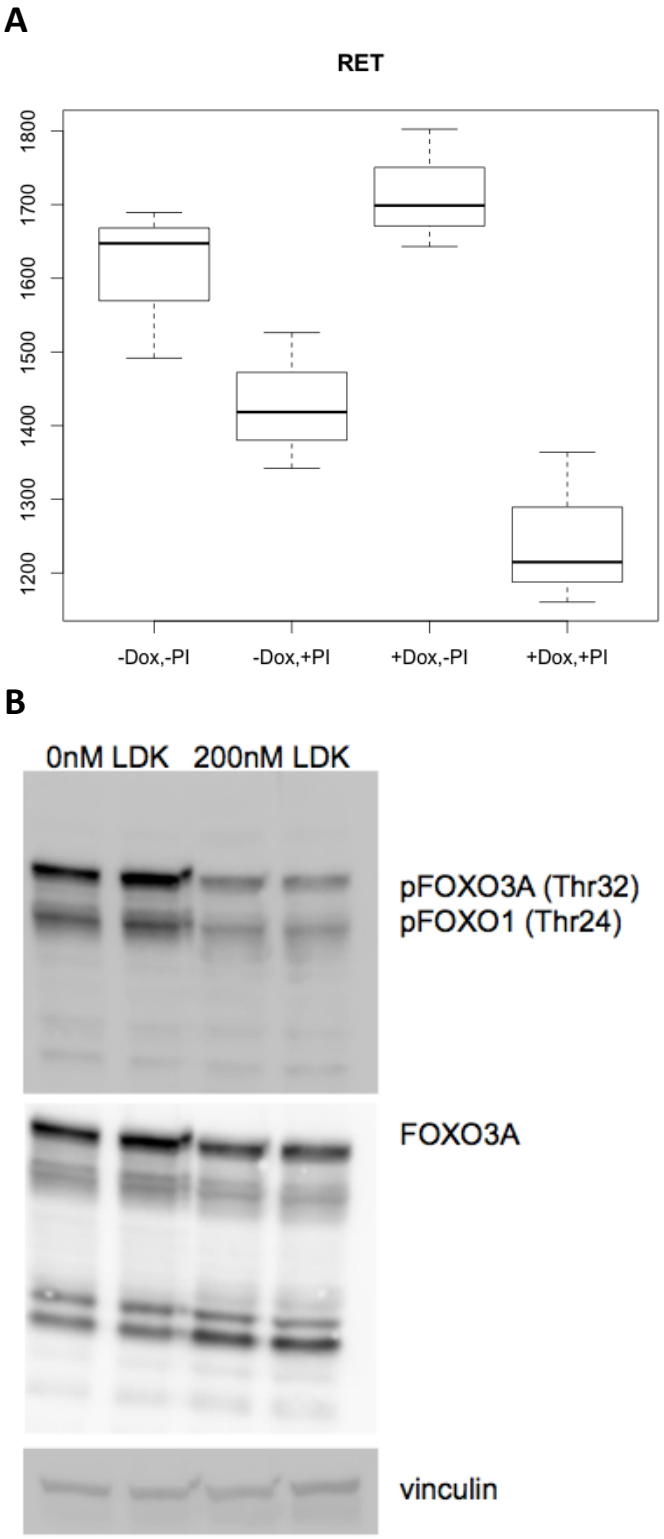

Supplemental data 15.

A. RET mRNA expression levels upon FOXO3 activation (+Dox) and Pi3K/AKT inhibition (+PI) in cell line SY5Y (Santo et al., 2013, GEO-id: GSE42762); **B.** pFOXO3a levels upon ALK inhibition with the LDK-378 compound are downregulated

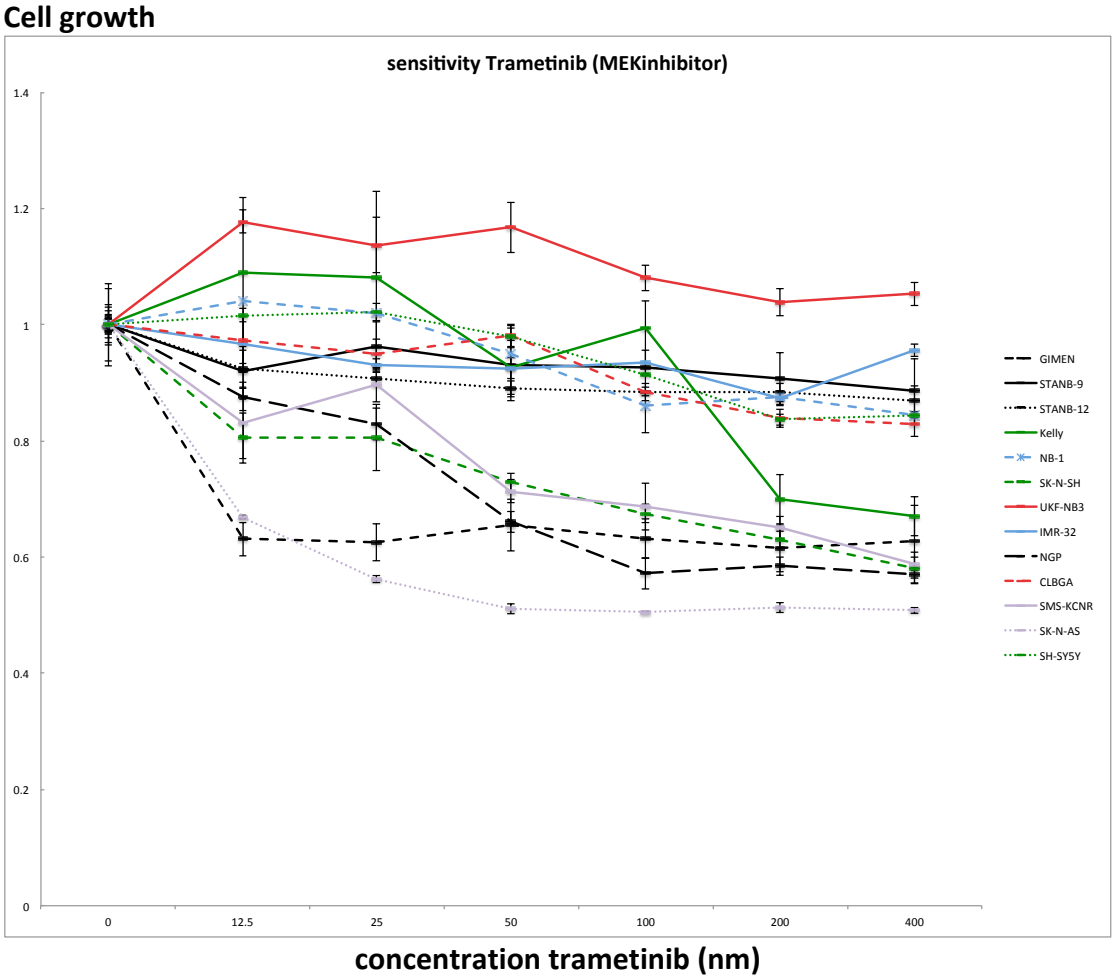

Supplemental data 16: Cell growth upon treatment of neuroblastoma cell lines with different concentrations of Trametinib (MAPK/MEK inhibitor) is only modestly affected

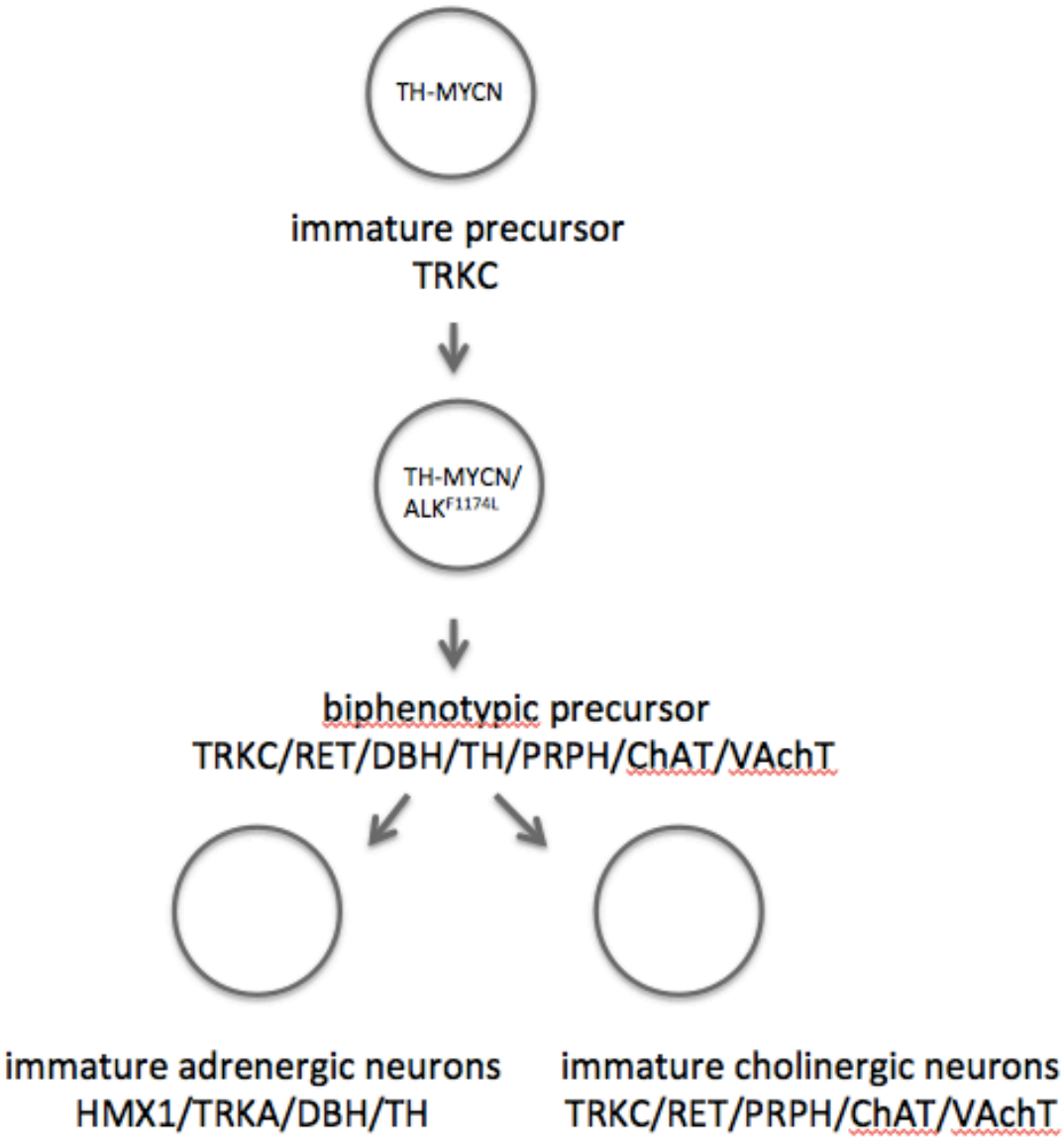

Supplemental Data 17: Scheme to clarify our hypothesis: During tumour formation in *Th-MYCN* mice, we speculate that overexpression of MYCN imposes a very immature phenotype with steeply decreased levels of both adrenergic and cholinergic differentiation markers. We hypothesize, based on our current findings, that mutant ALK may drive the cells somewhat further along the differentiation path with installment of the biphenotypic RET/TRKC positive proliferative progenitor cell type. Possibly, this sustained ALK signaling and upregulation of RET may positively impact on the survival of the cells during tumour initiation, thereby counteracting the initially observed apoptotic loss of most of the tumour precursor cells in early stages of tumour formation.

Chapter 4 Early and late effects of pharmacological ALK inhibition on the neuroblastoma transcriptome

Authors: **Shana Claeys** [1,2], Geertrui Denecker [1,2], Robrecht Cannoodt [1,2,3,4,5], Candy Kumps [1,6], Kaat Durinck [1,2], Frank Speleman [1,2], Katleen De Preter [1,2].

Paper published in Oncotarget in 2017

Author contribution:

Shana Claeys performed laboratory experiments and data analysis, was responsible for the design of the experiments, coordination of the research, generation of the figures and writing of the manuscript. Katleen De Preter and Robrecht Cannoodt assisted with the data analysis. Candy Kumps provided valuable discussions and feedback. Kaat Durinck and Geertrui Denecker supervised the laboratory experiments, were involved in the design of the experiments and coordination of the research. Katleen De Preter and Frank Speleman coordinated the research, designed experiments and helped writing the paper.

Early and late effects of pharmacological ALK inhibition on the neuroblastoma transcriptome

Authors: **Shana Claeys** [1,2], Geertrui Denecker [1,2], Robrecht Cannoodt [1,2,3,4,5], Candy Kumps [1,6], Kaat Durinck [1,2], Frank Speleman [1,2], Katleen De Preter [1,2].

4.1.1 Affiliations:

1. Center for Medical Genetics, Ghent University, Ghent, Belgium
2. Cancer Research Institute Ghent (CRIG), Ghent University, Ghent, Belgium
3. Bioinformatics Institute Ghent From Nucleotides to Networks (Big N2N), Ghent, Belgium
4. Data Mining and Modelling for Biomedicine group (DAMBI), VIB Inflammation Research Center, Ghent, Belgium
5. Department of Respiratory Medicine, Ghent University, Ghent, Belgium
6. Department of Uro-Gynaecology, Ghent University Hospital, Ghent, Belgium

4.1.2 Abstract

Background: Neuroblastoma is an aggressive childhood malignancy of the sympathetic nervous system. Despite multi-modal therapy, survival of high-risk patients remains disappointingly low, underscoring the need for novel treatment strategies. The discovery of *ALK* activating mutations opened the way to precision treatment in a subset of these patients. Previously, we investigated the transcriptional effects of pharmacological ALK inhibition on neuroblastoma cell lines, six hours after TAE684 administration, resulting in the 77-gene ALK signature, which was shown to gradually decrease from 120 minutes after TAE684 treatment, to gain deeper insight into the molecular effects of oncogenic ALK signaling.

Aim: Here, we further dissected the transcriptional dynamic profiles of neuroblastoma cells upon TAE684 treatment in a detailed timeframe of ten minutes up to six hours after inhibition, in order to identify additional early targets for combination treatment.

Results: We observed an unexpected initial upregulation of positively regulated MYCN target genes following subsequent downregulation of overall MYCN activity. In addition, we identified adrenomedullin (ADM), previously shown to be implicated in sunitinib resistance, as the earliest response gene upon ALK inhibition.

Conclusion: We describe the early and late effects of ALK inhibitor TAE684 treatment on the neuroblastoma transcriptome. The observed unexpected upregulation of *ADM* warrants further investigation in relation to putative ALK resistance in neuroblastoma patients currently undergoing ALK inhibitor treatment.

4.1.3 INTRODUCTION

Neuroblastoma (NB) is a childhood cancer arising from malignant transformation of cells from the sympatho-adrenergic lineage of the developing neural crest [1] and is characterized by a large clinical heterogeneity, including patients with tumours that spontaneously regress as well as patients with metastasis and refractory disease despite intensive therapy regimens [2]. For these high-risk neuroblastoma cases, a better understanding of the genes and pathways that are involved in disease development and progression is currently fuelling the identification of new molecular targets for therapy [3].

Overall, given the low frequency of mutations in neuroblastoma, options for targeted therapy are relatively limited. However, the recurrent somatic mutations of the tyrosine kinase receptor *ALK* identified in 8-10% of primary neuroblastoma tumours [4–8] and the emergence of *ALK* mutations at relapse mark ALK as an important novel drug target [9,10]. Several orally available small molecule ALK inhibitors have been developed and successfully applied in patients with other ALK mutant tumour entities, so-called ALKoma tumours, most notably a subset of lung cancers [11–17]. Several of these small molecule ALK inhibitors have recently gone into phase 1 clinical trials for patients with refractory neuroblastoma, inflammatory myofibroblastic tumour, non-small-cell lung cancer (NSCLC) and anaplastic large-cell lymphoma (ALCL) [18,19].

Despite the promising therapeutic potential of ALK inhibitors, an important drawback is the rapid occurrence of resistance due to escape mechanisms including secondary mutations or activation of other kinase signaling pathways [17,20–30]. A better understanding of the downstream ALK signaling cascades can inspire the development of more rationally designed combinatorial treatment approaches. In a previous study, ALK downstream signaling was characterized by in depth transcriptome analysis of neuroblastoma cells treated for six hours with the ALK inhibitor TAE684, resulting in the 77-gene ALK signature and the identification of a negative MAPK feedback loop and of RET as ALK activated target gene [31]. Moreover, we generated transcriptome data between 10 minutes and 6 hours after pharmacological ALK inhibition to show that our established 77-gene signature is gradually decreasing starting from 2 hours after the treatment. Here, we further

explore this dynamic transcriptome data generated upon treatment with the ALK inhibitor TAE684 in order to look in more detail into the dynamics of early transcriptional responses following ALK inhibition to improve our understanding on downstream ALK signaling and identify novel targets for combination therapy. To this end, we performed differential gene expression analysis at different time points following TAE684 treatment of the neuroblastoma cell line CLB-GA with an activating ALK^{R1275Q} mutation.

4.1.4 RESULTS AND DISCUSSION

MAPK, PI_3K, RET and MYC(N) signaling pathways are downregulated starting from 1 to 2 hours after TAE684 treatment

In order to gain more insights into the early dynamics of transcriptional changes after pharmacological inhibition of ALK signaling in neuroblastoma cells, the neuroblastoma cell line CLB-GA, which harbours an ALK^{R1275Q} mutation, was treated with the ALK inhibitor TAE684 and DMSO as control. While TAE684 did not go into clinical trials, TAE684 is a valid ALK inhibitor as we previously showed that the transcriptional responses for this drug and the more clinically relevant ones, such as crizotinib, LDK378 and X396, are very similar [31]. RNA expression profiling was performed on cells harvested 10 and 30 minutes, 1, 2, 4 and 6 hours after treatment (Supplementary Fig. 1).

Our previously established 77-gene ALK signature [31] significantly decreases from 2 hours after ALK inhibitor treatment, as shown earlier by Lambertz *et al.* [31]. In this study, we evaluated the dynamic regulation of known ALK downstream pathways, i.e. MAPK, PI_3K, RET and MYC/MYCN signaling pathways [4–7,31–34], by calculating signature activity scores for drugs specifically blocking these pathways. These drug signature scores summarize the transcriptional response of the components of a given signaling pathway upon pharmacological pathway inhibition. Our data confirm ALK regulation of these pathways and furthermore show that MAPK, PI_3K and RET pathway activity is decreased as early as 1 to 2 hours after the start of TAE684 treatment, as the corresponding inhibitor scores become activated at those time points (Figs. 1A, 1B, 1C; Supplementary Figs. 2A, 2B, 2C, 3A, 3B, 3C). Furthermore, we observed that *MYCN* expression levels significantly drop 1 hour after the treatment ($p=0.0015$) (Fig. 1D; Supplementary Fig. 2D). As expected, MYC(N)

activity scores [35,36] follow a delayed response at later time points (Figs. 1E, 1F; Supplementary Figs. 2E, 2F ,3D, 3E). These results are in line with the previously established regulatory role on MYCN transcription initiation for ALK, in addition to its effect on MYCN activity via phosphorylation [32,34,37–39].

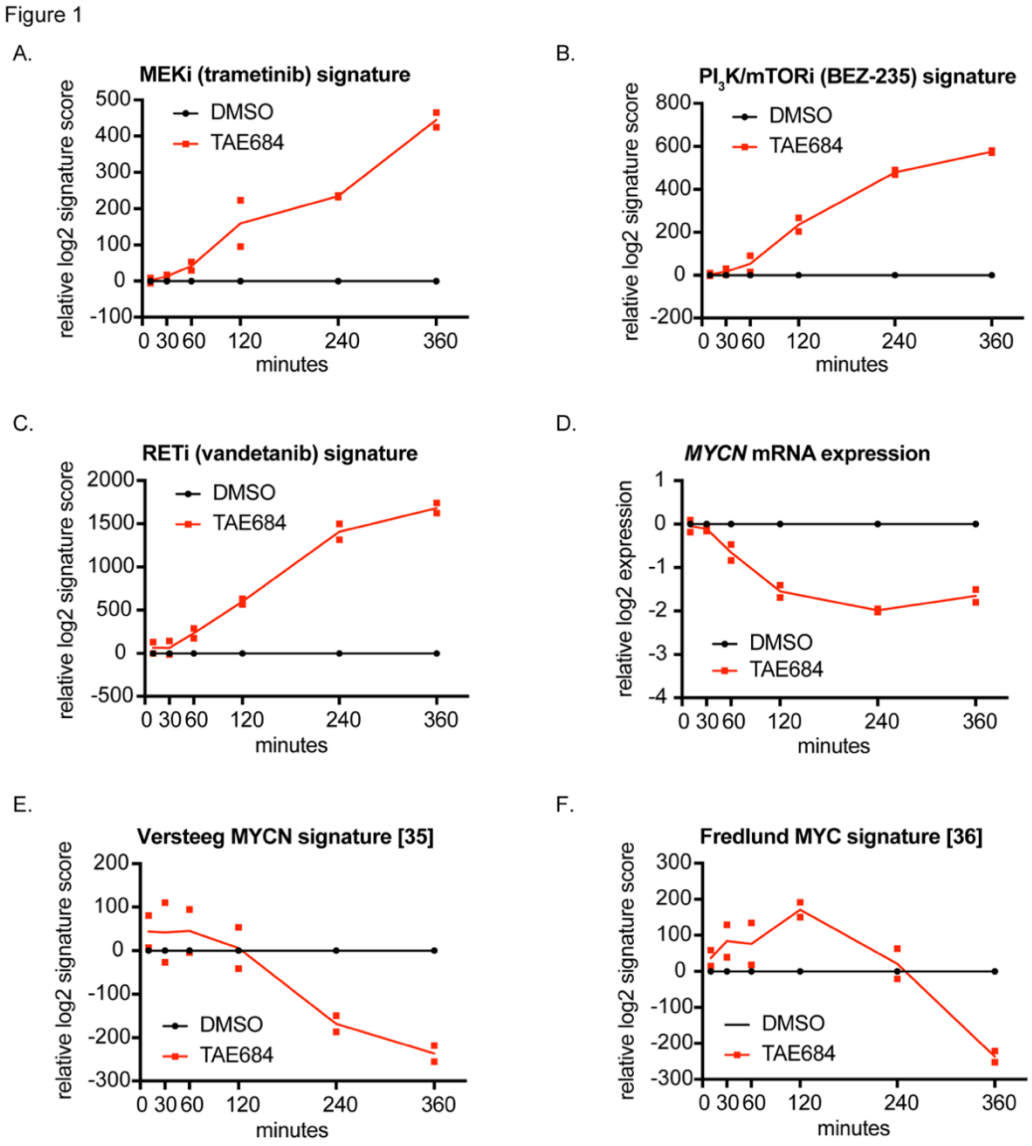

Figure 1: Signature score analysis for MAPK, PI_3K, RET and MYC(N) signaling pathways, downregulated starting from 1 or 2 hours after TAE684 treatment

A.-E. MEK inhibitor (trametinib) (A), PI_3K/mTOR inhibitor (BEZ-235) (B) and RET inhibitor (vandetanib) (C) signatures are upregulated from 1 or 2 hours after treatment of the CLB-GA cell line with 320 nM TAE684, while *MYCN* mRNA expression levels (D) are downregulated from 1 hour after treatment and the MYCN activity score from Valentijn *et al.* [35] (E) and the MYC signature score from Fredlund *et al.* [36] (F) from respectively 2 and 4 hours after

pharmacological ALK blockade. Log2 transformed ratios of expression levels of TAE684 treated vs DMSO control samples are plotted.

To identify other dynamically regulated pathways upon ALK inhibition, functional enrichment analysis was performed on a set of k-means clusters of genes with similar transcriptional responses over the timeframe. After k-means clustering with 9 centers, as defined by the elbow method, we combined clusters with similar expression patterns over time yielding a total of 6 different clusters (Fig. 2A; Supplementary Figs. 4A, 4B, 5A). Moreover, 4 of these clusters, namely cluster A, B, D and E, are showing a clear dynamic pattern, with a change in expression starting at 120 or 240 minutes and increasing over time, while the other 2 are showing a more modest pattern over time with only a small change at the latest time point (Fig. 2A, Supplementary Fig. 5A). Functional characterization of these 4 clusters through evaluating the enrichment for gene ontology terms (MSigDB ‘c5 Gene Ontology (GO) Biological Process Ontology (BP) v6.0’), oncogenic signatures (MSigDB ‘c6 Oncogenic Signatures v5.0’) and pathways of the Reactome Database [40,41] confirmed that these clusters consist of MYC, MAPK or mTOR targets and are involved in regulation of the MAPK cascade, in keeping with the downregulation of the MYC(N), PI_3K-AKT-mTOR and MAPK pathway (Fig. 2B; Supplementary Figs. 5B, 5C). Moreover, cluster E is also enriched for genesets linked to epigenetic processes, regulating amongst others chromatin structure and gene expression (Fig. 2B; Supplementary Figs. 5B, 5C).

Taken together, this analysis provides insights into the dynamics of inactivation of ALK-driven downstream pathways in ALK mutant neuroblastoma cells upon ALK inhibition and validates the applicability of the presented dataset to further scrutinize early temporal effects of ALK inhibition.

Figure 2

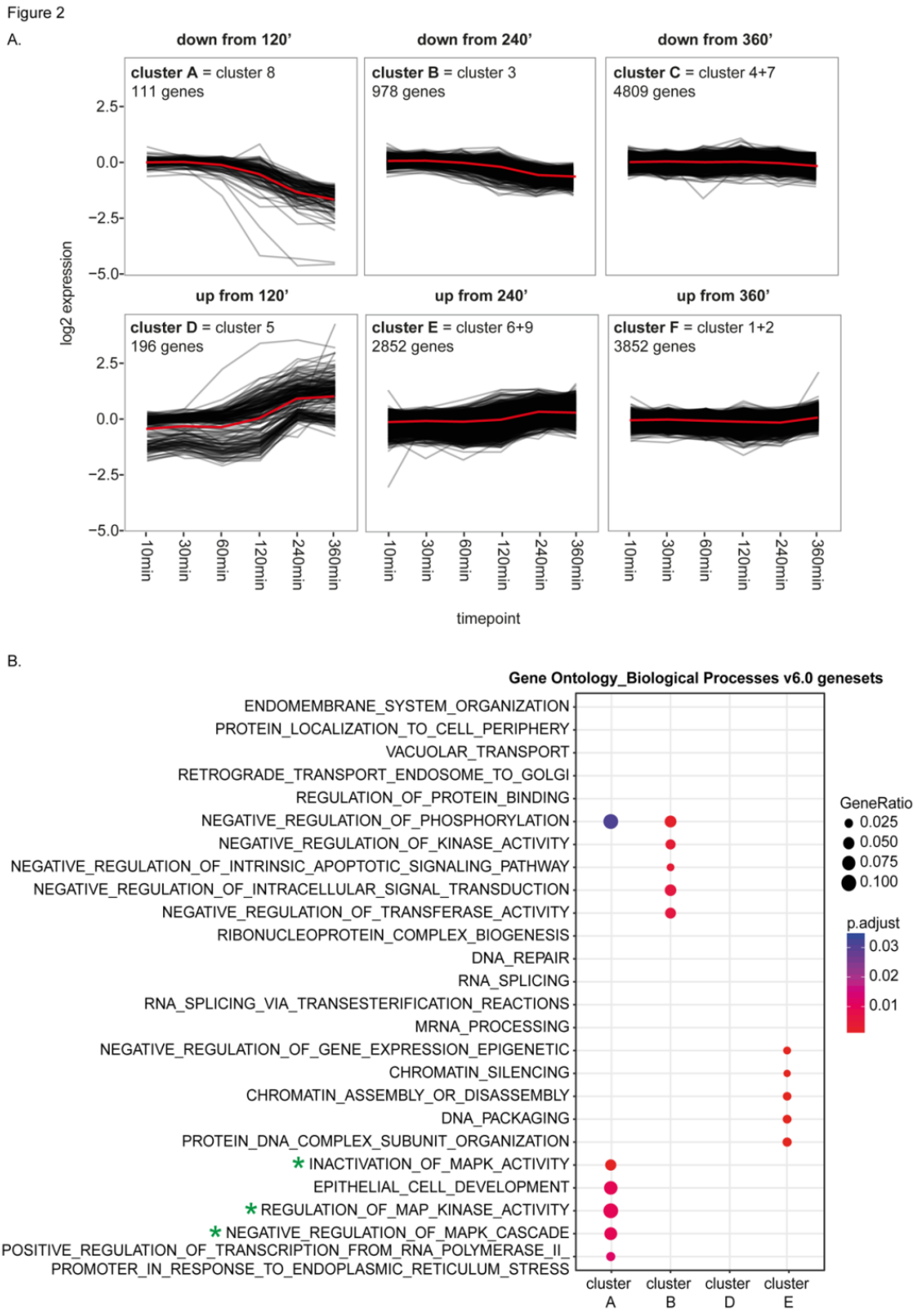

Figure 2: Functional characterization of the genes in the clusters with the MSigDB 'c5 Gene Ontology (GO) Biological Process Ontology (BP) v6.0',

A. The cluster plots represent the dynamic pattern of the expression of the genes belonging to 1 of the 6 clusters. The mean of the ratio of the expression in the TAE684 vs DMSO treated sample is plotted for each gene. The red lines show the average dynamic pattern of

the expression of the genes belonging to these clusters, calculated by the average of the mean of the ratio of the expression in the TAE684 vs DMSO treated sample. **B.** Plot showing the MSigDB 'c5 Gene Ontology (GO) Biological Process Ontology (BP) v6.0' genesets that are enriched in at least one of the four clusters, which are showing a clear dynamic pattern (clusters A, B, D, E). The size of each node corresponds to the number of genes overlapping between the cluster and the gene set and the colour represents the adjusted p-value of the enrichment test. Green stars indicate the genesets related to the MYC(N), KRAS-MAPK, PI_3K/mTOR pathways.

MYC(N) signaling is upregulated immediately following ALK inhibition

To functionally scrutinize the transcriptional changes upon ALK inhibitor treatment, Gene Set Enrichment Analysis (GSEA [42]) was performed using the 'Hallmarks v5.0' genesets from the Molecular Signatures Database (MSigDB) (software.broadinstitute.org/gsea/msigdb) at the different time points. This analysis further validates that the signaling pathways KRAS (MAPK) and PI_3K-mTOR are significantly repressed (Fig. 3A). Remarkably, one of the MYC genesets (HALLMARK_MYC_TARGETS_1) is significantly enriched for genes upregulated 30 minutes after treatment and significantly enriched for genes downregulated 6 hours after pharmacological ALK blockade (Fig. 3A, indicated in red). Moreover, we observed a significant increase in the Fredlund MYC signature [36] 2 hours after ALK inhibition ($p=0.0038$) (Fig. 1F, Supplementary Fig. 2F). Therefore, we also performed GSEA on other MYC(N) activity signatures and confirmed for 4 other genesets an initial upregulation (at 10 or 30 minutes after ALK inhibitor treatment) followed by a downregulation (from 2 hours after ALK inhibitor treatment) (Fig. 3B). The observation of this initial upregulation of MYCN activity scores is intriguing and needs further investigation.

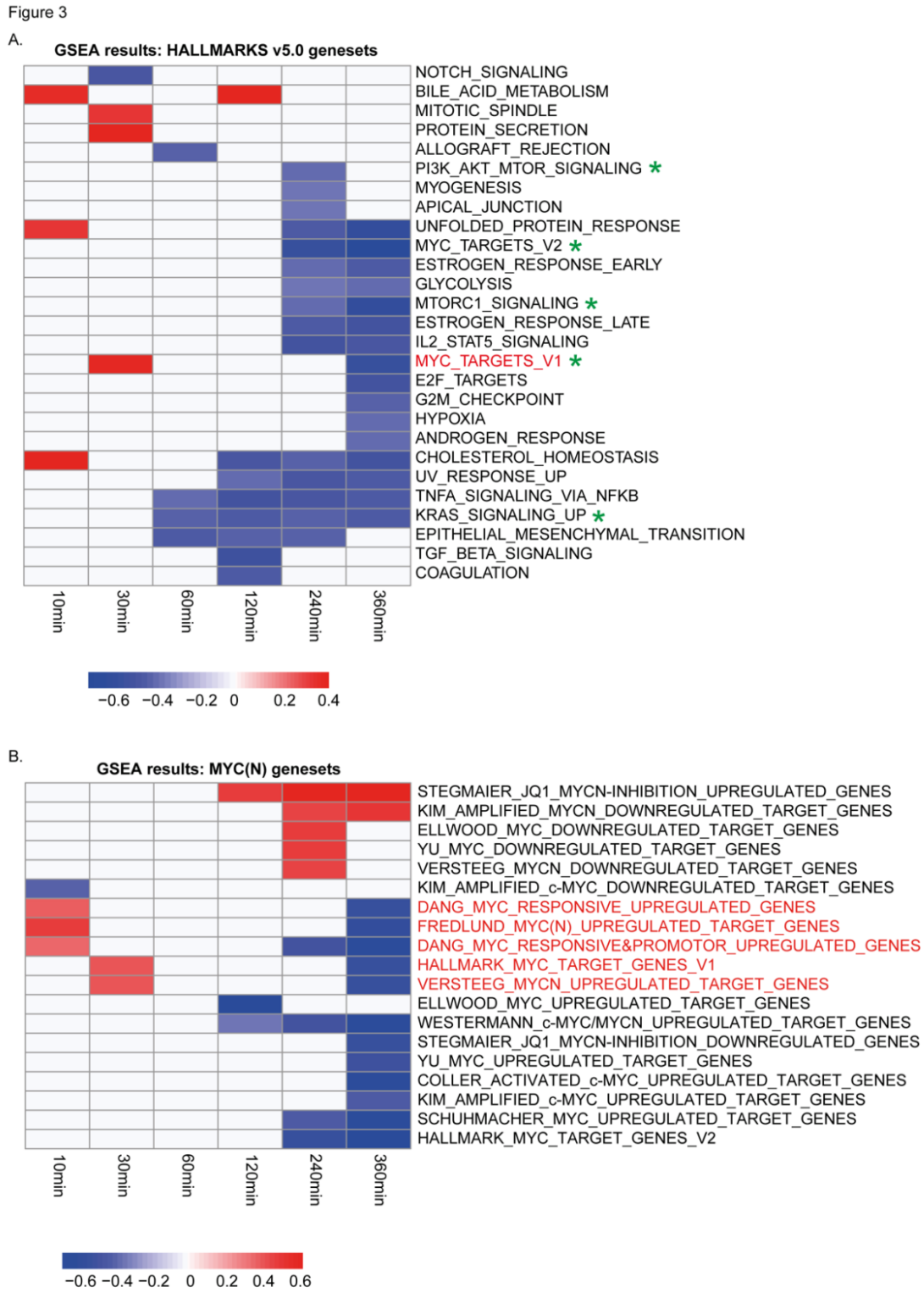

Figure 3: Gene Set Enrichment Analysis (GSEA) with the hallmarks and the MYC(N) signaling genesets shows that MYC(N) signaling is upregulated immediately following ALK inhibition

A. and B. Heatmap showing the genesets of the 'Hallmarks v5.0' genesets from MSigDB (A) and an in house compiled gene set collection containing all MYC target genesets from this

hallmark catalogue as well as publically available MYC(N) activity or target signatures [35,60–66] (B), that are enriched among the genes upregulated after ALK inhibition (positively enriched) (red) or that are enriched among the genes downregulated after ALK inhibition (negatively enriched) (blue) according to GSEA (with FDR < 0.1) [41]. Indicated in red are the genesets that are upregulated at earlier and downregulated at the later time points following ALK inhibition. Green stars indicate the genesets related to the MYC(N), KRAS-MAPK, PI_3K/mTOR pathways.

Adrenomedullin (ADM) is the earliest upregulated gene upon pharmacological ALK inhibition of NB cells

In order to identify the set of early and late genes that significantly change transcriptionally, differential gene expression analysis comparing TAE684 treated cells with DMSO treated controls was performed at each time point. This analysis revealed that no significant transcriptional changes occur as early as 10 or 30 minutes after treatment (using adjusted p-value (False Discovery Rate (FDR)) < 0.05), while starting from 2 hours after treatment an increasing number of significantly, differentially expressed genes are identified (Supplementary Table I). Our observations are in line with these from Lai *et al.* [43], who have shown that transcriptional events occur between 2 and 4 hours after inhibition of a receptor tyrosine kinase.

Interestingly, one gene showed significant differential upregulation 1 hour post-TAE684 treatment, i.e. adrenomedullin (*ADM*) (Fig. 4A; Supplementary Fig. 6A). Interestingly, using second- and third-generation ALK inhibitors [31], the upregulation of *ADM* upon ALK inhibition was confirmed in CLB-GA and Kelly (Supplementary Figs. 6B, 6C). Moreover, we could validate *ADM* upregulation 6 hours after treatment with TAE684 in more NB cell lines with an ALK amplification, an ALK^{R1275Q} or ALK^{F1174L} mutation (Fig. 4B). Furthermore, the early upregulation of *ADM* was validated in the cell line NB-1 upon pharmacological ALK inhibition with TAE684 (Fig. 4C), as the increase was already detectable 1 hour after the treatment. In addition, *ADM* expression levels are also significantly induced in the CLB-GA cell line, following PI_3K/mTOR inhibitor BEZ-235, MEK antagonist trametinib and RET repressor vandetanib treatment [31] (Supplementary Fig. 6D). Interestingly, *ADM* upregulation was also observed in the Anaplastic Large Cell Lymphoma (ALCL) cell line TS treated with three different ALK inhibitors for 6 hours [44] (Fig. 4D).

Adrenomedullin is upregulated under hypoxic conditions in neuroblastoma

As ADM is known to be induced under hypoxia [45–51], we investigated publically available transcriptome data from hypoxic versus normoxic neuroblastoma cells [52] and confirmed *ADM* upregulation under hypoxic conditions in these cells (Fig. 4E). Of further interest, *ADM* is higher expressed in more aggressive neuroblastoma tumours (stage 4 versus other stages) (Fig. 4F).

Furthermore, the observed *ADM* upregulation is intriguing and has a potentially important translational consequence. In addition to ADM activation upon hypoxia [45–51], ADM was also shown to act as growth factor, prevent apoptosis-mediated cell death, increase tumour cell motility and metastasis and induce angiogenesis in various cancer types [47–49,51,53–59]. Of further importance, it has been reported that hypoxia, which can activate ADM [45–51], induces resistance to ALK inhibitors in non-small cell lung cancer [60] and that ADM expression levels are increased in tyrosine kinase inhibitor sunitinib resistant renal cell carcinoma [61]. In view of these observations, we evaluated whether combining an adrenomedullin receptor antagonist (ADM22-52) [61] together with TAE684 would sensitize NB cells to ALK inhibition. No additional effects on decrease in cell viability were observed (data not shown). This observation could be due to the fact that elevated ADM levels have no effect on sensitivity for ALK inhibitors in neuroblastoma cells. Alternatively, given that the cell lines tested are very sensitive to the inhibitor with immediate strong and massive apoptotic effects, under these conditions elevated ADM levels may have no immediate effects on cell viability, while in a later stage in cells rendered resistant to ALK inhibition, combined exposure to both ALK inhibition and the ADM inhibitor might have effect.

Figure 4

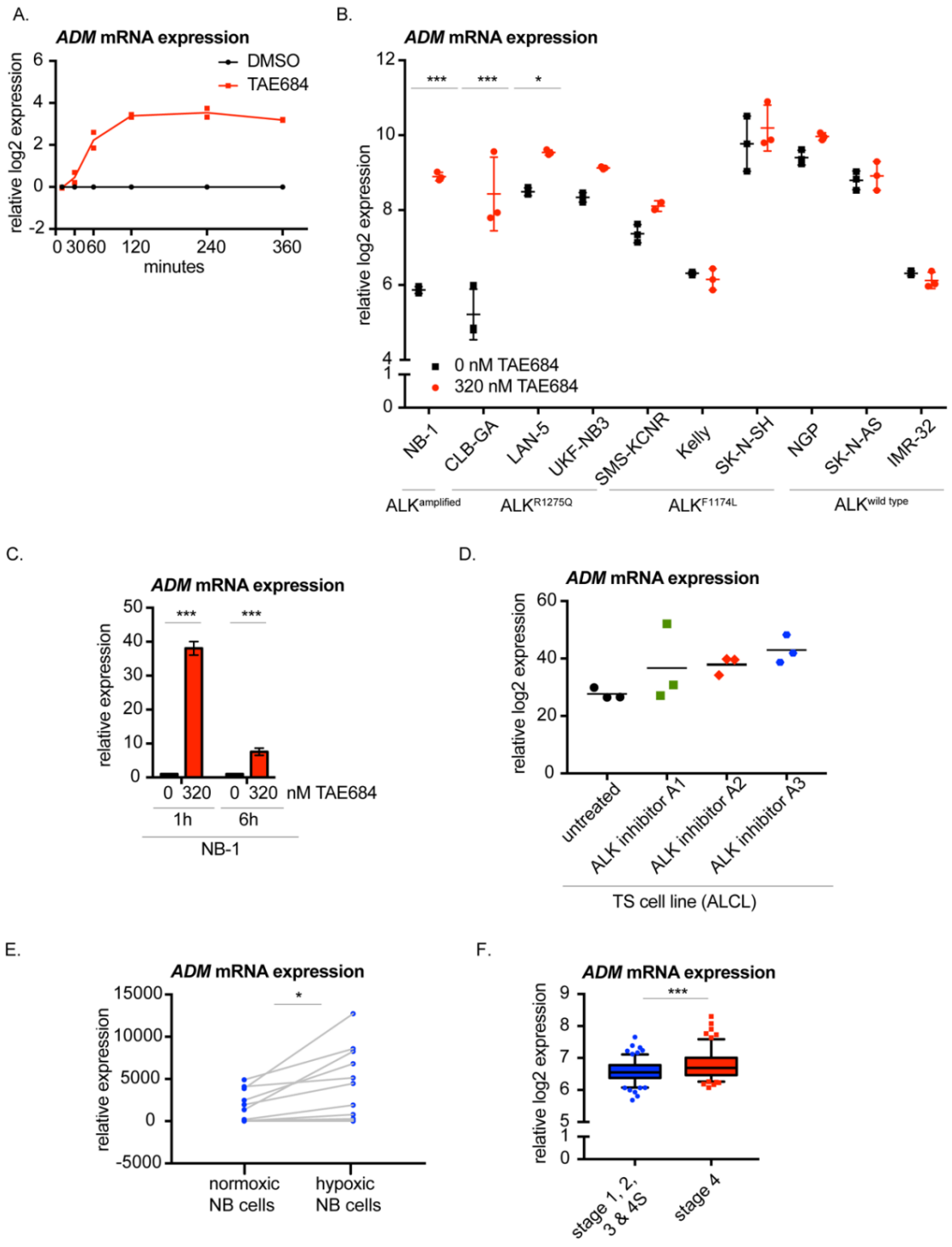

Figure 4: Adrenomedullin (ADM) is the earliest upregulated gene upon pharmacological ALK inhibition of NB cells

A. *ADM* mRNA is significantly upregulated starting from 1 hour after TAE684 treatment of the CLB-GA cell line. Ratios of log2 transformed expression levels of TAE684 treated vs DMSO control samples are plotted. **B.** *ADM* mRNA expression levels shown in several ALK wild

type (NGP, SK-N-AS, IMR-32) and ALK mutant (NB-1, CLB-GA, LAN-5, UKF-NB3, SMS-KCNR, Kelly, SK-N-SH) cell lines treated for 6 hours with 0.32 µM TAE684 or DMSO. **C.** *ADM* mRNA expression levels are upregulated in NB cell line NB-1 (ALKamp) 1 hour and 6 hours after treatment with 0.32 µM TAE684 compared to the DMSO control. **D.** *ADM* expression levels are upregulated 6 hours upon ALK inhibition with three different ALK inhibitors in the ALCL cell line TS. **E.** *ADM* mRNA expression levels are upregulated in 11 NB cell lines under hypoxic conditions. **F.** *ADM* expression levels are higher in stage 4 primary neuroblastoma tumours versus neuroblastoma tumours of stage 1, 2, 3 and 4S. Boxplots represent mean ± 95% confidence interval.
Statistical analyses: unpaired one-way ANOVA with Bonferroni correction (B. & C. & D.), paired t-test (E.) and unpaired t-test (F.). * $P < 0.05$, ** $P < 0.01$, *** $P < 0.001$

4.1.5 CONCLUSION

In summary, dynamic expression profiling following ALK inhibition of ALK mutated neuroblastoma cells revealed (1) unexpected early *ADM* upregulation with potential implications for design of more effective ALK targeted therapy, (2) an initial increase of MYC(N) activity immediately after ALK inhibition and (3) confirmed inhibition after 1 to 2 hours of the ALK downstream MAPK, PI3K-AKT, RET and MYC(N) pathways.

4.1.6 MATERIAL AND METHODS

CLB-GA time series dataset

The CLB-GA time series dataset has been described before [31]. The neuroblastoma CLB-GA cell line (ALK^{R1275Q}) was cultured in RPMI-1640 medium (Invitrogen), supplemented with fetal bovine serum (10%), kanamycin (100 µg/ml) penicillin/streptomycin (100 IU/ml), L-glutamine (2 mM) and HEPES (25 mM) (Life Technologies), and maintained at 37°C in a 5% C02-humidified environment. At different time points (10, 30 minutes, 1, 2, 4 and 6 hours) after treatment with 0.32 µM of the small molecule ALK inhibitor NVP-TAE684 (hereafter TAE684) (SelleckChem, S1108) or DMSO (VWR) as solvent control, cells were harvested and RNA quality was analysed using Experion (Bio-Rad) prior to gene-expression profiling. Samples were labelled and hybridized to the Sureprint G3 human GE 8x60K microarrays (Agilent Technologies), according to the manufacturer's guidelines and starting from 200 ng RNA. The data was normalized with the vsn method in R version

3.3.3 (packages vsn and limma). The R package BioMart was used to annotate gene names to their corresponding probes. Probes detecting at least a two-fold higher expression than the negative control probes of the array in at least 60% of the DMSO or TAE samples, were selected as background correction. Data can be accessed through ArrayExpress (accession number E-MTAB-3206) [31].

Signature score analysis

To establish MAPK, PI_3K/mTOR and RET inhibitor signatures, we used published gene expression profiling data (ArrayExpress accession number E-MTAB-3206) [31]. This dataset contains expression profiling data of the CLB-GA cell line 6 hours after treatment with MAPK inhibitor trametinib, the dual PI_3K/mTOR repressor BEZ-235 or RET antagonist vandetanib and DMSO as control. Using the limma R-package, differential expression analysis was performed comparing the DMSO-control and the inhibitor treated samples. The established signatures consist of the differentially expressed genes with adjusted p-value (False Discovery Rate (FDR)) < 0.05. In addition, a published MYCN and a published MYC signature were used to establish the MYC(N) pathway activity [35,36]. Signatures score analysis was conducted using a rank-scoring algorithm as described previously [31,36]. For each time point and each duplicate separately, both the ratio between the TAE684 treated sample and his corresponding control sample (Figure 1) as the absolute values (Supplementary Figure 2) were plotted using GraphPad Prism 7.

Gene set enrichment analysis

Gene set enrichment analysis (GSEA [42]) was performed using the MSigDB 'Hallmarks v5.0' gene sets (software.broadinstitute.org/gsea/msigdb) and an in house compiled gene set catalogue containing all MYC target genesets from this hallmark catalogue as well as publically available MYC(N) activity or target signatures [35,36,62–67]. The genesets, showing positively or negatively enrichment at minimum one time point and with a FDR < 0.1 are plotted in a heatmap. Data was plotted as the mean of the ratio of the TAE684 treated sample and his corresponding control sample at every time point.

Cluster analysis and pathway enrichment analysis in the clusters

Using the Bayesian Information Criterion (BIC) and the elbow method, 9 was defined as the optimal number of clusters in the dataset (Supplementary Figs. 4A, 4B). K-means clustering was performed on the expression level ratios of TAE684/DMSO samples for each time point in R (with k=9). However, visual inspection of the expression patterns of the genes in the clusters showed that some clusters have a similar pattern over time (clusters 1 and 2, 4 and 7, 6 and 9) (Supplementary Fig. 4B) and were therefore merged, ending with 6 final clusters (Supplementary Fig. 5A). For every cluster, the average response of the genes was plotted as a line (red line). The 4 clusters that are showing a clear dynamic pattern over time, were screened for MSigDB 'c5 Gene Ontology (GO) Biological Process Ontology (BP) v6.0' (software.broadinstitute.org/gsea/msigdb), MSigDB 'c6 Oncogenic Signatures v5.0' and overrepresented Reactome pathways [40,41] using the R-packages clusterProfiler and Reactome Pathway Analysis [68,69].

Differential expression analysis

At every time point, differential expression analysis was performed using the R package limma, comparing the DMSO-control and the TAE684-treated sample. The duplicate experiments, independently generated at different time points, were set as blocking factor. Significantly differentially expressed genes refer to those with an adjusted p-value (FDR) < 0.001. Results are shown in Supplementary Table I.

Analysis of ADM expression levels after ALK inhibition using qPCR

ADM expression levels were measured in CLB-GA (ALK^{R1275Q}) and Kelly (ALK^{F1174L}) cells that were treated for 6 hours with DMSO as control solvent and 0.09 µM of ALK inhibitor, PF06463922 acetate (Sigma-Aldrich, PZ0271) (dissolved in sterile DMSO and diluted to the final concentration in culture medium) and in NB-1 (ALK^{amp}) cells that were treated for 1 and 6 hours with DMSO as control solvent and 0.32 µM of TAE684 (dissolved in sterile DMSO and diluted to the final concentration in culture medium).

RNA extraction, cDNA synthesis and RT-qPCR of these samples was performed as described earlier [31]. The Cq-values for ADM expression were normalized with data

of at least two reference genes (TBP, YWHAZ, B2M, HPRT1 and SDHA) (primer sequences: Supplementary Table II) using qBasePlus software (Biogazelle).

Evaluation of ADM expression in public mRNA expression datasets

ADM expression levels were evaluated in (1) CLB-GA cells treated with 0.2 μM LDK378, 0.32 μM TAE684, 0.06 μM X396, 0.5 μM crizotinib, 0.05 μM trametinib (MEK inhibitor), 0.5 μM BEZ-235 (dual PI_3K/mTOR inhibitor) and 9.5 μM vandetanib for 6 hours (ArrayExpress accession number E-MTAB-3206) [31], (2) 10 NB cell lines treated with 0.32 μM TAE684 for 6 hours (ArrayExpress accession number E-MTAB-3205) [31], (3) the ALCL TS cell line treated with three different ALK inhibitors for 6 hours (GEO accession number GSE6184) [44], (4) 11 NB cell lines that were cultured under normoxic and hypoxic conditions (1% O2 instead of 20%) for 18 hours (GEO accession number GSE17714) [52] and (5) a cohort of 283 neuroblastoma tumour samples (GEO accession number GSE85047).

Statistical analyses

Statistical significance was calculated with GraphPad Prism7 by unpaired one-way ANOVA with Bonferroni correction when comparing more than two unmatched groups, while (un)-paired t-test was chosen when comparing two groups.

4.1.7 ACKNOWLEDGEMENTS

We thank Jeroen Schacht, Fanny De Vloed, Jolien Van Laere and Els De Smet for their outstanding technical assistance.

4.1.8 FUNDING

S.C. is supported by a pre-doctoral fellowship of the Research Foundation – Flanders (FWO; 11J8313N) and an Emmanuel van der Schueren grant (‘Kom op tegen Kanker’). K.D. is supported by Ghent University (BOF; BOF16/PDO/043) and R.C. by a pre-doctoral fellowship of the Research Foundation – Flanders (FWO).
The authors would further like to thank the following funding agencies: the Belgian Foundation against Cancer (project 2014-175) to F.S., Ghent University (BOF10/GOA/019, BOF16/GOA/23) to F.S., the Belgian Program of Interuniversity Poles of Attraction (IUAP Phase VII - P7/03) to F.S., the Fund for Scientific Research

Flanders (Research projects G053012N, G050712N, G051516N to F.S) and 'Stichting Villa Joep' to F.S.

4.1.9 CONFLICT OF INTEREST

The authors declare no conflict of interest.

4.1.10 REFERENCES

1. Louis CU, Shohet JM. Neuroblastoma: molecular pathogenesis and therapy. Annu Rev Med. 2015; 66: 49–63. doi: 10.1146/annurev-med-011514-023121.
2. Matthay K, Maris J, Schleiermacher G, Nakagawara A, Mackall C, Diller L, Weiss W. Neuroblastoma. Nat Rev Dis Primers. 2016; 2: 16078. doi: 10.1038/nrdp.2016.78.
3. Moreno L, Caron H, Geoerger B, Eggert A, Schleiermacher G, Brock P, Valteau-Couanet D, Chesler L, Schulte JH, De Preter K, Molenaar J, Schramm A, Eilers M, et al. Accelerating drug development for neuroblastoma - New Drug Development Strategy: an Innovative Therapies for Children with Cancer, European Network for Cancer Research in Children and Adolescents and International Society of Paediatric Oncology Europe Neuroblastoma project. Expert Opin Drug Discov. 2017; 12: 801–11. doi: 10.1080/17460441.2017.1340269.
4. George R, Sanda T, Hanna M, Fröhling S, II W, Zhang J, Ahn Y, Zhou W, London W, McGrady P, Xue L, Zozulya S, Gregor V, et al. Activating mutations in ALK provide a therapeutic target in neuroblastoma. Cah Rev The. 2008; 455: 975–8. doi: 10.1038/nature07397.
5. Mossé Y, Laudenslager M, Longo L, Cole K, Wood A, Attiyeh E, Laquaglia M, Sennett R, Lynch J, Perri P, Laureys G, Speleman F, Kim C, et al. Identification of ALK as a major familial neuroblastoma predisposition gene. Nature. 2008; 455: 930–5. doi: 10.1038/nature07261.
6. Chen Y, Takita J, Choi Y, Kato M, Ohira M, Sanada M, Wang L, Soda M, Kikuchi A, Igarashi T, Nakagawara A, Hayashi Y, Mano H, et al. Oncogenic mutations of ALK kinase in neuroblastoma. Cah Rev The. 2008; 455: 971–4. doi: 10.1038/nature07399.
7. Janoueix-Lerosey I, Lequin D, Brugières L, Ribeiro A, Pontual L, Combaret V, Raynal V, Puisieux A, Schleiermacher G, Pierron G, Valteau-Couanet D, Frebourg T, Michon J, et al. Somatic and germline activating mutations of the ALK kinase receptor in neuroblastoma. Cah Rev The. 2008; 455: 967–70. doi: 10.1038/nature07398.
8. Bellini A, Bernard V, Leroy Q, Frio T, Pierron G, Combaret V, Lapouble E, Clement N, Rubie H, Thebaud E, Chastagner P, Defachelles A, Bergeron C, et al. Deep Sequencing Reveals Occurrence of Subclonal ALK Mutations in

Neuroblastoma at Diagnosis. Clin Cancer Res. 2015; 21: 4913–21. doi: 10.1158/1078-0432.CCR-15-0423.

9. Schleiermacher G, Javanmardi N, Bernard V, Leroy Q, Cappo J, Rio Frio T, Pierron G, Lapouble E, Combaret V, Speleman F, de Wilde B, Djos A, Ora I, et al. Emergence of new ALK mutations at relapse of neuroblastoma. J Clin Oncol. 2014; 32: 2727–34. doi: 10.1200/JCO.2013.54.0674.

10. Eleveld TF, Oldridge DA, Bernard V, Koster J, Daage LC, Diskin SJ, Schild L, Bentahar NB, Bellini A, Chicard M, Lapouble E, Combaret V, Legoix-Né P, et al. Relapsed neuroblastomas show frequent RAS-MAPK pathway mutations. Nat Genet. 2015; 47: 864–71. doi: 10.1038/ng.3333.

11. Friboulet L, Li N, Katayama R, Lee C, Gainor J, Crystal A, Michellys P-Y, Awad M, Yanagitani N, Kim S, Pferdekamper A, Li J, Kasibhatla S, et al. The ALK Inhibitor Ceritinib Overcomes Crizotinib Resistance in Non–Small Cell Lung Cancer. Cancer Discov. 2014; 4: 662–73. doi: 10.1158/2159-8290.CD-13-0846.

12. Shaw A, Friboulet L, Leshchiner I, Gainor J, Bergqvist S, Brooun A, Burke B, Deng Y-L, Liu W, Dardaei L, Frias R, Schultz K, Logan J, et al. Resensitization to Crizotinib by the Lorlatinib ALK Resistance Mutation L1198F. New Engl J Medicine. 2016; 374: 54–61. doi: 10.1056/NEJMoa1508887.

13. Lovly C, McDonald N, Chen H, Ortiz-Cuaran S, Heukamp L, Yan Y, Florin A, Ozretić L, Lim D, Wang L, Chen Z, Chen X, Lu P, et al. Rationale for co-targeting IGF-1R and ALK in ALK fusion-positive lung cancer. Nat Med. 2014; 20: 1027–34. doi: 10.1038/nm.3667.

14. Shaw A, Kim D-W, Mehra R, Tan D, Felip E, Chow L, Camidge R, Vansteenkiste J, Sharma S, Pas T, Riely G, Solomon B, Wolf J, et al. Ceritinib in ALK-Rearranged Non–Small-Cell Lung Cancer. New Engl J Medicine. nejm; 2014; 370: 1189–97. doi: 10.1056/NEJMoa1311107.

15. Shaw A, Kim D-W, Nakagawa K, Seto T, Crinó L, Ahn M-J, Pas T, Besse B, Solomon B, Blackhall F, Wu Y-L, Thomas M, O'Byrne K, et al. Crizotinib versus Chemotherapy in Advanced ALK-Positive Lung Cancer. New Engl J Medicine. 2013; 368: 2385–94. doi: 10.1056/NEJMoa1214886.

16. Sakamoto H, Tsukaguchi T, Hiroshima S, Kodama T, Kobayashi T, Fukami T, Oikawa N, Tsukuda T, Ishii N, Aoki Y. CH5424802, a Selective ALK Inhibitor Capable of Blocking the Resistant Gatekeeper Mutant. Cancer Cell. sciencedirect; 2011; 19: 679–90. doi: 10.1016/j.ccr.2011.04.004.

17. Thomas R. Overcoming Drug Resistance in ALK-Rearranged Lung Cancer. New Engl J Medicine. 2014; 370: 1250–1. doi: 10.1056/NEJMe1316173.

18. Mossé Y, Lim M, Voss S, Wilner K, Ruffner K, Laliberte J, Rolland D, Balis F, Maris J, Weigel B, Ingle A, Ahern C, Adamson P, et al. Safety and activity of crizotinib for paediatric patients with refractory solid tumours or anaplastic large-cell lymphoma: a Children's Oncology Group phase 1 consortium study. The Lancet Oncology. 2013; 14: 472–80. doi: 10.1016/S1470-2045(13)70095-0.

19. Guan, Tucker, Wan, Chand, Danielson, Ruuth, Wakil E, Witek, Jamin, Umapathy, Robinson, Johnson, Smeal, et al. The ALK inhibitor PF-06463922 is

effective as a single agent in neuroblastoma driven by expression of ALK and MYCN. Dis Model Mech. highwire; 2016; 9: 941–52. doi: 10.1242/dmm.024448.
20. Amin AD, Li L, Rajan SS, Gokhale V, Groysman MJ, Pongtornpipat P, Tapia EO, Wang M, Schatz JH. TKI sensitivity patterns of novel kinase-domain mutations suggest therapeutic opportunities for patients with resistant ALK+ tumors. Oncotarget. 2016; 7: 23715–29. doi: 10.18632/oncotarget.8173.
21. Pall G. The next-generation ALK inhibitors. Curr Opin Oncol. 2015; 27: 118. doi: 10.1097/CCO.0000000000000165.
22. Duncan JS, Whittle MC, Nakamura K, Abell AN, Midland AA, Zawistowski JS, Johnson NL, Granger DA, Jordan NV, Darr DB, Usary J, Kuan P-F, Smalley DM, et al. Dynamic Reprogramming of the Kinome in Response to Targeted MEK Inhibition in Triple-Negative Breast Cancer. Cell. 2012; 149: 307–21. doi: 10.1016/j.cell.2012.02.053.
23. Toyokawa, Seto. Updated Evidence on the Mechanisms of Resistance to ALK Inhibitors and Strategies to Overcome Such Resistance: Clinical and Preclinical Data. Oncology Research and Treatment. 2015; 0: 291–8. doi: 10.1159/000430852.
24. Bresler SC, Wood AC, Haglund EA, Courtright J, Belcastro LT, Plegaria JS, Cole K, Toporovskaya Y, Zhao H, Carpenter EL, Christensen JG, Maris JM, Lemmon MA, et al. Differential inhibitor sensitivity of anaplastic lymphoma kinase variants found in neuroblastoma. Sci Transl Med. 2011; 3: 108ra114. doi: 10.1126/scitranslmed.3002950.
25. Bresler SC, Weiser DA, Huwe PJ, Park JH, Krytska K, Ryles H, Laudenslager M, Rappaport EF, Wood AC, McGrady PW, Hogarty MD, London WB, Radhakrishnan R, et al. ALK Mutations Confer Differential Oncogenic Activation and Sensitivity to ALK Inhibition Therapy in Neuroblastoma. Cancer Cell. 2014; 26: 682–94. doi: 10.1016/j.ccell.2014.09.019.
26. Heuckmann J, Hölzel M, Sos M, Heynck S, Balke-Want H, Koker M, Peifer M, Weiss J, Lovly C, Grütter C, Rauh D, Pao W, Thomas R. ALK Mutations Conferring Differential Resistance to Structurally Diverse ALK Inhibitors. Clinical Cancer Research. 2011; 17: 7394–401. doi: 10.1158/1078-0432.CCR-11-1648.
27. Yan X, Kennedy C, Tilkens S, Wiedemeier O, Guan H, Park J-I, Chan A. Cooperative Cross-Talk between Neuroblastoma Subtypes Confers Resistance to Anaplastic Lymphoma Kinase Inhibition. Genes & Cancer. 2011; 2: 538–49. doi: 10.1177/1947601911416003.
28. Debruyne D, Bhatnagar N, Sharma B, Luther W, Moore N, Cheung N-K, Gray N, George R. ALK inhibitor resistance in ALKF1174L-driven neuroblastoma is associated with AXL activation and induction of EMT. Oncogene. 2015; 35: 3681–91. doi: 10.1038/onc.2015.434.
29. Isozaki H, Ichihara E, Takigawa N, Ohashi K, Ochi N, Yasugi M, Ninomiya T, Yamane H, Hotta K, Sakai K, Matsumoto K, Hosokawa S, Bessho A, et al. Non–Small Cell Lung Cancer Cells Acquire Resistance to the ALK Inhibitor Alectinib by Activating Alternative Receptor Tyrosine Kinases. Cancer Res. highwire; 2015; 76: 1506–16. doi: 10.1158/0008-5472.CAN-15-1010.

30. Lovly C, Shaw A. Molecular Pathways: Resistance to Kinase Inhibitors and Implications for Therapeutic Strategies. Clin Cancer Res. highwire; 2014; 20: 2249–56. doi: 10.1158/1078-0432.CCR-13-1610.
31. Lambertz I, Kumps C, Claeys S, Lindner S, Beckers A, Janssens E, Carter DR, Cazes A, Cheung BB, De Mariano M, De Bondt A, De Brouwer S, Delattre O, et al. Upregulation of MAPK Negative Feedback Regulators and RET in Mutant ALK Neuroblastoma: Implications for Targeted Treatment. Clin Cancer Res. 2015; 21: 3327–39. doi: 10.1158/1078-0432.CCR-14-2024.
32. Schönherr C, Ruuth K, Kamaraj S, Wang C-L, Yang H-L, Combaret V, Djos A, Martinsson T, Christensen J, Palmer R, Hallberg B. Anaplastic Lymphoma Kinase (ALK) regulates initiation of transcription of MYCN in neuroblastoma cells. Oncogene. Oncogene; 2012; 31: 5193–200. doi: 10.1038/onc.2012.12.
33. Heukamp L, Thor T, Schramm A, Preter K, Kumps C, Wilde B, Odersky A, Peifer M, Lindner S, Spruessel A, Pattyn F, Mestdagh P, Menten B, et al. Targeted Expression of Mutated ALK Induces Neuroblastoma in Transgenic Mice. Sci Transl Medicine. 2012; 4: 141ra91–141ra91. doi: 10.1126/scitranslmed.3003967.
34. Berry T, Luther W, Bhatnagar N, Jamin Y, Poon E, Sanda T, Pei D, Sharma B, Vetharoy W, Hallsworth A, Ahmad Z, Barker K, Moreau L, et al. The ALKF1174L Mutation Potentiates the Oncogenic Activity of MYCN in Neuroblastoma. Cancer Cell. sciencedirect; 2012; 22: 117–30. doi: 10.1016/j.ccr.2012.06.001.
35. Valentijn LJ, Koster J, Haneveld F, Aissa RA, van Sluis P, Broekmans ME, Molenaar JJ, van Nes J, Versteeg R. Functional MYCN signature predicts outcome of neuroblastoma irrespective of MYCN amplification. Proc Natl Acad Sci USA. 2012; 109: 19190–5. doi: 10.1073/pnas.1208215109.
36. Fredlund E, Ringnér M, Maris JM, Påhlman S. High Myc pathway activity and low stage of neuronal differentiation associate with poor outcome in neuroblastoma. Proc Natl Acad Sci USA. 2008; 105: 14094–9. doi: 10.1073/pnas.0804455105.
37. Zhu S, Lee J-S, Guo F, Shin J, Perez-Atayde A, Kutok J, Rodig S, Neuberg D, Helman D, Feng H, Stewart R, Wang W, George R, et al. Activated ALK Collaborates with MYCN in Neuroblastoma Pathogenesis. Cancer Cell. sciencedirect; 2012; 21: 362–73. doi: 10.1016/j.ccr.2012.02.010.
38. Chesler L, Schlieve C, Goldenberg DD, Kenney A, Kim G, McMillan A, Matthay KK, Rowitch D, Weiss WA. Inhibition of phosphatidylinositol 3-kinase destabilizes Mycn protein and blocks malignant progression in neuroblastoma. Cancer Res. 2006; 66: 8139–46. doi: 10.1158/0008-5472.CAN-05-2769.
39. De Brouwer S, De Preter K, Kumps C, Zabrocki P, Porcu M, Westerhout E, Lakeman A, Vandesompele J, Hoebeeck J, Van Maerken T, De Paepe A, Laureys G, Schulte J, et al. Meta-analysis of Neuroblastomas Reveals a Skewed ALK Mutation Spectrum in Tumors with MYCN Amplification. Clinical Cancer Research. Clinical Cancer Research; 2010; 16: 4353–62. doi: 10.1158/1078-0432.CCR-09-2660.
40. Fabregat A, Sidiropoulos K, Garapati P, Gillespie M, Hausmann K, Haw R, Jassal B, Jupe S, Korninger F, McKay S, Matthews L, May B, Milacic M, et al. The Reactome pathway Knowledgebase. Nucleic Acids Res. 2016; 44: D481–7. doi: 10.1093/nar/gkv1351.

41. Croft D, Mundo AF, Haw R, Milacic M, Weiser J, Wu G, Caudy M, Garapati P, Gillespie M, Kamdar MR, Jassal B, Jupe S, Matthews L, et al. The Reactome pathway knowledgebase. Nucleic Acids Res. 2014; 42: D472–7. doi: 10.1093/nar/gkt1102.
42. Subramanian A, Tamayo P, Mootha V, Mukherjee S, Ebert B, Gillette M, Paulovich A, Pomeroy S, Golub T, Lander E, Mesirov J. Gene set enrichment analysis: A knowledge-based approach for interpreting genome-wide expression profiles. P Natl Acad Sci Usa. 2005; 102: 15545–50. doi: 10.1073/pnas.0506580102.
43. Lai AZ, Cory S, Zhao H, Gigoux M, Monast A, Guiot M-CC, Huang S, Tofigh A, Thompson C, Naujokas M, Marcus VA, Bertos N, Sehat B, et al. Dynamic reprogramming of signaling upon met inhibition reveals a mechanism of drug resistance in gastric cancer. Sci Signal. 2014; 7: ra38. doi: 10.1126/scisignal.2004839.
44. Piva R, Pellegrino E, Mattioli M, Agnelli L, Lombardi L, Boccalatte F, Costa G, Ruggeri BA, Cheng M, Chiarle R, Palestro G, Neri A, Inghirami G. Functional validation of the anaplastic lymphoma kinase signature identifies CEBPB and BCL2A1 as critical target genes. J Clin Invest. 2006; 116: 3171–82. doi: 10.1172/JCI29401.
45. Kitamuro T, Takahashi K, Totsune K, Nakayama M, Murakami O, Hida W, Shirato K, Shibahara S. Differential expression of adrenomedullin and its receptor component, receptor activity modifying protein (RAMP) 2 during hypoxia in cultured human neuroblastoma cells. Peptides. 2001; 22: 1795–801.
46. Dötsch J, Harmjanz A, Christiansen H, Hänze J, Lampert F, Rascher W. Gene expression of neuronal nitric oxide synthase and adrenomedullin in human neuroblastoma using real-time PCR. Int J Cancer. 2000; 88: 172–5.
47. Park S-J, Kim J-G, Son T, Yi J, Kim N, Yang K, Heo K. The histone demethylase JMJD1A regulates adrenomedullin-mediated cell proliferation in hepatocellular carcinoma under hypoxia. Biochem Bioph Res Co. 2013; 434: 722–7. doi: 10.1016/j.bbrc.2013.03.091.
48. Wang S, Yang W-L. Circulating hormone adrenomedullin and its binding protein protect neural cells from hypoxia-induced apoptosis. Biochimica Et Biophysica Acta Bba - Gen Subj. 2009; 1790: 361–7. doi: 10.1016/j.bbagen.2009.03.012.
49. Larráyoz IM, Martínez-Herrero S, García-Sanmartín J, Ochoa-Callejero L, Martínez A. Adrenomedullin and tumour microenvironment. J Transl Med. 2014; 12: 339. doi: 10.1186/s12967-014-0339-2.
50. Sena J, Wang L, Pawlus M, Hu C-J. HIFs Enhance the Transcriptional Activation and Splicing of Adrenomedullin. Mol Cancer Res. 2014; 12: 728–41. doi: 10.1158/1541-7786.MCR-13-0607.
51. Keleg S, Kayed H, Jiang X, Penzel R, Giese T, Büchler M, Friess H, Kleeff J. Adrenomedullin is induced by hypoxia and enhances pancreatic cancer cell invasion. Int J Cancer. 2007; 121: 21–32. doi: 10.1002/ijc.22596.
52. Fardin P, Barla A, Mosci S, Rosasco L, Verri A, Versteeg R, Caron HN, Molenaar JJ, Ora I, Eva A, Puppo M, Varesio L. A biology-driven approach identifies

the hypoxia gene signature as a predictor of the outcome of neuroblastoma patients. Mol Cancer. 2010; 9: 185. doi: 10.1186/1476-4598-9-185.

53. Uemura M, Yamamoto H, Takemasa I, Mimori K, Mizushima T, Ikeda M, Sekimoto M, Doki Y, Mori M. Hypoxia-inducible adrenomedullin in colorectal cancer. Anticancer Res. 2011; 31: 507–14.

54. Oehler MK, Fischer DC, Orlowska-Volk M, Herrle F, Kieback DG, Rees MC, Bicknell R. Tissue and plasma expression of the angiogenic peptide adrenomedullin in breast cancer. Br J Cancer. 2003; 89: 1927–33. doi: 10.1038/sj.bjc.6601397.

55. Wu X-Y, Hao C-P, Ling M, Guo C-H, Ma W. Hypoxia-induced apoptosis is blocked by adrenomedullin via upregulation of Bcl-2 in human osteosarcoma cells. Oncol Rep. 2015; doi: 10.3892/or.2015.4011.

56. Li F, Yang R, Zhang X, Liu A, Zhao Y, Guo Y. Silencing of hypoxia‑inducible adrenomedullin using RNA interference attenuates hepatocellular carcinoma cell growth in vivo. Mol Med Rep. 2014; 10: 1295–302. doi: 10.3892/mmr.2014.2320.

57. Chen P, Huang Y, Bong R, Ding Y, Song N, Wang X, Song X, Luo Y. Tumor-Associated Macrophages Promote Angiogenesis and Melanoma Growth via Adrenomedullin in a Paracrine and Autocrine Manner. Clin Cancer Res. 2011; 17: 7230–9. doi: 10.1158/1078-0432.CCR-11-1354.

58. Belloni AS, Albertin G, Forneris ML, Nussdorfer GG. Proadrenomedullin-derived peptides as autocrine-paracrine regulators of cell growth. Histol Histopathol. 2001; 16: 1263–74.

59. Qiao F, Fang J, Xu J, Zhao W, Ni Y, Akuo B, Zhang W, Liu Y, Ding F, Li G, Liu B, Wang H, Shao S. The role of adrenomedullin in the pathogenesis of gastric cancer. Oncotarget. 2017; doi: 10.18632/oncotarget.18881.

60. KOGITA A, TOGASHI Y, HAYASHI H, SOGABE S, TERASHIMA M, VELASCO M, SAKAI K, FUJITA Y, TOMIDA S, TAKEYAMA Y, OKUNO K, NAKAGAWA K, NISHIO K. Hypoxia induces resistance to ALK inhibitors in the H3122 non-small cell lung cancer cell line with an ALK rearrangement via epithelial-mesenchymal transition. Int J Oncol. 2014; 45: 1430–6. doi: 10.3892/ijo.2014.2574.

61. Gao Y, Li J, Qiao N, Meng Q, Zhang M, Wang X, Jia J, Yang S, Qu C, Li W, Wang D. Adrenomedullin blockade suppresses sunitinib-resistant renal cell carcinoma growth by targeting the ERK/MAPK pathway. Oncotarget. 2016; 7: 63374–87. doi: 10.18632/oncotarget.11463.

62. Puissant A, Frumm S, Alexe G, Bassil C, Qi J, Chanthery Y, Nekritz E, Zeid R, Gustafson W, Greninger P, Garnett M, McDermott U, Benes C, et al. Targeting MYCN in Neuroblastoma by BET Bromodomain Inhibition. Cancer Discovery. 2013; 3: 308–23. doi: 10.1158/2159-8290.CD-12-0418.

63. Coller H, Grandori C, Tamayo P, Colbert T, Lander E, Eisenman R, Golub T. Expression analysis with oligonucleotide microarrays reveals that MYC regulates genes involved in growth, cell cycle, signaling, and adhesion. Proc National Acad Sci. 2000; 97: 3260–5. doi: 10.1073/pnas.97.7.3260.

64. Ellwood-Yen K, Graeber TG, Wongvipat J, Iruela-Arispe ML, Zhang J, Matusik R, Thomas GV, Sawyers CL. Myc-driven murine prostate cancer shares molecular features with human prostate tumors. Cancer Cell. 2003; 4: 223–38.

65. Zeller K, Jegga A, Aronow B, O'Donnell K, Dang C. An integrated database of genes responsive to the Myc oncogenic transcription factor: identification of direct genomic targets. Genome Biol. 2003; 4: 1–10. doi: 10.1186/gb-2003-4-10-r69.
66. Yu D, Cozma D, Park A, Thomas-Tikhonenko A. Functional validation of genes implicated in lymphomagenesis: an in vivo selection assay using a Myc-induced B-cell tumor. Ann N Y Acad Sci. 2005; 1059: 145–59. doi: 10.1196/annals.1339.047.
67. Kim Y, Girard L, Giacomini C, Wang P, Hernandez-Boussard T, Tibshirani R, Minna J, Pollack J. Combined microarray analysis of small cell lung cancer reveals altered apoptotic balance and distinct expression signatures of MYC family gene amplification. Oncogene. 2005; 25: 130–8. doi: 10.1038/sj.onc.1208997.
68. Yu G, He Q-Y. ReactomePA: an R/Bioconductor package for reactome pathway analysis and visualization. Mol Biosyst. 2015; 12: 477–9. doi: 10.1039/C5MB00663E.
69. Yu G, Wang L-G, Han Y, He Q-Y. clusterProfiler: an R Package for Comparing Biological Themes Among Gene Clusters. Omics J Integr Biology. 2012; 16: 284–7. doi: 10.1089/omi.2011.0118.

4.1.11 TABLES

Supplementary Table I: Significantly, differentially expressed genes (excel)

Supplementary data table listing the significantly differentially expressed genes upon ALK inhibition at every time point (FDR < 0.001). The first sheet is a summary of the significantly differentially expressed genes, the second sheet contains the genes upregulated upon ALK inhibition and the third sheet shows the downregulated genes.

Supplementary Table II: primer sequences

Primer sequences used for qPCR expression analysis of the ADM gene and 5 reference genes.

Gene	Primer	Sequence
ADM	Forward	GAATCCGAGTGTTTGCCAGG
	Reverse	ACACGCATTGCACTTTTCCT
TBP	Forward	CACGAACCACGGCACTGATT
	Reverse	TTTTCTTGCTGCCAGTCTGGAC
YWHAZ	Forward	ACTTTTGGTACATTGTGGCTTCAA
	Reverse	CCGCCAGGACAAACCAGTAT
SDHA	Forward	TGGGAACAAGAGGGCATCTG
	Reverse	CCACCACTGCATCAAATTCATG
B2M	Forward	TGCTGTCTCCATGTTTGATGTATCT
	Reverse	TCTCTGCTCCCCACCTCTAAGT
HPRT1	Forward	TGACACTGGCAAAACAATGCA
	Reverse	GGTCCTTTTCACCAGCAAGCT

4.1.12 SUPPLEMENTARY FIGURES & LEGENDS

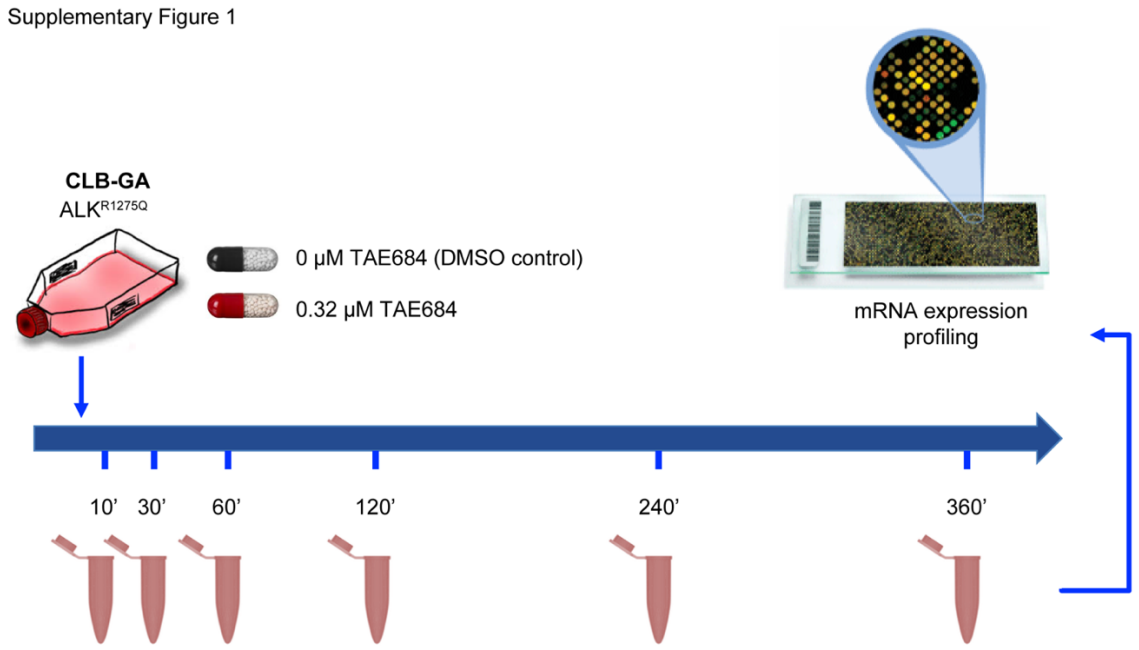

Supplementary Figure 1: Workflow to generate the time course dataset upon pharmacological ALK inhibition

CLB-GA, an ALK^{R1275Q} mutated NB cell line, was treated in duplicate with 0.32 µM TAE684 or DMSO. Cells were collected for RNA 10 and 30 minutes, 1, 2, 4 and 6 hours after the treatment. RNA was extracted, quality was checked and samples were used for mRNA expression profiling with the Sureprint G3 human GE 8x60K microarrays (Agilent Technologies).

Supplementary Figure 2

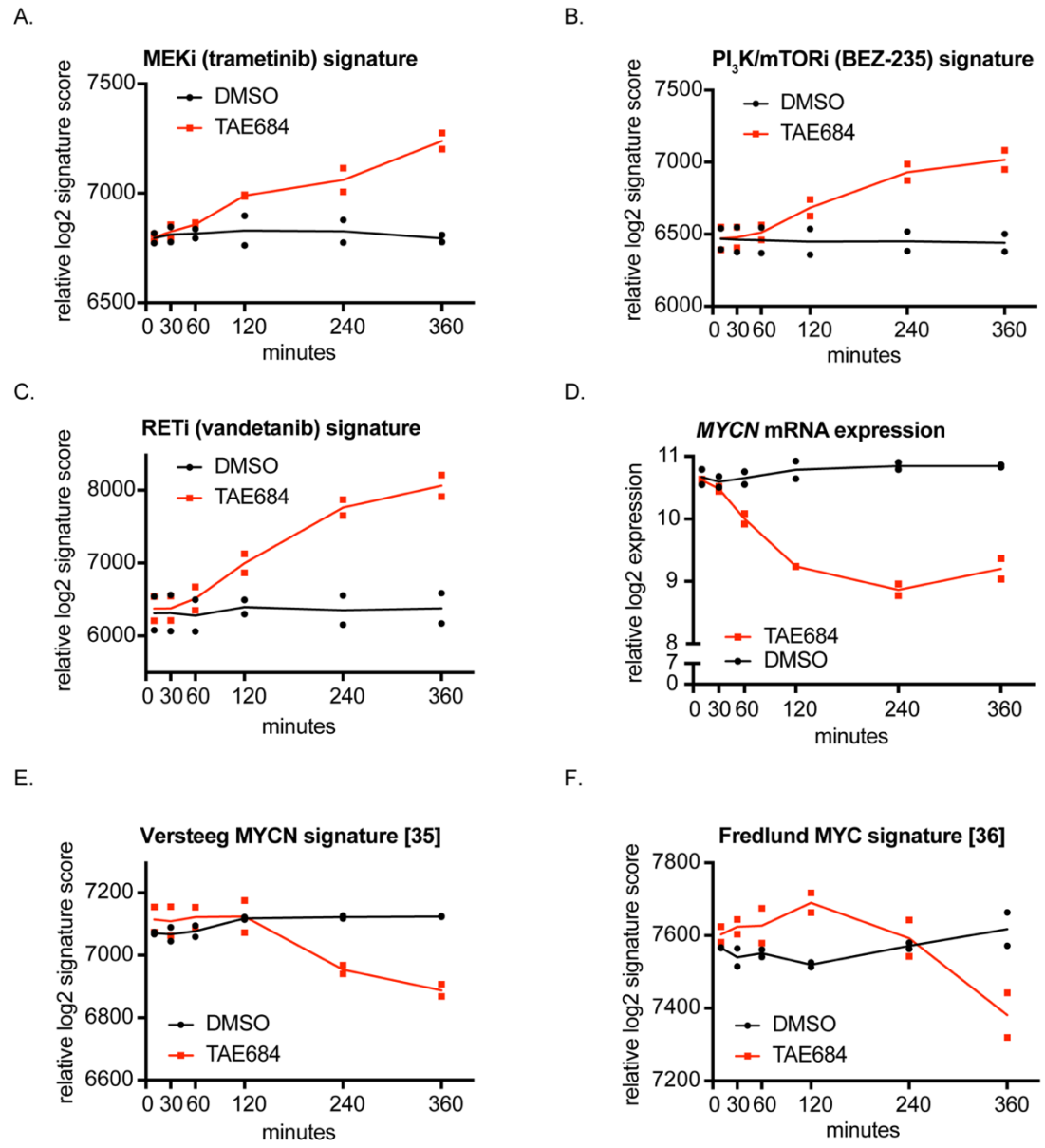

Supplementary Figure 2: Signature score analysis for MAPK, PI_3K, RET and MYC(N) signaling pathways, downregulated starting from 1 or 2 hours after TAE684 treatment (absolute values)

A.-F. MEK inhibitor (trametinib) (A), PI_3K/mTOR inhibitor (BEZ-235) (B) and RET inhibitor (vandetanib) (C) signatures are upregulated from 1 or 2 hours after treatment of the CLB-GA cell line with 320 nM TAE684, while *MYCN* mRNA expression levels (D) are downregulated from 1 hour after treatment and the MYCN activity score from Valentijn *et al.* [35] (E) and the MYC signature score from Fredlund *et al.* [36] (F) from respectively 2 and 4 hours after pharmacological ALK blockade. Log2 transformed expression levels of TAE684 treated and DMSO control samples are plotted.

Supplementary Figure 3

A.

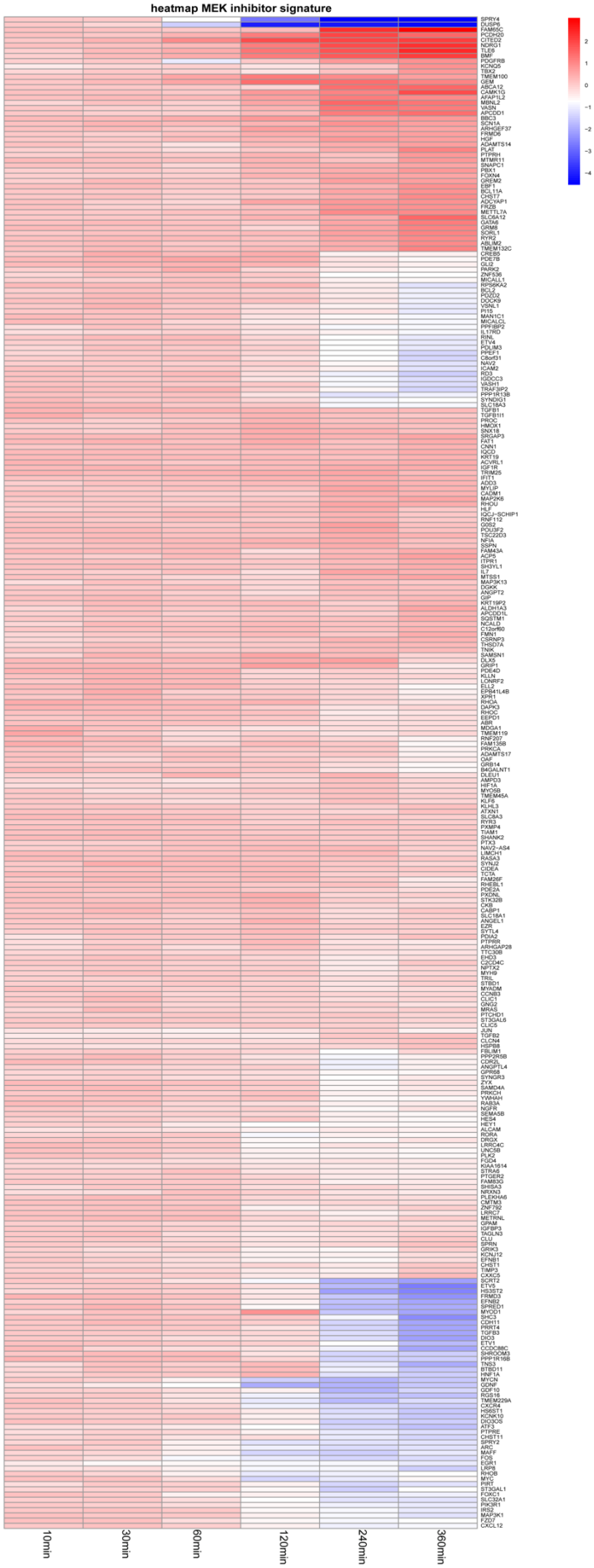

Supplementary Figure 3

B.

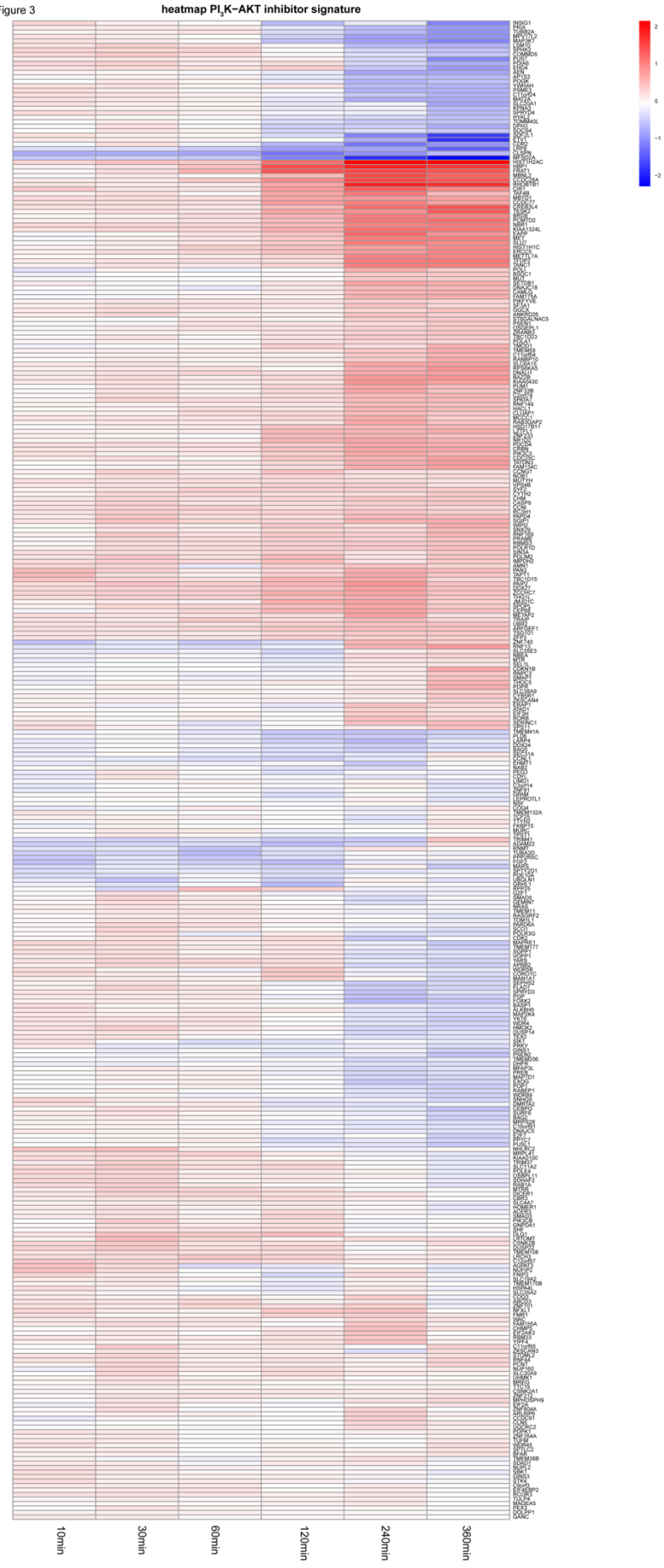

Supplementary Figure 3

C.

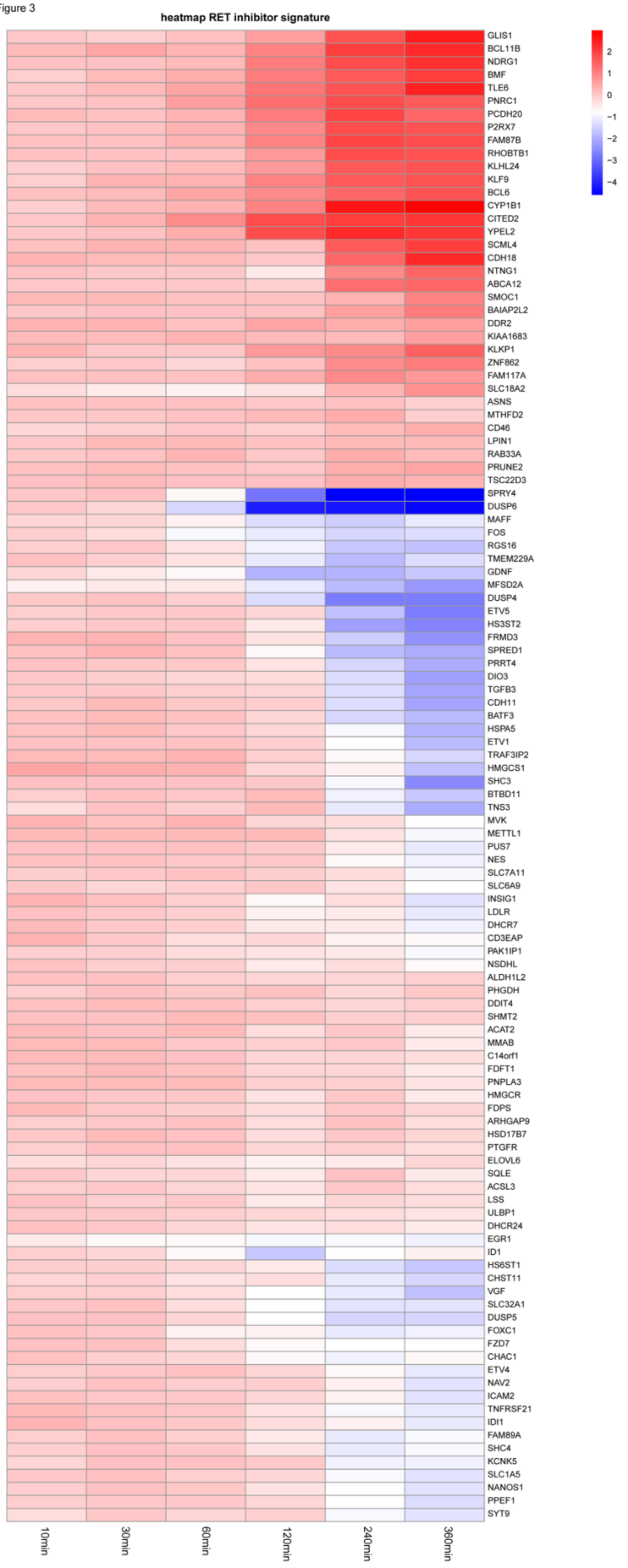

Supplementary Figure 3

D.

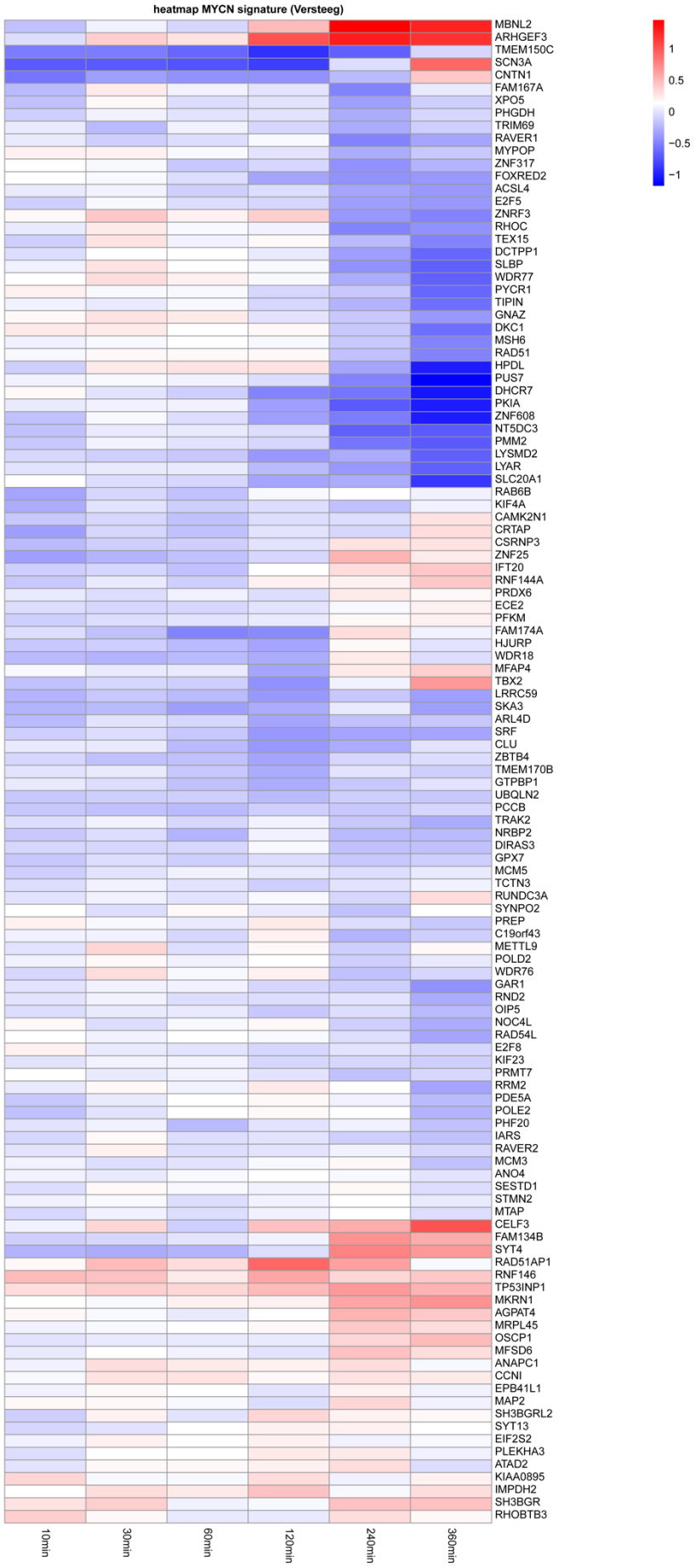

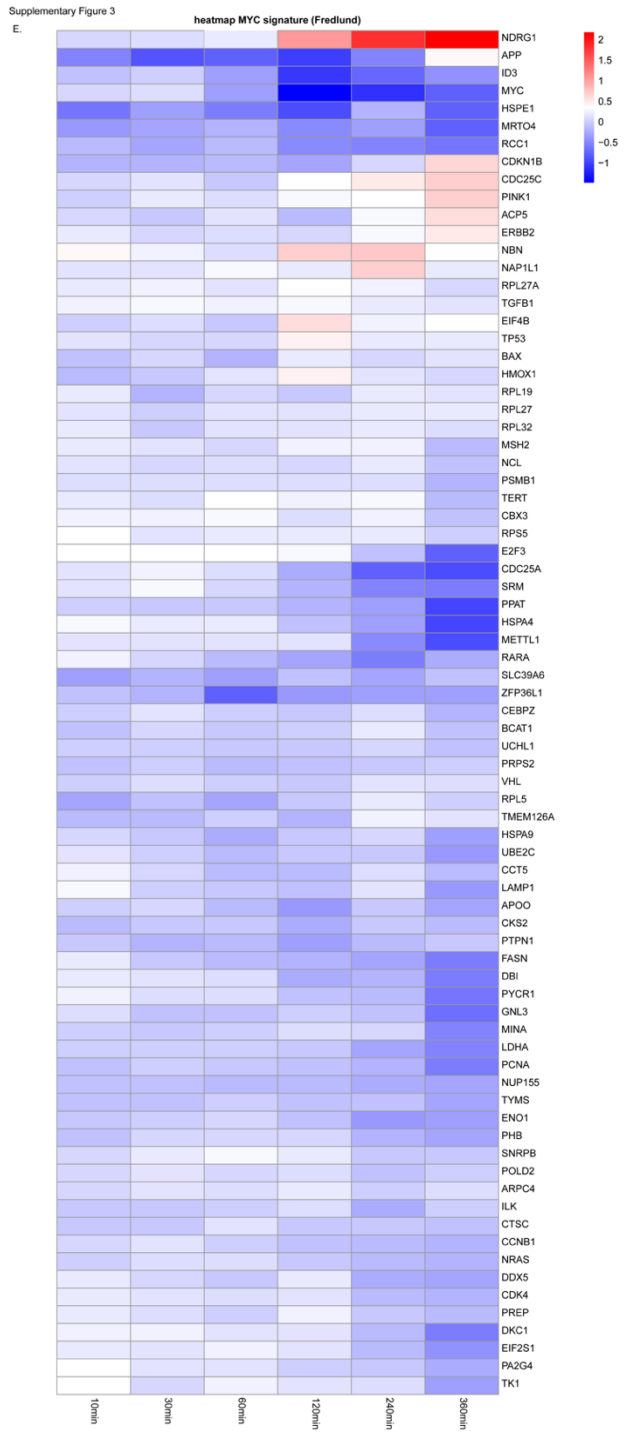

Supplementary Figure 3: Heatmaps representing the genes from the signature score analysis for MAPK, PI_3K, RET and MYC(N) signaling pathways

A.-E. Heatmaps showing the dynamic expression over time for the genes from the MEK inhibitor (trametinib) (A.), the PI_3K-AKT inhibitor (B.), the RET inhibitor (vandetanib) (C.), the Versteeg MYCN [35] signature (D.) and the Fredlund MYC [36] signature (E.). The mean of the ratio of the expression in the TAE684 vs DMSO treated sample is plotted for each gene over time.

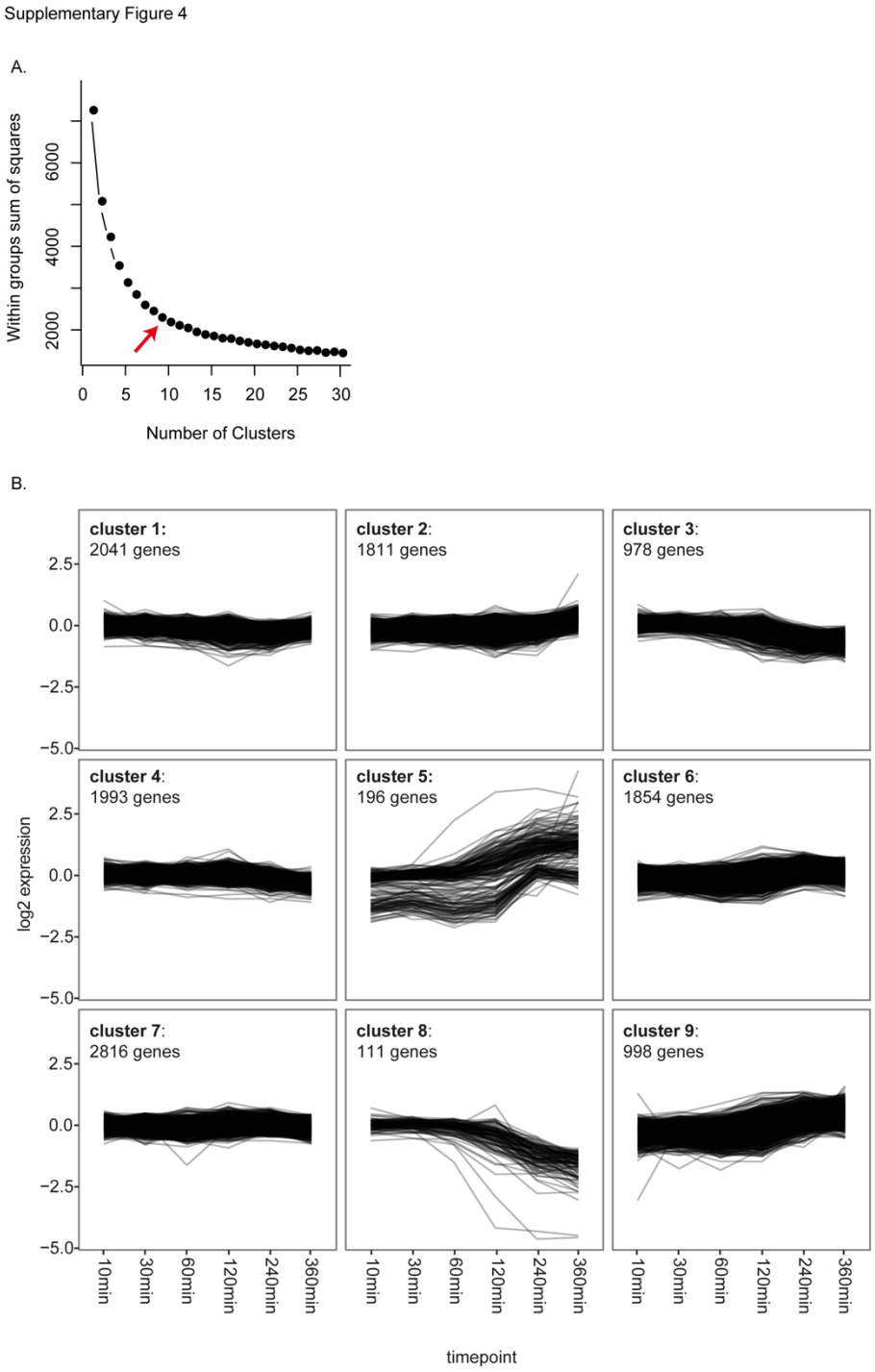

Supplementary Figure 4: K-means clustering of the expression data

A. Plot illustrating the choice to perform k-means clustering with k=9 (red arrow) as determined by the elbow method. The y-axis shows the variability within the groups and the x-axis the number of clusters. **B.** The cluster plots represent the dynamic pattern of the expression of the genes belonging to 1 of the 9 clusters. The mean of the ratio of the expression in the TAE684 vs DMSO treated sample is plotted for each gene.

Supplementary Figure 5

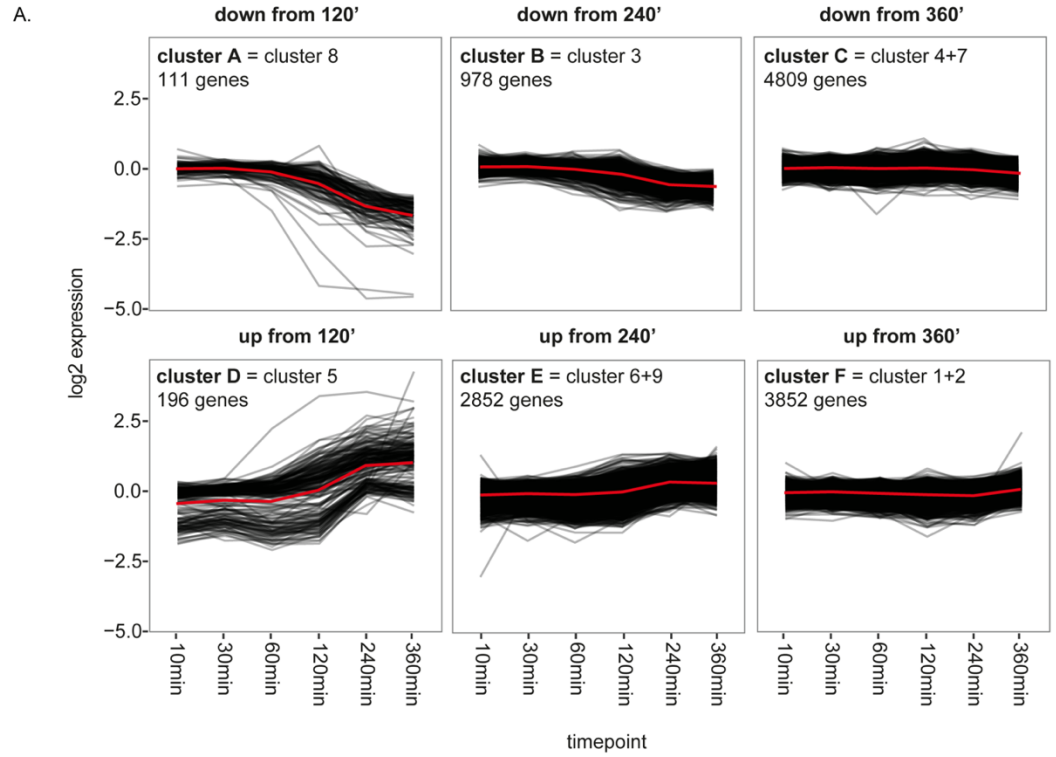

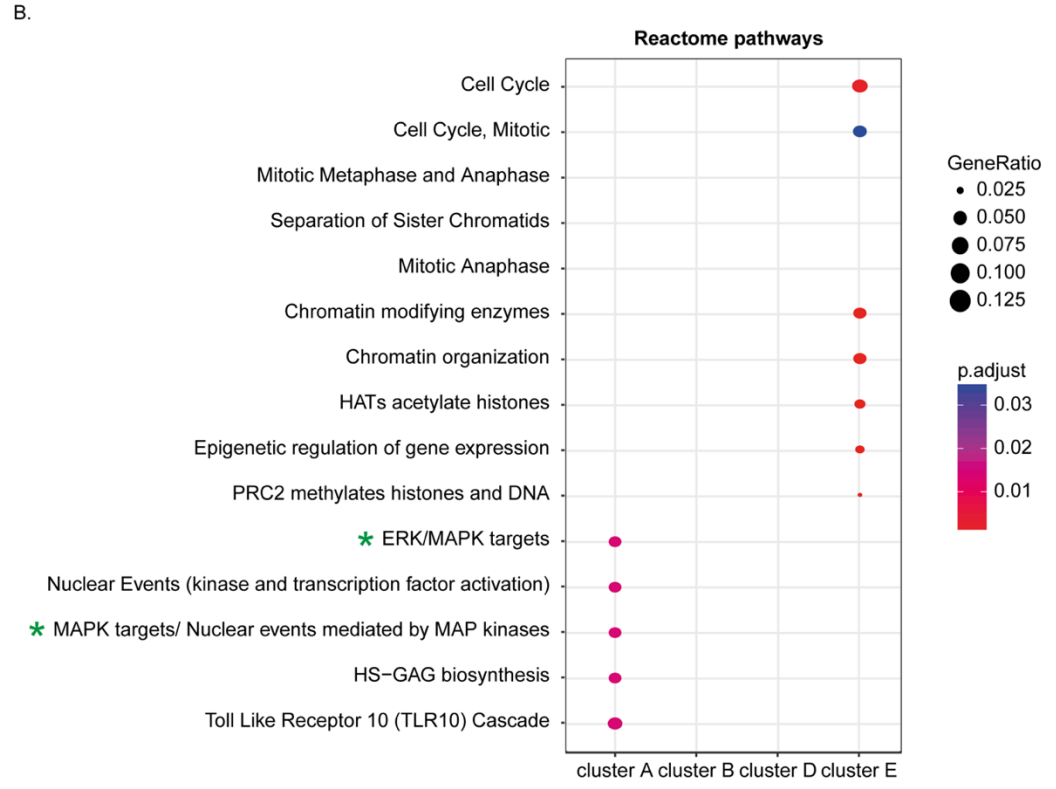

Supplementary Figure 5

C.

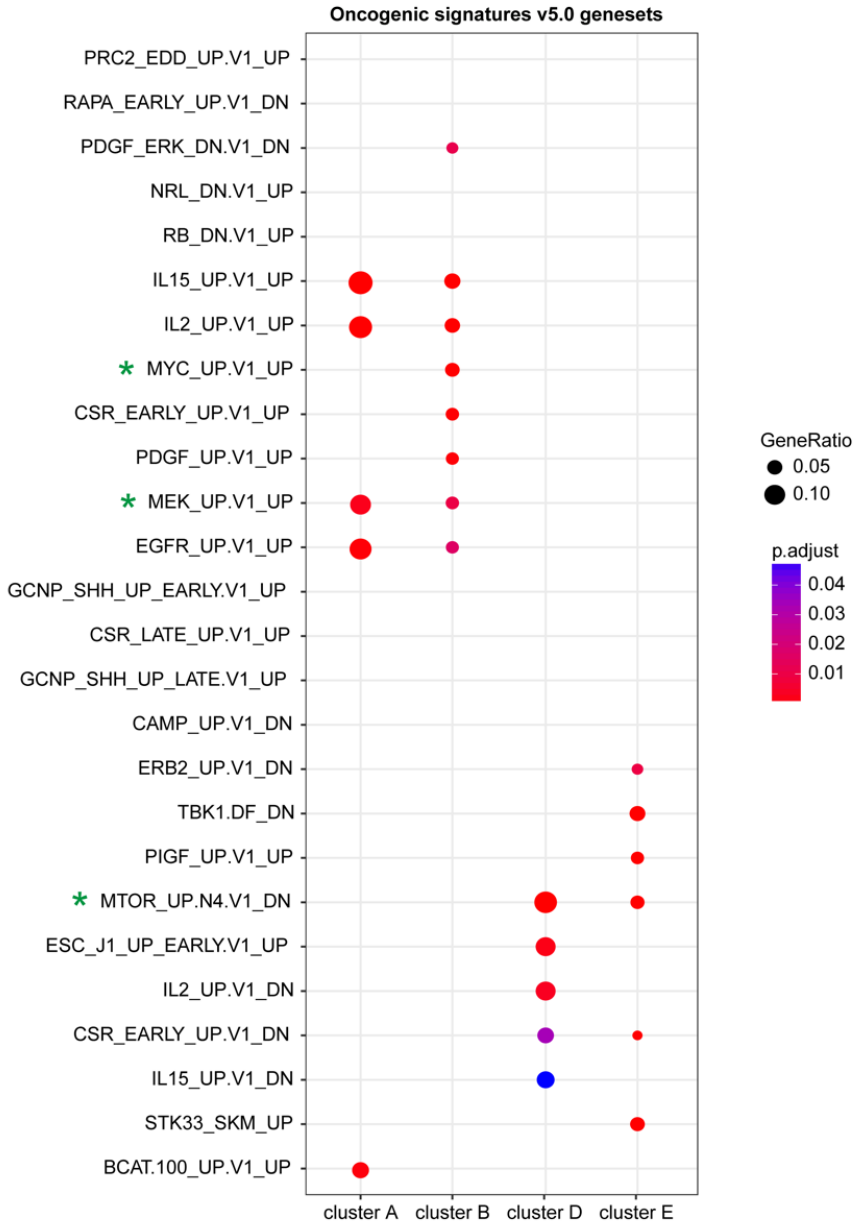

Supplementary Figure 5: Functional characterization of the genes in the clusters with the Reactome Pathways and MSigDB 'c6 Oncogenic Signatures v5.0'

A. The cluster plots represent the dynamic pattern of the expression of the genes belonging to 1 of the 6 clusters. The mean of the ratio of the expression in the TAE684 vs DMSO treated sample is plotted for each gene. The red lines show the average dynamic pattern of the expression of the genes belonging to these clusters, calculated by the average of the mean of the ratio of the expression in the TAE684 vs DMSO treated sample. **B.** The plot shown pathways of the Reactome Database that are enriched in at least one of the four

clusters, which are showing a clear dynamic pattern (clusters A, B, D, E). The size of each node corresponds to the number of genes overlapping between the cluster and the gene set and the colour represents the adjusted p-value of the enrichment test. **C.** The plot shown the MSigDB 'c6 Oncogenic Signatures v5.0' genesets that are enriched in at least one of the four clusters, which are showing a clear dynamic pattern (clusters A, B, D, E). The size of each node corresponds to the number of genes overlapping between the cluster and the gene set and the colour represents the adjusted p-value of the enrichment test. Green stars indicate the genesets related to the MYC(N), KRAS-MAPK, PI_3K/mTOR pathways.

Supplementary Figure 6

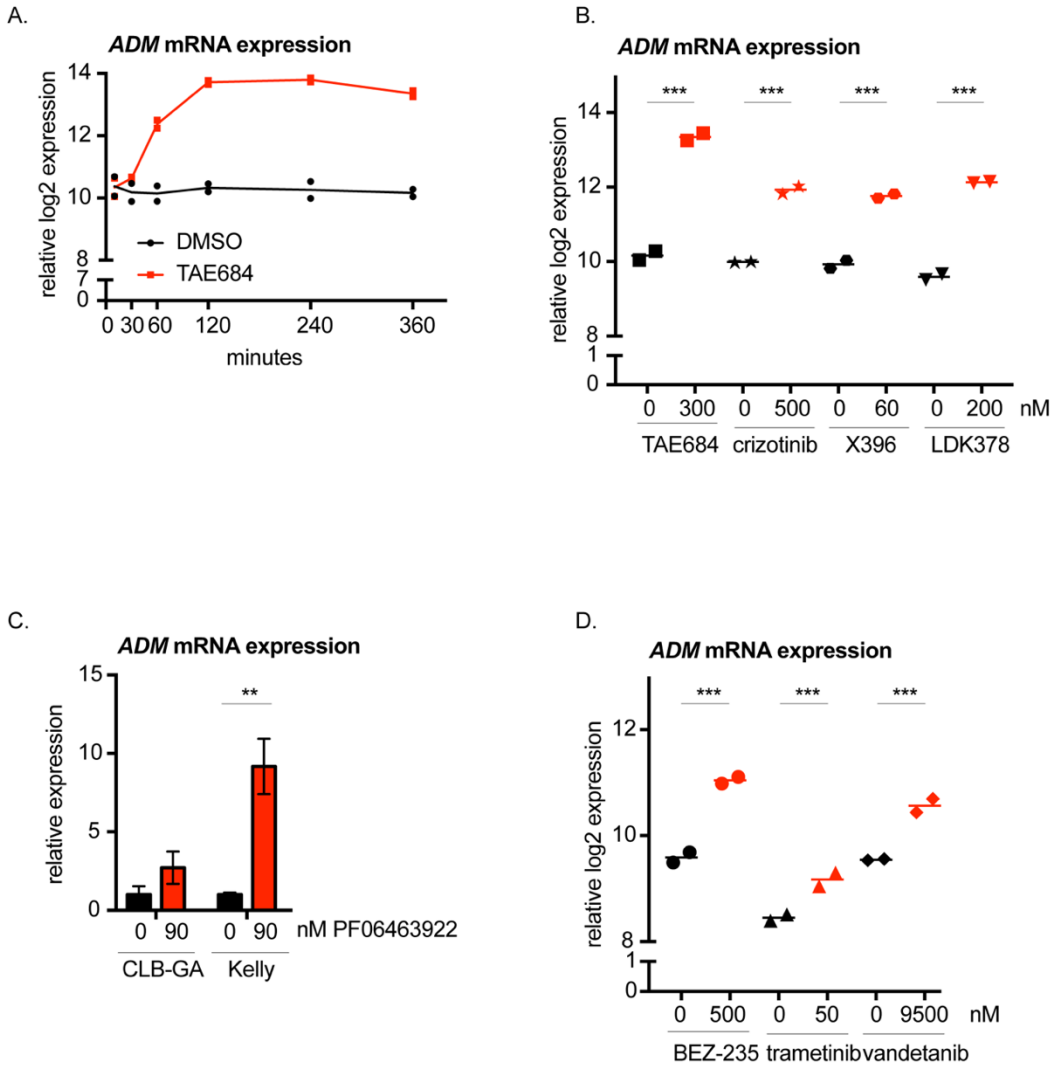

Supplementary Figure 6: *ADM* expression upon pharmacological blockade of ALK and ALK downstream signaling in NB cells

A. *ADM* mRNA is significantly upregulated starting from 1 hour after TAE684 treatment of the CLB-GA cell line. Log2 transformed expression levels of TAE684 treated and DMSO control samples are plotted. **B.** *ADM* mRNA expression levels are increased in CLB-GA treated for 6h with 0.32 µM TAE684, 0.5 µM crizotinib, 0.06 µM X396, 0.2 µM LDK378 compared to the DMSO control. **C.** *ADM* mRNA expression levels are upregulated in NB cell lines CLB-GA (ALKR1275Q) and Kelly (ALKF1174L) treated for 6 hours with 0.09 µM PF06463922 (new-generation ALK inhibitor) compared to the DMSO control. **D.** *ADM* mRNA expression levels are increased in CLB-GA treated with 0.5 µM BEZ-235, 0.05 µM trametinib, 9.5 µM vandetanib compared to DMSO for 6h.

Statistical analyses: unpaired one-way ANOVA with Bonferroni correction (B. & C. & D.). * $P < 0.05$, ** $P < 0.01$, *** $P < 0.001$

Chapter 5 ALK positively regulates MYCN activity through repression of HBP1 expression

Authors: **Shana Claeys** [1,2], Geertrui Denecker [1,2], Kaat Durinck [1,2*], Bieke Decaesteker [1,2*], Siebe Loontiens [1,2], Suzanne Vanhauwaert [1,2], Kristina Althoff [3], Caroline Wigerup [4], Daniel Bexell [4], Emmy Dolman [5], Kai-Oliver Henrich [6], Lea Wehrmann [6], Ellen M. Westerhout [7], Jean-Baptiste Demoulin [8], Candy Kumps [1,9], Tom Van Maerken [1,2], Genevieve Laureys [2,10], Christophe Van Neste [1,2], Bram De Wilde [1,2,10], Olivier De Wever [2,11], Frank Westermann [6], Rogier Versteeg [7], Jan J. Molenaar [5], Sven Påhlman [4] , Johannes H. Schulte [3,12,13,14,15], Katleen De Preter [1,2], Frank Speleman [1,2]

* shared 3rd author

Paper submitted to Oncogene, under revision

Author contribution:

Shana Claeys performed most of the laboratory experiments and data analysis, was responsible for the design of the experiments, coordination of the research, generation of the figures and writing of the manuscript. Katleen De Preter assisted with the bio-informatics analysis. Bieke Decaesteker, Kaat Durinck, Siebe Loontiens, Suzanne Vanhauwaert, Johannes H. Schulte, Emmy Dolman, Frank Westermann, Jean-Baptist Demoulin, Tom Van Maerken, Genevieve Laureys, Christophe Van Neste, Bram De Wilde, Rogier Versteeg and Jan J. Molenaar provided valuable discussions and feedback. Kristina Althoff and Johannes H. Schulte were responsible for the experiment with the LSL-*MYCN;dßh-i*Cre mice. Caroline Wigerup, Daniel Bexell and Sven Påhlman were responsible for the experiments with the PDX-derived cell line LU-NB-2. Olivier De Wever coordinated experiments on the incucyte. Kai-Oliver Henrich, Lea Wehrmann, and Frank Westermann provided PRC2-related information. Ellen M. Westerhout and Rogier Versteeg provided FOXO3 manipulated cell lines. Geertrui Denecker supervised the laboratory experiments, were involved in the design of the experiments and coordination of the research. Katleen De Preter

and Frank Speleman coordinated the research, designed experiments and helped writing the paper.

ALK positively regulates MYCN activity through repression of HBP1 expression

Authors: **Shana Claeys** [1,2], Geertrui Denecker [1,2], Kaat Durinck [1,2*], Bieke Decaesteker [1,2*], Siebe Loontiens [1,2], Suzanne Vanhauwaert [1,2], Kristina Althoff [3], Caroline Wigerup [4], Daniel Bexell [4], Emmy Dolman [5], Kai-Oliver Henrich [6], Lea Wehrmann [6], Ellen M. Westerhout [7], Jean-Baptiste Demoulin [8], Candy Kumps [1,9], Tom Van Maerken [1,2], Genevieve Laureys [2,10], Christophe Van Neste [1,2], Bram De Wilde [1,2,10], Olivier De Wever [2,11], Frank Westermann [6], Rogier Versteeg [7], Jan J. Molenaar [5], Sven Påhlman [4] , Johannes H. Schulte [3,12,13,14,15], Katleen De Preter [1,2], Frank Speleman [1,2]

* shared 3rd author

5.1.1 Affiliations:

1. Center for Medical Genetics Ghent (CMGG), Ghent University, Ghent, Belgium
2. Cancer Research Institute Ghent (CRIG), Ghent University, Ghent, Belgium
3. Department of Pediatric Oncology and Hematology, University Children's Hospital Essen, Essen, Germany
4. Translational Cancer Research, Lund University Cancer Center at Medicon Village, Lund University, Lund, Sweden
5. Princess Maxima Center for Pediatric cancer, Utrecht, The Netherlands
6. Neuroblastoma Genomics B087, German Cancer Research Center, Heidelberg, Germany
7. Department of Oncogenomics, Academic Medical Center, Amsterdam, The Netherlands
8. De Duve Institute, Université catholique de Louvain, Brussels, Belgium
9. Department of Uro-gynaecology, Ghent University Hospital, Ghent, Belgium
10. Department of Pediatric Oncology and Hematology, Ghent University Hospital, Ghent, Belgium
11. Laboratory of Experimental Cancer Research (LECR), Ghent University, Ghent, Belgium
12. Department of Pediatric Oncology/Hematology, Charite University Hospital Berlin, Berlin, Germany
13. Berlin Institute of Health (BIH), Berlin, Germany.
14. German Translational Cancer Research Consortium (DKTK), Berlin, Germany
15. German Translational Cancer Research Consortium (DKFZ), Heidelberg, Germany

5.1.2 FINANCIAL SUPPORT

S.C. is supported by a pre-doctoral fellowship of the Research Foundation – Flanders (FWO; 11J8313N) and an Emmanuel van der Schueren grant ('Kom op tegen Kanker'). S.V. is funded by the VLK (Flemish League against cancer) and 'Stichting Villa Joep'. B.D. and S.L. are supported by a pre-doctoral fellowship of the FWO Research Foundation – Flanders (FWO). K.D. is supported by Ghent University (BOF; BOF16/PDO/043). C.V., B.D.W. and T.V.M. are senior clinical investigators of the Research Foundation – Flanders (FWO; 18B1716N (B.D.W.), 12N6917N (C.V.), 1803115N (T.V.M.)). The authors would further like to thank the following funding agencies: the Belgian Foundation against Cancer (project 2014-175) to F.S., Ghent University (BOF10/GOA/019, BOF16/GOA/23) to F.S., the Belgian Program of Interuniversity Poles of Attraction (IUAP Phase VII - P7/03) to F.S., the Fund for Scientific Research Flanders (Research projects G053012N, G050712N, G051516N to F.S) and 'Stichting Villa Joep' to FS.

Word count: 4492 words / Figures: 5 / Tables: 2

5.1.3 ABSTRACT

ALK mutations occur in 10% of primary neuroblastoma and represent a major target for precision treatment. In combination with *MYCN* amplification, *ALK* mutations infer an ultra-high-risk phenotype resulting in very poor patient prognosis. To open up opportunities for future precision drugging, a deeper understanding of the molecular consequences of constitutive ALK signaling and its relationship to MYCN activity in this aggressive pediatric tumor entity will be essential. We show that mutant ALK downregulates the *'HMG-box transcription factor 1'* (HBP1) through the PI_3K-AKT-FOXO3a signaling axis. HBP1 inhibits both the transcriptional activating and repressing activity of MYCN, the latter being mediated through PRC2 activity. HBP1 itself is under negative control of MYCN through miR-17~92. Combined targeting of HBP1 by PI_3K antagonists and MYCN signaling by BET or HDAC inhibitors blocks MYCN activity and significantly reduces tumor growth, suggesting a novel targeted therapy option for high-risk neuroblastoma.

5.1.4 INTRODUCTION

Neuroblastoma (NB) is a childhood tumor arising from the embryonic sympatho-adrenal lineage of the neural crest and represents the primary cause of cancer-related death in young children ages one to five [1]. These tumors are characterized by a heterogeneous clinical course, ranging from spontaneous regression to highly aggressive, metastatic disease refractory to therapy [2]. Sequencing efforts have resulted in a detailed molecular characterization of the neuroblastoma genomic landscape, exhibiting few recurrent driver mutations in a background of highly recurrent DNA copy number alterations [3]. *MYCN* amplification is observed in half of the high-stage tumors and more than 10% exhibit activating *anaplastic lymphoma kinase (ALK)* receptor mutations [2,4–7]. These mutations are preferred targets for precision medicine and clinical trials using ALK inhibitors have been initiated [8,9]. However, as single compound approaches almost invariably lead to therapy resistance [10–20], a more detailed understanding of components implicated in ALK downstream signaling is warranted.

Previous studies have suggested genetic interaction between MYCN and ALK in neuroblastoma cells. We previously identified an ultra-high-risk patient subgroup with combined *MYCN* amplification and ALK^{F1174L} mutation [21]. Subsequently, a mouse and zebrafish neuroblastoma model revealed accelerated tumor formation when both MYCN and ALKF1174L were expressed in sympathetic neuronal progenitor cells [22,23]. Further, ALK was shown to control *MYCN* transcription levels and MYCN protein stabilization through the PI_3K-AKT pathway [24–27], providing insight into the possible mechanism of mutant ALK mediated increased tumor aggressiveness. In this study, we further explored the interrelationship between ALK and MYCN based on our previously established ALK-driven 77-gene signature [28]. We identified consistent ALK controlled downregulation of HBP1 (*'high-mobility-group (HMG) box protein'*), a previously established negative regulator of MYC(N) activity [29,30] and investigated the transcriptional and phenotypical effects of HBP1 modulation in ALK mutated and MYCN amplified neuroblastoma cells. Finally, we also investigated the effects of different single and combined drug combinations on HBP1 levels.

5.1.5 RESULTS

ALK downregulates HBP1 mRNA and protein expression levels

To further investigate the possible regulatory relationship between ALK and MYCN, we looked for hitherto unrecognized proteins implicated in MYCN regulation in neuroblastoma cells. To this end, we verified our previously published ALK-driven 77-gene signature[28] and identified the negative MYC regulator HBP1 as an ALK down regulated target. We first confirmed upregulation of HBP1 expression levels after pharmacological inhibition of ALK with TAE684 in six selected neuroblastoma cell lines. These included three ALK mutant cell lines with *ALK* amplification (NB-1), an ALK^{F1174L} mutation (SK-N-SH) and an ALK^{R1275Q} mutation (CLB-GA). Furthermore, we also selected two *ALK* wild type non-responding to the TAE684 ALK inhibitor (SK-N-AS, IMR-32) and one ALK wild type cell line that responded to ALK inhibition (Supplementary Fig. 1A) [28,31]. We confirmed increase in *HBP1* mRNA expression levels in the ALK mutant cell lines and the ALK wild type responder NGP, while no notable effects were observed in wild type non-responders SK-N-AS and IMR32 (Fig. 1A). We then analyzed the *HBP1* expression over several time points in ALK^{R1275Q} mutant CLB-GA cells following TAE684 treatment and observed *HBP1* upregulation as early as two hours after drug exposure (Supplementary Fig. 1B). ALK mediated HBP1 repression was confirmed by several next generation ALK inhibitors in CLB-GA cells [8,32] (Fig. 1B-C). We could also confirm the effect of inhibition of mutant ALK signaling on *HBP1* expression levels *in vivo* in mouse xenografted SH-SY5Y neuroblastoma cells treated with TAE684 and crizotinib (Fig. 1D).

The effects of ALK induction on HBP1 expression was tested *in vitro* using SK-N-AS (ALK^{wt}) neuroblastoma cells transduced with tetracycline-inducible overexpression constructs for ALK^{wt}, ALK^{F1174L} and ALK^{R1275Q} (Fig. 1E). Furthermore, in a cohort of 283 primary human neuroblastoma tumors (GSE85047), a significant negative correlation between *HBP1* and *ALK* gene expression was observed in keeping with the proposed negative regulatory effects of ALK on HBP1 (Supplementary Fig. 1C).

Given the role of ALK activation in a subset of lung carcinomas, we analyzed a dataset of EML4/ALK fusion positive non-small-cell lung carcinoma cells (NSCLC) [33] and observed higher HBP1 expression levels upon ALK inhibition (Fig. 1F). In Ba/F3 (murine pro-B) cells with ALK^{F1174L}, ALK^{R1275Q} or EML4/ALK, HBP1 levels decreased

in ALK mutant cells, while HBP1 levels were restored upon ALK inhibition (Supplementary Fig. 1D). Taken together, our data support that ALK leads to downregulation of HBP1 expression levels in neuroblastoma cells as well as in other cell types including NSCLC.

HBP1 levels are controlled through ALK-PI$_3$K/AKT-FOXO3a

To test which of the two major ALK downstream pathways (MAPK versus PI$_3$K/AKT) [4–7,28,34,35] controls HBP1 expression, ALK mutant cells were treated with either a MEK inhibitor (U0126) or a PI$_3$K/mTOR inhibitor (BEZ-235). HBP1 upregulation was observed after exposure to the PI$_3$K/mTOR inhibitor, while MEK inhibition only slightly affect *HBP1* levels (Fig. 1G-H). Similar results were obtained using the PI$_3$K inhibitor pictilisib (Supplementary Fig. 1E). In further support of these findings, the PI$_3$K/AKT inhibitor signature score [36] positively correlated with *HBP1* gene levels in the cohort of 283 NB patients (GSE85047) (Supplementary Fig. 1F).

Based on previously reported observations showing negative regulation of FOXO3a by ALK through the PI$_3$K-AKT pathway in neuroblastoma [28,36] and anaplastic large cell lymphoma (ALCL) [37] and the control of HBP1 by FOXO3a in fibroblasts [38], we explored the role of FOXO3a in ALK controlled HBP1 regulation in neuroblastoma. First, we assessed a FOXO3a signature [36] in a cohort of 283 NB patients and observed positive correlation of the signature with *HBP1* gene levels (GSE85047) (Supplementary Fig. 1G). Next, we looked into an available transcriptome dataset based on doxycycline-inducible FOXO3a overexpression in combination with the PI$_3$K/mTOR inhibitor PI-103 in the NB cells SH-SY5Y (ALK^{F1174L}) [36] and confirmed transcriptional upregulation of *HBP1* upon enhanced FOXO3a expression and PI-103 treatment in these cells (Fig. 1I). Collectively, our data support that ALK negatively regulates HBP1 expression levels through the PI$_3$K-AKT-FOXO3a pathway in neuroblastoma.

Figure 1

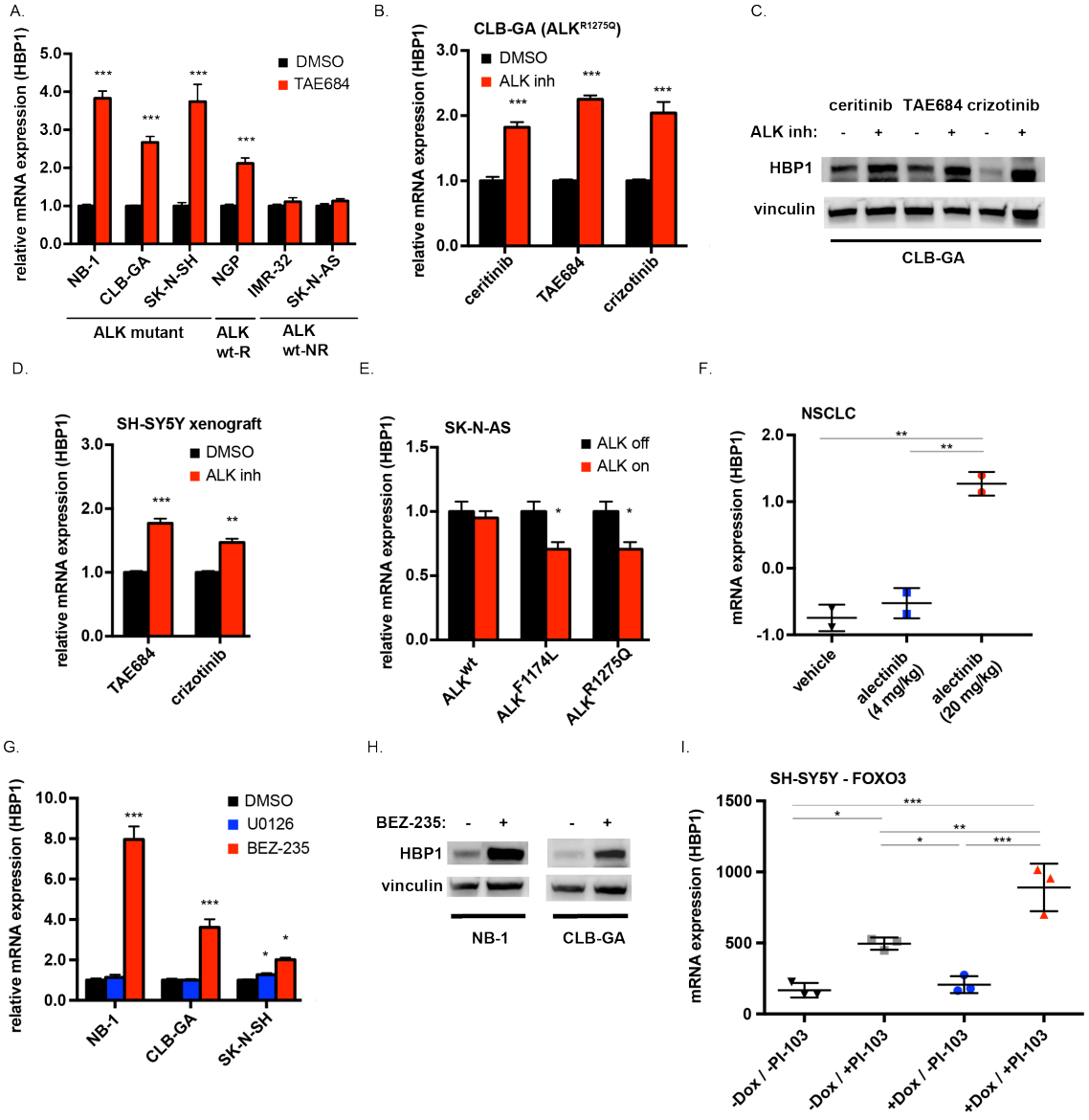

Figure 1: ALK signaling downregulates HBP1 expression through PI_3K/AKT - FOXO3a signaling in neuroblastoma and other ALKoma tumours.

A, H*BP1* mRNA expression in several ALK wild type (NGP, IMR-32, SK-N-AS) and ALK mutant (SK-N-SH, CLB-GA, NB-1) cell lines treated for 6 hours with 0.3 µM TAE684 or DMSO relative to the levels in DMSO treated cells. **B,** *HBP1* mRNA levels in CLB-GA treated with 0.2 µM LDK378, 0.32 µM TAE684, 0.5 µM crizotinib or DMSO for 6h, relative to the DMSO control of each compound. **C,** Western blot analysis showing HBP1 protein levels 24h after treating the CLB-GA cell line with different ALK inhibitors (0.2 µM LDK378, 0.32 µM TAE684, 0.5 µM crizotinib or DMSO). **D,** *HBP1* mRNA levels in SH-SY5Y xenografted mice treated with TAE68, crizotinib or carrier solution, relative to the carrier solution. **E,** HBP1 mRNA levels in SK-N-AS cell lines with TET-inducible ALK^{wt}, ALK^{F1174L} or ALK^{R1275Q}

constructs treated with tetracycline or ethanol for 24h, relative to the ethanol control of each cell line. **F,** *HBP1* expression in EML4/ALK fusion positive non-small-cell lung carcinoma cells (NSCLC)-xenografted mice treated with 4 or 20 mg/kg of the ALK inhibitor alectinib. Data represents mean ± SD of 2 biological replicates. **G,** *HBP1* mRNA levels in a small panel of NB cell lines (one ALK^{amp}, ALK^{R1275Q}, ALK^{F1174L} cell line) treated with 8 μM MEK inhibitor U0126, 0.5 μM PI_3K/mTOR inhibitor BEZ-235 or DMSO for 6 hours, relative to the DMSO control of each cell line. **H,** Western blot analysis showing HBP1 protein levels 24h after treating NB-1 and CLB-GA with the PI_3K/mTOR inhibitor (0.5 μM BEZ-235 or DMSO). **I,** *HBP1* mRNA levels in cells treated with 0.1 μg/ml doxycycline or nothing for 24 hours to induce overexpression of HA-tagged FOXO3A and then treated with either 1 μM PI_3K inhibitor PI-103 or DMSO for 6 additional hours.

Error bars represents mean ± SD of respectively 2 technical replicates (A, B, G), 2 biological replicates (F), 2 biological replicates, each containing 2 technical replicates (D, E) or 3 biological replicates (I) and are calculated following error propagation. * $P < 0.05$, ** $P < 0.01$, *** $P < 0.001$

HBP1 is negatively regulated by MYCN through the miR-17~92 cluster

In view of the previously reported negative regulation of HBP1 through the *miR-17~92* cluster in breast cancer, leukemia and lymphoma cells [39,40] and the known positive regulation of *miR-17~92* by MYCN in NB, leukemia and lymphoma cells [40–42], we decided to investigate this MYCN - *miR-17~92* - HBP1 regulatory axis in more detail in the context of NB cells. To this end, we first evaluated HBP1 protein expression levels following shRNA-mediated MYCN knockdown in the neuroblastoma IMR-5/75 cell line and found elevated HBP1 protein levels upon MYCN knockdown (Fig. 2A). In line with this finding, we also show that in MYCN-driven mouse tumor formation, *Hbp1* is transcriptionally downregulated (Supplementary Fig. 2A). The presumed MYCN control of HBP1 by the *miR-17~92* cluster was then confirmed using the previously validated tetracycline-inducible miR-17~92 overexpression model in SH-EP neuroblastoma cells [41], showing HBP1 downregulation upon induction of miR-17~92 (Fig. 2B-C, Supplementary Fig. 2B-C). In summary, these data are in keeping with negative HBP1 regulation through MYCN induced elevated miR-17~92 levels.

HBP1 is a suppressor of MYCN activity in neuroblastoma cells

Previous studies showed that HBP1 acts as a transcriptional repressor through direct interaction with other transcription factors, including MYC(N) [29,30]. As the functional interaction of HBP1 with MYCN in neuroblastoma has not been investigated thus far, we first performed co-immunoprecipitation for MYCN in the NGP NB cell line with stable HBP1 overexpression (NGP-HBP1up) and confirmed HBP1 and MYCN as interaction partners (Supplementary Fig. 2D). To further explore the role of HBP1 in regulation of MYCN activity in neuroblastoma, we analyzed the transcriptomes of the NGP-HBP1up versus NGP-parental cell line. Gene set enrichment analysis (GSEA [43]) of the genes upregulated upon HBP1 overexpression in NGP-HBP1up revealed enrichment (FDR < 0.25) for 11 out of 26 gene sets related to MYC(N) regulation and activity [44,45] (Fig. 2D, Supplementary Fig. 2E-F).

To explore the functional relationship between HBP1 and MYCN in primary human tumors, we established a HBP1up pathway signature based on the differentially expressed genes in NGP-HBP1up cells as compared to the NGP-parental cells and tested this signature in a cohort of 283 primary human NB tumor samples (GSE85047), demonstrating strong inverse correlation between the HBP1up pathway signature and MYCN gene expression and MYCN activity score [44] (Fig. 2E-F).

Taken together, our data are in keeping with HBP1 acting as a suppressor of MYCN activity in neuroblastoma cells.

The PRC2 complex cooperates with HBP1 in repression of gene activity

Gene set enrichment analysis (GSEA) of the NGP-HBP1up versus NGP-parental data using the ‘c6 Oncogenic Signatures v5.0’ from the Molecular Signatures Database (MSigDB), revealed positive enrichment for two PRC2 gene sets (Fig. 2G, Supplementary Fig. 2G) containing genes reported to be occupied by the Polycomb Repressive Complex 2 (PRC2) components SUZ12 or EZH2 [46], thus suggesting an upregulation by HBP1 of genes occupied by the PRC2 complex. Next, motif analysis using iRegulon [47] on the NGP-HBP1up versus NGP-parental differentially expressed genes revealed enrichments for SUZ12 motifs among the downregulated genes (Supplementary Fig. 2H). To test whether HBP1 and SUZ12 physically interact to mediate these transcriptional changes, we performed co-immunoprecipitation in NGP-HBP1up cell line and confirmed HBP1 and SUZ12 interaction (Supplementary

Fig. 2I). Moreover, a positive correlation between *HBP1* gene levels as well as the HBP1up pathway signature scores and an EZH2 inhibitor signature score, generated upon EPZ6438 EZH2 inhibitor treatment in SK-N-BE(2c) cells [48], was observed in the cohort of 283 NB patients (GSE85047) (Fig. 2H-I).

In summary, we identified HBP1 as a negative regulator of MYCN activity and suggest that HBP1 interacts with the PRC2 complex in gene repression.

Figure 2

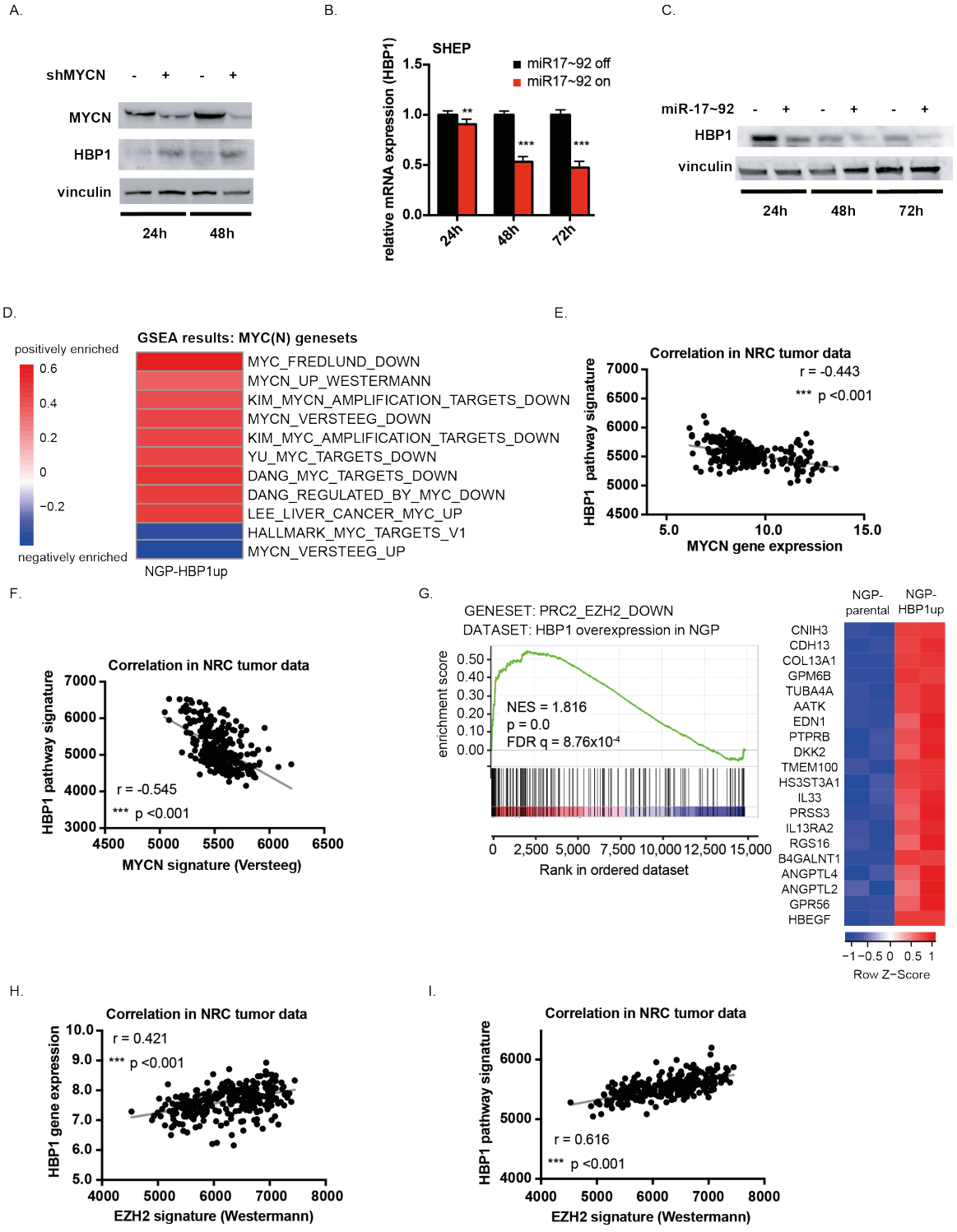

Figure 2: HBP1 is negatively regulated by MYCN through the miR-17~92 miRNA cluster and represses MYCN activity.

A, Western blot showing HBP1 and MYCN protein levels in the neuroblastoma IMR-5/75 cells upon shRNA-mediated MYCN knockdown. **B,** *HBP1* mRNA levels in SHEP cells treated with tetracycline (or ethanol as control) to induce the miR-17~92 cluster, expressed relative

to the corresponding control. **C,** Western blot analysis showing HBP1 protein levels at the same time points after inducing the miR-17~92 cluster in the SHEP cell line as in B. **D,** Heatmap showing the genesets of an in house compiled gene set collection containing all publically available MYC(N) activity or target signatures[44,45,52,64–68], that are positively or negatively enriched upon HBP1 overexpression according to GSEA (with FDR < 0.25). **E and F,** Spearman correlation between the HBP1 pathway signature and the *MYCN* gene levels (E) or the MYCN signature (F) in a cohort of 283 NB patients. **G,** GSEA for the EZH2 down geneset in the HBP1 overexpression data and heatmap showing the leading edge (top 22 genes) of this geneset plotted in the HBP1 overexpression dataset. **H and I,** Spearman correlation between *HBP1* gene levels (H) or HBP1 pathway signature (I) and the EZH2 signature in a cohort of 283 NB patients.

Error bars represents mean ± SD of 3 biological replicates, each containing 2 technical replicates (B) and are calculated following error propagation. * P < 0.05, ** P < 0.01, *** P < 0.001

Increased HBP1 levels represses tumor aggressiveness

To elucidate the role of HBP1 on the neuroblastoma cellular phenotype, we evaluated the functional characteristics of the NGP-HBP1up cell line versus the NGP-parental cells. HBP1 overexpression increased the apoptotic response, negatively affected colony forming capacity and repressed cell growth both with normal and lower serum concentrations, as shown by a marked reduction in viability rate (Fig. 3A-C, Supplementary Fig. 3A-B). Moreover, NGP-parental cells form compacted spheres within 3 days, an activity which is prevented by overexpression of HBP1 as indicated by the presence of loose aggregates where individual cells are recognizable (Fig. 3D).

Notably, HBP1 activity has previously been connected to cell differentiation in leukemic myeloid cells and in the cortical region of mouse brains [49,50]. In keeping with this, we also observed higher scores for the differentiation signature of Frumm [51], in HBP1 overexpressing versus NGP-parental cells (Supplementary Fig. 3C).

Importantly, we also revealed that the lowest HBP1 mean expression was observed in the *MYCN* amplified subgroup and in the stage 4 subgroup in a cohort of 283 neuroblastoma patients (GSE85047) (Supplementary Fig. 3D-E). Additionally, high levels of *HBP1* expression significantly correlated with better event-free and overall survival in all tumor types and in stage 4 tumors only (Fig. 3E-F, Supplementary Fig.

3F-G). Moreover, *HBP1* expression is a significant predictor of overall survival, independently of INSS stage, *MYCN* amplification and age ($p = 0.02$). To the best of our knowledge, no deletions nor inactivating mutations in HBP1 have been reported so far in NB primary tumors or cell lines.

Collectively, these data indicate that lower HBP1 levels mark tumor aggressiveness and that HBP1 could act as tumor suppressor in neuroblastoma.

Figure 3

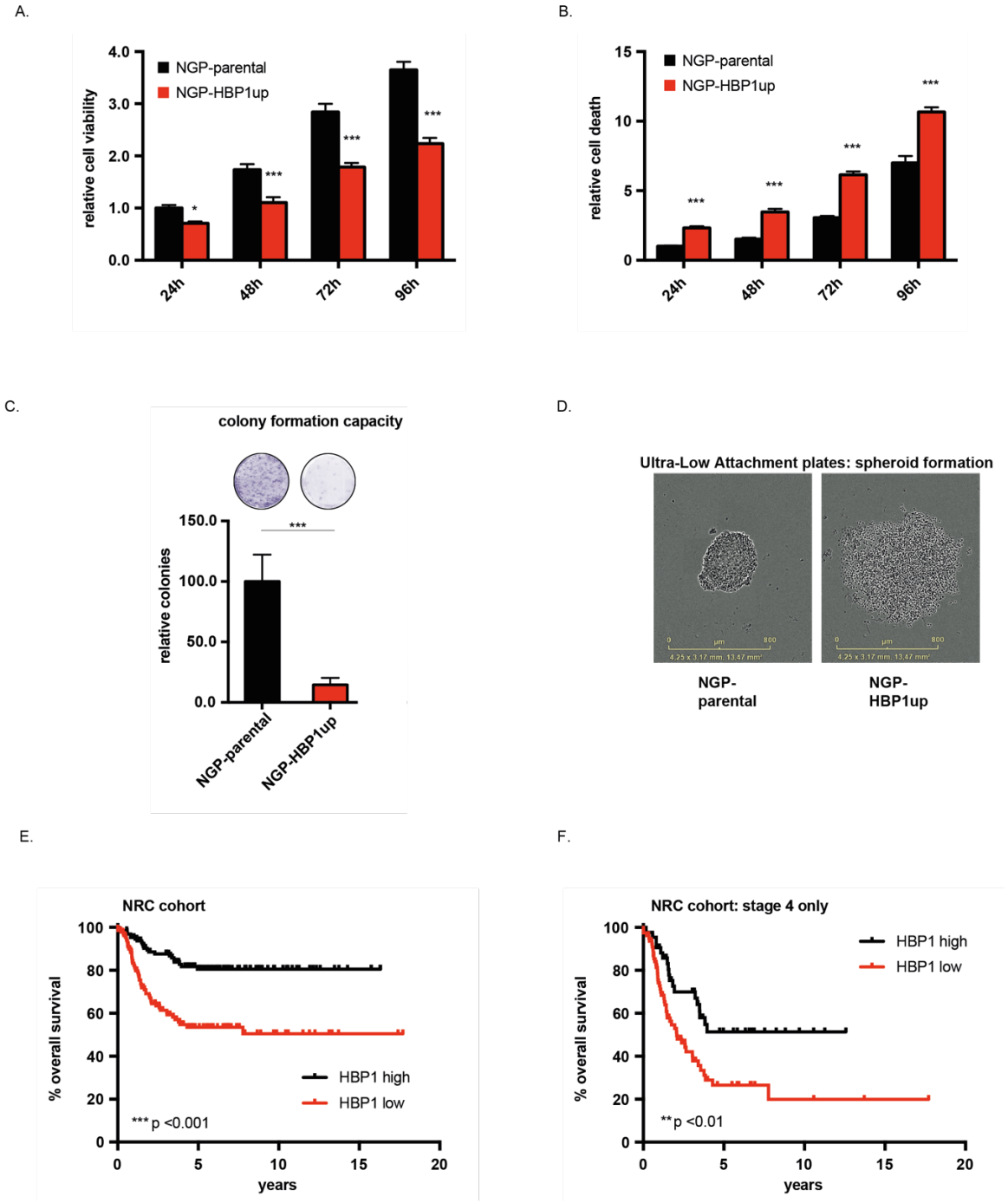

Figure 3: Increased HBP1 levels represses tumor aggressiveness

A and B, Cell viability (A) and cell death (B) of NGP-parental cell line and the NGP cell line with stable HBP1 overexpression at the indicated time points **C,** Clonogenic survival assays in the parental and HBP1 overexpressing NGP cell lines, with the quantification of three independent experiments, each consisting of 5 replicates, shown in the graph. **D,** NGP cell line with stable HBP1 overexpression forms a loose aggregate, while the NGP-parental cell line forms a dense spheroid on ultra-low-attachment plates. **E and F,** Kaplan Meier plot

showing percentage of overall survival in patients with high or low *HBP1* expression in tumors of all stages (E) and only stage 4 tumors (F) in the cohort of 283 NB patients.
Error bars represents mean ± SD of at least 3 biological replicates, each consisting of 2 technical replicates (A, B) and are calculated following error propagation. * P < 0.05, ** P < 0.01, *** P < 0.001

Combined pharmacological upregulation of HBP1 and repression of MYCN induces synergistic effects

In view of the new insights into HBP1 regulation and MYCN regulation in neuroblastoma cells (Fig. 4A-B), we decided to explore possibilities for drugging this regulatory axis. We initially tested the green tea polyphenol epigallocatechin-3-gallate (EGCG) previously shown to reduce breast cancer cell proliferation through increase of HBP1 mRNA stability. As a more clinically relevant compound, the PI_3K/mTOR dual inhibitor BEZ-235 was found to induce HBP1 expression (Fig. 1G). First, we demonstrate HBP1 upregulation and decreased cell viability after EGCG treatment in the ALK mutant cell lines NB-1 and CLB-GA, while no effects were noted in the ALK wild type TAE684 ALK inhibitor non-responder SK-N-AS cells (Fig. 4C-D). Next, we performed combination drugging for EGCG and BEZ-235 with the BET inhibitor JQ1, known to repress transcription elongation and MYCN expression, in *MYCN* amplified cell lines [52], and observed synergistic effects (Combination Index (CI) < 1) on cell growth and on MYCN protein levels as compared to treatment with the individual compounds in neuroblastoma cell lines (Fig. 4E-F-G-H; Supplementary Fig. 4A-B-C-D). We tested EGCG and JQ1 combination further *in vivo* in LSL-*MYCN;dßh-i*Cre tumors engrafted in immunocompromised mice and showed significant effects on tumor growth, proliferation, apoptosis and survival of mice receiving this combination (Fig. 5A-B-C-D; Supplementary Fig. 4E-F). We further observed a partial rescue for synergistic BEZ-235/JQ1 effects on viability (Fig. 5E, Supplementary Fig. 4G) in NGP cells with stable HBP1 knock down (shHBP1) as compared with the parental cell line.

Figure 4

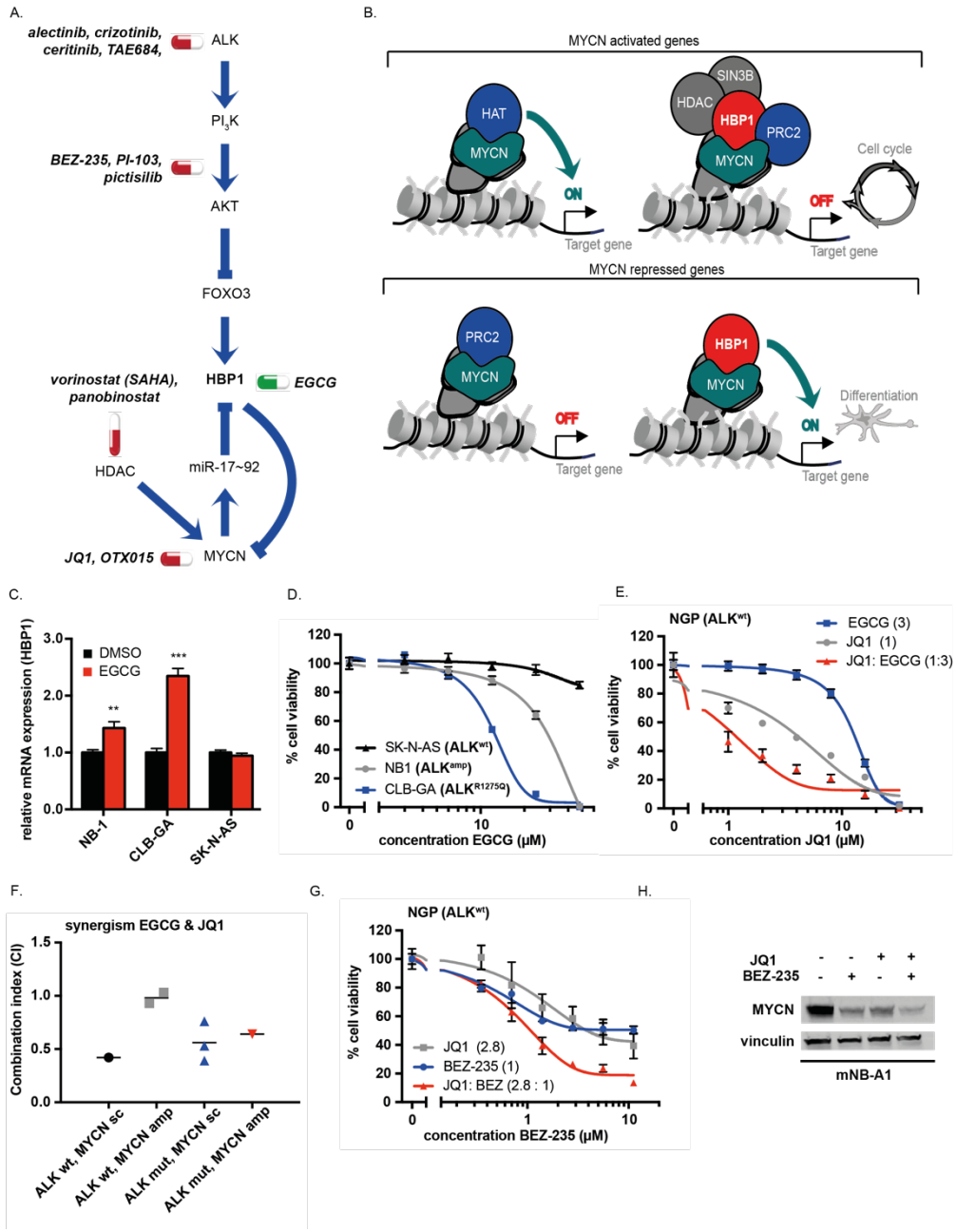

Figure 4: Combined pharmacological upregulation of HBP1 and repression of MYCN induces synergistic effects on tumor growth

A. ALK regulates MYCN activity through several mechanisms. It enhances MYCN protein stability by blocking GSK3β through PI_3K, while it simultaneously phosphorylates FOXO3 through this same pathway. In this way, FOXO3 stays cytoplasmatic and can't activate HBP1, which is a negative regulator of MYCN activity. MYCN itself inhibits HBP1 through induction of the miR-17-92 cluster, thereby forming a negative feedback loop. To block these pathways in order to upregulate HBP1 while negatively affecting MYCN activity, there are several nodes that can be targeted by compounds: ALK inhibitors (TAE684, crizotinib,

LDK378, alectinib), GSK3β inhibitors, PI_3K inhibitors (BEZ-235, PI-103, pictilisib), HDAC inhibitors (SAHA, panobinostat), JQ1 which inhibits BRD3 and in this way MYCN indirectly, while the green tea component EGCG upregulates HBP1 expression directly. **B,** Hypothetical scheme showing how HBP1 has an impact on the dual role of MYCN: HBP1 causes downregulation of genes involved in cell cycle that are positively regulated by MYCN, while it upregulates differentiation genes that are repressed by MYCN. **C,** *HBP1* mRNA levels in a small panel of NB cell lines (one ALK^{wt}, ALK^{amp}, ALK^{R1275Q} cell line) treated with 25 µM EGCG or DMSO, relative to the DMSO control of each cell line. **D,** Cell viability assay of the same cell lines as in C, showing the EGCG dose response curves 48h after treatment. **E,** Cell viability of the NGP cell line, showing the dose response curves of EGCG, JQ1 and the combination 48h after treatment. **F,** Combination index (CI)-values at IC-50 showing synergistic effect in a panel of 7 NB cell lines with different ALK and MYCN status. Synergy: CI < 1.0, additive: CI = 1.0, antagonism: CI > 1.0. **G,** Cell viability of the NGP cell line, showing the dose response curves of BEZ-235, JQ1 and the combination 48h after treatment. **H,** Western blot analysis showing MYCN protein levels 48h after treating the mNB-A1 cells with DMSO, 0.405 µM BEZ-235, 1.215 µM JQ1 or the combination.
Error bars represents mean ± SD of 2 technical replicates (C) or of at least 3 biological replicates, each consisting of 2 technical replicates (D, E, G) and are calculated following error propagation. * P < 0.05, ** P < 0.01, *** P < 0.001

Given the reported effect of HDAC inhibitors on MYCN protein levels [53], we also tested the effects of combined BEZ-235 and HDAC inhibitor SAHA (vorinostat) treatment in a panel of 8 cell lines and in the patient-derived xenograft (PDX)-derived cell line (LU-NB-2) [54,55], showing synergistic effects on cell survival (Fig. 5F; Supplementary Fig. 5A-B-C-D) and a synergistic effect on HBP1 and MYCN levels in the CLB-GA cell line (Supplementary Fig. 5E). Moreover, analysis of transcriptomes of the treated cells demonstrates downregulation of *MYCN* expression and more importantly, the MYCN activity score[44], thus indicating the expected reduction in MYCN activity (Fig. 5G-H). Finally, as for the BEZ-235 and JQ1 combination, we also observed increased cell viability in the shHBP1 cell line compared with the parental cell line for this BEZ-235 and SAHA combination (Fig. 5I, Supplementary Fig. 5F). Finally, we also tested the more recently developed potent HDAC inhibitor panobinostat [56], also demonstrating the expected synergism on cell viability in the tested neuroblastoma cell lines and the patient-derived xenograft (PDX)-derived cell

line (LU-NB-2) [54,55] (Fig.5J; Supplementary Fig. 5G-H-I) and synergistic upregulation of *HBP1* mRNA the CLB-GA cell line upon the BEZ-235 and panobinostat combination (Supplementary Fig. 5J).

Figure 5

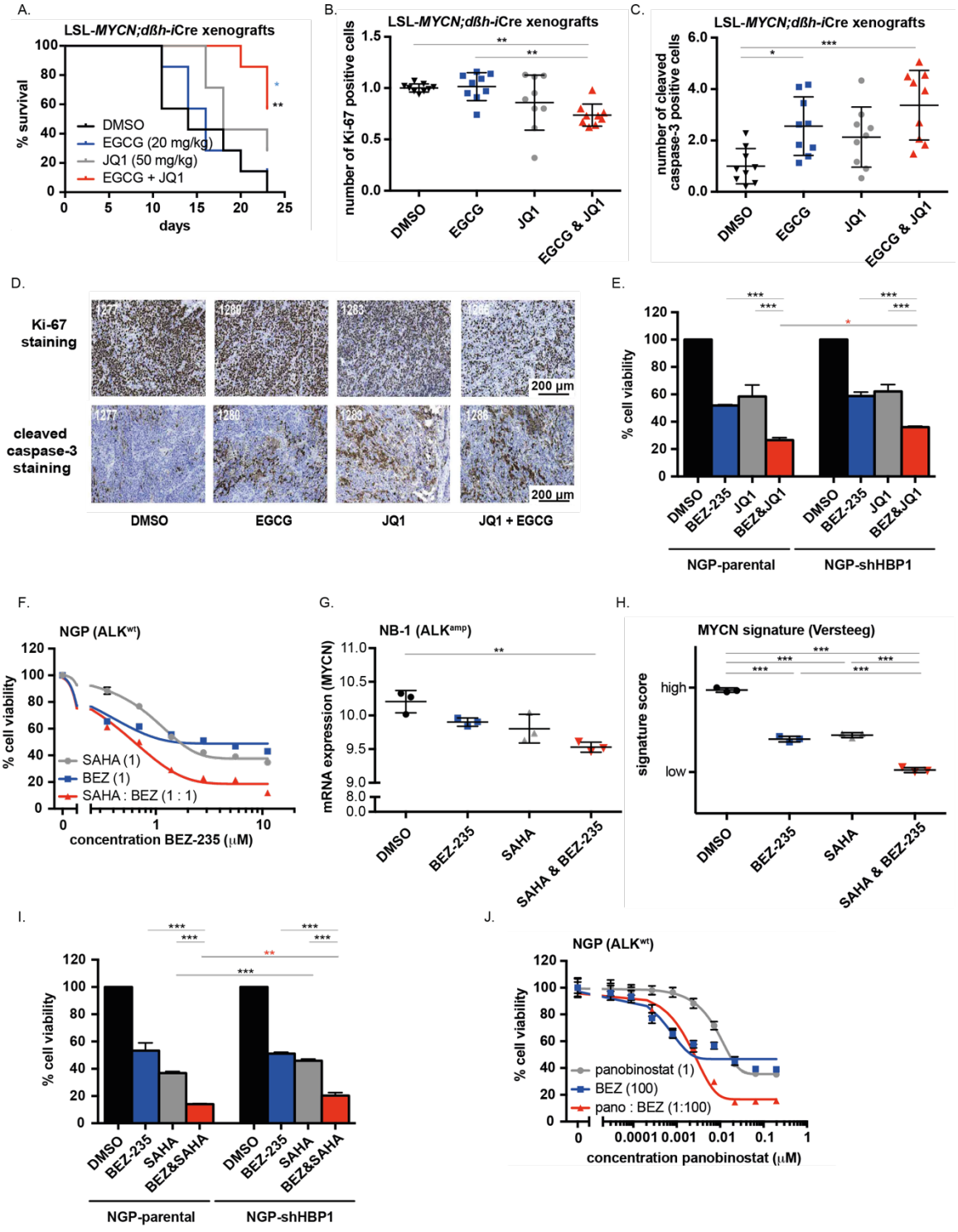

Figure 5: BEZ-235 in combination with JQ1 or HDACi synergistically upregulates HBP1 levels with concomitant repression of MYCN activity

A, Kaplan Meier plot showing percentage survival of LSL-*MYCN;dßh-i*Cre grafted mice treated with DMSO, EGCG (20 mg/kg), JQ1 (50 mg/kg) or the combination. Black stars: survival DMSO vs combination, blue stars: survival EGCG vs combination, n = 7 mice/group.

B and C, Graphs showing Ki-67 positive cells (B) and cleaved caspase-3 positive cells (C) in immunohistochemistry (IHC) staining in tumor sections of the forced treatment group of mice. **D,** IHC staining for the proliferative cells (Ki-67) and apoptotic cells (cleaved caspase-3) mentioned in B and C. Scale bar = 200 µm. **E,** Barplots showing % cell viability in the NGP-parental and shHBP1 cell line upon treatment with 2.8 µM BEZ-235, 8 µM JQ1 or the combination. **F,** Cell viability of the NGP cell line, showing the dose response curves of BEZ-235, SAHA and the combination 48h after treatment. **G and H,** MYCN expression (G) and MYCN activity score (H) in NB-1 cells treated with DMSO, 0.5 µM BEZ-235, 0.5 µM SAHA or the combination. **I,** Barplots showing % cell viability in the NGP-parental and shHBP1 cell line upon treatment with 2.8 µM BEZ-235, 2.8 µM SAHA or the combination. **J,** Cell viability of the NGP cell line, showing the dose response curves of BEZ-235, panobinostat and the combination 48h after treatment.

Error bars represents mean ± SD of 7 biological replicates (B, C), of at least 2 biological replicates, each consisting of 2 technical replicates (E, F, I, J) or of 3 biological replicates (G, H) and are calculated following error propagation. * $P < 0.05$, ** $P < 0.01$, *** $P < 0.001$

5.1.6 DISCUSSION

We provide *in vitro* and *in vivo* evidence for the existence of another mechanism for activation of MYCN activity through ALK-PI_3K-FOXO3a controlled down regulation of the negative regulator of MYC(N) activity HBP1. Together with the previously described ALK-ERK5-driven transcriptional induction of MYCN and regulation of the oncogenic activity of MYCN through increased mRNA levels and protein phosphorylation by the ALK-PI_3K/mTOR-GSK3β axis[24–27,57,58], this represents a third mechanism of ALK controlled MYCN activation. We also show that in neuroblastoma cells MYCN itself indirectly represses HBP1 expression levels through its downstream upregulated miRNA cluster miR-17~92 that targets HBP1.As such, a complex inter-regulatory network emerges where ALK regulates MYCN through three distinct mechanisms[24–27,55,56], MYCN transcriptionally activates ALK[59] and both ALK and MYCN repress HBP1 expression levels. Given the proven role of MYCN as driver oncogene in neuroblastoma oncogenesis[2], our data provide a further mechanistic explanation for the previously reported increased tumor aggressiveness in patients with combined *MYCN* amplification and *ALK^{F1174}* mutations and mouse

and zebrafish modeling which demonstrated a key role for mutated ALK in accelerated MYCN-driven neuroblastoma formation[21–23].

In this study, we investigated for the first time the functional interaction of HBP1 with MYCN in the context of neuroblastoma. We showed evidence for physical interaction between MYCN and HBP1, while HBP1 overexpression revealed significant enrichment for gene sets related to MYC(N) regulation and activity. Furthermore, in a cohort of 283 primary human NB tumor samples, we demonstrated strong inverse correlation between the HBP1 upregulated pathway signature and *MYCN* gene expression and MYCN activity score. Taken together, these data support the role of HBP1 as a suppressor of MYCN activity in neuroblastoma cells.

Unexpectedly, the data mining of the transcriptome alterations upon HBP1 overexpression and EZH2 inhibitor signature scores suggest that HBP1 abrogates the MYCN/PRC2 controlled repression of pro-differentiation genes. Our findings provide further evidence for a role for EZH2 and SUZ12 as components of the PRC2 complex in the MYCN mediated gene repression[48,60] and for the first time assigns a putative function to HBP1 as regulatory factor mediating the release of transcriptional repression by the MYCN/EZH2 complex. Further, HBP1 upregulation also leads to repression of MYCN activated genes, possibly through recruitment of HDAC and SIN3B as described for MYC [40]. Taken together, while the exact mode-of-action of HBP1 in relation to MYCN and PRC2 remains to be resolved, our data support previous findings that HBP1 affects both the MYC(N) transcriptional activating and repressing activity [29]. As such, our findings also support the recently suggested role for PRC2 in MYCN controlled gene repression [48,60].

Unraveling of the ALK signaling cascade has previously provided novel putative drugging approaches as illustrated by the finding of RET and ERK5 as druggable downstream ALK targets [28,57]. In this study, we explored several drug combinations targeting HBP1 and/or MYCN to explore possible synergistic interactions. We tested a PI3K/mTOR inhibitor aimed to activate (amongst others) HBP1 expression in combination with BET inhibitor JQ1, a known negative regulator of MYC(N) activity in MYCN amplified cell lines [52], in order to further decrease cell viability as well as MYC(N) activity and observed strong synergistic effects in neuroblastoma cells. Secondly, we combined the same PI3K/mTOR inhibitor with different HDAC inhibitors mediating MYCN suppression [53] and previously shown to give promising effects on

MYC-driven medulloblastoma[56] and Burkitt lymphoma[61] and also observed synergistic effects, both on conventional neuroblastoma as well as PDX-derived cell lines[54]. In addition to these combinations (Fig. 4A-B), other approaches can be envisioned to target MYCN or MYCN activity, thus offering the potential for consecutive series of different drug combinations to achieve sustained blocking of MYCN activity in neuroblastoma. Such approaches and other potent drug combinations as well as novel immunotherapeutic approaches may ultimately lead to accomplish the final goal to achieve better and long-term survival for NB patients.

5.1.7 MATERIAL AND METHODS

Cell lines and reagents

Human neuroblastoma cells were cultured in RPMI-1640 medium (Invitrogen), supplemented with fetal bovine serum (10%), kanamycin (100 μg/ml), penicillin/streptomycin (100 IU/ml), L-glutamin (2 mM) and HEPES (25 mM) (Life Technologies), while the mouse mNB-A1 cells were cultured in this medium supplemented with N-2 Supplement and B-27 Serum-Free Supplement (Life Technologies). The PDX-derived LU-NB-2 cell line, derived from a MYCN amplified neuroblastoma, orthotopically xenografted in NSG mice forming metastasizing tumors, was cultured under serum-free, stem-cell promoting culture conditions [54,55]. Cells were maintained at 37°C in a 5% C02-humidified environment.

The compounds NVP-TAE684 (ALK inhibitor, S1108), BEZ-235 (PI3K/mTOR inhibitor, S1009), pictilisib (PI3K inhibitor, S1065), U0126 (MEK inhibitor, S1102), EGCG (S2250) and panobinostat (HDAC inhibitor, S1030) were purchased from SelleckChem, crizotinib (ALK inhibitor, PZ0191) and SAHA (vorinostat, HDAC inhibitor, SML0061) from Sigma-Aldrich, LDK-378 (ALK inhibitor, A-1189-5) from Hoelzel Biotech and JQ1 (BET inhibitor, 27401) from BPS Bioscience. Compounds were dissolved in sterile DMSO, stored at -20°C and further diluted to an appropriate final concentration in culture medium at the time of use. DMSO was used as solvent control for every treatment.

Evaluation of HBP1 expression upon ALK and downstream pathway inhibition

HBP1 expression levels were evaluated in (1) 6 NB cell lines with different ALK status (ALK^{wt}, ALK^{F1174L}, ALK^{R1275Q}, ALK^{amp}) treated with 0.32 µM TAE684 for 6 hours, (2) the CLB-GA cell line (ALK^{R1275Q}) treated with 0.32 µM TAE684 and harvested at different time points (10, 30, 60, 120, 240, 360 min) (E-MTAB-3205 [28]), (3) CLB-GA cells treated with 0.2 µM LDK378, 0.32 µM TAE684, 0.06 µM X396, 0.5 µM crizotinib, 0.05 µM trametinib, 0.5 µM BEZ-235 and 9.5 µM vandetanib for 6 hours (E-MTAB-3206 [28]), (4) SK-N-AS cell lines with tetracycline-inducible ALK^{wt}, ALK^{F1174L} or ALK^{R1275Q} constructs treated with 2 µg/ml tetracycline or ethanol for 24 hours (E-MTAB-3207 [28]), (5) NB-1 and CLB-GA treated with 0.5 µM BEZ-235, 0.5 µM pictilisib or 8 µM U0126 for 6 hours for RNA and protein, (6) mice with subcutaneously xenografted SH-SY-5Y neuroblastoma cells, treated with TAE684 and crizotinib, (7) Ba/F3 (murine pro-B) cells with an ALK^{wt}, ALK^{F1174L}, ALK^{R1275Q} or EML4/ALK fusion-protein construct treated with 0.32 µM TAE684 for 6 hours, (8) publically available data of NSCLC treated with Alectinib (GSE25118 [33]), (9) a published dataset of a FOXO3-inducible SH-SY5Y cell line (GSE42762 [36]) and (10) a cohort of 283 neuroblastoma tumor samples (GSE85047)

Testing synergism of drug combinations *in vitro*

Neuroblastoma cells were seeded in 96-well tissue culture plates in triplicate at 30% confluency, allowed to recover overnight and subsequently treated with a range of concentrations of the two inhibitors while keeping the final concentration of DMSO constant. 48 hours after treatment, cell viability was measured using Cell-Titer Glo (Promega), according to the manufacturer's protocol and luminescence was measured with the GloMax®-Multi Detection System (Promega). To evaluate possible synergism, combination indexes (CI) for each combination were calculated using the CalcuSyn software (Biosoft, Ferguson, MO), which uses the Median Effect method [62]. Synergism is defined as a CI-value less than 1.0, while additive effects result in a CI-value equal to 1.0.

Synergistic effects of EGCG and JQ1 *in vivo*

LSL-*MYCN;dßh-i*Cre tumors were re-grafted in the flank of immuno-deficient mice.

The short-term treatment experiment consisted of 4 groups each containing 3 mice: vehicle (12,5% DMSO in 5% glucose), EGCG (20 mg/kg), JQ1 (50 mg/kg) or the combination (EGCG + JQ1). When tumors reached a volume of around 500 mm^3, mice were treated twice daily (100 µl i.p.) during 3 days. Hereafter, mice were sacrificed by cervical dislocation. Tumors were excised, formalin-fixed, analyzed for histology (H&E) and immunohistochemically stained for Ki-67 and cleaved caspase-3.

To monitor the effects on tumor growth and survival, a long-term experiment was performed. After tumors reached a volume of around 100-150 mm^3, 28 mice were randomly assigned to the 4 groups. Mice were treated daily (100 µl i.p.) for a period of maximal 23 days. When tumor sizes exceeded 3000 mm^3, mice were sacrificed by cervical translocation.

SHEP-miR-17~92 system

The miR-17~92 cluster was induced with 2 µg/ml tetracycline or ethanol (control) in the previously described SHEP-TR-miR-17~92 model system[41] and cells were harvested at different time points (0, 24, 48, 72 hours).

RNA isolation, cDNA synthesis and RT-qPCR

RNA isolation, cDNA synthesis and RT-qPCR of the generated samples was performed as we described earlier [28]. The Cq-values for target gene expression were normalized with at least three reference genes (primer sequences: Supplementary Table I.) and qBasePlus software (Biogazelle) was used to analyze the results [63].

Establishment of stable HBP1 overexpressing cell lines

NGP cells were transduced with Precision LentiORF Human HBP1 viral particles (ThermoScientific). Transduced cells were selected using blasticidin (20 µg/ml), subsequently maintained and harvested for further experiments.

In vitro assessment of HBP1 effect

NGP-parental and NGP HBP1 cells were seeded in white 96-well tissue culture plates in triplicate at 30% confluency and allowed to recover overnight. Cell viability was measured in triplicate using Cell-Titer Glo (Promega) 24h, 48h, 72h and 96h after seeding, while Caspase Glo (Promega) was used to evaluate cell death, both according to the manufacturer's protocol. Additionally, NGP-HBP1up and the NGP-parental cell lines were seeded at 70000 cells/well in sextuple in 96-well tissue culture plates in the presence of 10, 5, 1 or 0.1% serum and monitored and quantified using IncuCyte ZOOM technology (Essen BioScience).

To assess the colony formation capacity, cells were seeded in 5-fold at a concentration of 2000 cells per 6-cm dish. Cells were allowed to recover and to form colonies during a period of at least one week, followed by fixation of the cells by adding 0,5 ml 4% formaldehyde to each dish. After 1 hour, dishes were washed and colonies were colored with 0,005% crystal violet. After washing and air-drying, the dishes were scanned and evaluated with ImageJ and OpenCFU to quantify the differences.

For the spheroid formation, NGP-parental and NGP-HBP1up cells were seeded at 4000 cells/well in 48-fold in hydrogel coated 96 well plates, termed ultra-low attachment plates (ULA, Corning 7007) and monitored and quantified using IncuCyte ZOOM technology (Essen BioScience).

Co-immunoprecipitation

10 million NGP HBP1 cells were grown in T175s. After washing in ice-cold PBS, harvesting and centrifugation, cells were lysed with RIPA-buffer. 1/10 of the lysate was kept for input. Samples were incubated for 4 hours with 2 µg of the appropriate antibody (anti-MYCN (B8.4.B, sc-53993) from Santa Cruz Biotechnology or anti-HBP1 (11746-1-AP) from ProteinTech), followed by incubation with ProteinA Ultralink Resin beads (Thermo Scientific, 53139) at 4°C overnight. After washing, proteins were denatured with denaturation buffer (per condition: 20 µl 2x laemmli buffer + 19 µl RIPA buffer + 1 µl beta-mercapto-ethanol) and shaking the samples in a heat-block at 95°C. The eluate was used for Western.

Protein isolation, antibodies and western blotting

Protein isolation and western blotting was performed as we described earlier 28. MYCN (9405, 1:1000), SUZ12 (3737, 1:1000), secondary anti-rabbit (7074, 1:50000) and anti-mouse (7076, 1:50000) antibodies were obtained from Cell Signaling, while antibodies against the loading proteins vinculin (V9141, 1:10000) and α-tubulin (T4026, 1:10000) from Sigma Aldrich and the HBP1 (A-5) antibody (sc-376831, 1:400) from Santa Cruz Biotechnology.

Microarray-based gene expression profiling

RNA quality was analyzed using Experion (Bio-Rad). Samples from the parental and NGP HBP1 cell lines were labelled and hybridized to the Sureprint G3 human GE 8x60K microarrays (Agilent Technologies), according to the manufacturer's guidelines and starting from 200 ng RNA. The data were normalized with the vsn method, using the vsn and Limma packages in R.

Signature score generation and analysis and GSEA

Using the limma R-package, differential expression analysis was performed comparing the parental and NGP HBP1 samples. The established signatures consist of the differentially expressed genes with adjusted p-value (False Discovery Rate (FDR)) < 0.05. Next, we generated an EZH2 inhibitor signature, based on public data of EHZ2 inhibition with EPZ6438 in the SK-N-BE(2c) cell line[48] and a differentiation signature, based on public data of treating SK-N-BE(2c) and SH-SY5Y with pro-differentiating agents [51]. Signature score analyses were conducted using a rank-scoring algorithm[28]. Gene set enrichment analysis (GSEA [43]) was performed using the MSigDB 'c6 Oncogenic Signatures v5.0' gene sets (software.broadinstitute.org/gsea/msigdb) and an in house compiled gene set catalogue containing all MYC target genesets from the MSigDB 'Hallmark v5.0' catalogue as well as publically available MYC(N) activity or target signatures [44,45,52,64–68]. The genesets, showing positively or negatively enrichment and with a FDR < 0.25 are plotted in a heatmap.

RNA sequencing after SAHA and BEZ

RNA quality was evaluated using the Fragment Analyzer (Advanced Analytics). Library prep was performed with the TruSeq Stranded mRNA Library Prep Kit LT (Illumina), following manufacturer's instructions. Quality of the library was assessed with BioAnalyzer (Agilent) and concentrations were checked with the Kapa Library Quantification Kit (Kapa Biosystems). After pooling the samples, RNA sequencing was performed with the NextSeq 500 High Output kit, V2, 75 cycli, single-end (Illumina), following manufacturer's instructions, on the NextSeq 500 (Illumina). Quality of the data was checked by fastQC. Thereafter, the data was mapped to Hg38 by STAR and count data was generated using RSEM. Differential expression analysis was performed with Limma-voom in R.

Statistical analyses

Statistical significance was calculated with GraphPad Prism7 by unpaired one-way ANOVA with Bonferroni correction when comparing more than two unmatched groups, while unpaired t-test was chosen when comparing two groups.

5.1.8 ACCESSION NUMBER

The data have been deposited in NCBI's Gene Expression Omnibus and is accessible through GEO Series accession number GSE95193.

5.1.9 CONFLICT OF INTEREST:

The authors declare no conflict of interest.

5.1.10 ACKNOWLEDGEMENTS

We thank Jeroen Schacht, Jolien Van Laere, Fanny De Vloed, Givani Dewyn and Els De Smet from our lab as well as Glenn Wagemans from the LECR for their outstanding technical assistance. Furthermore, we thank Els Janssens, Annelies Fieuw, Sara De Brouwer and Irina Lambertz for their guidance during this project.

5.1.11 SUPPLEMENTARY INFORMATION accompanies the paper on the Oncogene website (http://www.nature.com/onc).

5.1.12 REFERENCES

1. Louis, C. U. & Shohet, J. M. Neuroblastoma: molecular pathogenesis and therapy. Annu. Rev. Med. 66, 49–63 (2015).
2. Cheung, N.-K. & Dyer, M. Neuroblastoma: developmental biology, cancer genomics and immunotherapy. Nat Rev Cancer 13, 397–411 (2013).
3. Molenaar, J. J. et al. Sequencing of neuroblastoma identifies chromothripsis and defects in neuritogenesis genes. Nature 483, 589–93 (2012).
4. Mossé, Y. et al. Identification of ALK as a major familial neuroblastoma predisposition gene. Nature 455, 930–935 (2008).
5. George, R. et al. Activating mutations in ALK provide a therapeutic target in neuroblastoma. Cah Rev The 455, 975–978 (2008).
6. Chen, Y. et al. Oncogenic mutations of ALK kinase in neuroblastoma. Cah Rev The 455, 971–974 (2008).
7. Janoueix-Lerosey, I. et al. Somatic and germline activating mutations of the ALK kinase receptor in neuroblastoma. Cah Rev The 455, 967–970 (2008).
8. Carpenter, E. L. & Mossé, Y. P. Targeting ALK in neuroblastoma--preclinical and clinical advancements. Nat Rev Clin Oncol 9, 391–9 (2012).
9. Guan et al. The ALK inhibitor PF-06463922 is effective as a single agent in neuroblastoma driven by expression of ALK and MYCN. Dis Model Mech 9, 941–952 (2016).
10. Amin, A. D. et al. TKI sensitivity patterns of novel kinase-domain mutations suggest therapeutic opportunities for patients with resistant ALK+ tumors. Oncotarget 7, 23715–29 (2016).
11. Pall, G. The next-generation ALK inhibitors. Curr Opin Oncol 27, 118 (2015).
12. Duncan, J. S. et al. Dynamic Reprogramming of the Kinome in Response to Targeted MEK Inhibition in Triple-Negative Breast Cancer. Cell 149, 307–321 (2012).
13. Toyokawa & Seto. Updated Evidence on the Mechanisms of Resistance to ALK Inhibitors and Strategies to Overcome Such Resistance: Clinical and Preclinical Data. Oncology Research and Treatment 0, 291–298 (2015).
14. Bresler, S. C. et al. Differential inhibitor sensitivity of anaplastic lymphoma kinase variants found in neuroblastoma. Sci Transl Med 3, 108ra114 (2011).
15. Bresler, S. C. et al. ALK Mutations Confer Differential Oncogenic Activation and Sensitivity to ALK Inhibition Therapy in Neuroblastoma. Cancer Cell 26, 682–694 (2014).
16. Heuckmann, J. et al. ALK Mutations Conferring Differential Resistance to Structurally Diverse ALK Inhibitors. Clinical Cancer Research 17, 7394–7401 (2011).

17. Yan, X. et al. Cooperative Cross-Talk between Neuroblastoma Subtypes Confers Resistance to Anaplastic Lymphoma Kinase Inhibition. Genes & Cancer 2, 538–549 (2011).
18. Debruyne, D. et al. ALK inhibitor resistance in ALKF1174L-driven neuroblastoma is associated with AXL activation and induction of EMT. Oncogene 35, 3681–3691 (2015).
19. Isozaki, H. et al. Non–Small Cell Lung Cancer Cells Acquire Resistance to the ALK Inhibitor Alectinib by Activating Alternative Receptor Tyrosine Kinases. Cancer Res 76, 1506–1516 (2015).
20. Lovly, C. & Shaw, A. Molecular Pathways: Resistance to Kinase Inhibitors and Implications for Therapeutic Strategies. Clin Cancer Res 20, 2249–2256 (2014).
21. De Brouwer, S. et al. Meta-analysis of Neuroblastomas Reveals a Skewed ALK Mutation Spectrum in Tumors with MYCN Amplification. Clinical Cancer Research 16, 4353–4362 (2010).
22. Zhu, S. et al. Activated ALK Collaborates with MYCN in Neuroblastoma Pathogenesis. Cancer Cell 21, 362–373 (2012).
23. Berry, T. et al. The ALKF1174L Mutation Potentiates the Oncogenic Activity of MYCN in Neuroblastoma. Cancer Cell 22, 117–130 (2012).
24. Schönherr, C. et al. Anaplastic Lymphoma Kinase (ALK) regulates initiation of transcription of MYCN in neuroblastoma cells. Oncogene 31, 5193–5200 (2012).
25. Chesler, L. et al. Inhibition of phosphatidylinositol 3-kinase destabilizes Mycn protein and blocks malignant progression in neuroblastoma. Cancer research 66, 8139–46 (2006).
26. Cage, T. A. et al. Downregulation of MYCN through PI3K Inhibition in Mouse Models of Pediatric Neural Cancer. Front Oncol 5, 111 (2015).
27. Vaughan, L. et al. Inhibition of mTOR-kinase destabilizes MYCN and is a potential therapy for MYCN-dependent tumors. Oncotarget 7, 57525–57544 (2016).
28. Lambertz, I. et al. Upregulation of MAPK Negative Feedback Regulators and RET in Mutant ALK Neuroblastoma: Implications for Targeted Treatment. Clin. Cancer Res. 21, 3327–39 (2015).
29. Escamilla-Powers, J. et al. The Tumor Suppressor Protein HBP1 Is a Novel c-Myc-binding Protein That Negatively Regulates c-Myc Transcriptional Activity. J Biol Chem 285, 4847–4858 (2010).
30. Tevosian, S. et al. HBP1: a HMG box transcriptional repressor that is targeted by the retinoblastoma family. Genes Dev 11, 383–396 (1997).
31. Passoni, L. et al. Mutation-Independent Anaplastic Lymphoma Kinase Overexpression in Poor Prognosis Neuroblastoma Patients. Cancer Research 69, 7338–7346 (2009).
32. Mossé, Y. et al. Safety and activity of crizotinib for paediatric patients with refractory solid tumours or anaplastic large-cell lymphoma: a Children's Oncology Group phase 1 consortium study. The Lancet Oncology 14, 472–480 (2013).
33. Sakamoto, H. et al. CH5424802, a Selective ALK Inhibitor Capable of Blocking the Resistant Gatekeeper Mutant. Cancer Cell 19, 679–690 (2011).

34. Heukamp, L. et al. Targeted Expression of Mutated ALK Induces Neuroblastoma in Transgenic Mice. Sci Transl Medicine 4, 141ra91–141ra91 (2012).
35. Moore, N. F. et al. Molecular rationale for the use of PI3K/AKT/mTOR pathway inhibitors in combination with crizotinib in ALK-mutated neuroblastoma. Oncotarget 5, 8737–49 (2014).
36. Santo, E. et al. FOXO3a Is a Major Target of Inactivation by PI3K/AKT Signaling in Aggressive Neuroblastoma. Cancer Res 73, 2189–2198 (2013).
37. Gu, T.-L. L. et al. NPM-ALK fusion kinase of anaplastic large-cell lymphoma regulates survival and proliferative signaling through modulation of FOXO3a. Blood 103, 4622–9 (2004).
38. Coomans de Brachène, A. et al. The expression of the tumour suppressor HBP1 is down-regulated by growth factors via the PI3K/PKB/FOXO pathway. The Biochemical journal 460, 25–34 (2014).
39. Li, H., Bian, C., Liao, L., Li, J. & Zhao, R. miR-17-5p promotes human breast cancer cell migration and invasion through suppression of HBP1. Breast Cancer Res Tr 126, 565–575 (2011).
40. Li, Y., Choi, P. S., Casey, S. C., Dill, D. L. & Felsher, D. W. MYC through miR-17-92 Suppresses Specific Target Genes to Maintain Survival, Autonomous Proliferation, and a Neoplastic State. Cancer Cell 26, 262–272 (2014).
41. Mestdagh et al. MYCN/c-MYC-induced microRNAs repress coding gene networks associated with poor outcome in MYCN/c-MYC-activated tumors. Oncogene 29, 1394–1404 (2009).
42. Althoff et al. A Cre-conditional MYCN-driven neuroblastoma mouse model as an improved tool for preclinical studies. Oncogene 34, 3357–3368 (2015).
43. Subramanian, A. et al. Gene set enrichment analysis: A knowledge-based approach for interpreting genome-wide expression profiles. P Natl Acad Sci Usa 102, 15545–15550 (2005).
44. Valentijn, L. J. et al. Functional MYCN signature predicts outcome of neuroblastoma irrespective of MYCN amplification. Proc. Natl. Acad. Sci. U.S.A. 109, 19190–5 (2012).
45. Zeller, K., Jegga, A., Aronow, B., O'Donnell, K. & Dang, C. An integrated database of genes responsive to the Myc oncogenic transcription factor: identification of direct genomic targets. Genome Biol 4, 1–10 (2003).
46. Bracken, A., Dietrich, N., Pasini, D., Hansen, K. & Helin, K. Genome-wide mapping of Polycomb target genes unravels their roles in cell fate transitions. Gene Dev 20, 1123–1136 (2006).
47. Janky, R. et al. iRegulon: From a Gene List to a Gene Regulatory Network Using Large Motif and Track Collections. Plos Comput Biol 10, e1003731 (2014).
48. Henrich, K.-O. et al. Integrative Genome-Scale Analysis Identifies Epigenetic Mechanisms of Transcriptional Deregulation in Unfavorable Neuroblastomas. Cancer Res 76, 5523–5537 (2016).

49. Watanabe, N., Kageyama, R. & Ohtsuka, T. Hbp1 regulates the timing of neuronal differentiation during cortical development by controlling cell cycle progression. Development 142, 2278–2290 (2015).
50. Yao, C., Works, K., Romagnoli, P. & Austin, G. Effects of overexpression of HBP1 upon growth and differentiation of leukemic myeloid cells. Leukemia 19, 1958–1968 (2005).
51. Frumm, S. M. et al. Selective HDAC1/HDAC2 Inhibitors Induce Neuroblastoma Differentiation. Chem Biology 20, 713–725 (2013).
52. Puissant, A. et al. Targeting MYCN in Neuroblastoma by BET Bromodomain Inhibition. Cancer Discovery 3, 308–323 (2013).
53. Cortés, C., Kozma, S., Tauler, A. & Ambrosio, S. MYCN concurrence with SAHA-induced cell death in human neuroblastoma cells. Cell Oncol 38, 341–352 (2015).
54. Braekeveldt, N. et al. Neuroblastoma patient-derived orthotopic xenografts retain metastatic patterns and geno- and phenotypes of patient tumours. Int J Cancer 136, E252–E261 (2015).
55. Persson, C. U. et al. Neuroblastoma patient-derived xenograft cells cultured in stem-cell promoting medium retain tumorigenic and metastatic capacities but differentiate in serum. Sci Rep 7, 10274 (2017).
56. Pei, Y. et al. HDAC and PI3K Antagonists Cooperate to Inhibit Growth of MYC-Driven Medulloblastoma. Cancer Cell 29, 311–323 (2016).
57. Umapathy, G. et al. The kinase ALK stimulates the kinase ERK5 to promote the expression of the oncogene MYCN in neuroblastoma. Sci Signal 7, ra102–ra102 (2014).
58. Duffy, D., Krstic, A., Schwarzl, T., Higgins, D. & Kolch, W. GSK3 Inhibitors Regulate MYCN mRNA Levels and Reduce Neuroblastoma Cell Viability through Multiple Mechanisms, Including p53 and Wnt Signaling. Molecular Cancer Therapeutics 13, 454–467 (2014).
59. Hasan, K. et al. ALK is a MYCN target gene and regulates cell migration and invasion in neuroblastoma. Sci Reports 3, 3450 (2013).
60. Corvetta, D. et al. Physical Interaction between MYCN Oncogene and Polycomb Repressive Complex 2 (PRC2) in Neuroblastoma FUNCTIONAL AND THERAPEUTIC IMPLICATIONS. J Biol Chem 288, 8332–8341 (2013).
61. Ferreira, A., de-Freitas-Junior, J., Morgado-Díaz, J., Ridley, A. & Klumb, C. Dual inhibition of histone deacetylases and phosphoinositide 3-kinases: effects on Burkitt lymphoma cell growth and migration. J Leukocyte Biol 99, 569–578 (2016).
62. Chou, T.-C. & Talalay, P. Analysis of combined drug effects: a new look at a very old problem. Trends Pharmacol Sci 4, 450–454 (1983).
63. Hellemans, J., Mortier, G., Paepe, A., Speleman, F. & Vandesompele, J. qBase relative quantification framework and software for management and automated analysis of real-time quantitative PCR data. Genome Biol 8, 1–14 (2007).

64. Coller, H. et al. Expression analysis with oligonucleotide microarrays reveals that MYC regulates genes involved in growth, cell cycle, signaling, and adhesion. Proc National Acad Sci 97, 3260–3265 (2000).
65. Ellwood-Yen, K. et al. Myc-driven murine prostate cancer shares molecular features with human prostate tumors. Cancer Cell 4, 223–38 (2003).
66. Fredlund, E., Ringnér, M., Maris, J. M. & Påhlman, S. High Myc pathway activity and low stage of neuronal differentiation associate with poor outcome in neuroblastoma. Proc. Natl. Acad. Sci. U.S.A. 105, 14094–9 (2008).
67. Yu, D., Cozma, D., Park, A. & Thomas-Tikhonenko, A. Functional validation of genes implicated in lymphomagenesis: an in vivo selection assay using a Myc-induced B-cell tumor. Ann. N. Y. Acad. Sci. 1059, 145–59 (2005).
68. Kim, Y. et al. Combined microarray analysis of small cell lung cancer reveals altered apoptotic balance and distinct expression signatures of MYC family gene amplification. Oncogene 25, 130–138 (2005)

5.1.13 TABLES

Supplementary Table I.: primer sequences

Primer sequences for the target and reference genes.

Gene	Primer	Sequence	
HBP1	Forward	TAGAGCTGAAGGCTGTGATA	Target genes
	Reverse	ACAGACTCGCCAAATGATAC	
MYCN	Forward	AGGCATCGTTTGAGGATCAG	
	Reverse	AGGACACCCTGAGCGATTC	
UBC	Forward	ATTTGGGTCGCGGTTCTTG	Reference genes
	Reverse	TGCCTTGACATTCTCGATGGT	
TBP	Forward	CACGAACCACGGCACTGATT	
	Reverse	TTTTCTTGCTGCCAGTCTGGAC	
B2M	Forward	TGCTGTCTCCATGTTTGATGTATCT	
	Reverse	TCTCTGCTCCCCACCTCTAAGT	
YWHAZ	Forward	ACTTTTGGTACATTGTGGCTTCAA	
	Reverse	CCGCCAGGACAAACCAGTAT	
HPRT1	Forward	TGACACTGGCAAAACAATGCA	
	Reverse	GGTCCTTTTCACCAGCAAGCT	
HMBS	Forward	GGCAATGCGGCTGCAA	
	Reverse	GGGTACCCACGCGAATCAC	
SDHA	Forward	TGGGAACAAGAGGGCATCTG	
	Reverse	CCACCACTGCATCAAATTCATG	

Supplementary Table II.: GSEA results (excel)

Supplemental data containing the results of the GSEA for the NGP HBP1 data. First two files contain the genesets from an in-house build collection that are respectively positively and negatively enriched in the NGP HBP1 dataset, while the last two files the genesets from c6 collection (Broad Institute) that are respectively positively and negatively enriched in the NGP HBP1 dataset.

5.1.14 SUPPLEMENTARY FIGURES

Supplementary figure 1

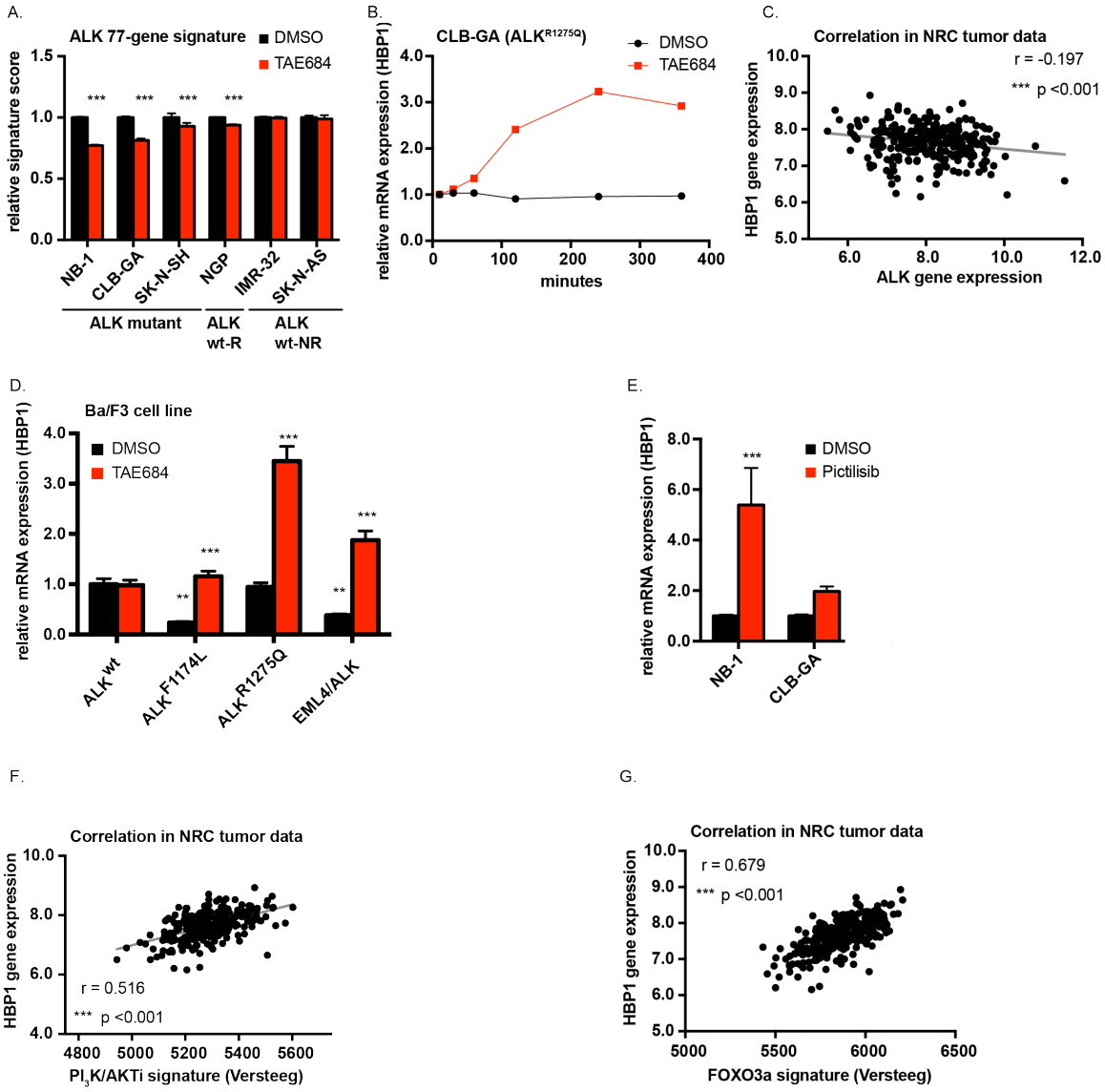

Supplementary figure 1: HBP1 is downregulated by mutant through PI_3K-AKT-FOXO3a.

A, ALK 77-gene signature score in several ALK wild type (NGP, IMR-32, SK-N-AS) and ALK mutant (SK-N-SH, CLB-GA, NB-1) cell lines treated for 6 hours with 0.3 μM TAE684 or DMSO relative to the levels in DMSO treated cells. **B,** *HBP1* expression in CLB-GA cells after treatment with 0.32 μM TAE684 or DMSO at the indicated time points, relative to the DMSO control at the 0 minutes time point. **C,** Spearman correlation between *HBP1* and *ALK* gene expression in a cohort of 283 NB tumors. **D,** *HBP1* mRNA levels in Ba/F3 (murine pro-B) cells with an ALK^{wt}, ALK^{F1174L}, ALK^{R1275Q} or the EML4/ALK fusion-protein construct treated with 0.32 μM of the ALK inhibitor TAE684 or DMSO for 6 hours. **E,** *HBP1* mRNA levels in a

small panel of NB cell lines (one ALK^{amp} and one ALK^{R1275Q}) treated with 0.5 µM PI_3K inhibitor pictilisib or DMSO, relative to the DMSO control of each cell line. **F and G,** Spearman correlation between PI_3K/AKT inhibitor signature score and the *HBP1* gene expression level in a NB cell line panel (F) and in a cohort of 283 NB tumors (G).

Error bars represents mean ± SD of respectively 3 biological replicates (A), 2 biological replicates (B) or 2 technical replicates (D, E) and are calculated following error propagation. * $P < 0.05$, ** $P < 0.01$, *** $P < 0.001$

Supplementary figure 2

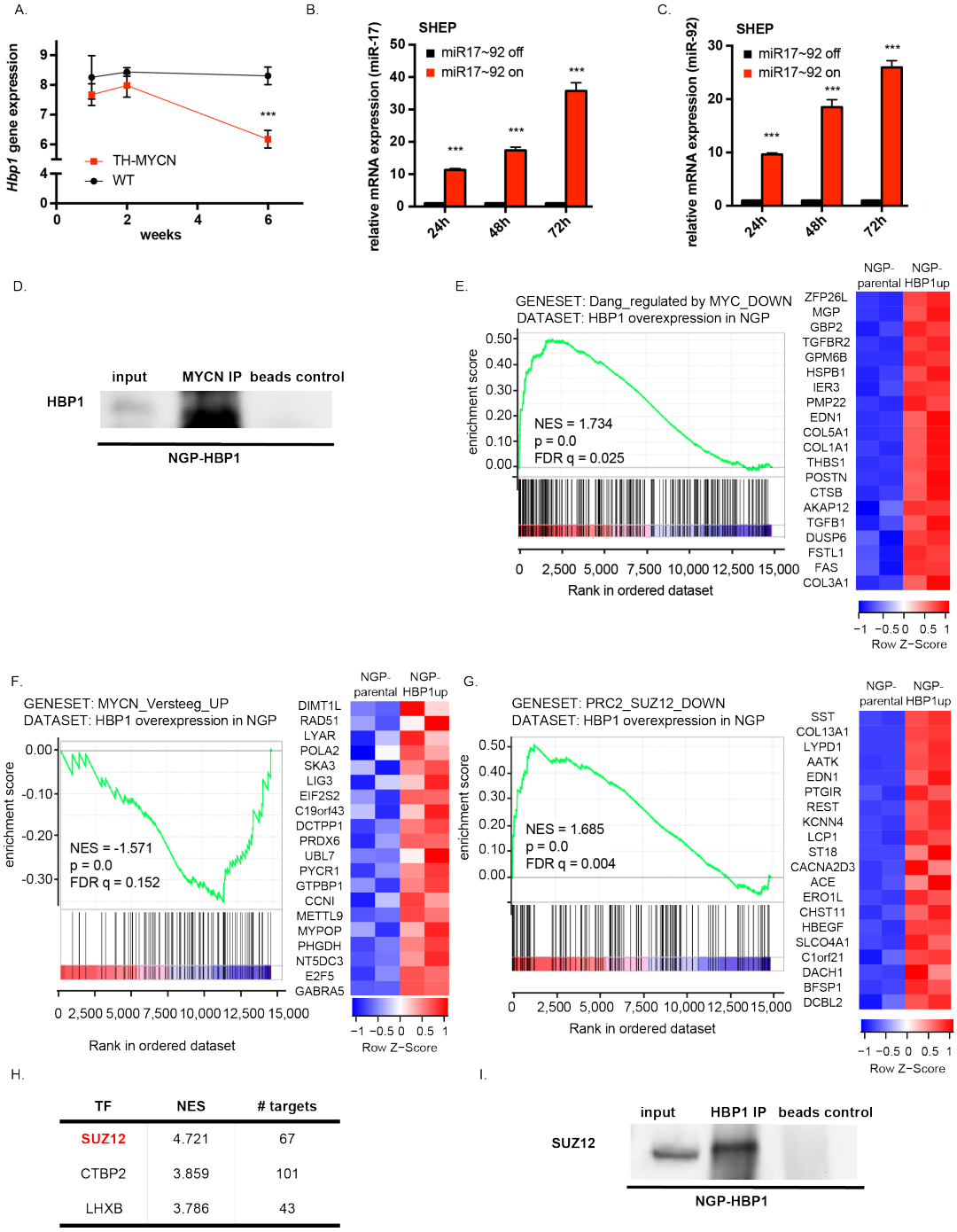

TF	NES	# targets
SUZ12	4.721	67
CTBP2	3.859	101
LHXB	3.786	43

Supplementary figure 2: HBP1 is negatively regulated by MYCN through the miR-17~92 miRNA cluster and represses MYCN activity.

A, Expression of *Hbp1* in normal ganglia and neuroblasts hyperplasia from 1 week, 2 weeks and 6 weeks old wild type or *Th-MYCN* mice. Data represent mean gene expression ± SD of 4 samples. **B and C,** *miR-17* (B) and *miR-92a1* (C) mRNA levels in SHEP cells treated with tetracycline (or ethanol as control) to induce the miR-17~92 cluster, expressed relative to the corresponding control. **D,** Co-immunoprecipitation between HBP1 and MYCN in NGP HBP1

cell line. **E,** GSEA for the MYC down geneset (Dang) in the HBP1 overexpression data and heatmap showing the leading edge (top 28 genes) of this geneset plotted in the HBP1 overexpression dataset. **F,** GSEA for the MYCN up geneset (Versteeg) in the HBP1 overexpression data and heatmap showing the leading edge (top 2O genes) of this geneset plotted in the HBP1 overexpression dataset. **G,** GSEA for the SUZ12 down geneset in the HBP1 overexpression data and heatmap showing the leading edge (top 22 genes) of this geneset plotted in the HBP1 overexpression dataset. **H,** Table showing top 3 results of the iRegulon analysis on the genes differentially downregulated upon HBP1 overexpression in NGP, enriched track ID SUZ12: WgEncodeSydhTfbsNt2d1Suz12UcdPh. **I,** Co-immunoprecipitation between HBP1 and SUZ12 in NGP HBP1 cell line.
Error bars represents mean gene expression ± SD of 4 samples (A) or mean ± SD of 3 biological replicates, each containing 2 technical replicates (B, C) and are calculated following error propagation. * $P < 0.05$, ** $P < 0.01$, *** $P < 0.001$

Supplementary figure 3

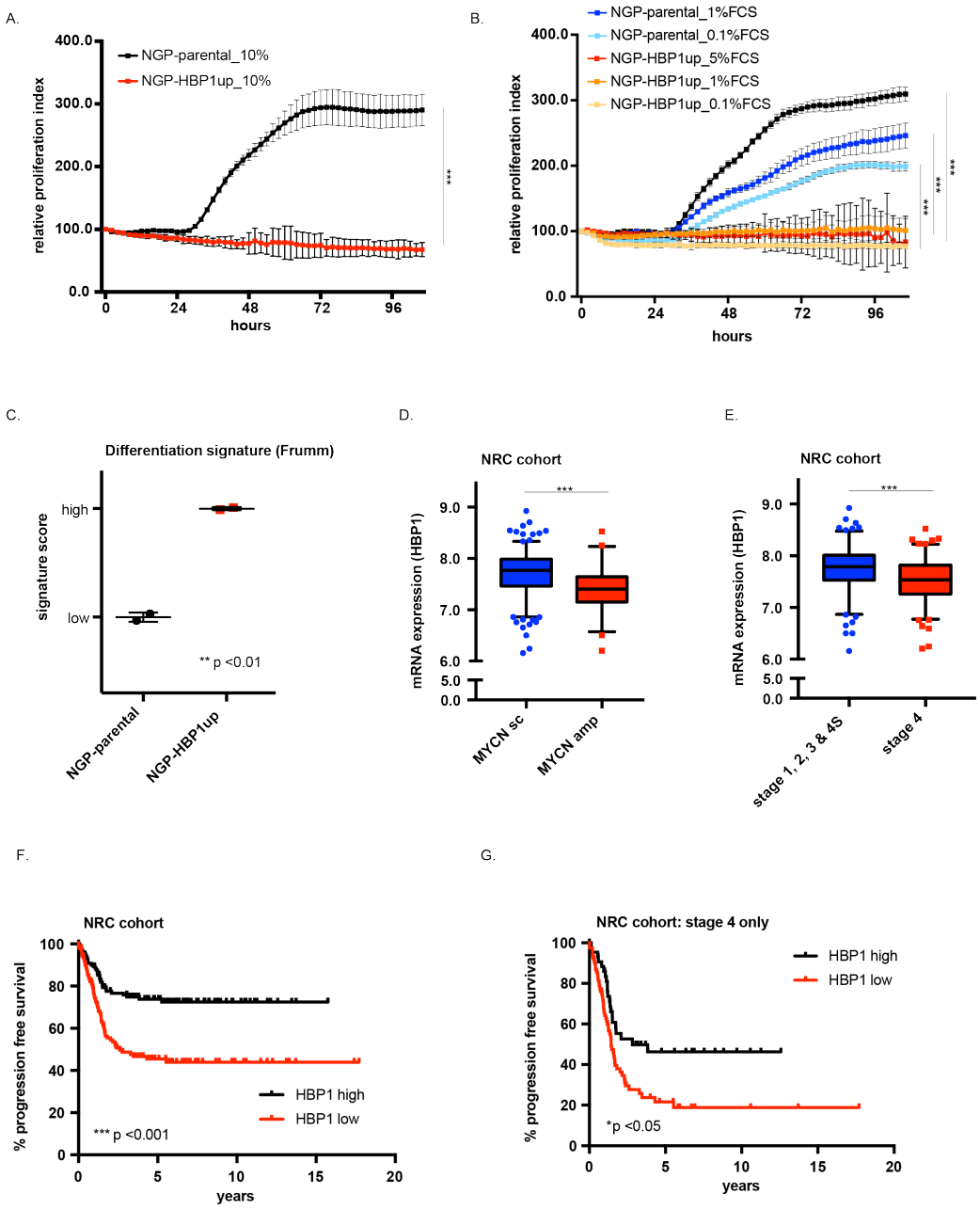

Supplementary figure 3: Increased HBP1 levels represses tumor aggressiveness

A and B, Cell proliferation index of NGP-parental cell line and the NGP cell line with stable HBP1 overexpression at the indicated time points with normal FBS percentages (A) or lower serum concentrations (B). **C,** The differentiation signature score in the parental and HBP1 overexpressing cell lines. **D,** *HBP1* expression in the cohort of 283 NB patients with MYCN amplified vs MYCN single copy tumors. **E,** *HBP1* expression in the cohort of 283 NB patients with low stage (stage 1, 2, 3 & 4S) vs high stage (stage 4) tumors. **F and G,** Kaplan Meier

plot showing percentage of event-free survival in patients with high or low *HBP1* expression in tumors of all stages (F) and only stage 4 tumors (G) in the cohort of 283 NB patients.
Error bars represents mean ± SD of at least 3 technical replicates (A, B), 2 biological replicates (C), while boxplots represent mean ± 95% confidence interval (D, E) and are calculated following error propagation. * $P < 0.05$, ** $P < 0.01$, *** $P < 0.001$

Supplementary figure 4

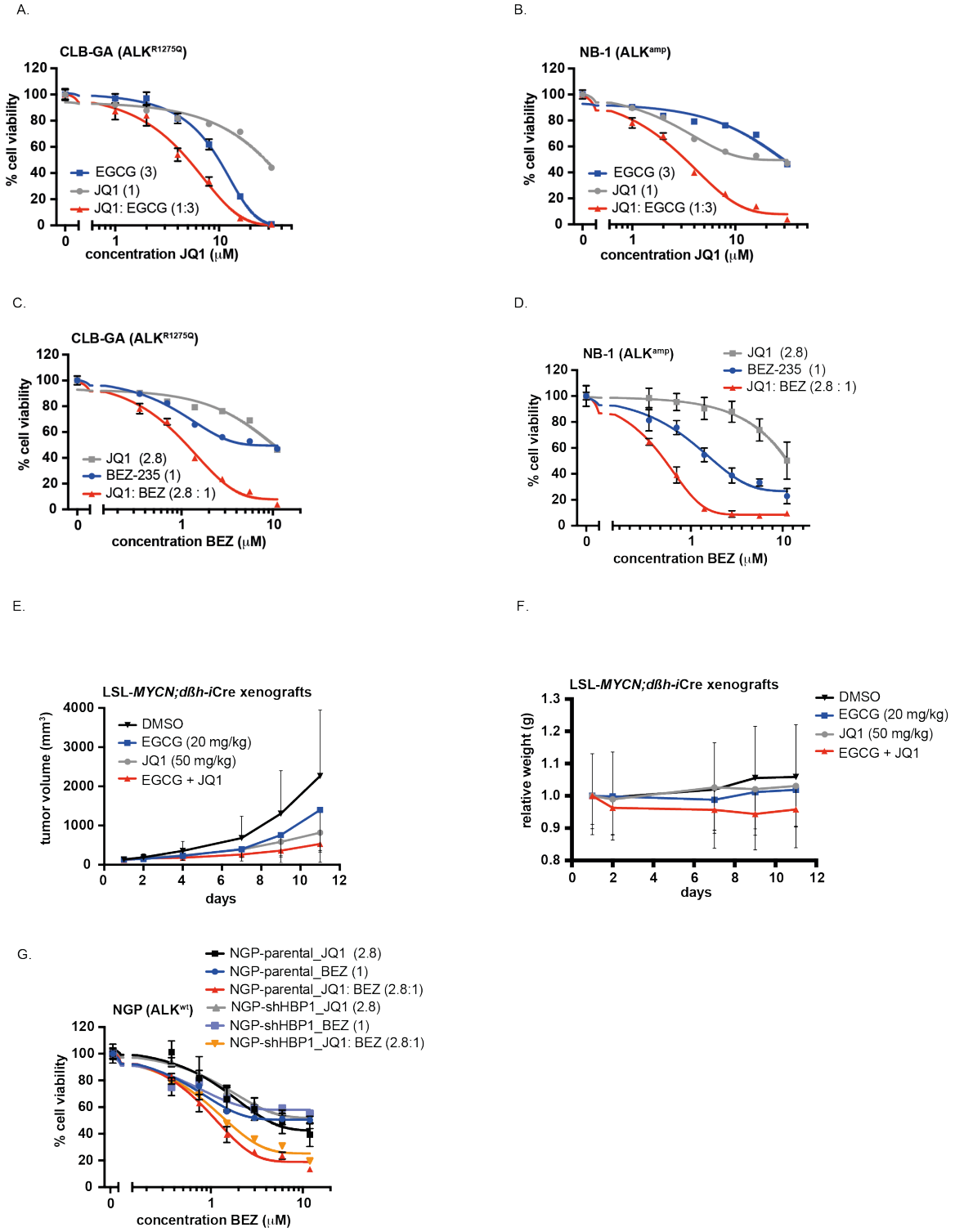

Supplementary figure 4: Combined pharmacological upregulation of HBP1 and repression of MYCN induces synergistic effects on tumor growth

A and B, Cell viability of the CLB-GA cell line (A) and the NB-1 cell line (B), showing the dose response curves of EGCG, JQ1 and the combination 48h after treatment. **C and D,** Cell viability of the CLB-GA cell line (C) and the NB-1 cell line (D), showing the dose response

curves of BEZ-235, JQ1 and the combination 48h after treatment. **E,** Plot showing tumor volume (mm3) of LSL-*MYCN;dßh-i*Cre grafted mice treated with DMSO, EGCG (20 mg/kg), JQ1 (50 mg/kg) or the combination, n = 7 mice/group. **F,** Plot showing the weight (g) of LSL-*MYCN;dßh-i*Cre grafted mice treated with DMSO, EGCG (20 mg/kg), JQ1 (50 mg/kg) or the combination, n = 7 mice/group. **G,** Cell viability of the NGP-parental and shHBP1, showing the dose response curves of BEZ-235, JQ1 and the combination 48h after treatment.
Error bars represents mean ± SD of at least 3 biological replicates, each consisting of 2 technical replicates (A, B, C, D, F) and are calculated following error propagation. * $P < 0.05$, ** $P < 0.01$, *** $P < 0.001$

Supplementary figure 5

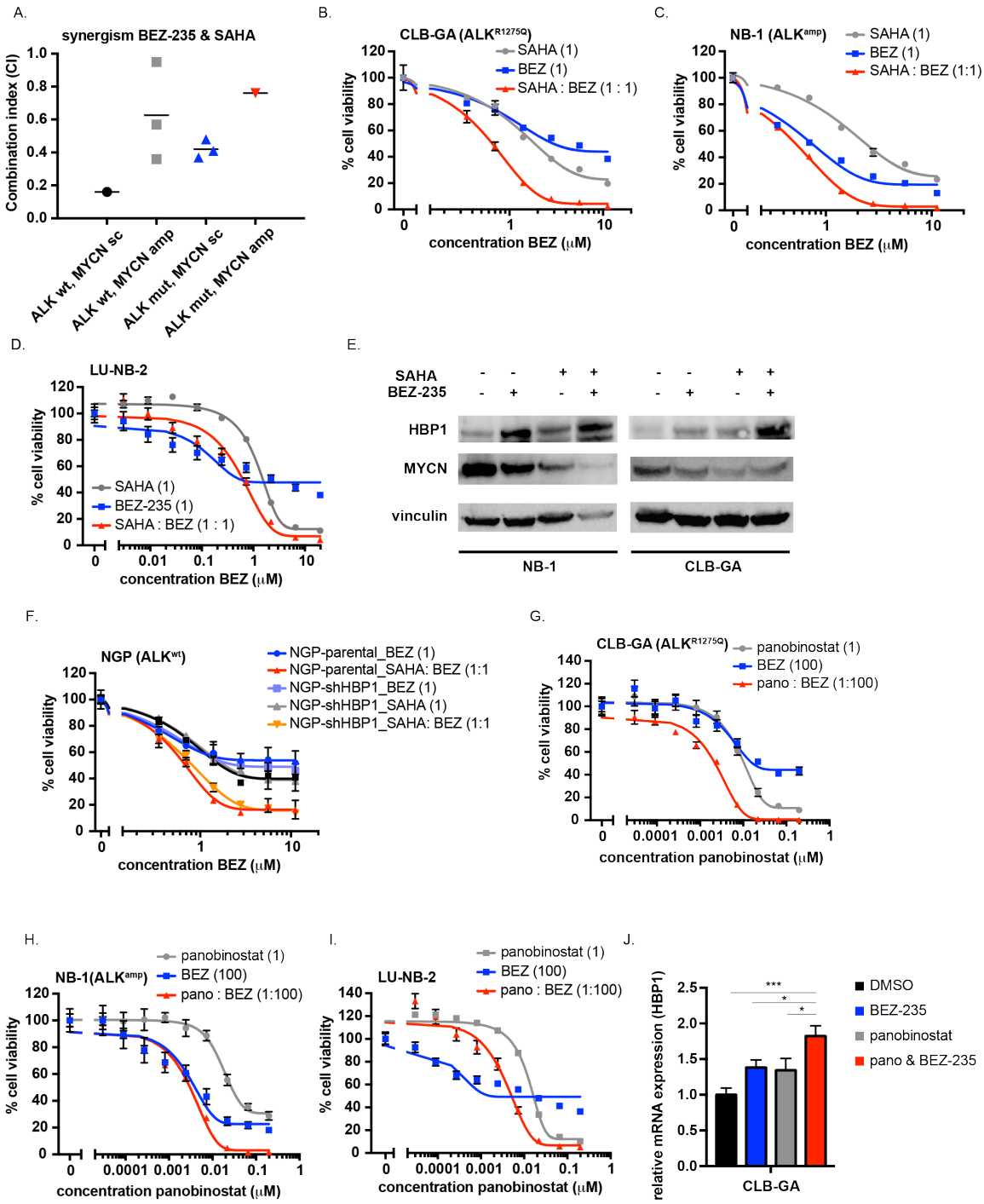

Supplementary figure 5: BEZ-235 induced HBP1 levels in combination with HDACi induces synergistic effects on tumor growth

A, CI-values at IC-50 of the BEZ-235 and SAHA combination, showing synergistic effect in a panel of 8 NB cell lines with different ALK and MYCN status. Synergy: CI < 1.0, additive: CI = 1.0, antagonism: CI > 1.0. **B and C,** Cell viability of the CLB-GA cell line (B) and the NB-1 cell line (C), showing the dose response curves of BEZ-235, SAHA and the combination 48h after treatment. **D,** Cell viability of the PDX-derived cell line LU-NB-2, showing the dose

response curves of BEZ-235, SAHA and the combination 48h after treatment. **E,** Western blot analysis showing HBP1 and MYCN protein levels 48h after treating NB-1 and CLB-GA with DMSO, 0.5 μM BEZ-235, 0.5 μM SAHA or the combination. **F,** Cell viability of the NGP-parental and shHBP1, showing the dose response curves of BEZ-235, SAHA and the combination 48h after treatment. **G and H,** Cell viability of the CLB-GA cell line (G) and the NB-1 cell line (H), showing the dose response curves of BEZ-235, panobinostat and the combination 48h after treatment. **I,** Cell viability of the PDX-derived cell line LU-NB-2, showing the dose response curves of BEZ-235, panobinostat and the combination 48h after treatment. **J,** *HBP1* mRNA levels in CLB-GA cells treated with DMSO, 0.243 μM BEZ-235, 0.00243 μM panobinostat or the combination for 48h, showed relative to the DMSO control. Error bars represents mean ± SD of at least 3 biological replicates, each consisting of 2 technical replicates (B, C, D, F, G, H, I) or of 2 technical replicates (J) and are calculated following error propagation. * $P < 0.05$, ** $P < 0.01$, *** $P < 0.001$

Part IV: discussion and future perspectives

Let us make our future now,
and let us make our dreams
tomorrow's reality.
~Malala Yousafzai~

Chapter 6 Discussion and future perspectives

ALK has become a subject of intensive neuroblastoma research since the discovery of constitutively activating mutations in its kinase domain in 2008 by several groups, including the teams at Ghent University [1–4]. Two important questions were addressed during my research project. The first aim was triggered by the availability of an FDA approved small molecule inhibitor targeting the kinase domain of ALK tested in other ALK-driven cancer entities, which accelerated the opening of phase 1 clinical trials in children with neuroblastoma [5,6]. At the time such trials were initiated, our knowledge of the oncogenic regulated networks and target genes downstream of ALK in neuroblastoma however was still incomplete. Given that resistant clones often emergence after initial successful treatment with small molecule inhibitors, ***I first focussed on more detailed dissection of ALK signaling*** in order to predict possible resistance mechanism and detect new vulnerable downstream targets. Next, several observations, including studies from the Ghent team [7, 8,9], provided evidence that the presence of ALK mutations could contribute to tumour aggressiveness, specifically in combination with MYCN amplification. Therefore, ***I exploited the ALK-driven transcriptome signature*** to identify novel ALK targets that could provide insight into the contribution of mutant ALK in tumour aggressiveness.

6.1 General discussion

6.1.1 Deciphering mutant ALK activated signaling in neuroblastoma cells

One of the primary aims of my thesis was to unravel the activated pathways downstream of mutated ALK in neuroblastoma. To this end, we established the ALK 77-gene signature, which captures the transcriptomic effects of pharmacological inhibition of ALK. This signature was generated through profiling of a panel of neuroblastoma cell lines with different ALK mutational status and was further validated in ALK-driven human and mouse tumours (paper 1) [10]. Previous knowledge of ALK downstream networks was mainly based on studies of the role of oncogenic ALK fusion proteins in non-small cell lung carcinoma (NSCLC) and anaplastic large cell lymphoma (ALCL), showing the involvement of different downstream pathways,

including the MAPK, PI_3K/mTOR, PLCγ, SHH, CRKl-C3G-RAP1, JAK-STAT and Jun pathways [11,12]. In neuroblastoma, PLCγ, SHH, CRKl-C3G-RAP1, JAK-STAT and Jun were not detected as downstream effectors of the signal, while we mainly observed ALK-driven MAPK, PI_3K/mTOR and MYC(N) signaling, in keeping with findings by others [1–4,9,13,14]. Differences in signaling pathways downstream of a given receptor can be explained by cellular context, the tumour type and the identity of the mutation or fusion partner of ALK [11,12].

The MAPK signaling axis is of particular importance in neuroblastoma tumorigenesis, given the observation that mutations in RAS/MAPK pathway components are enriched in relapsed cases [15]. More intriguingly, our ALK 77-gene signature [10] revealed that several MAPK negative regulators are downregulated upon pharmacological ALK inhibition, suggesting that the negative feedback will be abolished and the MAPK pathway may become re-activated. Therefore, we have tested the use of MAPK inhibitors in neuroblastoma cell lines with different ALK status. However, this treatment only resulted in modest changes in cell viability. Nevertheless, a combination of a compound targeting the MAPK pathway with an ALK inhibitor could be beneficial to keep the MAPK pathway repressed and in this way, circumvent relapse caused by MAPK activation. Moreover, recently, it has been shown that neuroblastoma cells without ERK phosphorylation were almost not sensitive to MEK inhibitors, while a significant growth inhibition and suppression of MYCN was observed in cells with ERK phosphorylation [16]. Moreover, a dual inhibitor of RAS and MEK results in more effective tumour suppression of neuroblastoma, since the upregulation of the negative feedback loop observed upon MEK inhibition alone is counteracted by the effect on RAS [16].

The activation of MYC(N) signaling is in line with previous findings and in keeping with the reported effects of activation of PI_3K-AKT-GSK3ß controlled MYCN protein stabilization and MAPK-ERK5 enhanced *MYCN* transcription [14,17–20]. Importantly, further exploration of the 77-gene signature allowed us to identify HBP1 as a mutant ALK downregulated gene implicated in yet another pathway driving MYCN activity (see further). In view of these novel findings, one could envision that combined treatments targeting MYCN activity, e.g. using ALK inhibitors in combination with BET or HDAC inhibitors, could act synergistically and offer novel venues for therapeutic

intervention in relapsed or ultra-high-risk patients with *ALK*^{mutant} and *MYCN*^{amplified} tumours.

Of further notice, we also detected ETV5, a member of the PEA3 family of ETS transcription factors and a known oncogene [21,22], as being upregulated by mutant ALK. ETV5 is involved in diverse cellular processes, including cell cycle control, proliferation and tissue remodelling and is involved in differentiation of neural crest progenitors [21–23]. Further studies by our team (not part of this thesis), recently showed that ETV5 contributes to proliferation and invasion of neuroblastoma cells, thus possibly explaining the increased incidence of ALK mutations in relapsed tumours [24] (Mus *et al.*, in preparation).

6.1.2 RET is regulated through the ALK-PI$_3$K-AKT-FOXO3a axis downstream of mutant ALK in neuroblastoma

We identified a mutant ALK-PI$_3$K-AKT-FOXO3a-RET signaling axis in neuroblastoma cells and a strong correlation between RET expression and our ALK 77-gene signature (paper 1) [10]. Furthermore, the 77 genes from the signature show the same response upon treatment with the RET inhibitor vandetanib as upon ALK inhibition, suggesting cross-talk between RET and ALK. This underscores our hypothesis that combining an ALK inhibitor with a RET inhibitor could synergistically shut down the involved pathways. Therefore, further dissection of the role of RET in neuroblastoma and more specifically in ALK signaling in neuroblastoma needs further investigation. Moreover, since ALK is necessary for proliferation of immature sympathetic neurons [25] and RET is needed for migration, proliferation, differentiation and survival of neural crest cells [26], the cross-talk between ALK and RET observed by us and the group of Janoueix-Lerosey [10,27] suggests that ALK mediates its effects on neuronal proliferation at least partly through RET.

6.1.3 MYCN activated genes are unexpectedly upregulated upon pharmacological ALK inhibition

To further unravel the dynamic transcriptional responses following ALK inhibition, we explored mRNA profiling data at different time points after drug admission in the neuroblastoma cell line CLB-GA carrying an ALK^{R1275Q} mutation (paper 2). First, we

confirmed the presence of PI_3K/mTOR, MAPK and MYC(N) signaling downstream of ALK, thus also validating the experimental setting. Next, we could show effects on the transcriptome as early as 1 to 2 hours after treatment with the ALK inhibitor TAE684. An intriguing and unexpected finding was the increase in genes activated by MYCN after 30 to 60 minutes (paper 2), before the overall MYCN activity goes down at 60 to 120 minutes as initially reported (paper 1) [10]. While interesting and intriguing, this result should be further investigated. At present, we can only speculate on the underlying mechanism for this observation. As depicted in figure A, several mechanisms are now known through which ALK impacts on MYCN activity. The current finding described in paper 2 could possibly be explained by a feedback mechanism that senses ALK inactivation and further transiently enhances the transcription or stabilisation of targets activated by MYCN, while leaving the MYCN repressed targets untouched. Moreover, this observation was only evaluated in one cell line, so additional analyses in other neuroblastoma cell lines and if possible, neuroblastoma tumours are necessary.

6.1.4 ALK wild type responders to pharmacological ALK inhibition

An interesting observation, which was not investigated in detail in this thesis, was the finding that not only mutant ALK, but also some ALK wild type neuroblastoma cell lines responded to the tested ALK inhibitors, showing effects on reduced survival and similar downstream transcriptional responses (paper 1, supplemental data 6; paper 3, figure 1 and supplementary figure 1). Moreover, it has been shown that wild type ALK can be oncogenic if a certain, critical threshold of ALK expression has been achieved [28]. Furthermore, several cell lines expressing the ALK wild type receptor express abundantly ALK on their cell surface [29]. The molecular basis of this finding is not completely understood, but could have important impact as it may increase the number of patients eligible to ALK inhibitor treatment as only 8-10% of patients present with ALK mutated tumours at diagnosis.

6.1.5 Resistance against ALK inhibitors

Despite an initial response to the ALK inhibitors, ultimately most if not all of the tumours will develop resistance, as also observed for other TKIs [30]. These resistance mechanisms can be classified in two major groups, namely ALK dominant or ALK

non-dominant mechanisms [31]. The ALK dominant mechanisms include secondary mutations and copy number gains or amplifications of the ALK gene. Indeed, new secondary mutations in the ALK gene have been reported in relapsed neuroblastoma cases [24]. ALK non-dominant resistance is caused by activation of bypass pathways, such as EGFR, KRAS, KIT, MET, IGF-1R, SRC and AXL [30–33]. Moreover, pharmacological resistance is caused by suboptimal exposure of the drug in the central nervous system (CNS) and is mainly observed upon treatment with the ALK inhibitor crizotinib due to low penetration through the blood-brain barrier (BBB) and high efflux by P-glycoprotein [30,32].

6.1.6 Newer ALK inhibitors

During the course of my investigation, several new next-generation ALK inhibitors have been developed [30]. Ceritinib or LDK378 is an ATP-competitive ALK inhibitor, which is more potent than crizotinib [30]. Moreover, this drug was shown to be efficient against most of the crizotinib resistance-mediating ALK mutations [30]. Furthermore, ceritinib was also active in cases with IGF1-R bypass activation [30].

Alectinib, another second-generation ALK inhibitor, also showed activity against most of the known resistance-mediating ALK mutations and more importantly, against CNS metastases [30]. Additionally, alectinib is also more effective than crizotinib in ALK inhibitor naive tumours [30]. Administration of this compound to neuroblastoma cells and xenografts resulted in apoptosis by blocking the ALK-mediated PI_3K-AKT-mTOR pathway [34]. Furthermore, survival of *Th-MYCN* mice receiving this compound was prolonged [34].

PF-06463922 or lorlatinib is a third next-generation ATP-competitive ALK inhibitor [30,32], showing dramatic tumour inhibition in xenografts and in the *Th-ALK^{F1174L}/MYCN* neuroblastoma mouse model [6]. Moreover, this inhibitor is more potent than the three above mentioned inhibitors (crizotinib, ceritinib and alectinib) against wild type ALK and is effective against all clinically relevant crizotinib-, ceritinib- and/or alectinib-resistant ALK mutations [6,32,35]. More importantly, this compound demonstrated superior anti-tumour activity against brain metastases compared to either crizotinib or alectinib [32], probably due to the enhanced potency of the compound and its increased ability to cross the BBB by avoiding transporter-mediated efflux [32].

6.1.7 *ADM*, earliest upregulated gene and a possible resistance mechanism upon ALK inhibition in neuroblastoma.

Next to the development of second- and third-generation ALK inhibitors, it is a priority to identify unknown resistance mechanisms. Therefore, we explored the dynamic transcriptional responses upon ALK inhibition and identified *ADM* as the first gene emerging as differentially upregulated following ALK inhibition as early as one hour after the treatment (paper 2). This finding was of particular interest given the known role of ADM in resistance to sunitinib in renal cancer [36]. Moreover, this gene is higher expressed during hypoxia [37–43], which is a known resistance mechanism against ALK inhibitors in NSCLC [44]. Therefore, we evaluated the combination of an adrenomedullin receptor antagonist (ADM22-52) [36] together with the ALK inhibitor TAE684 in a small panel of neuroblastoma cell lines, but in this experiment, no additional decreasing effects on cell viability were observed. Given that the neuroblastoma cell lines tested are already very sensitive to the ALK inhibitor, we propose that the combination should be tested in ALK inhibitor resistant neuroblastoma cells.

ADM upregulation could also reactivate the MYCN activity as ADM increases MAX levels [45], which will lead to more formation of MYC(N)-MAX heterodimers and higher MYC(N) activity. However, in a later phase, due to the steep ADM increase, MAX levels will become too high to complex with the present MYC(N) proteins leading to the formation of MAX-MAD complexes that will inhibit MYC(N)-MAX heterodimers, unless the MYC(N) proteins are upregulated by another mechanism. However, this hypothesis needs further investigation to see if MYCN activity is indeed influenced by *ADM* upregulation upon ALK inhibition in neuroblastoma cell lines or mouse models.

Taken together, monitoring of *ADM* levels during therapy in the context of emerging ALK inhibitor resistant subclones could be of interest. While repeated biopsies to this end are not possible, the use of liquid biopsies to this purpose could offer an interesting possibility for such monitoring [46]. Indeed, a simple blood sample can be used, as tumours shed tumour material into the blood, including circulating tumour cells (CTCs), circulating or cell-free tumour DNA (ctDNA) and tumour-derived exosomes [47]. Such liquid biopsies have a broad range of clinical applications, ranging

from screening and early detection of cancer to prognosis, detection of residual disease and identifications of therapeutic targets [48,49]. More importantly, they can be used for real-time monitoring of therapies in order to detect drug resistance and the mechanisms behind [48,49]. Moreover, for neuroblastoma, the detection of 17q gain in circulating DNA helps to define patient prognosis, optimize therapy stratification and provide more appropriate treatment [50]. Similarly, the detection of circulating *MYCN* DNA in peripheral blood is a valuable prognostic marker for neuroblastoma and can also be used as a non-invasive assay to follow-up patients with a higher risk for relapse [51]. Intriguingly, the sensitivity to determine *MYCN* DNA in serum depends on stage of disease, since higher levels of circulating *MYCN* DNA is found in patients with metastatic neuroblastoma compared with those with localized neuroblastoma, particularly those with low tumour burden [52]. Therefore, this assay may be particularly interesting for patients with stage 3 neuroblastoma and metastatic disease, for whom a wait and see strategy is currently recommended, to assess their *MYCN* status [52]. Additionally, ALK^{F1174L} and ALK^{R1275Q} hotspot mutations can be identified in patients with neuroblastoma by analysis of ctDNA from only 200 μl serum or plasma at diagnosis [53].

6.1.8 Mutant ALK downregulation of HBP1 is a fourth component of ALK controlled MYCN activity.

Given the existence of an ultra-high-risk group of neuroblastoma patients with tumours harbouring both *MYCN* amplification and ALK^{F1174L} mutation [7] and the observation that mouse and zebrafish models show accelerated tumour formation when both *MYCN* and ALK^{F1174L} are expressed in sympathetic neuronal progenitor cells [8,9], we looked for mechanisms explaining this cooperativity. Three ALK-driven regulatory mechanisms impacting on MYCN activity have been described. ALK increases the initiation of transcription activity of the promoter upstream of the *MYCN* gene [14] and regulates *MYCN* transcription level as well through the PI_3K-AKT-MEKK3-MEK5-ERK5 pathway [20], while ALK stabilizes MYCN protein levels through the PI_3K-AKT-GSK3β pathway [17–19] (Figure A).

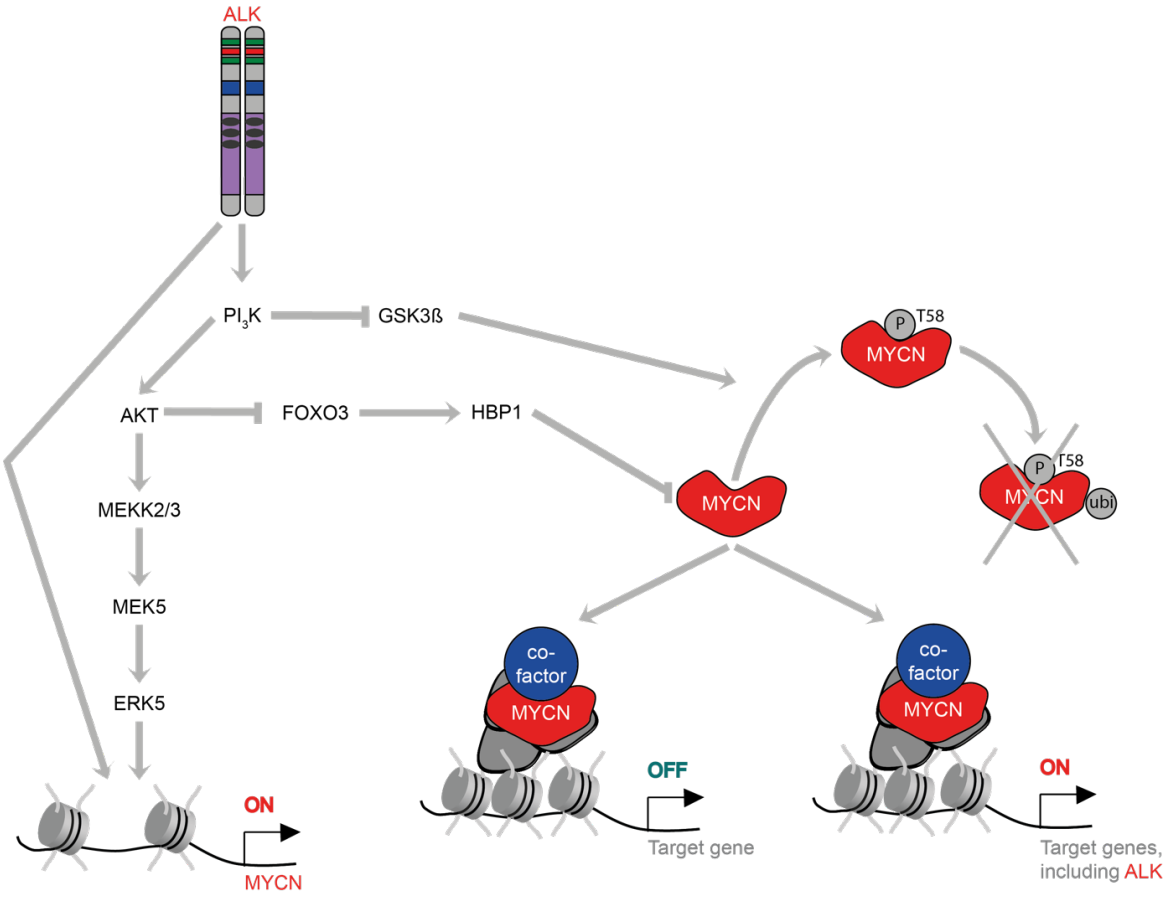

Figure A: mechanisms for cooperativity between ALK and MYCN.

Different mechanisms are found for the ALK and MYCN cooperativity in neuroblastoma. Firstly, ALK induces *MYCN* mRNA levels by increased transcriptional initiation of the *MYCN* gene. Secondly, ALK enhances MYCN protein levels through the PI_3K-AKT-GSK3β pathway. Thirdly, *MYCN* transcription is further boosted by the PI_3K-AKT-MEKK3-MEK5-ERK5 pathway. As fourth mechanism, ALK negatively controls HBP1, a MYCN repressor, through the PI_3K-AKT-FOXO3a axis. Moreover, MYCN itself enhances *ALK* transcription, creating a positive feedback loop. Figure adapted from [14,17–20].

Exploration of the ALK 77-gene signature [10] revealed HBP1, a known negative regulator of c-MYC and MYCN [54,55] and was therefore thoroughly investigated in the context of neuroblastoma (paper 3). We first confirmed that HBP1 was negatively regulated by ALK through the PI_3K-AKT-FOXO3a pathway. More importantly, we could confirm in neuroblastoma that HBP1 represses MYCN activity. Surprisingly, HBP1 inhibits both the repressor as activator function of MYCN, since MYCN repressed genes were upregulated, while MYCN activated targets became downregulated upon HBP1 overexpression in neuroblastoma cells. Moreover, MYCN itself negatively regulates HBP1 by inducing the miR-17~92 cluster.

We therefore identified a fourth and important new mechanism for the ALK-MYCN cooperativity (Figure A). Further studies, including chromatin immunoprecipitation followed by sequencing (ChIP-seq) in neuroblastoma cells with regulable HBP1 constructs could shed more light onto how and with which MYCN target genes HBP1 interacts and to understand the role of the PRC2 complex in this regulation.

6.1.9 MYCN targeting, drugging the undruggable?

Several research groups have focused on finding ways to reduce MYCN levels and activity in neuroblastoma, giving its role as main oncogenic driver. However, as mentioned in the introduction, directly targeting MYCN has long been difficult and alternative ways to negatively regulate MYCN activity are therefore necessary. Based on our observations that HBP1 negatively impacts the dual MYCN activity, we therefore looked for drugs regulating HBP1 levels to use as single compound or in combinations with other drugs to decrease MYCN levels.

As tool compound, we selected the green tea component EGCG, as it was shown to increase *HBP1* mRNA stability in order to block the WNT pathway in breast cancer [56]. Therefore, we verified the effect of EGCG on *HBP1* and cell viability in neuroblastoma and indeed, we could confirm *HBP1* upregulation and a decrease in cell viability upon EGCG administration. Moreover, the combination of this compound together with JQ1, a BET inhibitor that negatively impacts MYCN levels, further decreased cell viability as well as MYCN expression and activity.

However, the effect of EGCG is not only caused by HBP1 upregulation, as this green tea component targets many additional genes and pathways. EGCG can have antiproliferative, anti-mutagenic, antioxidant, antibacterial, antiviral and chemo-preventive effects [57,58], through regulating the JAK-STAT, MAPK, PI_3K-AKT, WNT, Notch, NF-κB and AP-1 pathways [57,58]. Moreover, EGCG induces the tumour suppressive genes p53, p21, p16 and RB1 [57,58]. Furthermore, EGCG induces epigenetic changes, by inhibiting DNMT1 and RNA polymerase III, by modulating hTERT activity and by repressing promoter methylation of *p16* and *p15* [57,58]. Moreover, in breast cancer and NSCLC, EGCG suppresses angiogenesis by

inhibiting HIF1α [59,60]. EGCG can also be used as therapeutic adjuvant, as it enhances 5-fluorouracil–chemosensitivity in colorectal cancer [61].
More importantly, in the context of neuroblastoma, EGCG treatment results in a dose-dependent decrease in cell proliferation, an increase in apoptosis and a complete inhibition of sphere formation [62]. Moreover, the addition of EGCG to neuroblastoma cells results in a decrease in cell viability and induction of cell death by blocking GRP78 [63], one of the other interesting genes of our ALK 77-gene signature. Moreover, the effects of EGCG can be enhanced in neuroblastoma by overexpression of miR-7-1 [64] or by knockdown of BIRC5 [65].
Next to these anti-carcinogenic effects, EGCG has neuroprotective effects, showing promising results as dietary supplement for Alzheimer Disease [66,67].
In summary, EGCG has a lot of benefits for your health, but response depends on the levels achieved in plasma and tissue [68].

Nevertheless, to confirm that the effects of EGCG on neuroblastoma cell viability and MYCN activity are partly caused by upregulation of HBP1, we tested a more specific, clinically relevant compound, namely the dual PI_3K/mTOR inhibitor BEZ-235, based on our observation of the existence of the PI_3K-AKT-FOXO3a-HBP1 axis in neuroblastoma. Indeed, we were able to confirm the upregulation of HBP1 and the simultaneously decrease in MYCN activity and cell viability. However, BEZ-235 not only causes a decrease in MYCN activity through HBP1, but destabilises as well MYCN proteins through upregulating GSK3β and *MYCN* transcription via repressing the PI_3K-AKT-MEKK3-MEK5-ERK5 pathway [14,17–20]. Nevertheless, knockdown of HBP1 partly rescued the effect on cell viability observed upon the combination, confirming that at least a part of the effect is caused by upregulating HBP1 levels.

6.2 Future perspectives

6.2.1 Digging deeper into ALK signaling

While I was able to discover several important novel translationally relevant findings in relation to ALK signaling in neuroblastoma cells, this work also represents a step towards further investigations in relation to mutant ALK in neuroblastoma cells.

First, as the ligand for ALK was not known when we started our study, we made use of ALK inhibitors and ALK stimulation using monoclonal antibodies to a lesser extent [69–71]. Given the availability of the ALK ligands [72,73], it is now possible to study the dynamic regulation of ALK signaling upon activation as was previously reported for e.g. EGFR [74,75]. Such studies indeed revealed transcriptional waves following RTK activation (Figure B) [74,75]. Upon binding of the ligand and the subsequent activation of the receptor, the first wave observed consists of the immediate turnover of the immediately downregulated microRNAs (ID-miRs). The targets of these ID-miRs are the immediate early genes (IEGs). Therefore, upon degradation of these ID-miRs, the expression of the IEGs will increase. Subsequently, these IEGs are responsible for the transcription of the third wave, the delayed early genes (DEGs), which will cause a decrease in expression of the IEGs. The latest group that is activated, harbours the secondary response genes (SRG), which are responsible for the phenotypic outcome [74,75].

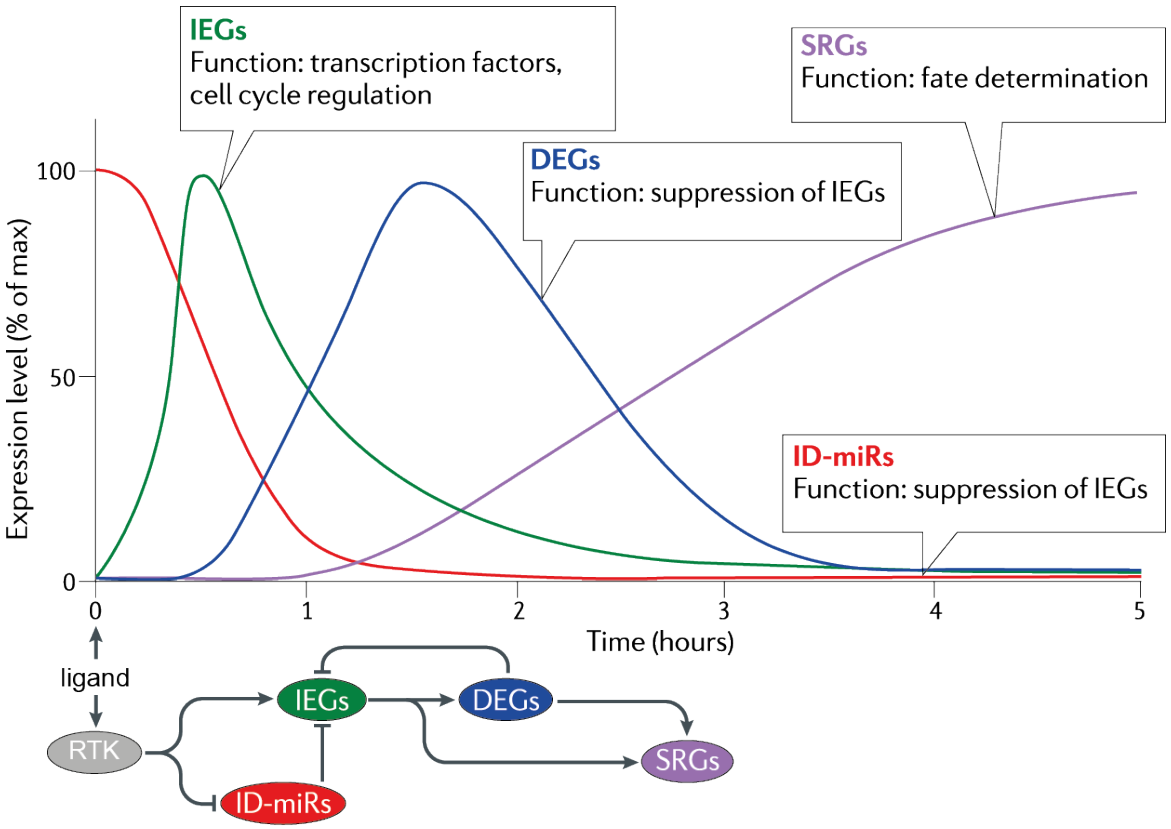

Figure B: transcriptional waves upon RTK activation.

First, a set of miRNAs are immediately downregulated (immediately downregulated miRNAs or ID-miRs), which subsequently causes an increase in the immediate early genes (IEGs). This is followed by transcription of the delayed early genes (DEGs). As last group, the secondary response genes (SRGs) are activated. Figure adapted from [74,75].

In our study, we also discovered response to ALK inhibitors in neuroblastoma cell lines expressing wild type ALK (so called responders). This is potentially important given that we described a prognostic significance for the 77-gene signature in a cohort of patients with primary neuroblastoma. This suggests that in certain tumours with wild type ALK, downstream signaling is active and that such patients could possibly benefit from ALK inhibitors.

Further, in our studies, we investigated protein coding mRNAs and did not explore in-depth the noncoding transcriptome. As shown by the host lab and other teams, noncoding RNAs including microRNAs (miRNAs) and long noncoding RNAs (lncRNAs) are also important effectors downstream of various signaling pathways.

Therefore, further studies investigating the “dark side” of the genome could reveal further important novel findings in the context of ALK.

As referred to in the introduction, RTKs transduce extracellular signals through a cascade of phosphorylation events, which finally elicit effects on gene expression. Therefore, a thorough investigation of the phospho-proteomic and proteomic landscape is necessary. During my PhD thesis, I participated in an EU project, ASSET, of which part aimed at deciphering ALK downstream effects on phosphorylation using quantitative mass spectrometry-based proteomics in collaboration with the Olson lab (Denmark). To this end, I fine-tuned the experimental set-up, using the neuroblastoma cell line NB-1 (harbouring amplification of full-length ALK) and selected a time point at 30 minutes after compound administration with three ALK inhibitors TAE684, crizotinib and LDK378 (Emdal K.B. *et al*., Science Signaling, submitted). By this strategy, four signaling layers were investigated: interactome, phosphotyrosine-interactome, phospho-proteome and proteome. In this way, we created a multi-layered proteomic resource of aberrant ALK signaling in neuroblastoma. Moreover, through this study, IRS2 was identified as a new immediate downstream transmitter, linking ALK to the PI_3K-AKT-FOXO3 axis. Additionally, we integrated our transcriptomic data with the phospho-proteomic data in the NB-1 cell line to find differentially phosphorylated transcription factors with targets enriched in the up- or downregulated genes after ALK inhibition (unpublished data). This analysis showed that differentially phosphorylated FOXO3 and CDC5L have enriched target genes in the upregulated genes, while the downregulated genes are enriched for the targets of the differentially phosphorylated CIC, ERF and ETV3. Moreover, MYC(N), MAZ, MEIS1 and JUN are differentially phosphorylated and have targets both in the up- and downregulated genes. Moreover, targets from the transcription factor HBP1, which is not differentially phosphorylated, but transcriptionally upregulated, are strongly enriched in the genes downregulated upon ALK inhibition.

6.2.2 New emerging therapeutic strategies for patients with high-risk or relapsed neuroblastoma

In this thesis, we mainly focused on the use of small molecule inhibitors against ALK or his downstream pathways. However, additional strategies exist to target a RTK.
First of all, as discussed in the introduction, monoclonal antibodies directed against the extracellular domain have been developed targeting several RTKs. In 2005, Moog-Lutz *and colleagues* [69] have tested several activating and inhibiting monoclonal antibodies against the ALK receptor. The activating ones, mAb46 and mAb48 induce activation through dimerization, while the inactivating one, mAb30, blocks the receptor in an inactive state by dimerization [69]. However, already 6 hours after exposure to these monoclonal antibodies, they monitored a slight decrease in the effect on phosphorylated ERK [69], maybe explaining why these monoclonal antibodies are not used in the clinic. Moreover, we have not used the inactivating monoclonal antibody, because we wanted to discover the affected downstream pathways and the possible resistance mechanisms, specific for small molecule inhibition of ALK.
Secondly, antisense oligonucleotides, which are designed to interact with mRNA to reduce expression of the targeted RNA, are made to target EGFR, VEGFR, IGF-1R and TGF-αR [76,77]. However, the molecules need to pass through the cell membrane of their targeted cell to fulfil their action, which is often difficult with the current safe delivery strategies [78]. Moreover, until today, these are not used to target ALK.

Furthermore, as nicely reviewed by Brodeur *and colleagues* [79], several additional, potential targets in neuroblastoma exist, which can be classified in four categories: (1) genes activated by mutation, amplification, translocation or overexpression, (2) genes inactivated by deletion, mutation or epigenetic silencing, (3) membrane-molecules selectively expressed on most neuroblastoma tumours and (4) targets common to neuroblastoma and other cancers (Figure C).

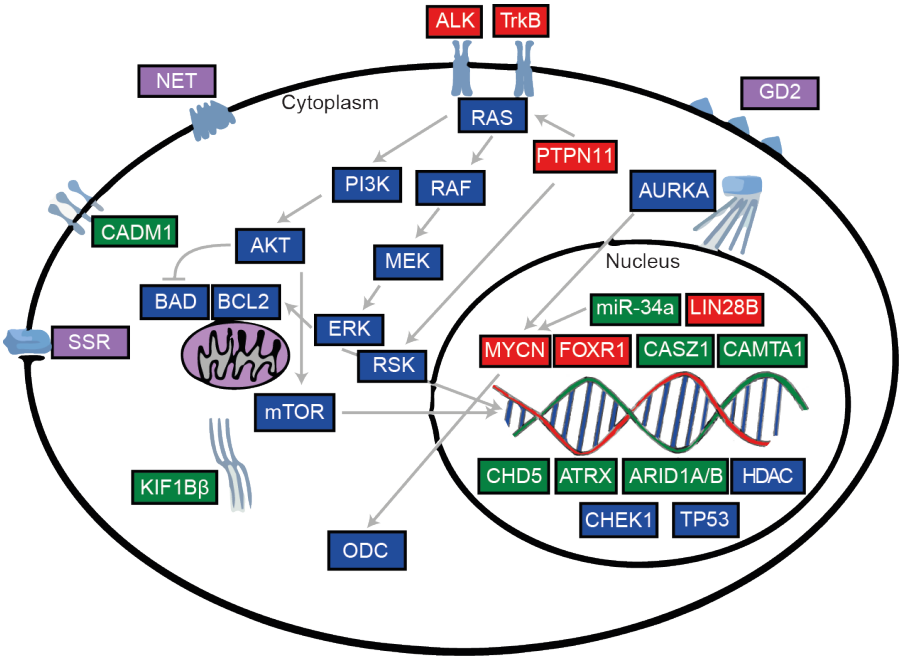

Figure C: Targets for precision therapy in neuroblastoma.

Scheme showing the intracellular location of therapeutic targets in neuroblastoma. Activated genes and their proteins are depicted in red, while inactivated ones are shown in green. Proteins expressed selectively on the membrane of neuroblastoma cells are in purple, while targets common to neuroblastoma and other cancers are depicted in blue. Figure adapted from [79].

Indeed, as detailed summarised by Castel *and colleagues* in 2014 [80] and by Berlanga *and colleagues* in 2017 [81], several inhibitors against these potential targets are tested as single compound or in combination with other agents in preclinical and clinical phases to treat neuroblastoma patients, with the main focus on high-risk neuroblastoma. Amongst these are second- and third-generation ALK inhibitors, mTOR as well as AKT inhibitors, HDAC inhibitors including SAHA or vorinostat, Aurora A and EGFR inhibitors, ODC1 inactivators, angiogenesis and proteasome repressors [80,81].

Moreover, recent research confirmed the effectiveness of PARP inhibitors alone and in combination with CHK1 targeted therapy in MYCN-driven neuroblastoma [82]. Additionally, histone demethylases inhibitors repress MYCN signaling simultaneously with oxidative phosphorylation, resulting in a decrease in cell viability and in tumour growth and an increase in differentiation in MYCN-driven neuroblastoma [83]. Furthermore, the use of compounds targeting PHOX2B expression resulted in more apoptosis and less proliferation of neuroblastoma cells, suggesting that these

compounds could be beneficial for neuroblastoma patients [84]. Moreover, components of the Rho/Rac signaling cascade, important for migration and differentiation of neural crest cells, are mutated in neuroblastoma tumours [85]. Further research showed that inhibitors of ROCK2, a kinase involved in this pathway, induced differentiation of neuroblastoma cells, while repressing migration, cell growth and invasion [85]. Moreover, this effect is caused by inhibiting GSK3β-dependent MYCN phosphorylation [85].

Further research has also focused on finding the appropriate single drug that binds to multiple proteins or the perfect combination of highly selective inhibitors in order to target the tumour cell at multiple levels. In this way, they hope to simultaneously circumvent the resistance rapidly occurring against drugs targeting only one molecule [77]. In this way, sorafinib, a multikinase inhibitor, has been identified to be effective as antiproliferative and anti-angiogenesis molecule and is currently evaluated in a phase I trial in combination with cyclophosphamide and topotecan [81]. Moreover, the p53 tumour suppressor is mostly non-mutated in neuroblastoma. However, amplification and increased expression of MDM2, which interacts with p53 to inactivate the tumour suppressor, and suppression of CDKN2A, which is an inactivator of MDM2, are frequently observed in neuroblastoma [86]. Therefore, the combination of a MDM2 inhibitor with a BLC2 inhibitor was evaluated and resulted in a highly synergistic increase in apoptosis in a panel of neuroblastoma cell lines and in orthotopic neuroblastoma xenografts [86]. Simultaneously, another group have combined such MDM2 antagonists together with mTORC1 inhibitors [87]. This combination also caused synergistic inhibition of tumour growth in p53 wild type neuroblastoma [87].

An important challenge given the rapidly growing number of molecular targets in neuroblastoma is to translate the preclinical findings into the clinic through initial phase I studies to determine undesired effects and critical doses [88]. This requires careful coordination through international collaborative studies e.g. under supervision of SIOPEN or COG. Disappointingly, the overall average rate of successful translation from animal models to clinical cancer trials is less than 8% [89]. Such failure could be caused by an inappropriate design of the clinical trial and thus better designs should be pursued in the future [90]. Moreover, crucial genetic, molecular, immunologic and cellular differences between humans and mice prevent the successful translation [90]. An important issue here is that genetic heterogeneity is

difficult to model in animals [90]. Thus, ideally, the compound or the combination should be tested in multiple animals, with different ages and diverse genetic backgrounds, better mimicking the human situation [90]. Additionally, the laboratory environment can cause stress, which will have a significant effect on experimental results [89]. Currently, these confounding issues are under evaluation by the ITCC consortium (http://www.itcc-consortium.org/about-itcc.php), which aims to carefully select novel drug targets on one hand and tries to accelerate phase I studies on the other hand. Only by a thoroughly investigation and properly designed clinical trials [89,90], new treatments can be found that are more effective and less toxic on short- and long-term, resulting in better survival and higher quality of life.

Next to the development of targeted therapy, major advances have been made in immunotherapy. Different strategies of immunotherapy exist to amplify the existent anti-tumour immune response or to induce anti-tumour immune response [91]. One way is by using monoclonal antibodies against antigens specific for the tumour cells, such as ch14.18 to target GD2 on neuroblastoma cells [79,91,92]. This anti-GD2 monoclonal antibody therapy demonstrated promising effects in high-risk neuroblastoma, suggesting it should be considered to be included in frontline therapy for patients with such high-risk tumours [91]. Moreover, such monoclonal antibodies can be conjugated to toxins or drugs to specifically kill the tumour cells [91]. Additionally, bispecific antibodies activate a receptor on an immune effector cell, while recognizing an antigen on the tumour cell [91]. However, since anti-GD2 therapy is toxic due to the presence of GD2 on noci-receptor-containing peripheral nerves, the search for new immunotherapeutic targets is urgently needed [93]. By searching for genes encoding proteins with extracellular domains, that are differentially expressed on neuroblastoma compared to normal tissues, GPC2 has been identified as a promising new immunotherapeutic target [93]. Indeed, cellular cytotoxicity was observed in neuroblastoma cells *in vitro* upon treatment with a GPC2 targeting antibody-drug conjugate [93]. Moreover, *in vivo* administration to neuroblastoma mouse models improved their survival [93]. Another strategy is to reactivate the T cells present in and around the tumour by using immune checkpoint inhibitors [91,94]. They block cell surface molecules like CTLA4 and PD-1, which are expressed on the T cells and transmit inhibitory signals [91,94]. A third method are the tumour vaccines, targeting the defined tumour antigens [91]. Several studies are ongoing in children, but first results

show that these tumour vaccines are safe to administer, but tumour regression is rarely observed [91]. Chimeric antigen receptor T-cells (CAR-Ts) represent another strategy. T-cells are expanded *ex vivo* and genetically engineered, so that they express the CAR on their surface. These CARs will recognize the antigens on the targeted tumour cells and the T-cells can kill them [91,92].
Moreover, the combination of such immunotherapy and molecularly targeted agents represent a new strategy to treat these patients. Recently, the combination of melphalan, a chemotherapeutic used to treat high-risk neuroblastoma, with BSO, a glutathione synthesis inhibitor, was investigated in patients with recurrent/refractory high-risk neuroblastoma, showing good responses in this subgroup of patients, even after extensive prior therapy [95]. However, such combinations need further investigation to evaluate the survival and the durability of responses [94].

6.2.3 New kids on the block: epigenetics and single cell analysis

Recent papers have described core regulatory circuits controlling (two) different phenotypes present within neuroblastoma tumours cells [96,97]. These core regulatory circuits are controlled by super-enhancer marked transcription factors and other key genes implicated in neuroblastoma biology, such as ALK. In view of this finding and given that epigenetic mutations are amongst the most common genetic alterations in cancer, further dissection of the epigenetic control of normal sympathetic nervous development and key events leading to neuroblastoma development will be of utmost importance. As part of these investigations, further study of ALK in these processes in the context of epigenetics should be performed in order to further complete the complex picture of deregulated gene regulatory and signaling pathways in neuroblastoma.

Bulk analysis methods, such as the microarray and RNA sequencing approaches applied in this thesis, capture a global picture of the entire tumour sample. However, it has long been known that tumours are heterogeneous subpopulations of cells at the phenotypic and (epi)genomic level [46,98]. Indeed, a tumour is a complex ecosystem, with interaction between the malignant cells and their microenvironment, including amongst others the immune, epithelial and stromal cells [99]. This intra-tumour heterogeneity has an impact on tumour progression, metastasis, response

and relapse [98,100], as this is the underlying driving force for selection of therapy resistant cancer cells leading to relapse and often death of the patient [98]. For long, this has represented a major challenge in cancer research towards deeper understanding of tumour behaviour. Until recently, single cell analyses were limited due to the lack of appropriate methodology and equipment [46,101,102].This picture is now rapidly changing with recent introduction of new procedures for the study of genome, methylome, transcriptome and even protein analysis at single cell level [46,101].

Yet another challenge is spatial tumour heterogeneity with differences between different sites in the tumour or between a primary tumour and his metastasis [103]. Another spectacular recent technical evolution that can yield insights into this spatial tumour heterogeneity is the study of liquid biopsies which may yield a more broader picture of genomic tumour features. Moreover, liquid biopsies also offer a powerful option for the study of cancer progression, therapy response and resistance, either through the analysis of circulating DNA, RNA or even single circulating tumour cells [48]. As a prelude to the power of this methodology, the host lab explored liquid biopsy analysis for detection of copy number alterations at diagnosis [104] and Chicard *and colleagues* showed that genomic copy number profiling using ctDNA highlights heterogeneity in neuroblastoma [103]. Moreover, deep sequencing of neuroblastoma tumours showed the existence of subclonal ALK mutations at diagnosis [105] and the mutational difference between tumours at diagnosis and relapse [15,106]. Given the success of these early studies, it can be assumed that further exploration of the power of liquid biopsies will have great impact on the study of tumour heterogeneity and tumour follow-up in neuroblastoma.

6.3 Concluding remarks

ALK mutations represented a major new finding in the understanding of the biology of neuroblastoma when I started this thesis. I was able to make substantial contributions to novel insights into ALK, helping to better understand neuroblastoma biology and offering new venues for therapeutic interventions. During this thesis, novel discoveries in the study of neuroblastoma have significantly increased our understanding of neuroblastoma, but also raise new questions. The emergence of novel drug targets has initiated initiatives for precision medicine in several countries

and has spurred discussion towards selecting drug combinations for inclusion into phase 1 clinical trials, e.g. as part of the ITCC initiative (http://www.itcc-consortium.org/about-itcc.php), in which the host lab is participating. Moreover, immunotherapy is rapidly changing the face of contemporary cancer treatment and has also been introduced for neuroblastoma. Together with our contributions in this field and the many ongoing research collaborations worldwide, we can be hopeful, that, like for childhood leukaemia, we can dramatically increase survival rates for neuroblastoma patients in the near future and reduce toxic short- and long-time effects to save lives and increase quality of life for children surviving neuroblastoma.

6.4 References:

1. Mossé, Y. *et al.* Identification of ALK as a major familial neuroblastoma predisposition gene. *Nature* **455,** 930–935 (2008).
2. George, R. *et al.* Activating mutations in ALK provide a therapeutic target in neuroblastoma. *Cah Rev The* **455,** 975–978 (2008).
3. Chen, Y. *et al.* Oncogenic mutations of ALK kinase in neuroblastoma. *Cah Rev The* **455,** 971–974 (2008).
4. Janoueix-Lerosey, I. *et al.* Somatic and germline activating mutations of the ALK kinase receptor in neuroblastoma. *Cah Rev The* **455,** 967–970 (2008).
5. Carpenter, E. L. & Mossé, Y. P. Targeting ALK in neuroblastoma--preclinical and clinical advancements. *Nat Rev Clin Oncol* **9,** 391–9 (2012).
6. Guan *et al.* The ALK inhibitor PF-06463922 is effective as a single agent in neuroblastoma driven by expression of ALK and MYCN. *Dis Model Mech* **9,** 941–952 (2016).
7. De Brouwer, S. *et al.* Meta-analysis of Neuroblastomas Reveals a Skewed ALK Mutation Spectrum in Tumors with MYCN Amplification. *Clinical Cancer Research* **16,** 4353–4362 (2010).
8. Zhu, S. *et al.* Activated ALK Collaborates with MYCN in Neuroblastoma Pathogenesis. *Cancer Cell* **21,** 362–373 (2012).
9. Berry, T. *et al.* The ALKF1174L Mutation Potentiates the Oncogenic Activity of MYCN in Neuroblastoma. *Cancer Cell* **22,** 117–130 (2012).
10. Lambertz, I. *et al.* Upregulation of MAPK Negative Feedback Regulators and RET in Mutant ALK Neuroblastoma: Implications for Targeted Treatment. *Clin. Cancer Res.* **21,** 3327–39 (2015).
11. Hallberg & Palmer. The role of the ALK receptor in cancer biology. *Ann Oncol Official J European Soc Medical Oncol Esmo* **27 Suppl 3,** iii4–iii15 (2016).
12. Hallberg, B. & Palmer, R. Mechanistic insight into ALK receptor tyrosine kinase in human cancer biology. *Nature Reviews Cancer* **13,** 685–700 (2013).
13. Heukamp, L. *et al.* Targeted Expression of Mutated ALK Induces Neuroblastoma in Transgenic Mice. *Sci Transl Medicine* **4,** 141ra91–141ra91 (2012).
14. Schönherr, C. *et al.* Anaplastic Lymphoma Kinase (ALK) regulates initiation of transcription of MYCN in neuroblastoma cells. *Oncogene* **31,** 5193–5200 (2012).
15. Eleveld, T. F. *et al.* Relapsed neuroblastomas show frequent RAS-MAPK pathway

mutations. *Nat. Genet.* **47,** 864–71 (2015).
16. Tanaka, T. *et al.* MEK inhibitors as a novel therapy for neuroblastoma: Their in vitro effects and predicting their efficacy. *J Pediatr Surg* **51,** 2074–2079 (2016).
17. Chesler, L. *et al.* Inhibition of phosphatidylinositol 3-kinase destabilizes Mycn protein and blocks malignant progression in neuroblastoma. *Cancer research* **66,** 8139–46 (2006).
18. Cage, T. A. *et al.* Downregulation of MYCN through PI3K Inhibition in Mouse Models of Pediatric Neural Cancer. *Front Oncol* **5,** 111 (2015).
19. Vaughan, L. *et al.* Inhibition of mTOR-kinase destabilizes MYCN and is a potential therapy for MYCN-dependent tumors. *Oncotarget* **7,** 57525–57544 (2016).
20. Umapathy, G. *et al.* The kinase ALK stimulates the kinase ERK5 to promote the expression of the oncogene MYCN in neuroblastoma. *Sci Signal* **7,** ra102–ra102 (2014).
21. Sizemore, G., Pitarresi, J., Balakrishnan, S. & Ostrowski, M. The ETS family of oncogenic transcription factors in solid tumours. *Nat Rev Cancer* **17,** 337–351 (2017).
22. Oh, S., Shin, S. & Janknecht, R. ETV1, 4 and 5: An oncogenic subfamily of ETS transcription factors. *Biochimica Et Biophysica Acta Bba - Rev Cancer* **1826,** 1–12 (2012).
23. Paratore, C., Brugnoli, G., Lee, H.-Y., Suter, U. & Sommer, L. The Role of the Ets Domain Transcription Factor Erm in Modulating Differentiation of Neural Crest Stem Cells. *Dev Biol* **250,** 168–180 (2002).
24. Schleiermacher, G. *et al.* Emergence of new ALK mutations at relapse of neuroblastoma. *J. Clin. Oncol.* **32,** 2727–34 (2014).
25. Reiff, T. *et al.* Midkine and Alk signaling in sympathetic neuron proliferation and neuroblastoma predisposition. *Development* **138,** 4699–4708 (2011).
26. Mulligan, L. RET revisited: expanding the oncogenic portfolio. *Nat Rev Cancer* **14,** nrc3680 (2014).
27. Cazes, A. *et al.* Activated Alk triggers prolonged neurogenesis and Ret upregulation providing a therapeutic target in ALK-mutated neuroblastoma. *Oncotarget* **5,** 2688–702 (2014).
28. Passoni, L. *et al.* Mutation-Independent Anaplastic Lymphoma Kinase Overexpression in Poor Prognosis Neuroblastoma Patients. *Cancer Research* **69,** 7338–7346 (2009).
29. Carpenter, E. *et al.* Antibody targeting of anaplastic lymphoma kinase induces cytotoxicity of human neuroblastoma. *Oncogene* **31,** onc2011647 (2012).
30. Pall, G. The next-generation ALK inhibitors. *Curr Opin Oncol* **27,** 118 (2015).
31. Toyokawa & Seto. Updated Evidence on the Mechanisms of Resistance to ALK Inhibitors and Strategies to Overcome Such Resistance: Clinical and Preclinical Data. *Oncology Research and Treatment* **0,** 291–298 (2015).
32. Zou, H. *et al.* PF-06463922, an ALK/ROS1 Inhibitor, Overcomes Resistance to First and Second Generation ALK Inhibitors in Preclinical Models. *Cancer Cell* **28,** 70–81 (2015).
33. Debruyne *et al.* ALK inhibitor resistance in ALK(F1174L)-driven neuroblastoma is associated with AXL activation and induction of EMT. *Oncogene* **35,** 3681–91 (2016).
34. Lu, J. *et al.* The second-generation ALK inhibitor alectinib effectively induces apoptosis in human neuroblastoma cells and inhibits tumor growth in a TH-MYCN transgenic neuroblastoma mouse model. *Cancer Lett* **400,** 61–68 (2017).
35. Infarinato, N. R. *et al.* The ALK/ROS1 Inhibitor PF-06463922 Overcomes Primary Resistance to Crizotinib in ALK-Driven Neuroblastoma. *Cancer Discov* **6,** 96–107 (2016).
36. Gao, Y. *et al.* Adrenomedullin blockade suppresses sunitinib-resistant renal cell carcinoma growth by targeting the ERK/MAPK pathway. *Oncotarget* **7,** 63374–63387 (2016).
37. Kitamuro, T. *et al.* Differential expression of adrenomedullin and its receptor component, receptor activity modifying protein (RAMP) 2 during hypoxia in cultured human neuroblastoma cells. *Peptides* **22,** 1795–801 (2001).
38. Sena, J., Wang, L., Pawlus, M. & Hu, C.-J. HIFs Enhance the Transcriptional

Activation and Splicing of Adrenomedullin. *Mol Cancer Res* **12,** 728–741 (2014).
39. Dötsch, J. *et al.* Gene expression of neuronal nitric oxide synthase and adrenomedullin in human neuroblastoma using real-time PCR. *Int. J. Cancer* **88,** 172–5 (2000).
40. Larráyoz, I. M., Martínez-Herrero, S., García-Sanmartín, J., Ochoa-Callejero, L. & Martínez, A. Adrenomedullin and tumour microenvironment. *J Transl Med* **12,** 339 (2014).
41. Keleg, S. *et al.* Adrenomedullin is induced by hypoxia and enhances pancreatic cancer cell invasion. *Int J Cancer* **121,** 21–32 (2007).
42. Park, S.-J. *et al.* The histone demethylase JMJD1A regulates adrenomedullin-mediated cell proliferation in hepatocellular carcinoma under hypoxia. *Biochem Bioph Res Co* **434,** 722–727 (2013).
43. Wang, S. & Yang, W.-L. Circulating hormone adrenomedullin and its binding protein protect neural cells from hypoxia-induced apoptosis. *Biochimica Et Biophysica Acta Bba - Gen Subj* **1790,** 361–367 (2009).
44. KOGITA, A. *et al.* Hypoxia induces resistance to ALK inhibitors in the H3122 non-small cell lung cancer cell line with an ALK rearrangement via epithelial-mesenchymal transition. *Int J Oncol* **45,** 1430–1436 (2014).
45. Shichiri, M., Kato, H., Doi, M., Marumo, F. & Hirata, Y. Induction of max by adrenomedullin and calcitonin gene-related peptide antagonizes endothelial apoptosis. *Mol. Endocrinol.* **13,** 1353–63 (1999).
46. Tellez-Gabriel, M., Ory, B., Lamoureux, F., Heymann, M.-F. F. & Heymann, D. Tumour Heterogeneity: The Key Advantages of Single-Cell Analysis. *Int J Mol Sci* **17,** (2016).
47. Speicher, M. R. & Pantel, K. Tumor signatures in the blood. *Nat. Biotechnol.* **32,** 441–3 (2014).
48. Alix-Panabières, C. & Pantel, K. Clinical Applications of Circulating Tumor Cells and Circulating Tumor DNA as Liquid Biopsy. *Cancer Discov* **6,** 479–91 (2016).
49. Siravegna, G. & Bardelli, A. Genotyping cell-free tumor DNA in the blood to detect residual disease and drug resistance. *Genome Biol.* **15,** 449 (2014).
50. Combaret, V. *et al.* Determination of 17q gain in patients with neuroblastoma by analysis of circulating DNA. *Pediatr Blood Cancer* **56,** 757–61 (2011).
51. Combaret, V. *et al.* Circulating MYCN DNA as a tumor-specific marker in neuroblastoma patients. *Cancer Res.* **62,** 3646–8 (2002).
52. Combaret, V. *et al.* Influence of neuroblastoma stage on serum-based detection of MYCN amplification. *Pediatr Blood Cancer* **53,** 329–31 (2009).
53. Combaret, V. *et al.* Detection of tumor ALK status in neuroblastoma patients using peripheral blood. *Cancer Med* **4,** 540–50 (2015).
54. Tevosian *et al.* HBP1: a HMG box transcriptional repressor that is targeted by the retinoblastoma family. *Genes & Development* **11,** 383–396 (1997).
55. Escamilla-Powers, J. *et al.* The Tumor Suppressor Protein HBP1 Is a Novel c-Myc-binding Protein That Negatively Regulates c-Myc Transcriptional Activity. *J Biol Chem* **285,** 4847–4858 (2010).
56. Kim, J. *et al.* Suppression of Wnt signaling by the green tea compound (-)-epigallocatechin 3-gallate (EGCG) in invasive breast cancer cells. Requirement of the transcriptional repressor HBP1. *J. Biol. Chem.* **281,** 10865–75 (2006).
57. Schramm, L. Going Green: The Role of the Green Tea Component EGCG in Chemoprevention. *J Carcinog Mutagen* **04,** (2013).
58. Singh, B., Shankar, S. & Srivastava, R. Green tea catechin, epigallocatechin-3-gallate (EGCG): Mechanisms, perspectives and clinical applications. *Biochem Pharmacol* **82,** 1807–1821 (2011).
59. Gu, J.-W. W. *et al.* EGCG, a major green tea catechin suppresses breast tumor

angiogenesis and growth via inhibiting the activation of HIF-1α and NFκB, and VEGF expression. *Vascular cell* **5,** 9 (2013).
60. He, L. *et al.* (−)-Epigallocatechin-3-gallate inhibits human papillomavirus (HPV)-16 oncoprotein-induced angiogenesis in non-small cell lung cancer cells by targeting HIF-1α. *Cancer Chemoth Pharm* **71,** 713–725 (2013).
61. Toden, S., Tran, H.-M. M., Tovar-Camargo, O. A., Okugawa, Y. & Goel, A. Epigallocatechin-3-gallate targets cancer stem-like cells and enhances 5-fluorouracil chemosensitivity in colorectal cancer. *Oncotarget* **7,** 16158–71 (2016).
62. Nishimura, N. *et al.* Epigallocatechin gallate inhibits sphere formation of neuroblastoma BE(2)-C cells. *Environ Heal Prev Medicine* **17,** 246–251 (2012).
63. Martin, S. *et al.* Inducing apoptosis of cancer cells using small-molecule plant compounds that bind to GRP78. *Brit J Cancer* **109,** 433–443 (2013).
64. Chakrabarti, M., Ai, W., Banik, N. & Ray, S. Overexpression of miR-7-1 Increases Efficacy of Green Tea Polyphenols for Induction of Apoptosis in Human Malignant Neuroblastoma SH-SY5Y and SK-N-DZ Cells. *Neurochem Res* **38,** 420–432 (2013).
65. Hossain, M. M., Banik, N. L. & Ray, S. K. Survivin knockdown increased anti-cancer effects of (-)-epigallocatechin-3-gallate in human malignant neuroblastoma SK-N-BE2 and SH-SY5Y cells. *Exp. Cell Res.* **318,** 1597–610 (2012).
66. Rezai-Zadeh, K. *et al.* Green Tea Epigallocatechin-3-Gallate (EGCG) Modulates Amyloid Precursor Protein Cleavage and Reduces Cerebral Amyloidosis in Alzheimer Transgenic Mice. *J Neurosci* **25,** 8807–8814 (2005).
67. Levites, Y., Amit, T., Mandel, S. & Youdim, M. B. Neuroprotection and neurorescue against Abeta toxicity and PKC-dependent release of nonamyloidogenic soluble precursor protein by green tea polyphenol (-)-epigallocatechin-3-gallate. *FASEB J.* **17,** 952–4 (2003).
68. Mereles, D. & Hunstein, W. Epigallocatechin-3-gallate (EGCG) for Clinical Trials: More Pitfalls than Promises? *Int J Mol Sci* **12,** 5592–5603 (2011).
69. Moog-Lutz, C. *et al.* Activation and Inhibition of Anaplastic Lymphoma Kinase Receptor Tyrosine Kinase by Monoclonal Antibodies and Absence of Agonist Activity of Pleiotrophin. *Journal of Biological Chemistry* **280,** 26039–26048 (2005).
70. Mazot, P. *et al.* Internalization and Down-Regulation of the ALK Receptor in Neuroblastoma Cell Lines upon Monoclonal Antibodies Treatment. *Plos One* **7,** e33581 (2012).
71. Mazot, P. *et al.* The constitutive activity of the ALK mutated at positions F1174 or R1275 impairs receptor trafficking. *Oncogene* **30,** 2017–2025 (2011).
72. Guan, J. *et al.* FAM150A and FAM150B are activating ligands for anaplastic lymphoma kinase. *eLife* **4,** e09811 (2015).
73. Reshetnyak, A. *et al.* Augmentor α and β (FAM150) are ligands of the receptor tyrosine kinases ALK and LTK: Hierarchy and specificity of ligand–receptor interactions. *Proc National Acad Sci* **112,** 15862–15867 (2015).
74. Avraham, R. & Yarden, Y. Feedback regulation of EGFR signalling: decision making by early and delayed loops. *Nature Reviews Molecular Cell Biology* **12,** 104–117 (2011).
75. Amit, I. *et al.* A module of negative feedback regulators defines growth factor signaling. *Nat Genet* **39,** ng1987 (2007).
76. Madhusudan, S. & Ganesan, T. S. Tyrosine kinase inhibitors in cancer therapy. *Clin. Biochem.* **37,** 618–35 (2004).
77. Knight, Z., Lin, H. & Shokat, K. Targeting the cancer kinome through polypharmacology. *Nature reviews. Cancer* **10,** 130–7 (2010).
78. Xu, L. & Anchordoquy, T. Drug delivery trends in clinical trials and translational medicine: challenges and opportunities in the delivery of nucleic acid-based therapeutics. *J Pharm Sci* **100,** 38–52 (2011).

79. Brodeur, G. *et al.* Therapeutic targets for neuroblastomas. *Expert Opin Ther Tar* **18,** 277–292 (2014).
80. Castel, V., Segura, V. & Berlanga, P. Emerging drugs for neuroblastoma. *Expert Opin Emerg Dr* **18,** 155–171 (2013).
81. Berlanga, P., Cañete, A. & Castel, V. Advances in emerging drugs for the treatment of neuroblastoma. *Expert Opin Emerg Dr* (2017). doi:10.1080/14728214.2017.1294159
82. Colicchia, V. *et al.* PARP inhibitors enhance replication stress and cause mitotic catastrophe in MYCN-dependent neuroblastoma. *Oncogene* **36,** 4682–4691 (2017).
83. Yang, J. *et al.* Targeting Histone Demethylases in MYC-Driven Neuroblastomas with Ciclopirox. *Cancer Res* **77,** 4626–4638 (2017).
84. Di Zanni, E. *et al.* Targeting of PHOX2B expression allows the identification of drugs effective in counteracting neuroblastoma cell growth. *Oncotarget* **8,** 72133–72146 (2017).
85. Dyberg, C. *et al.* Rho-associated kinase is a therapeutic target in neuroblastoma. *Proc National Acad Sci* **114,** E6603–E6612 (2017).
86. Van Goethem, A. *et al.* Dual targeting of MDM2 and BCL2 as a therapeutic strategy in neuroblastoma. *Oncotarget* **8,** 57047–57057 (2017).
87. Moreno-Smith, M. *et al.* p53 Nongenotoxic Activation and mTORC1 Inhibition Lead to Effective Combination for Neuroblastoma Therapy. *Clin Cancer Res* (2017). doi:10.1158/1078-0432.CCR-17-0668
88. Gharwan, H. & Groninger, H. Kinase inhibitors and monoclonal antibodies in oncology: clinical implications. *Nature reviews. Clinical oncology* **13,** 209–27 (2016).
89. Mak, I. W., Evaniew, N. & Ghert, M. Lost in translation: animal models and clinical trials in cancer treatment. *Am J Transl Res* **6,** 114–8 (2014).
90. Lowenstein, P. R. & Castro, M. G. Uncertainty in the translation of preclinical experiments to clinical trials. Why do most phase III clinical trials fail? *Curr Gene Ther* **9,** 368–74 (2009).
91. Mackall, C., Merchant, M. & Fry, T. Immune-based therapies for childhood cancer. *Nat Rev Clin Oncol* **11,** nrclinonc.2014.177 (2014).
92. Seeger, R. Immunology and immunotherapy of neuroblastoma. *Semin Cancer Biol* **21,** 229–237 (2011).
93. Bosse, K. *et al.* Identification of GPC2 as an Oncoprotein and Candidate Immunotherapeutic Target in High-Risk Neuroblastoma. *Cancer Cell* **32,** 295–309.e12 (2017).
94. Sharma, P. & Allison, J. P. Immune Checkpoint Targeting in Cancer Therapy: Toward Combination Strategies with Curative Potential. *Cell* **161,** 205–214 (2015).
95. Villablanca, J. *et al.* A Phase I New Approaches to Neuroblastoma Therapy Study of Buthionine Sulfoximine and Melphalan With Autologous Stem Cells for Recurrent/Refractory High-Risk Neuroblastoma. *Pediatric Blood Cancer* **63,** 1349–1356 (2016).
96. Boeva, V. *et al.* Heterogeneity of neuroblastoma cell identity defined by transcriptional circuitries. *Nat Genet* **49,** 1408–1413 (2017).
97. Van Groningen, T. *et al.* Neuroblastoma is composed of two super-enhancer-associated differentiation states. *Nature Genetics* **49,** 1261–1266 (2017).
98. Fisher, R., Pusztai, L. & Swanton, C. Cancer heterogeneity: implications for targeted therapeutics. *Br. J. Cancer* **108,** 479–85 (2013).
99. Tirosh, I. *et al.* Dissecting the multicellular ecosystem of metastatic melanoma by single-cell RNA-seq. *Science* **352,** 189–96 (2016).
100. Meacham, C. E. & Morrison, S. J. Tumour heterogeneity and cancer cell plasticity. *Nature* **501,** 328–37 (2013).
101. Litzenburger, U. M. *et al.* Single-cell epigenomic variability reveals functional cancer heterogeneity. *Genome Biol.* **18,** 15 (2017).

102. Ziegenhain, C. *et al.* Comparative Analysis of Single-Cell RNA Sequencing Methods. *Mol. Cell* **65,** 631–643.e4 (2017).
103. Chicard, M. *et al.* Genomic Copy Number Profiling Using Circulating Free Tumor DNA Highlights Heterogeneity in Neuroblastoma. *Clin. Cancer Res.* **22,** 5564–5573 (2016).
104. Roy, N. *et al.* Shallow Whole Genome Sequencing on Circulating Cell-Free DNA Allows Reliable Noninvasive Copy-Number Profiling in Neuroblastoma Patients. *Clin Cancer Res* **23,** 6305–6314 (2017).
105. Bellini, A. *et al.* Deep Sequencing Reveals Occurrence of Subclonal ALK Mutations in Neuroblastoma at Diagnosis. *Clinical Cancer Research* **21,** 4913–4921 (2015).
106. Schramm, A. *et al.* Mutational dynamics between primary and relapse neuroblastomas. *Nat. Genet.* **47,** 872–7 (2015).

Part V: summary & samenvatting

Science is not only a discipline of reason,
but, also, one of romance and passion.
~Stephen Hawking~

Chapter 7 Summary

In this thesis, we describe the study of a particular receptor tyrosine kinase (RTK), ALK, which is recurrently mutated in up to 10% of neuroblastoma tumours, a paediatric tumour of the sympathetic nervous system. Like many other RTKs, ALK controls a complex downstream signaling cascade implicated in development and normal cell functions and implicated in various cancers through constitutive activating mutations or fusion proteins. Mutated ALK is an important target in neuroblastoma as few other recurrent mutations have been detected and given that this receptor, like many other RTKs, can be inhibited by new targeted drugs (small molecule inhibitors). Despite this promising outlook, optimism must be tempered as recent studies have shown that precision treatment using single drugs almost invariable leads to resistance due to second-line mutations, gene amplifications, aberrations in the downstream pathway or the activation of a bypass network. In order to circumvent such resistance mechanisms and to find additional vulnerable nodes for targeted treatment, in-depth knowledge of the networks regulated by ALK in neuroblastoma is essential.

We therefore further analysed the transcriptional network downstream of ALK and established a 77-gene signature for mutant ALK inhibition in neuroblastoma. Further dissection of this gene signature yielded several new important observations. In addition to confirmation of implication of the PI_3K-AKT-mTOR, MAPK and MYC(N) signaling pathways downstream of ALK in neuroblastoma, we observed a strong upregulation of (a) MAPK negative feedback loop regulators and (b) RET and RET-driven cholinergic neuronal markers.

In a second part, we decided to study in more detail the dynamic regulated transcriptome of ALK^{R1275Q} mutant CLB-GA neuroblastoma cells following treatment with the first-generation ALK inhibitor TAE684. We observed the expected downregulation of the downstream pathways, PI_3K-AKT-mTOR, MAPK and MYC(N) signaling, within 2 hours following treatment. Intriguingly, the positively regulated MYCN target genes showed initial upregulation, followed by the expected decrease in overall MYCN activity. Of further interest, the first differentially expressed gene,

adrenomedullin (ADM), was previously reported to be involved in sunitinib resistance in renal cancer. Therefore, we hypothesize that this gene could be implicated in the resistance mechanisms against ALK small molecules in neuroblastoma.

The discovery by our group that there is an ultra-high-risk patient subgroup, which has both *MYCN* amplification and *ALK*^{F1174L} mutation, suggested that ALK and MYCN cooperate in neuroblastoma tumorigenesis. Moreover, in a mouse and zebrafish neuroblastoma model system, the expression of both *MYCN* and *ALK*^{F1174L} in sympathetic neuronal progenitor cells accelerated tumour formation. Additionally, it was shown that ALK controls MYCN through two different mechanisms. First, ALK regulates *MYCN* transcription levels directly and through the PI_3K-AKT-MEKK3-MEK5-ERK5 pathway. Secondly, MYCN protein is stabilized by ALK via the PI_3K/AKT/GSK3β pathway. Moreover, MYCN itself transcriptionally activates *ALK*.
As a last part of this thesis, we focused on identifying additional mechanisms for this ALK – MYCN cooperativity with possible additional value of identifying new druggable nodes in this cross-talk. We therefore went back to our ALK 77-gene signature and identified HBP1 as a central component of a third mechanism of ALK regulated MYCN activity. We discovered that ALK negatively controls HBP1 levels through the PI_3K-AKT-FOXO3 signaling axis, while MYCN represses HBP1 through induction of the miR-17~92 cluster. More importantly, HBP1 inhibits both the transcriptional activation as repressing activity of MYCN, partly through interaction with the PRC2 complex. Moreover, forced overexpression of HBP1 in neuroblastoma cells showed an increase in cell death and a higher differentiation signature score, concomitant with decreased cell viability, colony formation capacity and spheroid formation, suggesting a possible tumour suppressive role in neuroblastoma. Of further interest, lowest HBP1 expression was observed in MYCN amplified and high stage neuroblastoma tumours, while high HBP1 levels were correlated with better event-free and overall survival, further confirming the repression of tumour aggressiveness by HBP1. Finally, combined targeting of HBP1 by PI_3K antagonists and MYCN signaling using BET or HDAC inhibitors synergistically represses MYCN activity and significantly reduces tumour growth, suggesting a novel targeted therapy option for the ultra-high-risk patient subgroup with both *MYCN* amplification and *ALK*^{F1174L} mutation.

Chapter 8 Samenvatting

In deze thesis beschrijven we de studie van ALK, een receptor tyrosine kinase (RTK) dat frequent gemuteerd is in 10% van de neuroblastoma tumoren, een pediatrische tumor van het sympathisch zenuwstelsel. Zoals vele andere RTKs, controleert ALK een complexe *downstream* signalisatie cascade, enerzijds betrokken in ontwikkeling en normale cellulaire functies maar anderzijds ook in verschillende kankers door constitutieve activerende mutaties of als fusiegen. Gezien een beperkt aantal andere frequente mutaties zijn ontdekt in neuroblastoma, is gemuteerd ALK een belangrijk doelwit in neuroblastoma. Daarenboven heeft deze receptor, zoals vele andere RTKs, het grote voordeel dat deze kan onderdrukt worden door nieuwe doelgerichte medicijnen (*small molecule inhibitors*).
Ondanks dit veelbelovend vooruitzicht, moet het optimisme getemperd worden. Recente studies hebben aangetoond dat “precisie-behandeling” door gebruik te maken van slechts één medicijn bijna steeds leidt tot resistentie door het ontstaan van andere mutaties, genamplificaties, aberraties in de *downstream* signaalwegen of door de activatie van een *bypass* netwerk. Om deze resistentie mechanismen te ontwijken en om nieuwe, additionele eiwitten te vinden die geschikt zijn voor doelgerichte therapie, is een grondige kennis van de netwerken die door ALK gereguleerd worden in neuroblastoma prioritair.

Daarom hebben we de transcriptionele netwerken die door ALK gereguleerd worden verder geanalyseerd en genereerden we een 77-genen signatuur voor gemuteerd ALK in neuroblastoma. Verdere dissectie van deze gensignatuur gaf aanleiding tot verschillende, nieuwe observaties. Naast de confirmatie van de betrokkenheid van de PI_3K-AKT-mTOR, MAPK en MYC(N) signaalwegen *downstream* van ALK in neuroblastoma, observeerden we ook een sterke opregulatie van (a) negatieve feedback regulatoren van de MAPK signaalweg en van (b) RET en RET-gestuurde cholinerge, neuronale merkers.

In het tweede deel, besloten we om het dynamisch transcriptioneel profiel van de ALK^{R1275Q} gemuteerde CLB-GA neuroblastoma cellen in meer detail te onderzoeken na behandeling met TAE684, een van de eerst ontwikkelde ALK inhibitoren. We

observeerden de verwachte neerregulatie van de downstream signaalwegen, PI_3K-AKT-mTOR, MAPK en MYC(N) reeds binnen 2 uur na behandeling. Intrigerend was ook de ontdekking dat de positief gereguleerde MYCN doelwitgenen eerst een initiële opregulatie vertoonden, die gevolgd werd door de verwachte daling in de volledige MYCN-activiteit. Ook interessant was dat het eerste gen dat differentieel tot expressie kwam adrenomedullin (ADM) was. Dit is een gen waarvan recent beschreven is dat het een rol heeft in sunitib resistentie in nierkanker. Daarom postuleren we dat dit gen ook betrokken kan zijn in resistentie mechanismen tegen ALK inhibitoren in neuroblastoma.

Onze onderzoeksgroep kwam tot de ontdekking dat er een *ultra-high-risk* patiënten subgroep bestaat, die zowel *MYCN* amplificaties als ALK^{F1174L} mutaties heeft, wat suggereert dat deze twee eiwitten samenwerken tijdens de ontwikkeling van neuroblastoma. Daarnaast werd in een muis en een zebravis modelsysteem aangetoond dat de simultane expressie van *MYCN* en ALK^{F1174L} in sympathische adrenerge precursor cellen zorgt voor een versnelde vorming van neuroblastoma tumoren. Bovendien wordt MYCN door ALK gecontroleerd via twee verschillende mechanismen. Enerzijds reguleert ALK de transcriptie van *MYCN* direct alsook via de PI_3K-AKT-MEKK3-MEK5-ERK5 axis. Anderzijds, wordt het MYCN eiwit gestabiliseerd door ALK via de PI_3K/AKT/GSK3β signaalweg. Daarnaast activeert MYCN zelf ook de transcriptie van *ALK*.

In het laatste gedeelte van deze thesis focusseerden we ons op het identificeren van nieuwe mechanismen voor de samenwerking tussen ALK en MYCN, waardoor we mogelijks andere eiwitten kunnen identificeren in deze *cross-talk* die kunnen gebruikt worden voor doelgerichte therapie. Daarvoor hebben we onze ALK 77-genen signatuur verder onderzocht en hebben we zo HBP1 geïdentificeerd als een derde manier waarop ALK MYCN aandrijft. We ontdekten dat ALK de HBP1 expressie negatief reguleert via de PI_3K-AKT-FOXO3 signalisatie weg, terwijl MYCN zorgt voor een onderdrukking van HBP1 door de inductie van de miR-17~92 cluster. Nog belangrijker is de ontdekking dat HBP1 zowel de transcriptionele activator als repressor functie van MYCN onderdrukt, deels door interactie met het PRC2 complex. Verder veroorzaakte overexpressie van HBP1 in neuroblastoma cellen meer celdood en een hogere differentiatie signatuurscore. Deze resultaten waren in

lijn met verminderde cel viabiliteit, kolonie vormende capaciteit en vorming van sferoïden, wat suggereert dat HBP1 mogelijks een tumorsuppressor gen is in neuroblastoma. Verder van belang was dat lage HBP1 expressie niveaus geobserveerd werden in tumoren met MYCN amplificatie en in stadium 4 neuroblastoma tumoren, terwijl hoge HBP1 levels gecorreleerd waren met een betere overleving. Dit alles benadrukt het belang van HBP1 in het onderdrukken van de agressiviteit van de tumor. Finaal toonden we aan dat de combinatie van PI_3K antagonisten om HBP1 op te reguleren samen met onderdrukking van MYCN signalisatie met BET of HDAC inhibitoren, zorgt voor een synergistische onderdrukking van de MYCN activiteit en voor een significantie reductie van tumorgroei, wat suggereert dat dit een optie is voor nieuwe doelgerichte therapie voor de *ultra-high-risk* patiënten subgroep met zowel *MYCN* amplificatie als ALK^{F1174L} mutatie.

Part VI: curriculum vitae and word of thanks

Scientific research is one of the most exciting and rewarding of occupations.
~Frederick Sanger~

Chapter 9 About the author

Personal details

name	Shana Claeys
address	Kerkhofstraat 1
	9890 Asper
	Belgium
telephone	+32-499-61-88-02
e-mail	Shana.Claeys@icloud.com
born	on July 16, 1989
	in Ghent
nationality	Belgian
social status	cohabiting
driver license B (2009)	

Professional records

2012 - present PhD fellowship in biomedical science
topic: Functional study of the ALK^{F1174} mutation in neuroblastoma
Ghent University, Center for Medical Genetics, Ghent,
De Pintelaan 185, 9000 Ghent, Belgium

Education

2012 - present Higher education
PhD fellowship in biomedical science
topic: Functional study of the ALK^{F1174} mutation in neuroblastoma
Ghent University, Center for Medical Genetics, Ghent,
De Pintelaan 185, 9000 Ghent, Belgium

2010 – 2012 higher education
masters's degree of Biomedical Sciences – discipline Genetics
Ghent University, 9000 Ghent, Belgium
thesis: high throughput functional characterisation of miRNAs
thesis place: Ghent University, Center for Medical Genetics, Ghent, De Pintelaan 185, 9000 Ghent, Belgium
graduated magna cum laude
- laboratory animal science: "attest B&C"
- clinical trials: "Certificate of training"

2007 – 2010 higher education
bachelor's degree of Biomedical Sciences
Ghent University, 9000 Ghent, Belgium
graduated magna cum laude
- bio-informatics: "HITS Level 1 Certification"

2001 – 2007 general secondary education
direction ASO, Latin – Mathematics
Sint-Bavohumaniora, Reep 4, 9000 Ghent, Belgium
graduated magna cum laude

Memberships, Awards and Grants

- Member of the Cancer Research Institute Ghent (CRIG), which covers all cancer research in the area of Ghent in order to empower the needed research.
- Emmanuel Van der Schueren research grant of "Kom op tegen Kanker". HBP1 as a new therapeutic target in ALK- and MYCN-driven neuroblastoma. November 24, 2016 in Ancienne Belgique, Brussels, Belgium.
- Best poster presentation by Young Investigator by BeSHG 2016. The HBP1 tumour suppressor is an epigenetic regulator of MYCN-driven neuroblastoma through interaction with the PRC2 complex. February 4 & 5, 2016, Leuven, Belgium.
- FWO PhD fellowship renewal grant. Functional study of the ALK^{F1174} mutation in neuroblastoma. June 25, 2014, Brussels, Belgium

- FWO PhD fellowship grant. Functional study of the ALK^{F1174} mutation in neuroblastoma. June 20, 2012, Brussels, Belgium.

Professional training, skills & experiences

1. Transferable skills

▪ Communication skills	How to get published, Ghent, Belgium, May 18 & 19, 2016
▪ Leadership and management	Personal effectiveness, Ghent, Belgium, May 8 & 22, June 11, 2014.
▪ Research and valorisation	Advanced statistical methods: the R package (module 1), Zwijnaarde, Belgium, September 11 & 18 & 25, October 2 & 9 & 16 & 23, 2013 (certificate of attendance + examination).

2. Specialist training

- Advanced statistical methods: statistical genome analysis (module 4), Zwijnaarde, Belgium. March 12 & 19 & 26, April 2 & 23 & 30, May 7 & 14 & 28, 2014 (examination).
- Advanced statistical methods: multivariate methods (module 3), Zwijnaarde, Belgium. January 15 & 22 & 29, February 5 & 12 & 19, 2014 (examination).
- Advanced statistical methods: non- parametric methods (module 2), Zwijnaarde, Belgium. November 6 & 13 & 20 & 27, 2013; December 4 & 11, 2013; January 8, 2014 (examination).

3. Other courses

- From Big Data to Bedside workshop, Ghent, Belgium, April 1, 2015.
- Introductory course: using computing infrastructure and (bio)informatics tools available in our lab, Ghent, Belgium, February 17, 2015.
- UGent Introduction Day for PhD students, Ghent, Belgium, February 5, 2013.

4. Computer skills

- Microsoft office — Word, Excel, PowerPoint
- Graphical tools — Adobe Illustrator, GraphPad Prism
- Data-analysis — qBASE+, R, GSEA, Bioconductor, R2, basic command line, Cytoscape iRegulon, Cytoscape enrichmentMap

5. Wet lab experience

- Cellular and molecular assays:
  cell culture, cell harvesting, transfections (siRNA, shRNA, miRNA, plasmids, nanoparticles), luciferase assay, cell titer glo assay, caspase glo assay, IncuCyte, ELISA cell death assay, xCELLigence assay, colony formation assay, scratch assay, FACS: cell cycle analysis, FACS: sorting
- Drugging assay:
  compound treatment, dual drugging experiments
- Protein work:
  protein isolation & concentration measurement, Western blotting, Immuno-precipitation, Immuno-fluorescence
- RNA related work:
  primer design, RNA isolation, cDNA synthesis, qPCR, miScript RT, miScript qPCR, Experion, BioAnalyzer, SingleShot, Cells-to-CT
- Bacterial work:
  general bacterial work, growing plasmids, plasmid isolation, transformation
- Viral work:
  selection marker kill curve, virus production, viral transduction
- Mouse work:
  subcutaneous injection of cell line in the flank of nude mice, tumor growth follow-up, cervical dislocation, paraffin embedding, TissueLyser
- Standard molecular work:
  site-directed mutagenesis, PCR, colony PCR, plasmid digestion, cloning, plasmid ligation

6. Varia

Languages	Dutch English French

A1 publications

- Emdal K.B, Pedersen A.K, Bekker-Jensen D.B, Lundby A, Claeys S, De Preter K, Speleman F, Francavilla C, Olsen J.. V. Integrated proximal proteomics (IPP) reveals IRS2 as a determinant of cell survival in ALK-driven neuroblastoma. Science Signaling, submitted on September 18, 2017.
- Claeys S, Denecker G, Cannoodt R, Kumps C, Durinck K, Speleman F, De Preter K. Early and late effects of pharmacological ALK inhibition on the neuroblastoma transcriptome. Oncotarget, 2017
- Claeys S, Denecker G, Durinck K*, Decaesteker B*, Loontiens S, Vanhauwaert S, Althoff K, Wigerup C, Bexell D, Dolman E, Henrich K-O, Wehrmann L, Westerhout E.M., Demoulin J-B, Kumps C, Van Maerken T, Laureys G, Van Neste C, De Wilde B, De Wever O, Westermann F, Versteeg R, Molenaar J.J., Pahlman S, Schulte J.H., De Preter K, Speleman F. ALK positively regulates MYCN activity through repression of HBP1 expression. Oncogene, revised paper, submitted on October 16, 2017.
- Van Peer G, Mets E, Claeys S, De Punt I, Lefever S, Ongenaert M, Rondou P, Speleman F, Mestdagh P, Vandesompele J. A high-throughput 3' UTR reporter screening identifies microRNA interactomes of cancer genes. Submitted for publication in PLoS One, June 2017.
- Lambertz I, Kumps C, Claeys S, Lindler S, Beckers A, Janssens E, Carter D, Cazes A, Cheung B, De Mariano M, De Bondt A, De Brouwer S, Delattre O, Gibbons J, Janoueix I, Laureys G, Liang C, Marshall G, Porcu M, Takita J, Camacho Trujillo D, Van Den Wyngaert I, Van Roy N, Van Goethem A, Van Maerken T, Zabrocki P, Cools J, Schulte J, Vialard J, Speleman F, De Preter K. Upregulation of MAPK negative feedback regulators and RET in mutant ALK neuroblastoma: implications for targeted treatment. Clinical Cancer Research, 2015.

Mentorship of students

- Hannah Kiss (2013). The unravelling of the signalisation of ALK in neuroblastoma. Thesis to obtain the diploma of master in de Biomedical sciences. Promotor: De Preter K., mentor: Kumps C., Claeys S., Lambertz I.
- Suzanne De Bruyn (2014). Functional characterization of ALK signaling in neuroblastoma. Thesis to obtain the diploma of master in de Biomedical sciences. Promotor: Lambertz I., mentor: Claeys S.
- Manolito De Bruycker (2013). The role of ALK in neuroblastoma. Z-line paper, 2d bachelor of Medicine. Promotor: Lambertz I., mentor: Claeys S.
- Thomas Maly (2013). The role of ALK in neuroblastoma. Z-line paper, 2d bachelor of Medicine. Promotor: Lambertz I., mentor: Claeys S.
- Magalie De Kezel (2014). Synthetic lethality in cancer. Z-line paper, 2d bachelor of Medicine. Promotor: De Preter K., mentor: Claeys S.
- Jules Demuynck (2015). Resistance mechanism by the treatment of the ELM4-ALk translocation with crizotinib. Z-line paper, 2d bachelor of Medicine. Promotor: De Preter K., mentor: Claeys S.
- Pieter Lammens (2015). Resistance mechanism by the administration of ALK inhibitors. Z-line paper, 2d bachelor of Medicine. Promotor: De Preter K., mentor: Claeys S.

Scientific Presentations

- Claeys S, Denecker G, Decaesteker B, Janssens E, Kumps C, De Brouwer S, Lambertz I, Fieuw A, Vanhauwaert S, Althoff K, Bate-Eya L, Dolman E, Wigerup C, Bexell D, Pahlman S, Henrich K-O, Wehrmann L, Hogarty M.D., Demoulin J-B, Van Maerken T, Laureys G, Van Neste C, De Wilde B, Durinck K, Westermann F, Molenaar J.J., Schulte J.H., De Preter K, Speleman F. The HBP1 tumour suppressor is a negative epigenetic regulator of MYCN-driven neuroblastoma through interaction with the PRC2 complex. f-TALES: cancer, an old dog with new tricks. Leuven, Belgium, March 6 & 7, 2017.

- Claeys S, Denecker G, Lambertz I, Janssens E, Vanhauwaert S, Decaesteker B, Van Maerken T, De Wilde B, Laureys G, Althoff K, Schulte J, Demoulin J-B, Bate-Eya L, Molenaar J.J., Westermann F, De Preter K, Speleman F. HBP1 is a negative epigenetic regulator of MYCN-driven neuroblastoma through interaction with the PRC2 complex. Opening Symposium for the new Treatment and Research Center for Pediatric Oncology and Haematology Heidelberg, Heidelberg, Germany, January 19 & 20, 2017.
- Claeys S, Lambertz I, Janssens E, Vanhauwaert S, Decaesteker B, Kumps C, De Brouwer S, Fieuw A, Van Maerken T, De Wilde B, Laureys G, Althoff K, Schulte J, Bate-Eya L, Molenaar J.J, Demoulin J-B, Look T. De Preter K, Speleman F. The HBP1 tumour suppressor is a negative epigenetic regulator of MYCN-driven neuroblastoma through interaction with the PRC2 complex. Advances in Neuroblastoma Research, Cairns, Australia, June 19 -24, 2016.
- Claeys S, Lambertz I, Van Goethem A, Kumps C, De Brouwer S, Fieuw A, Van Maerken T, Althoff K, Schulte J, Demoulin J-B, De Preter K, Speleman F. The HBP1 tumour suppressor is an epigenetic regulator of MYCN-driven neuroblastoma through interaction with the PRC2 complex. Research Day, Ghent, Belgium, March 16, 2016.
- Claeys S, Lambertz I, Janssens E, Vanhauwaert S, Decaesteker B, Kumps C, De Brouwer S, Fieuw A, Van Maerken T, De Wilde B, Laureys G, Althoff K, Schulte J, Bate-Eya L, Molenaar J.J, Demoulin J-B, Look T. De Preter K, Speleman F. The HBP1 tumour suppressor is a negative epigenetic regulator of MYCN-driven neuroblastoma through interaction with the PRC2 complex. Oncopoint meeting, Ghent, Belgium, March 2, 2016.
- Claeys S, Lambertz I, Van Goethem A, Kumps C, De Brouwer S, Fieuw A, Van Maerken T, Althoff K, Schulte J, Demoulin J-B, De Preter K, Speleman F. The HBP1 tumour suppressor is an epigenetic regulator of MYCN-driven neuroblastoma through interaction with the PRC2 complex. BeSHG, Leuven, Belgium, February 4 & 5, 2016.
- Claeys S, Lambertz I, Van Goethem A, Beckers A, Kumps C, Van Maerken T, Schulte J, De Preter K, Speleman F. The HBP1 tumour suppressor at multiple regulatory cross roads in neuroblastoma. CNIO frontiers meeting: new trends in anticancer drug development, Madrid, Spain, March 22 – 25, 2015.

- Claeys S, Lambertz I, Van Goethem A, Beckers A, Kumps C, Van Maerken T, Schulte J, De Preter K, Speleman F. Synergistic combined molecular treatment targeting the HBP1 tumour suppressor gene in neuroblastoma. OncoPoint meeting, Ghent, Belgium, February 11, 2015.
- Claeys S, Kumps C, Lambertz I, De Brouwer S, Lindner S, Van Goethem A, Van Maerken T, Vialard J, Cools J, Schulte J, De Preter K, Speleman F. The HBP1 tumour suppressor is a druggable ALK downregulated gene controlling MYCN activity. Advances in Neuroblastoma Research, Cologne, Germany, May 13 – 16, 2014.
- Claeys S, Kumps C, Lambertz I, De Brouwer S, Lindner S, Van Goethem A, Van Maerken T, Vialard J, Cools J, Schulte J, De Preter K, Speleman F. The HBP1 tumour suppressor is a druggable ALK downregulated gene controlling MYCN activity. BeSHG, Antwerp, Belgium, February 7, 2014.
- Claeys S, De Preter K, Speleman F, Lambertz I, Kumps C. Green tea compound EGCG activates HBP1: an ALK downstream suppressor gene in neuroblastoma. Oncopoint meeting, Ghent, Belgium, February 6, 2014.

Scientific Posters

- Denecker G, Claeys S, Lambertz I, Janssens E, Vanhauwaert S, Decaesteker B, Van Maerken T, De Wilde B, Laureys G, Althoff K, Schulte J, Demoulin J-B, Roberts S.S., Bate-Eya L, Molenaar J.J., Westermann F, De Preter K, Speleman F. The HBP1 tumour suppressor is a negative epigenetic regulator of MYCN-driven neuroblastoma through interaction with the PRC2 complex. AACR: annual meeting. Washington D.C., USA, April 1 – 5, 2017.
- Claeys S, Denecker G, Decaesteker B, Janssens E, Kumps C, De Brouwer S, Lambertz I, Fieuw A, Vanhauwaert S, Althoff K, Bate-Eya L, Dolman E, Wigerup C, Bexell D, Pahlman S, Henrich K-O, Wehrmann L, Hogarty M.D., Demoulin J-B, Van Maerken T, Laureys G, Van Neste C, De Wilde B, Durinck K, Westermann F, Molenaar J.J., Schulte J.H., De Preter K, Speleman F. The HBP1 tumour suppressor is a negative epigenetic regulator of MYCN-driven neuroblastoma through interaction with the PRC2 complex. f-TALES: cancer, an old dog with new tricks. Leuven, Belgium, March 6 & 7, 2017.

- Claeys S, Lambertz I, Van Goethem A, Kumps C, De Brouwer S, Fieuw A, Van Maerken T, Althoff K, Schulte J, Demoulin J-B, De Preter K, Speleman F. The HBP1 tumour suppressor is an epigenetic regulator of MYCN-driven neuroblastoma through interaction with the PRC2 complex. BeSHG, Leuven, Belgium, February 4 & 5, 2016.
- Claeys S, Lambertz I, Van Goethem A, Kumps C, De Brouwer S, Fieuw A, Van Maerken T, Althoff K, Schulte J, Demoulin J-B, Neuroblastoma Research Consortium, De Preter K, Speleman F. HBP1 downregulation through mutant ALK represents a novel mechanism for cooperative MYCN activation in neuroblastoma. 4th Neuroblastoma Research Symposium, Newcastle, UK, November 26 & 27, 2015.
- Claeys S, Kumps C, Lambertz I, Beckers A, Van Maerken T, Van Goethem A, Schulte J, Lindner S, Odersky A, Speleman F, De Preter K. The role of pleiotropic constitutive ALK signaling in acceleration of MYCN-driven neuroblastoma formation. ASSET GA Meeting, Vienna, Austria, June 9 – 11, 2013.

Scientific Participations

- f-TALES: cancer, an old dog with new tricks. Leuven, Belgium, March 6 & 7, 2017.
- f-TALES: Light on the dark side of the genome, Ghent, Belgium, September 15 & 16, 2016.
- Cell-VIB Symposium: Hallmarks of Cancer, Ghent, Belgium, December 11 – 13, 2016
- Neuroblastoma in Berlin, Berlin, Germany, December 13 – 15, 2015: short oral presentation
- ASSET GA Meeting, Vienna, Austria, October 7 – 9, 2015: oral presentation
- From Big Data to Bedside, Ghent, Belgium, April 2, 2015.
- ASSET GA Meeting, Vienna, Austria, December 4 & 5, 2014.
- Cancer Pharmacogenomics and Targeted Therapies 2014, Cambridge, United Kingdom, September 17 – 19, 2014.

- BeSSCR, Ghent, Belgium, September 12, 2014.
- IUAP Progress Meeting P7/03, Brussels, Belgium, June 12, 2014.
- Cancer Pharmacogenomics and Targeted Therapies 2013, Cambridge, United Kingdom, 15 – 17, September 2013.
- Pediatric tumours at the interface symposium, Vienna, Austria, June 6 – 9, 2013.
- SYSMED 2012 International Conference on Systems Medicine, Dublin, Ireland, September 9 – 13, 2012

Scientific abstracts

- Mus L, Lambertz I, Kumps C, Claeys S, Denecker G, Van Loocke W, Van Neste C, Koster J, Versteeg R, Van Roy N, De Wilde B, Laureys G, Schulte J, De Wever O, De Preter K, Speleman F. The ETV5 oncogene is a target of activated ALK signaling in neuroblastoma. Research Day Ghent University, Ghent, Belgium, April 20, 2017.
- Denecker G, Claeys S, Lambertz I, Janssens E, Vanhauwaert S, Decaesteker B, Van Maerken T, De Wilde B, Laureys G, Althoff K, Schulte J, Demoulin J-B, Bate-Eya L, Molenaar J.J., Westermann F, De Preter K, Speleman F. HBP1 is a negative epigenetic regulator of MYCN-driven neuroblastoma through interaction with the PRC2 complex. AACR Annual Meeting 2017, Washington DC, USA, April 1 – 5, 2017.
- Mus L, Lambertz I, Kumps C, Claeys S, Denecker G, Van Loocke W, Van Neste C, Koster J, Versteeg R, Van Roy N, De Wilde B, Laureys G, Schulte J, De Wever O, De Preter K, Speleman F. The ETV5 oncogene is a target of activated ALK signaling in neuroblastoma. OncoPoint meeting, Ghent, Belgium, March 15, 2017.
- Mus L, Lambertz I, Kumps C, Claeys S, Denecker G, Van Loocke W, Van Neste C, Koster J, Versteeg R, Van Roy N, De Wilde B, Laureys G, Schulte J, De Wever O, De Preter K, Speleman F. The ETV5 oncogene is a target of activated ALK signaling in neuroblastoma. f-TALES: cancer, an old dog with new tricks. Leuven, Belgium, March 6 & 7, 2017.
- Claeys S, Denecker G, Decaesteker B, Janssens E, Kumps C, De Brouwer S, Lambertz I, Fieuw A, Vanhauwaert S, Althoff K, Bate-Eya L, Dolman E, Wigerup

C, Bexell D, Pahlman S, Henrich K-O, Wehrmann L, Hogarty M.D., Demoulin J-B, Van Maerken T, Laureys G, Van Neste C, De Wilde B, Durinck K, Westermann F, Molenaar J.J., Schulte J.H., De Preter K, Speleman F. The HBP1 tumour suppressor is a negative epigenetic regulator of MYCN-driven neuroblastoma through interaction with the PRC2 complex. f-TALES: cancer, an old dog with new tricks. Leuven, Belgium, March 6 & 7, 2017.

- Claeys S, Denecker G, Lambertz I, Janssens E, Vanhauwaert S, Decaesteker B, Van Maerken T, De Wilde B, Laureys G, Althoff K, Schulte J, Demoulin J-B, Bate-Eya L, Molenaar J.J., Westermann F, De Preter K, Speleman F. HBP1 is a negative epigenetic regulator of MYCN-driven neuroblastoma through interaction with the PRC2 complex. Opening Symposium for the new Treatment and Research Center for Pediatric Oncology and Haematology Heidelberg, Heidelberg, Germany, January 19 & 20, 2017.
- Decaesteker B, Devloed F, Loontiens S, Denecker G, Van Loocke W, Gartlgruber M, Rombaut D, Beckers A, Claeys S, Henssen A, Vanhauwaert S, Westermann F, Schulte J, De Preter K*, Speleman F* (*equal contribution). The TBX2 super-enhancer marked transcription factor on 17q is overexpressed in neuroblastoma and infers poor prognosis. f-TALES: Light on the dark side of the genome, Ghent, Belgium, September 15 & 16, 2016.
- Claeys S, Lambertz I, Janssens E, Vanhauwaert S, Decaesteker B, Kumps C, De Brouwer S, Fieuw A, Van Maerken T, De Wilde B, Laureys G, Althoff K, Schulte J, Bate-Eya L, Molenaar J.J, Demoulin J-B, Look T. De Preter K, Speleman F. The HBP1 tumour suppressor is a negative epigenetic regulator of MYCN-driven neuroblastoma through interaction with the PRC2 complex. Advances in Neuroblastoma Research, Cairns, Australia, June 19 – 24, 2016.
- Lambertz I, Mus L, Kumps C, Claeys S, Van Loocke W, Van Neste C, Koster J, Versteeg R, Van Roy N, De Wilde B, Laureys G, Schulte J, De Wever O, De Preter K, Speleman F. Sensing mutant ALK: Capicua and ETV5 as executors of aberrant ALK-driven MAPK signaling. Advances in Neuroblastoma Research, Cairns, Australia, June 19 – 24, 2016.
- Claeys S, Lambertz I, Van Goethem A, Kumps C, De Brouwer S, Fieuw A, Van Maerken T, Althoff K, Schulte J, Demoulin J-B, De Preter K, Speleman F. The HBP1 tumour suppressor is an epigenetic regulator of MYCN-driven

neuroblastoma through interaction with the PRC2 complex. Research Day, Ghent, Belgium, March 16, 2016.

- Claeys S, Lambertz I, Janssens E, Vanhauwaert S, Decaesteker B, Kumps C, De Brouwer S, Fieuw A, Van Maerken T, De Wilde B, Laureys G, Althoff K, Schulte J, Bate-Eya L, Molenaar J.J, Demoulin J-B, Look T. De Preter K, Speleman F. The HBP1 tumour suppressor is a negative epigenetic regulator of MYCN-driven neuroblastoma through interaction with the PRC2 complex. Oncopoint meeting, Ghent, Belgium, March 2, 2016.
- Lambertz I, Mus L, Kumps C, Claeys S, Van Roy N, De Wilde B, Laureys G, Schulte J, De Wever O, De Preter K, Speleman F. ETV5 functionally connects ALK and CXCR4 signaling in neuroblastoma. Oncopoint meeting, Ghent, Belgium, March 2, 2016.
- Mus L, Claeys S, De Wilde B, Laureys G, Van Goethem A, Schulte J, De Preter K, Lambertz I, Speleman F. Dual targeting of ALK and RET: establishing a novel basis for the treatment of neuroblastoma. Oncopoint meeting, Ghent, Belgium, March 2, 2016.
- Claeys S, Lambertz I, Van Goethem A, Kumps C, De Brouwer S, Fieuw A, Van Maerken T, Althoff K, Schulte J, Demoulin J-B, De Preter K, Speleman F. The HBP1 tumour suppressor is an epigenetic regulator of MYCN-driven neuroblastoma through interaction with the PRC2 complex. BeSHG, Leuven, Belgium, February 4 & 5, 2016.
- De Wyn J, Janssens E, Vanhauwaert S, Claeys S, Beckers A, De Preter K, Speleman F. The splicing factor SRSF2 is a dosage sensitive candidate oncogene in neuroblastoma. BeSHG, Leuven, Belgium, February 4 & 5, 2016.
- Mus L, Lambertz I, Kumps C, Claeys S, Schulte J, De Preter K, Speleman F. Dual targeting of ALK and RET: establishing a novel basis for the treatment of neuroblastoma. BeSHG, Leuven, Belgium, February 4 & 5, 2016.
- Lambertz I, Claeys S, Kumps C, Mus L, Janssens E, Van Roy N, De Wilde B, Laureys G, Cools J, De Wever O, Schulte J, De Preter K, Speleman F. ETV5 functionally connects ALK and CXCR4 signaling in neuroblastoma. BeSHG, Leuven, Belgium, February 4 & 5, 2016.

- Claeys S, Lambertz I, Van Goethem A, Kumps C, De Brouwer S, Fieuw A, Van Maerken T, Althoff K, Schulte J, Demoulin J-B, Neuroblastoma Research Consortium, De Preter K, Speleman F. HBP1 downregulation through mutant ALK represents a novel mechanism for cooperative MYCN activation in neuroblastoma. 4th Neuroblastoma Research Symposium, Newcastle, UK, November 26 & 27, 2015.
- Lambertz I, Claeys S, Kumps C, Mus L, Beckers A, Janssens E, Van Roy N, Laureys G, Schulte J, De Wever O, De Preter K, Speleman F. ETV5 functionally connects ALK and RET signaling in neuroblastoma. 4th Neuroblastoma Research Symposium, Newcastle, UK, November 26 & 27, 2015.
- Lambertz I, Kumps C, Claeys S, Lindler S, Beckers A, Janssens E, Carter D, Cazes A, Cheung B, De Mariano M, Camacho Trujillo D, De Bondt A, De Brouwer S, Gibbons J, Janoueix I, Laureys G, Liang C, Marshall G, Porcu M, Takita J, Van Den Wyngaert I, Van Roy N, Van Goethem A, Van Maerken T, Zabrocki P, Cools J, Schulte J, Vialard J, Speleman F, De Preter K. Upregulation of MAPK negative feedback regulators and RET in mutant ALK neuroblastoma: implications for targeted treatment. CNIO frontiers meeting: new trends in anticancer drug development, Madrid, Spain, March 22 – 25, 2015.
- Claeys S, Lambertz I, Van Goethem A, Beckers A, Kumps C, Van Maerken T, Schulte J, De Preter K, Speleman F. The HBP1 tumour suppressor at multiple regulatory cross roads in neuroblastoma. CNIO frontiers meeting: new trends in anticancer drug development, Madrid, Spain, March 22 – 25, 2015.
- Lambertz I, Kumps C, Claeys S, Lindler S, Beckers A, Janssens E, Carter D, Cazes A, Cheung B, De Mariano M, Camacho Trujillo D, De Bondt A, De Brouwer S, Gibbons J, Janoueix I, Laureys G, Liang C, Marshall G, Porcu M, Takita J, Van Den Wyngaert I, Van Roy N, Van Goethem A, Van Maerken T, Zabrocki P, Cools J, Schulte J, Vialard J, Speleman F, De Preter K. Upregulation of MAPK negative feedback regulators and RET in mutant ALK neuroblastoma: implications for targeted treatment. 15th Annual Meeting of the Belgian Society of Human Genetics, Charleroi, Belgium, March 2015.
- Lambertz I, Kumps C, Claeys S, Lindler S, Beckers A, Janssens E, Carter D, Cazes A, Cheung B, De Mariano M, Camacho Trujillo D, De Bondt A, De Brouwer S, Gibbons J, Janoueix I, Laureys G, Liang C, Marshall G, Porcu M,

Takita J, Van Den Wyngaert I, Van Roy N, Van Goethem A, Van Maerken T, Zabrocki P, Cools J, Schulte J, Vialard J, Speleman F, De Preter K. Characterization of ALK-driven molecular networks identifies perturbed RET and cholinergic signaling in neuroblastoma. Science day, Ghent, Belgium, March 2015.

- Lambertz I, Kumps C, Claeys S, Lindler S, Beckers A, Janssens E, Carter D, Cazes A, Cheung B, De Mariano M, Camacho Trujillo D, De Bondt A, De Brouwer S, Gibbons J, Janoueix I, Laureys G, Liang C, Marshall G, Porcu M, Takita J, Van Den Wyngaert I, Van Roy N, Van Goethem A, Van Maerken T, Zabrocki P, Cools J, Schulte J, Vialard J, Speleman F, De Preter K. Upregulation of MAPK negative feedback regulators and RET in mutant ALK neuroblastoma: implications for targeted treatment. OncoPoint meeting, Ghent, Belgium, February 11, 2015.
- Claeys S, Lambertz I, Van Goethem A, Beckers A, Kumps C, Van Maerken T, Schulte J, De Preter K, Speleman F. Synergistic combined molecular treatment targeting the HBP1 tumour suppressor gene in neuroblastoma. OncoPoint meeting, Ghent, Belgium, February 11, 2015.
- Lambertz I, Kumps C, Claeys S, Lindler S, Beckers A, Janssens E, Carter D, Cazes A, Cheung B, De Mariano M, Camacho Trujillo D, De Bondt A, De Brouwer S, Gibbons J, Janoueix I, Laureys G, Liang C, Marshall G, Porcu M, Takita J, Van Den Wyngaert I, Van Roy N, Van Goethem A, Van Maerken T, Zabrocki P, Cools J, Schulte J, Vialard J, Speleman F, De Preter K. Characterization of ALK-driven molecular networks identifies perturbed RET and cholinergic signaling in neuroblastoma. Cancer Pharmacogenomics and Targeted Therapies 2014, Cambridge, United Kingdom, September 17 – 19, 2014
- Speleman F, Vandesompele J, De Preter K, Mestdagh P, Van Maerken T, Schulte J, Lambertz I, Claeys S, Van Goethem A, Zeka F. Integrated biology-driven diagnostic and therapeutic management of neuroblastoma. FOD: Guidance Committee Cancer Plan, Brussels, Belgium, July 3, 2014.
- Lambertz I, Kumps C, Claeys S, Beckers A, Janssens E, Vanhauwaert S, Look T, He S, Schulte J, De Wever O, De Preter K, Speleman F. Mutant ALK controls

the RET-ETV5 signaling axis in neuroblastoma. Advances in Neuroblastoma Research, Cologne, Germany, May 13 – 16, 2014.

- Claeys S, Kumps C, Lambertz I, De Brouwer S, Lindner S, Van Goethem A, Van Maerken T, Vialard J, Cools J, Schulte J, De Preter K, Speleman F. The HBP1 tumour suppressor is a druggable ALK downregulated gene controlling MYCN activity. Advances in Neuroblastoma Research, Cologne, Germany, May 13 – 16, 2014.
- Claeys S, Kumps C, Lambertz I, De Brouwer S, Lindner S, Van Goethem A, Van Maerken T, Vialard J, Cools J, Schulte J, De Preter K, Speleman F. The HBP1 tumour suppressor is a druggable ALK downregulated gene controlling MYCN activity. BeSHG, Antwerp, Belgium, February 7, 2014.
- Claeys S, De Preter K, Speleman F, Lambertz I, Kumps C. Green tea compound EGCG activates HBP1: an ALK downstream suppressor gene in neuroblastoma. Oncopoint meeting, Ghent, Belgium, February 6, 2014.
- Lambertz I, Claeys S, Kumps C, Beckers A, Janssens E, Vanhauwaert S, De Wever O, De Preter K, Speleman F. ETV5 is a strong candidate driver oncogene in neuroblastoma. Oncopoint meeting, Ghent, Belgium, February 6, 2014.
- Van Peer G, Mets E, Anckaert J, Volders PJ, Claeys S, De Punt I, Rondou P., Mestdagh P, Speleman F, Vandesompele J. An unbiased high-throughput microRNA library screen identifies microRNA-interactomes of key oncogenes and tumour suppressor genes implicated in different cancer types. Keystone Symposia: Noncoding RNAs in Development and Cancer, Vancouver, Canada, January 20 – 25, 2013

Chapter 10 Een woordje van dank

Gedurende de voorbije 5 jaar heb ik me vol overgave en met veel plezier verdiept in de duistere wereld van het neuroblastoomonderzoek. Tijdens deze periode vol experimenten, datamining en presentaties, word je jammer genoeg geconfronteerd met dipjes door tegenvallende experimenten, een toestel dat niet werkt of een paper die terugkeert met veel commentaren. Gelukkig zijn er ook succesjes, die je weer voldoening en moed geven om door te gaan. Al deze momenten heb ik kunnen delen met toffe mensen. Zonder hen was het dan ook moeilijk geweest om deze thesis tot een goed einde te brengen en daarom wil ik hen ook even in de *picture* plaatsen.

Eerst en vooral wil ik prof. dr. Frank Speleman en prof dr. ir. Katleen De Preter, mijn promotor en co-promotor, bedanken. Ze hebben me de mogelijkheid gegeven om op 1 oktober 2012 dit doctoraat te starten in het Medisch Centrum voor Genetica te Gent, alsook hebben ze me gedurende het hele traject gesteund en me de kans gegeven me te ontplooien tot een volwaardige en zelfstandige PhD'er. Frank, bedankt om me de mogelijkheid te geven om mijn projecten op binnen- en buitenlandse congressen te presenteren. Katleen, bedankt om me in contact te brengen en vooral me wegwijs te maken in de datamining wereld.
Daarnaast dank ik ook Candy Kumps , Sara De Brouwer en Irina Lambertz om me te begeleiden tijdens mijn eerste jaren en me de kennis over verschillende soorten experimenten bij te brengen. Ook Geertrui Denecker en Kaat Durinck wil ik bedanken, om mijn projecten mee te helpen sturen. Bij jullie kon ik ook terecht met alle vragen omtrent publicaties en het schrijven van een thesis. Bedankt ook Els Janssens voor de zebravis experimenten en de hulp gedurende mijn PhD.

Verder wil ik alle (ex)-collega's van het CMGG, zowel uit MRB1, MRB2 en Blok B bedanken voor de toffe sfeer, de leuke en grappige momenten, zowel in de refter, in de labo's als er buiten. Samen hebben we naast research, ook veel mooie momenten beleefd tijdens congressen en andere activiteiten, denk maar aan C4CC, ANR in Australië, de lab-retreats, de sportdagen, samen gaan spinnen of gaan zwemmen, … Kortom, te veel om op te noemen!

Daarnaast heeft ieder van jullie me wel iets bijgeleerd of me geholpen, zowel op het werk als ernaast, waarvoor dank!

Speciale dank ook aan Jeroen Schacht, Els Desmet, Fanny De Vloed en Jolien Van Laere. Dankzij jullie hulp bij de vele en soms grote experimenten, zijn deze papers tot stand gebracht. Ook bedankt aan al mijn bureaugenootjes, die over de jaren heen veranderd zijn, voor de grappige momenten, de wetenschappelijke discussies, alsook voor de mogelijkheid om af en toe stoom af te laten, om er dan terug vol goede moed in te springen. Bedankt aan iedereen van de FSP groep voor de vele mooie momenten en de toffe samenwerkingen! Bedankt ook aan mijn labsis, Liselot Mus!

De laatste, maar zeker ook belangrijkste “dankjewel” gaat naar mijn familie, schoonfamilie en vrienden, die steeds interesse toonden in wat ik deed. Jullie zorgden er ook voor dat ik kon relativeren en beseffen wat echt belangrijk is, alsook dat ik me kon ontspannen en kon genieten van het samenzijn met jullie. Maar, indien nodig, maakten jullie het ook mogelijk dat ik me ten volle op mijn PhD kon focussen. Bedankt mama en papa om me deze kansen te geven, me te steunen, in me te geloven en er te zijn voor mij! Bedankt zusje en Kenny om er te zijn voor mij als ik even het geloof in mezelf kwijt was en me op te beuren als ik het nodig had. Bedankt mama, papa en Kenny, om als testpubliek op te treden voor het aanhoren van de vele presentaties, onder andere over “HBP1, a tumor suppressor gene, …”. Hopelijk is vandaag duidelijk geworden wat HBP1 nu eigenlijk doet en hoe het in het bredere plaatje, namelijk neuroblastoma past.
Bedankt ook aan Kenny en mijn lieve collega’s, om me te helpen met het ontwerpen van de cover voor mijn thesis.

Bedankt aan iedereen om me bij te staan bij mijn doctoraat!

Shana Claeys

Alone, we can do so little,
Together, we can do so much.
~Helen Keller~